Identification and Targeting of Therapeutic Resistance Mechanisms in Inflammatory Breast Cancer

by

Jennifer L. Allensworth

Department of Pathology
Duke University

Date: July 24, 2013

Approved:

_____
Gayathri R. Devi, Supervisor

_____
Robin E. Bachelder

_____
Mark W. Dewhirst

_____
Bruce A. Sullenger

_____
Kevin P. Williams

Dissertation submitted in partial fulfillment of
the requirements for the degree of Doctor
of Philosophy in the Department of
Pathology in the Graduate School
of Duke University

2013

ABSTRACT

Identification and Targeting of Therapeutic Resistance Mechanisms in Inflammatory Breast Cancer

by

Jennifer L. Allensworth

Department of Pathology
Duke University

Date: July 24, 2013

Approved:

_____
Gayathri R. Devi, Supervisor

_____
Robin E. Bachelder

_____
Mark W. Dewhirst

_____
Bruce A. Sullenger

_____
Kevin P. Williams

An abstract of a dissertation submitted in partial fulfillment of the requirements for the degree of Doctor of Philosophy in the Department of Pathology in the Graduate School of Duke University

2013

Abstract

Inflammatory breast cancer (IBC) is a rare and highly aggressive form of breast cancer that is characterized by survival signaling through overexpression and/or activation of the epidermal growth factor receptors EGFR/ErbB1 and Her2/ErbB2 and defects in the apoptotic program. The development of therapeutic resistance is a significant barrier to successful treatment in IBC, and thus, strategies targeting the mechanisms that drive drug resistance could prevent or reverse therapeutic resistance, significantly improving patient prognosis. Based on analysis of previously developed models of therapeutic resistant IBC, we hypothesized that apoptotic dysregulation and redox adaptive mechanisms were central to the drug resistant phenotype in IBC cells, and that targeting of these mechanisms could overcome therapeutic resistance. Our objectives to address this hypothesis were: 1. to develop and characterize an isotype-matched IBC cellular model to investigate the mechanisms of acquired therapeutic resistance; 2. to characterize IAP-specific small molecule inhibitors as a means of targeting the mechanism of apoptotic dysregulation in IBC; and 3. to characterize a novel redox modulatory combination as a means of targeting redox adaptive mechanisms in IBC.

Analysis of cell viability, proliferation, and growth parameters, evaluation of protein expression and signaling via western immunoblot, and measurement of reactive

oxygen species (ROS), antioxidants, and apoptosis in patient-derived IBC cell lines and isogenic derivatives revealed that resistance to the ErbB1/2 inhibitor lapatinib was protective against other targeted agents and chemotherapeutics. Additionally, reversal of resistance was associated with enhanced ability to accumulate ROS and downregulation of anti-apoptotic and antioxidant proteins. Targeting of resistance mechanisms using small molecule IAP inhibitors and a redox modulatory strategy both effectively induced apoptosis in therapy resistant IBC cells. Together, these results confirm XIAP and the redox adaptive phenotype as promising therapeutic targets for IBC and demonstrate the feasibility of targeting those mechanisms in order to reverse therapeutic resistance.

Dedication

For my parents, who always believed in me and encouraged me.

Contents

List of Tables

List of Figures

List of Abbreviations

4E-BP1	eIF4E binding protein 1
8-OHdG	8-hydroxydeoxyguanosine
AI	aromatase inhibitor
ALDH	aldehyde dehydrogenase
AML	acute myeloid leukemia
AMPK	AMP-activated protein kinase
AP-1	activator protein-1
Apaf-1	apoptotic protease activating factor 1
ARE	antioxidant response element
Bcl-2	B cell lymphoma 2
BCS	bathocuproine sulfonate
bFGF	basic fibroblast growth factor
BH	Bcl-2 homology
BIR	baculovirus IAP repeat
BMI	body mass index
CAF	cyclophosphamide, doxorubicin, 5-fluorouracil
CCS	copper chaperone for superoxide dismutase
CDK	cyclin-dependent kinase

CEF	cyclophosphatmide, epirubicin, 5-fluoruracil
CI	combination index
cIAP	cellular inhibitor of apoptosis protein
COMMD1	copper metabolism Murr1 domain-containing protein 1
CR	clinical response
CSC	cancer stem cell
DEAB	diethylaminobenzaldehyde
DHE	dihydroethidium
DISC	death-inducing signaling complex
DMSO	dimethyl sulfoxide
DSF	disulfiram
DTP	drug tolerant persister
Dvl	disheveled
EGF	epidermal growth factor
EGFR/ErbB1	epidermal growth factor receptor
EMT	epithelial to mesenchymal transition
ER	estrogen receptor
ERK	extracellular signal-related kinase
FADD	Fas-associated protein with death domain
FTI	farnesyl transferase inhibitor

GSH	reduced glutathione
GSSG	oxidized glutathione
GSR	glutathione reductase
GPx	glutathione peroxidase
GST	glutathione S-transferase
H_2DCFDA	2',7'-dichlorodihydrofluorescein diacetate
HDAC	histone deacetylase
Her2/ErbB2	human epidermal growth factor receptor 2
HIF-1	hypoxia-inducible factor 1
HO-1	heme oxygenase 1
HSP	heat shock protein
IAP	inhibitor of apoptosis protein
IBM	IAP-binding motif
IKK	IκB kinase
ILPIP	ILP-interacting protein
IBC	inflammatory breast cancer
ILP2	inhibitor of apoptosis-like protein 2
IRES	internal ribosomal entry site
JNK	c-Jun N-terminal kinase
LABC	locally advanced breast cancer

MAPK	mitogen-activated protein kinase
MDA	malondialdehyde
ML-IAP	melanoma inhibitor of apoptosis protein (livin)
MMP	matrix metalloproteinase
MOMP	mitochondrial outer membrane permeabilization
mtDNA	mitochondrial DNA
MTT	3-[4, 5-dimethylthiazol-2yl]-2, 5 diphenyl tetrazolium bromide
NAIP	neuronal apoptosis inhibitory protein
NCI-DTP	National Cancer Institute Developmental Therapeutics Program
NF-κB	nuclear factor-kappa B
NIK	NF-κB-inducing kinase
Nrf2	nuclear factor (erythroid-derived 2)-like 2
Nrx	nucleoredoxin
NQO1	NADPH quinone oxidoreductase
PARP	poly-ADP ribose polymerase
pCR	pathologic complete response
PDGF	platelet-derived growth factor
PI3K	phosphatidylinositol 3-kinase
PKC	protein kinase C
PLC-γ	phospholipase C γ

PR	progesterone receptor
Prx	peroxiredoxin
PTEN	phosphatase and tensin homolog
PTP	protein tyrosine phosphatase
qHTS	quantitative high throughput screening
RING	really interesting new gene
ROS	reactive oxygen species
RT	room temperature
RTK	receptor tyrosine kinase
SAPK	stress-activated protein kinase
SCLC	small cell lung cancer
SERM	selective estrogen receptor modulators
Smac	second mitochondrial activator of caspases
STAT	signal transducer and activator of transcription
SOD	superoxide dismutase
TF	transcription factor
TGF-β	transforming growth factor β
TM	tetrathiomolybdate
TMRE	tetramethylrhodamine, ethyl ester, perchlorate
TN	triple negative

TNF-α	tumor necrosis factor α
TNFR	TNF-α receptor
TRAF	TNF receptor-associated factor
Trx	thioredoxin
VEGF	vascular endothelial growth factor
XIAP	X-linked inhibitor of apoptosis protein

Acknowledgements

I want to thank my wonderful husband James, who has stood by me through the good times and the bad. He's been my rock and always knows what goofy little thing to do to make me laugh when I might want to cry. He's also been there to celebrate my successes as my biggest cheerleader, and no victory would be half as sweet without him at my side. He makes my life better just by being a part of it, and I couldn't imagine it any other way.

Of course I have to thank my advisor, Gay, for all of her help and guidance over the years; she has helped me to grow as a scientist and taught me a lot about dealing with people and the importance of collaboration. I truly appreciate all the time and care she spent helping me get through graduate school successfully. I would also like to thank the members of my committee- Mark Dewhirst, Bruce Sullenger, Robin Bachelder, Kevin Williams, and Kim Lyerly- for their moral support, thoughtful advice, and scientific guidance. Additionally, I would like to thank my DGS Soman Abraham for his listening ear and invaluable advice throughout the process. All of you helped to make this success possible for me, and for that I am truly grateful.

I want to thank my friends, labmates, co-workers, and co-conspirators on the 4th floor of MSRB I, which has been my second home for the last four years. I have been so lucky to fall into such a wonderful group of people; Amy, Myron, Scott, and Katherine,

it has been so much fun getting to work with all of you that at times work didn't seem like work at all. You guys are like family to me, and I can't tell you how instrumental having you there for me has been. Katherine, you were such a great mentor and inspiration to me; seeing your brilliance in action inspired me to be a better scientist, and seeing your success after you left made me excited to continue my journey as well. Amy, you've been a part of my life from Day One in the Devi Lab all the way through to my graduation, and I hope you know that I couldn't have made it through without you!

I would also like to thank my amazing friends outside the lab; meeting people in a new place is always hard, but I feel so lucky that I came to know you guys. Having a lifeline outside of the lab has been so crucial; from trivia nights to camping trips, being able to escape science and just have fun with you guys helped me get through grad school with a smile.

Lastly, I would of course like to thank my family. Your love and support is always with me, and it's made me feel just a little less far from home knowing that. It's been hard to be so far away from you guys for this time, but I always knew it was only a temporary separation, and I can't wait to be close to you all again very soon.

1 Introduction

1.1 Inflammatory Breast Cancer

Inflammatory breast cancer (IBC) is a highly aggressive and lethal subtype of breast cancer that is distinct from other forms of locally advanced breast cancer (LABC). IBC is relatively rare, accounting for somewhere between 1 and 5% of all breast cancers diagnosed in the United States [1]. IBC progresses very rapidly, and is often not diagnosed until the patient has already progressed to Stage IIIb (lymph node and chest wall involvement) or IV (distant metastasis). Rapid progression combined with late stage at diagnosis and therapeutic intervention often results in poor patient prognosis; survival rates for IBC are much lower than those for other types of breast cancer, with a median overall survival of women with IBC at only three to four years. There has been little improvement in patient prognosis since the introduction of neoadjuvant chemotherapy over 30 years ago despite advances in multimodality treatment [2].

1.1.1 Clinical, pathological, and epidemiological features of IBC

IBC's rarity combined with non-classical breast cancer symptoms often results in misdiagnosis. IBC often presents as redness or erythema of the skin, which is diffuse and can extend to cover the entire breast; this is commonly also associated with swelling, or edema [3]. These clinical symptoms mimic an inflammatory response, which can cause the disease to be mistaken for relatively innocuous conditions such as mastitis or dermatitis. The onset of symptoms can occur very rapidly, sometimes even overnight,

which is generally more characteristic of an infectious process than cancer. [4]. In most cases there is no palpable mass, and less than half of cases show a discrete mass upon mammographic examination, a classical finding for most other types of breast cancer [5]. In addition to redness and swelling, the patient may present with peau d'orange (orange peel) appearance of the skin of the breast, dramatic changes in skin color, skin thickening, nodules that may ulcerate, and/or nipple retraction or blistering; however, each case is different, and some women exhibit very few symptoms, adding to the difficulty in diagnosing IBC [3]. At the time of detection, lymph node involvement is apparent in 55-85% of patients [6]. Distant metastases are also common at diagnosis due to rapid disease progression, and these contribute to the poor prognosis of IBC [7].

IBC tumor cells often display a ductal phenotype and high histological and nuclear grades. The disease tends to present as small clusters of tumor cells (emboli) in the dermal tissue rather than as a discrete tumoral mass. A skin punch biopsy is the best technique for tissue analysis when IBC is suspected as it allows for analysis of both the underlying breast tissue and the skin above. The primary pathological finding associated with IBC is the presence of tumor emboli in the dermal lymphatics [3]. Blockage of the lymphatic vessels by these emboli is generally the underlying cause of the edema that is common [5]. However, confirmation of dermal lymphatic involvement is not always achieved; less than 75% of diagnosed IBC cases are positively identified as

having dermal lymphovascular tumor emboli [8]. Thus, while this histopathological finding can confirm a suspected IBC diagnosis, its absence does not rule out IBC.

Epidemiologically, IBC is diagnosed at significantly higher rates in African American women than in Caucasian women, with about 50% higher incidence of IBC in that population comparatively; Asian and Pacific Islander women are believed to be at lowest risk [9, 10]. Age at diagnosis is significantly lower for IBC patients (median 58 years) than those with non-IBC breast cancer (median 68 years) regardless of race, and African American women tend to be diagnosed at a younger age than Caucasian patients [1]. Median survival is also shorter in African American patients by approximately one year [9]. In addition to race, obesity also correlates with the occurrence of IBC; women with a body mass index (BMI) of greater than 26 are at a significantly higher risk for IBC than those with a BMI below 22.3 [11]. Examination of a cohort of IBC patients at MD Anderson Cancer Center revealed that 50% of registry patients are considered to be obese (BMI over 30) [3]. There is also a significant geographical disparity in IBC occurrence; while the rate of incidence in the United States is between 1 and 5%, IBC is much more common in North African countries including Morocco, Algeria, Tunisia, and Egypt, where IBC reportedly accounts for as many as 10-15% of all breast cancer cases [12, 13].

1.1.2 Molecular features of IBC

Just as IBC is a distinct form of breast cancer clinically and histopathologically, there are certain molecular features that are common in or specific to IBC. Many of these features are involved in mediating IBC pathogenesis and may represent potential therapeutic targets in combating the disease. A summary of the prevalence of selected molecular phenotypes in IBC and non-IBC can be found in Table 1.1.

Table 1.1: Prevalence of molecular phenotypes in IBC and non-IBC breast cancer

Phenotype	IBC (%)	Non-IBC (%)	Reference
Basal type	34	16	[14]
Triple negative	29	10-20	[15, 16]
Her2 amplified	36-42	17	[17, 18]
EGFR positive	30	18	[19, 20]
ER/PR positive	59	69	[21]
p53 mutated	57	37	[22]
Highly vascular	51	14	[23]

1.1.2.1 Hormone receptor negativity

A large proportion of IBC tumors are negative for expression of progesterone and estrogen receptors (PR and ER respectively). IBC cases most often fall into one of two categories: the basal subtype, which is characterized by expression of genes usually found in normal basal or myoepithelial breast cells including cytokeratin 5/6, P-cadherin, and epidermal growth factor receptor (EGFR/ErbB1) [24, 25], or the human epidermal growth factor receptor 2 (Her2/ErbB2)-overexpressing subtype in which the oncogene Her2 is amplified or overexpressed [26]. Of the five molecular subtypes for

breast cancer as a whole (luminal A and B, basal, ERBB2-overexpressing and normal-like), basal and ErbB2-overexpressing are associated with the worst prognosis [14].

Basal type breast cancer is highly aggressive and associated with especially poor prognosis. IBC tumors show a high incidence of basal type tumors, with these cases making up 33.8% of IBC cases in one study compared to only 15.93% of non-IBC cases [14]. Tumors of the basal subtype are commonly also of the triple negative (TN) phenotype based on the absence of ER, PR, and Her2/ErbB2 [24]. Unlike ER and Her2 positive breast cancers, there are relatively fewer therapies available for these tumors, as they are insensitive to estrogen- or Her2-targeting therapies like tamoxifen and trastuzumab [27]. TN IBC tumors are associated with increased likelihood for locoregional recurrence (38.6% for TN IBC vs. 8-22.6% non-TN) and distant metastasis (56.7% for TN IBC vs. 28.8-52.1% non-TN) and poor overall survival (42.7% 5 year survival for TN IBC vs. 54-74% for non-TN) as compared to IBC patients with some combination of ER, PR, and Her2 positivity [15].

1.1.2.2 Survival and growth signaling

The other main subtype of breast cancer that makes up the IBC population is the ErbB2/Her2-overexpressing group, which comprises approximately 42% of IBC cases [18]. There is an increased frequency of this subtype in IBC specifically; in a panel of 178 non-IBC and 67 IBC patients, Prost et al. determined that ErbB2 is amplified in 36% of IBC specimens compared to only 17% of non-IBC samples [17]. ErbB2 is a

transmembrane receptor tyrosine kinase and member of the epidermal growth factor receptor (EGFR/ErbB) family. It mediates signal transduction through mitogen-activated protein kinase (MAPK), phosphatidylinositol 3-kinase (PI3K)/Akt, phospholipase C γ (PLC- γ), protein kinase C (PKC), and signal transducer and activator of transcription (STAT) pathways which promote survival and proliferation while inhibiting apoptosis [28]. Thus, inappropriate activation of ErbB2 signaling results in the uncontrolled cell growth and resistance to apoptosis that is characteristic of aggressive cancers like IBC.

EGFR/ErbB1 is another member of the EGFR/ErbB family of membrane receptors. EGFR overexpression is frequent in IBC and is commonly associated with the basal subtype; an immunohistochemical study found that EGFR overexpression occurs in approximately 30% of IBC cases, consistent with its association with basal type tumors, which account for ~33% of IBC [14, 19, 29]. Similarly to ErbB2, EGFR also stimulates cell signaling networks including the PLC-γ, MAPK, and PI3K/Akt pathways to promote cell proliferation, tumor progression, invasion, and metastasis [30, 31], thus playing a role in both tumorigenesis and tumor progression. EGFR has also shown strong prognostic significance for IBC patients, with overexpression correlating with increased risk of disease recurrence and a significantly worse 5 year survival rate compared to EGFR negative IBC tumors [19].

The nuclear factor κB (NF-κB) pro-survival transcription factor (TF) is also commonly activated in IBC, with a significant upregulation of NF-κB target genes in IBC

relative to non-IBC [18, 32-34]. NF-κB activation promotes tumorigenesis, tumor progression, and therapeutic resistance through a number of downstream transcriptional targets. NF-κB promotes survival through the expression of anti-apoptotic proteins from the B cell lymphoma 2 (Bcl-2) and inhibitor of apoptosis protein (IAP) families; cell cycle progression via upregulation of cyclin D1; resistance to oxidative stress through modulation of antioxidants; and metastasis through transcription of genes involved in invasion and angiogenesis including cell adhesion molecules, matrix metalloproteinases (MMPs), vascular endothelial growth factor (VEGF), and inflammatory cytokines [35-37].

1.1.2.3 p53 mutation

The p53 TF is a tumor suppressor that can either induce cell cycle arrest and DNA repair mechanisms or apoptotic cell death in response to cellular stresses. As a significant barrier to transformation and tumor progression, p53 is very commonly inactivated in cancer; p53 mutations are the most common mutations found amongst all cancers, and IBC is no different [38]. Compared with LABC, IBC patients have higher levels of mutated p53 protein [39]; Turpin et al. found that IBC exhibited a 57% rate of p53 mutation, while LABC showed only 37% [22]. The prognostic power of p53 mutation in IBC is powerful; patients with p53 mutation and nuclear overexpression of mutant p53 protein had an 8.6-fold higher risk of death than those without mutation or overexpression [40]. Mutations in p53 have been associated with more aggressive

tumors, anthracycline resistance, reduced progression free and overall survival, and less favorable long-term outcome in IBC [41]. Thus, p53 status is important when considering patient outcomes and potential treatment regimens.

1.1.2.4 Overexpression of E-cadherin and eIF4G1

E-cadherin is a transmembrane glycoprotein that mediates epithelial cell-to-cell adhesion. In most cancers, the epithelial to mesenchymal transition (EMT) represents a crucial switch toward an invasive phenotype and metastatic potential that is associated with poor prognosis [42], while expression of E-cadherin is predictive of low metastatic potential [43]. However, E-cadherin is highly expressed in IBC despite its characterization as highly aggressive and invasive [44]. That is because in IBC, E-cadherin is essential for the formation of tumor emboli through the promotion of tumor cell-to-tumor cell interactions rather than adherence to the surrounding stromal tissue [45]. In this way, E-cadherin actually promotes the dissemination of tumor cells through a form of continuous invasion called passive metastasis [46].

eIF4G1 is a translation initiation factor that acts in concert with eIF4E and eIF4A to form the eIF4F complex, which recruits ribosomes to capped mRNAs to initiate translation [47]. In the case of IBC, in which eIF4G1 is overexpressed, it has been determined that eIF4G1 preferentially promotes the cap-independent translation of internal ribosomal entry site (IRES)-containing mRNAs. This translational reprogramming by eIF4G1 contributes to the pathogenic properties of IBC through

upregulation of p120 catenin mRNA, which contains an IRES element in its 5′ region. p120 catenin is responsible for anchoring E-cadherin at cell adherens junctions, and is thus indispensable for the formation of tumor emboli by IBC cells [46]. Hence, eIF4G1 overexpression in IBC cells promotes their highly aggressive nature by enhancing p120 catenin mRNA translation, which works with E-cadherin to mediate the formation of tumor emboli and promote continuous invasion through passive metastasis.

1.1.2.5 Increased angiogenesis, lymphangiogenesis, and vasculogenesis

IBC tumors tend to be highly angiogenic; comparison of IBC and non-IBC tumors reveals a much higher percentage of tissue with moderate to high microvascular density in IBC patients compared to non-IBC patients (51% vs. 14%) [23]. In addition, IBC specimens show a significant increase in genes associated with angiogenesis including those that encode angiopoietin, bFGF-2 (basic fibroblast growth factor 2), VEGF receptor 2 (VEGFR2) and R3, and VEGF-C and -D [48].

In addition to p120 catenin, overexpression of eIF4G1 promotes the translation of IRES-containing VEGF mRNA as a means of driving IBC pathogenesis. VEGF is a key regulator of angiogenesis that promotes the growth of vascular endothelial cells [49]. Increased expression of VEGF in IBC enhances tumor vascularity and protects against damaging hypoxia [50]. As IBC displays upregulation of genes and TFs [such as activator protein 1 (AP-1) and hypoxia-inducible factor 1 (HIF-1)] activated by hypoxia and environmental stress, a high level of intratumoral hypoxia may be characteristic of

the disease [51]. Hypoxia induces a switch from cap-dependent to cap-independent translation, which promotes increased tumor angiogenesis in an eIF4G1- and eIF4E binding protein 1 (4E-BP1)-dependent manner [52]. Silvera et al. determined that IBC cells have adapted to mimic a state of constant hypoxia at the translational level by upregulation of eIF4G1 and constitutive activation of 4E-BP1 which promotes the production of proteins required for tumor emboli survival and dissemination including VEGF and p120 catenin. They postulate that this adaptive mechanism allows tumor emboli to continue growing despite constant cycling between hypoxia and normoxia in the tumor microenvironment [50].

Lymphatic metastasis was originally thought to occur via the pre-existing lymphatic network; however, analysis of animal models and human tumors indicates that tumors can induce growth and remodeling of lymphatic vessels [53, 54]. Lymphangiogenesis is the formation of new lymphatic vessels from pre-existing ones; because cancer cells tend to travel via the lymphatic system and the lymph nodes are often the first site of metastasis, this process is highly important to tumor invasion and metastatic potential [55]. IBC specimens show a significant increase in genes associated with lymphangiogenesis and contain significantly higher fractions of proliferating lymphatic endothelial cells than non-IBC breast cancer specimens [48], consistent with their highly metastatic behavior.

Vasculogenesis, also referred to as vascular mimicry, is the process by which tumor cells form vessel-like structures that allow the flow of oxygen and nutrients in the absence of endothelial cells [3]. Animal xenograft models of IBC indicate that vasculogenesis may play a role in the disease [56, 57], but further clinical studies are needed to determine whether this feature is relevant in the patient population [54].

1.1.2.6 Apoptotic dysregulation

The ability to resist apoptotic cell death is one of the hallmarks of cancer [58] and a common mechanism by which cancer cells do this is through the dysregulation of components of the apoptotic machinery. Comparison of IBC and non-IBC tumor samples indicates that IBC cells have an enhanced capability to avoid apoptosis; this will be discussed in detail in Section 1.2.5, after a thorough introduction of the apoptotic pathways and components.

1.1.3 Current treatment options for IBC

1.1.3.1 Standard of care treatment

The standard of care therapy for primary IBC has evolved over the last four decades to include a number of different approaches working in concert to combat this aggressive disease, which has resulted in distinct improvements in patient prognosis from what was once a mere 5% rate of 5 year overall survival [7]. Currently, the accepted therapeutic plan includes systemic neoadjuvant chemotherapy, most often a combination of anthracyclines and taxanes [59], in combination with trastuzumab in the

case of ErbB2 positivity or hormonal therapies in the case of ER positive cases, followed by surgery, radiotherapy, and possible continuation of targeted agents [3, 4, 7, 60].

The anthracycline family of chemotherapeutics includes daunorubicin, doxorubicin, and epirubicin. Anthracycline activity is related to the inhibition of topoisomerase II activity, which occurs as a result of DNA intercalation by the drug, and production of free oxygen radicals that damage cellular DNA and lipid membranes [61]. The taxane family of chemotherapeutics includes docetaxel and paclitaxel. Taxanes are a form of mitotic inhibitors that function via stabilization of microtubules within the cell, which blocks cell division [62]. Most often, chemotherapeutic combinations including cyclophosphamide, doxorubicin, 5-fluorouracil (CAF) or cyclophosphamide, epirubicin, 5-fluorouracil (CEF) are followed by paclitaxel for the treatment of IBC, since addition of paclitaxel improved pathologic complete response (pCR) rates from approximately 10% to 25% [3, 4, 7].

Although mastectomy alone provides no prognostic benefit to IBC patients, yielding 5 year survival rates of 0-10% [63], surgery is a key component of multimodality therapy in patients that respond to chemotherapy, which is intended to shrink the disease and allow for complete surgical resection. The most common surgical procedure for IBC is a mastectomy with axillary lymph node dissection [3, 4, 7]. A poor prognosis is associated with positive margins, highlighting the importance of complete tumor resection [64]. Due to this fact, patients who do not respond to chemotherapy may

not benefit from surgical resection, and it may be preferable to start radiation therapy and reevaluate the benefits of surgery later or seek out clinical trials for alternative therapies [65].

Aggressive radiotherapy is recommended for IBC patients following mastectomy; in this process, the chest wall, internal mammary regions, and the surrounding undissected lymph nodes (axillary, infraclavicular, and supraclavicular) are targeted. Coverage of the chest wall is critical in order to target tumor emboli that are located in the dermal lymphatic system [3, 4, 7]. Though radiation treatment regimens vary among institutions, it is common for patients to receive once or twice daily treatment with a total dose of up to 66 Gy, as greater benefit is observed with high doses [3, 7, 66]. In a study of 115 IBC patients, Liao et al. determined that escalation of dosage from 60 to 66 Gy in a twice daily delivery format increased 5 year locoregional control rates from 58% to 84% [67].

1.1.3.2 Introduction of targeted therapies

Targeted therapies are constantly being developed, and some have already been integrated into IBC treatment regimens [4]. The targeted approach is beneficial because in comparison to systemic chemotherapy, drug specificity toward certain molecular aspects of the disease results in lower systemic toxicity and high anti-tumoral efficacy.

Hormonal therapy targets ER and PR positive tumors, which require estrogen to survive and grow; the most commonly used hormonal therapies are the ER antagonist

tamoxifen, aromatase inhibitors (AI), which block the synthesis of estrogen, and ovarian ablation, which blocks estrogen production at the primary source [68]. In a recent study of 100 patients with non-metastatic IBC, those who received hormone therapy in addition to chemotherapy showed improvement in 3 year disease-free and overall survival rates [69]. However, a large proportion of IBC cases are negative for the hormone receptors and thus resistant to this strategy.

Trastuzumab (Herceptin) is a humanized monoclonal antibody that targets ErbB2/Her2 and is commonly used in combination with chemotherapy for Her2 positive IBC patients, which make up a large percentage of the IBC population. Mechanisms of action include inhibition of Her2-mediated PI3K/Akt and MAPK signaling, induction of cell cycle arrest through induction of the cyclin-dependent kinase (CDK) inhibitor p27, induction of apoptosis, inhibition of angiogenesis, promotion of immune targeting via the antibody-dependent cellular cytoxicity (ADCC) response, and inhibition of DNA repair mechanisms [70]. Addition of anti-Her2 therapy to the chemotherapeutic regimen has been noted to improve pCR rates in IBC patients; a study in 76 Her2 positive IBC patients found a 54.8% pCR rate in patients receiving the standard doxorubicin, paclitaxel, cyclophosphamide chemotherapy plus trastuzumab compared to a 19.3% pCR rate in patients receiving the same chemotherapeutic regimen without trastuzumab [71]. However, the majority of patients who achieve an initial response to trastuzumab-based regimens generally acquire resistance within 1 year [72, 73].

Lapatinib (Tykerb) is a dual tyrosine kinase inhibitor that blocks PI3K/Akt and MAPK signaling through ErbB1/EGFR and ErbB2/Her2 [74]. Over the years, alternative mechanisms for lapatinib anti-tumor efficacy have been discovered. Xia et al. found that ErbB2 regulates expression of the anti-apoptotic protein survivin, and that lapatinib efficacy is associated with inhibition of survivin [75]. Additionally, lapatinib was found to reverse multidrug resistance through inhibition of drug transporters including the ABC subfamily members ABCB1 and ABCG2, P-glycoprotein (Pgp), and breast cancer resistance protein (BCRP) [76, 77]. A recent study in our lab determined that lapatinib mediates oxidative stress-induced apoptosis in IBC cells [78]. Clinically, lapatinib has shown anti-tumoral efficacy; one study reported 50% clinical response (CR) in Her2-overexpressing patients; the expression of phosphorylated Her2 and Her3 predicted a favorable response to treatment, while response was low in EGFR+/Her2- tumors [79]. A more recent study incorporating lapatinib and paclitaxel showed a stronger response for the combination, with a 78.1% CR rate for patients with Her2 overexpression [80]. However, the efficacy of lapatinib is limited by the development of acquired resistance, which commonly occurs within 12 months of starting lapatinib therapy, even in patients who initially respond well to treatment [81].

The angiogenic process has also seen recent attention in the development of new targeted therapies. Bevacizumab is a human monoclonal antibody targeting VEGF which has shown efficacy in IBC; a clinical study combining bevacizumab with

chemotherapy showed a 67% response rate in 20 IBC patients, which was associated with reduction in phosphorylated VEGFR2 [82]. The small molecule inhibitor of VEGFR2 semaxinib has also been investigated for use in IBC patients; however, toxicities toward the cardiac system when used in combination with doxorubicin prevented further investigation [83]. Another angiogenesis inhibitor called pazopanib was recently studied in a Phase II trial with lapatinib in Her2 positive IBC; the overall response rates were improved from 47 and 31% with lapatinib or pazopanib monotherapy to 58% with the combination. However, single agent pazopanib and the combination were both associated with toxicities that resulted in increased patient discontinuation due to adverse effects [84].

The GTP-ase RhoC, a member of the Ras superfamily, has been found to be overexpressed in IBC as is associated with the highly metastatic phenotype [85]. Farnesyl transferase inhibitors (FTIs) have been investigated in preclinical models of IBC as a way to modulate RhoC expression and inhibit motility and invasion [86]. A recent clinical study combining the FTI tipifarnib with chemotherapy determined that 18% had a clinical complete response (compared to the historical rate of ~10-15% with chemotherapy) and 59% had a clinical partial response, yielding an overall clinical response rate of 77% [87].

1.1.4 Unmet needs for the disease

Despite significant advances in multimodality treatment which have greatly improved patient survival, most patients ultimately experience recurrence and succumb to the disease. For this reason, it is essential IBC research continues, with focuses on understanding the basic biology of this disease as well as the development of new therapies.

1.1.4.1 Increased IBC awareness and refinement of diagnostic parameters

One reason that patient prognosis is so poor for IBC patients is the fact that most patients have already progressed to Stage IIIb or Stage IV by the time of diagnosis. This is in part due to the rarity of the disease; patients often have never heard of it, and doctors may never have seen a case before. Increased patient awareness would decrease the "wait and see" approach when some of the early symptoms arise, compelling patients to seek medical help as soon as possible. Additionally, the current diagnostic approach for IBC is very subjective, with much emphasis placed on physical symptoms, which can vary significantly from patient to patient. Improved diagnostic parameters would allow physicians inexperienced with IBC to diagnose it rapidly, saving precious time during which cancer progression occurs in the absence of treatment. While standard multimodality therapy shows some efficacy in treating primary IBC, there is no standard of care for metastatic disease, and the associated prognosis is especially dismal

[3]. Thus, detection of the cancer before it has the opportunity to metastasize to other organs could significantly improve patient survival rates.

1.1.4.2 Identification of molecular targets that contribute to IBC's highly aggressive nature and development of strategies to target these pathways

As discussed in Section 1.1.2, several molecular features that contribute to IBC pathogenesis have been identified. These factors provide targets for the development of novel therapies against IBC. Some examples of these are already used clinically, including the ErbB2-targeting agents trastuzumab and lapatinib, and the anti-estrogens tamoxifen and AIs. Other potential molecular targets for anti-IBC therapy that have been investigated include p53 mutation, E-cadherin overexpression, and hyperactivation of NF-κB.

Gene therapy to restore wildtype p53 function has shown success in breast cancer; one clinical study of Ad5CMV-p53 (Advexin) in combination with chemotherapy observed a partial CR in all patients, which was attributed to increased chemotherapy-related apoptosis due to effective wt-p53 gene transfer and expression as well as activation of a local immune response directed against the gene-transduced cancer cells [88]. Preclinical data show that anti-E-cadherin treatment reduces tumorigenicity and emboli formation in IBC xenografts [89]. The proteasome inhibitor bortezomib, which blocks NF-κB activity, has been tested in combination with capecitabine in patients with metastatic breast cancer and showed moderate anti-tumor activity, with a 15% response rate and 40% stable disease [90].

The combination of pre-clinical studies in IBC and clinical studies in LABC suggest that these therapies might be effective against clinical IBC; however, none of these treatments has been tested in IBC patients as of yet [2]. The development of clinical trials to treat IBC patients with novel potential therapeutics like these will allow for the expansion of current IBC treatment regimens to include specific targeting of pathogenesis factors which may improve survival rates similar to the way that ER- and Her2-targeted therapies have. Additionally, further characterization of the basic biology of IBC in *in vitro* and animal models will elucidate other molecular determinants and pathogenesis factors that may prove to be viable therapeutic targets.

1.1.4.3 Development of drugs targeting therapeutic resistance mechanisms

While Her2-targeting agents have shown promise in IBC clinical trials, most patients develop acquired resistance within 12 months of starting therapy [72, 73, 81]. Therefore, studies to identify the mechanisms of trastuzumab and lapatinib resistance in IBC are needed in order to provide a durable response for patients.

Trastuzumab resistance has been extensively studied in many different breast cancer models and cohorts of patient samples. Noted trastuzumab resistance mechanisms include expression of the truncated, constitutively active p95-Her2 receptor [91, 92]; epitope masking by membrane-associated Muc4 [93] or a CD44/hyaluronan complex [94]; Her2-independent activation of downstream signaling via loss of the PI3K/Akt inhibitor PTEN [95] or activating mutations in PI3K [96, 97] or Akt [98]; co-

expression of the insulin-like growth factor IGF-1R [99, 100]; and downregulation of the CDK inhibitor p27 [101, 102]. A recent study in our lab was the first to examine trastuzumab sensitivity in an IBC model; this revealed that upregulation of the IAPs X-linked inhibitor of apoptosis protein (XIAP) and survivin in response to treatment was associated with resistance [103].

Although both agents target the Her2 pathway, resistance mechanisms to lapatinib are mostly distinct from those against trastuzumab. For example, loss of PTEN and PI3K mutations do contribute to lapatinib resistance [104-106], and expression of truncated p95-Her2 [92, 107, 108] and IGF-1R [109] are also unrelated. One reported mechanism of lapatinib resistance was elucidated in two non-IBC Her2-overexpressing models of breast cancer (BT474 and SKBR3). In these models, resistance is mediated by derepression of the FOXO3A forkhead box TF, which is negatively regulated by the PI3K/Akt pathway, as a result of Her2/PI3K/Akt inhibition by lapatinib. This promotes a switch from Her2 to ER signaling and induces upregulation of the anti-apoptotic protein survivin. This mechanism was confirmed in patient biopsies, in which some Her2 positive LABC tumors treated with lapatinib showed activation of FOXO3a and increased expression of ER and its gene products [81, 110]. Further study of the same lapatinib-resistant models revealed activation of a cytoprotective stress response mediated by the NF-κB family member RelA, which controls transcription of the IAPs; inhibition of RelA overcame therapeutic resistance, and examination of clinical

specimens revealed significant differences in p-RelA expression in lapatinib responders and non-responders, corroborating the *in vitro* findings [111]. Another model of lapatinib resistance in Her2-overexpressing breast cancer cell lines also indicated that resistance was mediated through NF-κB signaling [112]. Lapatinib resistance in a cell line model of colorectal cancer was determined to be the result of modulation of members of the Bcl-2 family of apoptosis-regulatory proteins; expression of anti-apoptotic Mcl-1 was increased in the resistant cells concurrent with a reduction in pro-apoptotic Bak and Bax protein activation [113]. These studies highlight the importance of the apoptotic pathways in lapatinib resistance mechanisms, although none were conducted in IBC models.

Development of two IBC models of acquired therapeutic resistance to lapatinib in our lab supports the involvement of apoptotic factors in lapatinib resistance. Acquired resistance in Her2-overexpressing (SUM190) and EGFR-activated (SUM149) IBC cell lines was associated with the upregulation of XIAP, and ectopic expression of XIAP in the parental cell lines reversed lapatinib sensitivity [114]. Further examination of the resistant cell lines revealed overexpression of antioxidant enzymes superoxide dismutase (SOD) 1/2 and an increase in cellular GSH; again, exogenous addition of antioxidants was able to reverse lapatinib sensitivity in the parental lines, revealing a novel mechanism of resistance in IBC [78]. These results suggest a multifactorial resistance mechanism and indicate that in addition to the apoptotic response, redox

modulation may be important to consider for therapies aimed at restoring lapatinib sensitivity.

Because Her2-overexpressing and EGFR-activated tumors make up the bulk of the IBC patient population, strategies aimed at enhancing therapeutic response to these targeted agents has the potential for significant clinical improvement. Development of novel therapeutics or identification of agents that may repurposed for combination with trastuzumab or lapatinib to provide a durable response for patients with IBC would be highly beneficial for the patient population [3].

1.2 Apoptotic Dysregulation and Therapeutic Resistance in Cancer

1.2.1 Overview of apoptosis

Apoptosis is a tightly controlled form of programmed cell death with a large number of modulatory factors; failure of those internal regulatory mechanisms promotes pathological conditions from autoimmunity to cancer [115]. Because apoptotic dysregulation is a key factor in IBC (detailed in Section 1.1.2.6), this section introduces apoptotic cell death and mechanisms by which the process can become dysregulated.

1.2.1.1 The apoptotic pathways

The caspase enzymes are a family of cysteine proteases activated by proteolytic cleavage [116] that act as the executioners of apoptotic cell death. Caspases cleave specific substrates, resulting in the hallmarks of apoptosis including cell shrinkage, membrane blebbing, chromatin condensation, and DNA fragmentation [115, 117].

There are two main pathways by which apoptosis occurs. The intrinsic, or mitochondrial pathway, is activated in response to internal stimuli including oxidative stress, DNA damage, and cytokine or nutrient deprivation, as well as stress induced by gamma irradiation and many chemotherapeutics [118, 119]. Activation of BH3-only proteins (Bid, Bad, and Bim) liberates Bak and Bax proteins from anti-apoptotic Bcl-2 family members. These oligomerize and insert into the mitochondrial membrane to promote mitochondrial outer membrane permeabilization (MOMP), allowing efflux of cytochrome c and second mitochondrial activator of caspases (Smac/DIABLO). Cytochrome c binds to apoptotic protease activating factor 1 (Apaf-1) to form the apoptosome, which recruits and activates pro-caspase-9 [115, 120]. The extrinsic, or death receptor (DR)-mediated pathway, is activated by the binding of extracellular ligands to DRs on the cell surface including TNF-TNFR1/2, Fas ligand-Fas/CD95, and TNF-α-related apoptosis-inducing ligand (TRAIL)-DR4/5. This recruits the Fas-associated protein with death domain (FADD) adaptor protein and pro-caspase-8 to form the death inducing signaling complex (DISC), which promotes activation of caspase-8 [115, 121]. The intrinsic and extrinsic pathways converge on the activation of effector caspases-3 and -7 by caspase-8 or -9. A summary of the apoptotic pathways can be found in Figure 1.1.

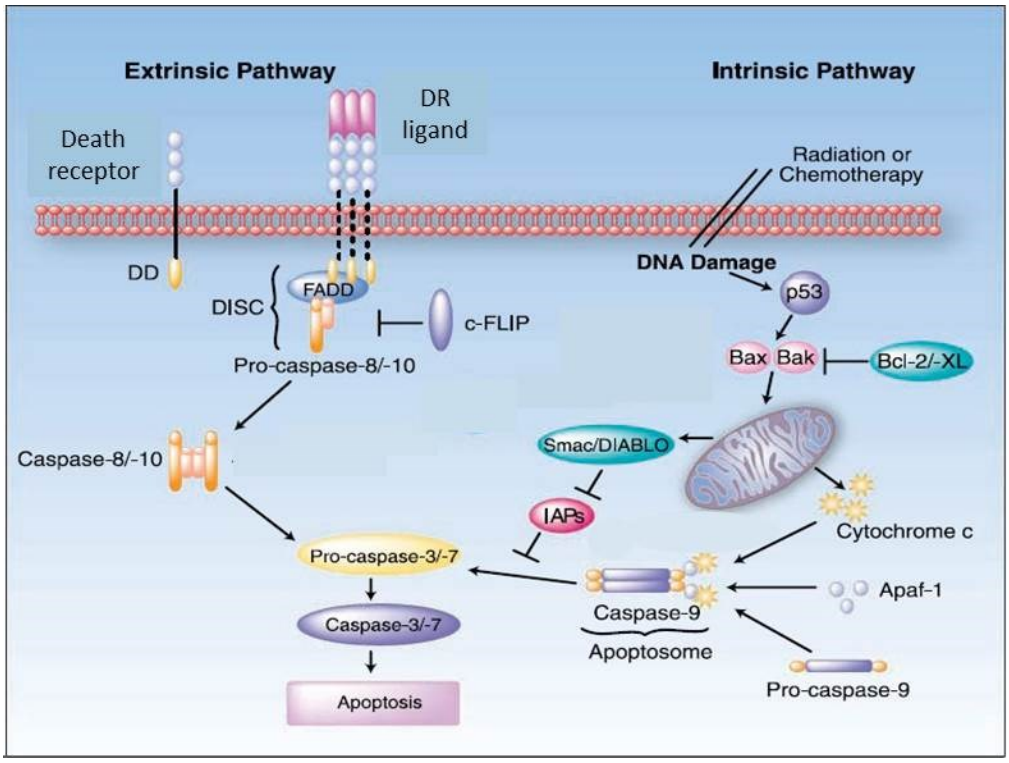

Figure 1.1: The apoptotic pathways

Adapted from [122].

1.2.1.2 Negative regulators of apoptosis

The Bcl-2 family is made up of over 20 proteins, all of which contain at least one Bcl-2 homology (BH) domain. Anti-apoptotic members include Bcl-2, Bcl-xL, Bcl-w, and Mcl-1; there are two groups of pro-apoptotic proteins: the BH3-only subfamily including Bim, Bid, Bad, Bmf, Noxa, and Puma, and the Bax subfamily, composed of Bax, Bak, and Bok [123]. Anti-apoptotic Bcl-2 proteins guard mitochondrial integrity and block apoptosis through the intrinsic pathway by interacting with pro-apoptotic members of the BH3-only subfamily [119, 124].

The IAPs are a family of caspase inhibitors that includes cellular IAP1/2 (cIAP1/2), XIAP, livin/melanoma IAP (ML-IAP), IAP-like protein 2 (ILP2), neuronal apoptosis-inhibitory protein (NAIP), Bruce/Apollon, and survivin [116]. IAPs can inhibit both intrinsic and extrinsic apoptotic pathways, suggesting they are potentially more potent apoptotic inhibitors than the Bcl-2 family [123]. IAPs are characterized by 1-3 baculovirus IAP repeat (BIR) motifs, and cIAP1/2, XIAP, ILP2, and livin/ML-IAP also contain a really interesting new gene (RING) domain which functions as an E3 ubiquitin ligase [125]. The IAPs bind to caspases through their BIR domains, although only XIAP can potently inhibit caspase activity through direct binding [126-128]. Some IAPs can ubiquitinate caspases to promote their inactivation or proteasomal degradation [129-134], and apoptogenic Smac/DIABLO is sequestered or targeted for degradation through ubiquitination by IAPs [131, 134-138]. IAPs can also ubiquitinate proteins such as the

TNF receptor-associated factors (TRAFs), receptor-interacting protein kinases (RIPKs), and NF-κB-inducing kinase (NIK) to mediate signaling [134, 135].

1.2.2 Dysregulation of apoptosis in cancer

Dysregulation of apoptosis can lead to disease, and the ability to evade apoptotic cell death is one of the hallmarks of cancer [58]. Mechanisms by which cancer cells achieve apoptotic dysregulation are detailed below.

1.2.2.1 Dysregulation of p53 and the mitochondrial pathway

The tumor suppressor p53 is a major mediator of the intrinsic apoptotic pathway. p53 loss or inactivation is a common event in human cancers; apoptotic stimuli induce p53-mediated upregulation of pro-apoptotic factors including Bcl-2 family members Bax, Bid, Noxa, and Puma. Cancer cells that have lost this p53-mediated response are thus desensitized to apoptosis associated with DNA damage and rendered insensitive to chemotherapy [124, 139, 140]. As p53 induces the intrinsic apoptotic pathway, defects in the activators of this pathway are associated with apoptotic dysregulation even in p53-competent cells [124]. Both loss of Apaf-1 expression and plasma membrane sequestration of Apaf-1 have been reported as mechanisms of chemoresistance [141-143].

1.2.2.2 Dysregulation of caspases

Inactivation of caspases can cripple the apoptotic response. Loss of pro-caspase-3 expression has been observed in breast cancer cells and results in resistance to some apoptosis-inducing treatments [115]. Downregulation of pro-caspase-3 expression levels

has also been shown to correlate with progression of gastric carcinoma and gastric lymphoma [144]. Hypermethylation of caspase-8 regulatory sequences resulting in reduced caspase-8 expression is associated with therapeutic resistance in a number of tumor cell lines and primary tumors [145]. Caspase-8 is frequently inactivated through gene deletion or DNA methylation in neuroblastomas and medulloblastomas, where it confers resistance to apoptosis and is a negative prognostic factor [146-149]. Caspase-8 is frequently silenced in small cell lung cancer (SCLC) tumors (79% of tumors tested) and cell lines, usually by aberrant promoter methylation. Inactivating point mutations in caspase-8 have also been associated with increased resistance to apoptosis [150, 151].

1.2.2.3 Dysregulation of death receptors and DISC components

DR pathways are downregulated in many tumors; Fas/CD95 expression is decreased in hepatocellular carcinomas and melanomas, and deletions or mutations in DR4/5 have also been observed in some cancers [141]. DISC components including DR5, FAS/CD95 and FASL are frequently lost in SCLC, which is associated with resistance to TRAIL-induced apoptosis [152, 153]. Additionally, expression of soluble DRs that act as decoys for death-inducing ligands can block extrinsic apoptosis. Soluble Fas/CD95 has been found in several cancer types, with elevated levels associated with poor prognosis [154-156]. Loss of CD95- or TRAIL-mediated apoptosis contributes to immune evasion, facilitating tumor metastasis [157].

Absence of the FADD adaptor protein, which helps to mediate caspase-8 activation by the DISC, has also been observed in human malignancies. A study of 70 acute myeloid leukemia (AML) patients found that leukemic cells from two thirds of patients expressed low or no FADD protein; this was an independent prognostic factor for poor response to chemotherapy in terms of remission rate and survival [158]. Overexpression of c-FLIP, a negative regulator of caspase-8 activity, has been reported in a number of human cancers [159] and renders many types of cancer cells resistant to DR-mediated apoptosis [160, 161]. c-FLIP expression is inversely correlated with TRAIL sensitivity in prostate cancer cells [162], and expression was associated with higher tumor stage and shorter survival times in colorectal carcinoma [163].

1.2.2.4 Dysregulation of the Bcl-2 family

The Bcl-2 family members are commonly dysregulated in human cancers. A chromosomal translocation that results in Bcl-2 upregulation is responsible for more than 50% of all non-Hodgkin's lymphomas (NHL) [115, 164], and elevated Bcl-2 levels have been found to correlate with chemoresistance and poor prognosis in patients with hematopoietic malignancies [165, 166]. Overexpression of Bcl-2 in MCF7 breast cancer cells is associated with enhanced resistance to TNF-α [167], and upregulation of Bcl-2 expression in metastatic breast cancer cells mediates resistance to chemotherapy [168]. Increased expression of Bcl-xL is associated with disease progression in colorectal and prostate cancers [169, 170], and a strong negative correlation was found between Bcl-xL

expression and sensitivity to standard chemotherapeutic agents in a panel of 60 cancer cell lines [171]. Increased expression of Mcl-1 has also been linked to poor chemotherapy response [172, 173].

As an alternative to increased expression of anti-apoptotic proteins, reduced expression of pro-apoptotic members can also enhance cell survival. Inactivating mutations of pro-apoptotic Bax are observed in several types of cancer [174-177], and reduction in Bax expression and/or the Bax:Bcl-2 ratio is associated with poor prognosis in chronic lymphocytic leukemia, colon, and gastric cancers [166, 178, 179]. Bax downregulation is also associated with poor response to chemotherapy and shortened survival in women with metastatic breast cancer [180].

1.2.2.5 Dysregulation of the IAPs

Many tumors have high expression of IAPs, which is associated with poor prognosis [181]. Though survivin is not found in normal adult tissues, it is highly expressed in many human cancers including lung, colon, pancreas, prostate, and breast [182-184]. Survivin expression has been associated with a significantly reduced 5 year survival rate in colon cancer patients [185] and poor prognosis in gastric cancer and neuroblastoma [186-188]. Amplification of the chromosome region that encompasses cIAP1 and cIAP2 has been observed in several cancers [189] and is regularly associated with cIAP1 overexpression in esophageal squamous cell carcinomas [190]. Upregulation of cIAP2 via chromosomal translocation is highly associated with marginal cell

lymphomas of the mucosa-associated lymphoid tissue [191, 192], and increased cIAP2 expression in prostate cancer is associated with decreased relapse-free survival [193]. Overexpression of the IAP livin has also been associated with chemotherapy resistance in primary cultures derived from melanoma patient tissue, and expression correlates negatively with melanoma patient survival [194, 195].

XIAP is the most potent IAP in part due to its unique ability to bind and suppress the activity of caspases directly [125, 161, 196]. XIAP also activates the PI3K/Akt signaling pathway and can participate in a pro-survival feedback loop by promoting the activity of its transcriptional regulator NF-κB [197, 198]. XIAP-mediated ubiquitination of copper metabolism Murr1 domain-containing protein 1 (COMMD1), a negative regulator of NF-κB activity, further promotes survival signaling through this pathway [199]. Overexpression of XIAP has been reported in many different types of cancer and has been associated with unfavorable response to chemotherapy [200-204], resistance to TRAIL [205], lymph node metastasis [206], poor tumor differentiation [207, 208], increased risk of relapse and metastasis [203, 209, 210], and shortened survival [200-202, 211-214]. XIAP expression correlates positively with tumor stage and pathological grade of breast, colorectal, and laryngeal carcinomas [215-217], suggesting a role of XIAP in disease progression. Increased XIAP expression in melanomas compared to benign nevi, with even higher expression in metastases, indicate that XIAP may also be involved in regulating the metastatic process [204].

1.2.3 Apoptotic dysregulation in IBC

As mentioned in Section 1.1.2.6, analysis of the molecular characteristics of IBC has revealed that apoptotic dysregulation is a relevant feature that separates IBC from LABC. IBC tumors show enhanced NF-κB activation compared to non-IBC tumors [18, 32-34], and a number of anti-apoptotic genes are transcriptionally activated by NF-κB including Bcl-2, Bcl-xL, cIAP1/2, XIAP, survivin, and TRAF1/2 [35]. The IAPs have also been reported to promote NF-κB activation, suggesting the presence of an anti-apoptotic feedback loop between the two [197, 218, 219]. Bertucci et al. determined that the anti-apoptotic genes defender against apoptotic cell death (DAD1), which encodes a protein that interacts with Mcl-1 [220], and ALS2CR2, which encodes the ILP-interacting protein (ILPIP) that interacts with XIAP to inhibit apoptosis via activation of c-Jun terminal kinase (JNK) [221], are upregulated in IBC relative to non-IBC [222]. Another gene profiling study discovered differential expression of the pro-apoptotic protein Bax in IBC patient samples compared to other types of breast cancer [223]. Iwamoto et al. found that genes associated with the apoptosis pathways were overexpressed in a subset of IBC tumors compared with non-IBC cancers of the same receptor phenotype [224]. A recent study of lapatinib resistance in IBC cell lines determined that the E3 ligase MDM2 inhibits apoptosis via ubiquitination and destabilization of p53 and the apoptosome activator CAS; MDM2 also ubiquitinates the E3 ligase HUWE1, blocking its inhibitory effects on the anti-apoptotic Mcl-1 protein to promote survival [225]. Our own studies in

IBC cell line models revealed that the anti-apoptotic proteins survivin and XIAP mediate resistance to Her2 targeted therapies trastuzumab and lapaitnib [103, 114]; together, these data highlight the importance of apoptotic dysregulation in IBC pathogenesis and indicate that therapies aimed at restoring normal function to the apoptotic pathways could benefit patients with IBC.

1.3 Oxidative Stress, Redox Adaptation, and Therapeutic Resistance in Breast Cancer

Recent studies in our lab indicate that redox adaptive mechanisms may play a role in acquired therapeutic resistance in IBC cell line models (discussed in detail in Section 1.4.2) [78]. Thus, thus section will provide an overview of oxidative stress and redox adaptation, as well as their roles in therapeutic resistance and sensitivity.

1.3.1 Reactive species are required for normal cell function

Although ROS are generally thought of as damaging to cells due to their ability to induce oxidative stress at high concentrations, low levels of ROS that act as second messengers in signaling cascades are essential for cellular responses to external stimuli [226]. Due to their high reactivities that preclude substrate specificity, most reactive species are not considered second messengers; however, the enzymatic production and degradation of H_2O_2, along with its preferential reactivity toward protein thiols make it a second messenger [227]. H_2O_2 oxidizes cysteine residues to relay signals, and substrate specificity is derived from the fact that not all cysteines are susceptible to H_2O_2-mediated oxidation. Most cysteine residues in the cell have pKas that are too high for H_2O_2 to react

with, but some exist as thiolate anions due to nearby charged amino acids and thus have low pKas [226, 228]. Protein tyrosine phosphatases (PTPs), whose function is the removal of phosphate groups from substrates, contain an active site cysteine with low pKa. Oxidation of cysteine residues in the catalytic domain of PTPs by H_2O_2 results in reversible inactivation, temporarily promoting a phosphorylated state for proteins in the vicinity [226, 228]. Oxidative inactivation of the PTP PTEN promotes activation of PI3K/Akt signaling [226, 229]. PTP inactivation plays an important role in cellular response to growth factors; binding of ligands like platelet-derived growth factor (PDGF) and epidermal growth factor (EGF) to receptors produces a burst of ROS that inactivates PTPs; blockage of that production inhibits normal signaling [230]. Binding of other ligands including bFGF, transforming growth factor β (TGF-β), and angiotensin II also elicits production of H_2O_2 to mediate downstream signaling events [226, 231].

ROS activate a number of cellular signaling pathways that regulate growth, proliferation, stress responses, and apoptosis, including the MAPKs. H_2O_2 promotes p38 and JNK MAPK signaling by relieving the inhibition of their activator ASK1 by Trx [227, 232]. H_2O_2 also modulates extracellular-reguated kinase (ERK) 1/2 signaling by inducing autophosphorylation of growth factor receptors such as EGFR and PDGF, which activates Ras and Raf/MEK/ERK [232-234]; alternatively, activation of Ras via oxidation can achieve the same effects [235, 236]. Wnt/β-catenin signaling is activated by H_2O_2 through oxidation of the Trx-like protein nucleoredoxin (Nrx), which binds Dishevelled

(Dvl) to suppress Wnt signaling under normal conditions. Nrx oxidation releases Dvl, resulting Wnt/β-catenin activation [226, 237]. Generation of H_2O_2 following cell attachment to the extracellular matrix results in oxidation of cysteine residues to activate the tyrosine kinase Src [238, 239].

ROS also mediate signaling through modification of redox-sensitive TFs such as NF-κB, HIF-1, p53, and AP-1; these contain cysteine residues in their DNA-binding domains that render them susceptible to activation by oxidative modification [238]. The TF nuclear factor (erythroid-derived 2)-like 2 (Nrf2) can also be activated by ROS via the oxidation of its negative regulator Keap1 [226, 240]. Thus, ROS are important for activation of signaling cascades that are essential for normal cell function.

1.3.2 High levels of ROS can be damaging to cells

Oxidative stress occurs when there is an imbalance between the levels of ROS within the cell and the antioxidant systems responsible for detoxifying ROS. While low to moderate doses of ROS are required for the propagation of cellular signals, high levels of ROS can damage cells through interactions with critical cellular components.

ROS promote mutagenesis through modifications of bases, the deoxyribose backbone, DNA strand breaks, and cross-linking to other molecules [241]. If the cells are allowed to survive and divide, those genomic alterations can promote oncogenesis (discussed in Section 1.3.3) [242]. However, high levels of irreparable damage to the genome promote cell death. DNA damage most commonly activates the intrinsic, or

mitochondrial, apoptotic pathway through the tumor suppressor p53 [243]. In addition to nuclear DNA, mitochondrial DNA (mtDNA) is a critical cellular target for oxidative damage [244]. mtDNA is especially susceptible to ROS due to its close proximity to the electron transport chain (the major source of cellular free-radical production) and lack of protective histones. Damage to mtDNA could lead to lethal cell injury through the loss of electron transport, mitochondrial membrane potential, and ATP generation [241].

Proteins are also sensitive to oxidative stress, which can result in oxidation of sulfhydryl groups, oxidative adducts on amino acid residues, reactions with aldehydes, protein-protein cross-linking, and protein fragmentation [241, 245]. Oxidation of amino acids promotes the formation of protein carbonyls, which alter protein structure and promote unfolding; this is associated with enhanced proteolytic degradation [241]. Due to the vital role of proteins in regulating cell signaling, cell structure, and enzymatic processes like metabolism, their oxidation rapidly contributes to oxidative stress [246].

Lipid peroxidation results in the conversion of unsaturated lipids to polar lipid hydroperoxides [247]; this process causes increased membrane fluidity, efflux of cytosolic solutes, and loss of membrane–protein activities. Extensive lipid peroxidation correlates with the ultimate disintegration of membrane integrity and cell death [248]. Additionally, products of lipid peroxidation including malondialdehyde (MDA) and 4-hydroxy-2-nonenal are themselves reactive and promote DNA degradation, further damaging the cell [248].

1.3.3 ROS can promote oncogenesis

As mentioned in Section 1.3.2, ROS can react with cellular and mitochondrial DNA, promoting the acquisition of mutations. Oxygen radicals react with DNA bases to produce a variety of adducts [249], which can result in mutations, deletions, gene amplification, and rearrangements [250]. Changes in the cellular DNA sequence can activate proto-oncogenes or inactivate tumor suppressor genes, both of which contribute to tumorigenesis. DNA damage as measured by levels of oxidative DNA lesions (8-hydroxydeoxyguanosine, 8-OHdG) has been noted in various tumors types [242]. While there are mechanisms to repair DNA lesions, defects in cell cycle arrest and apoptosis (such as p53 mutation) allow for the propagation of cells with DNA mutations [251]. Because the mitochondria, which are the primary source of intracellular ROS [241], are heavily involved in maintaining genomic stability through functions in DNA replication, repair, and recombination, oxidative damage to the mitochondria promotes increased mutation rates and contributes to oncogenesis [252].

Despite their potential for cellular damage, ROS are often upregulated in cancer cells; their role in promoting certain signaling cascades is one reason for this adaptation [253]. The EGFR signaling pathway, which requires H_2O_2 for activation and downstream signaling, is central to breast cancer pathogenesis. EGFR is a major oncogenic factor that is associated with large tumors, poor differentiation, and has been reported to correlate with poor prognosis [29, 254, 255]. While EGFR is found in all breast cancer subtypes, it

is overexpressed more frequently in TN and IBC breast cancers, both of which are highly aggressive [29]. Downstream targets of EGFR signaling include PLC-γ/PKC, PI3K/Akt, Ras/Raf/ERK, and the STATs; activation of these pathways promotes proliferation, tumorigenesis, invasion and metastasis, and therapeutic resistance [29, 31]. The PI3K/Akt signaling pathway, also promoted by ROS, has been noted to be upregulated in breast cancer, where it: inhibits apoptosis by upregulating survival factors such as NF-κB and downregulating pro-apoptotic proteins [256, 257]; stimulates cell cycle progression; promotes cell growth and proliferation; and plays a role in EMT through upregulation of the transcriptional repressor of E-cadherin, Snail [256]. ROS-mediated Raf/Mek/ERK signaling inhibits apoptosis through the suppression of pro-apoptotic mRNAs and proteins like Bim and Bad and increased expression of anti-apoptotic proteins including Bcl-2, Bcl-xL, and Mcl-1 [258]. The Wnt/β-catenin pathway is also induced by ROS; this pathway supports EMT through induction of vimentin [259] and Snail [260, 261], which are associated with the mesenchymal state. Further, Wnt/β-catenin signaling is positively correlated with expression of the stem cell marker CD44 and mediates radiation resistance in mouse mammary progenitor cells [260, 262, 263]. Thus, many important signaling pathways that are central to oncogenesis and tumor progression are regulated by ROS.

1.3.4 Redox adaptation in breast cancer cells promotes resistance to anti-tumoral therapies

Cancer cells are often characterized by increased levels of ROS due to aberrant metabolism, mitochondrial dysfunction, oncogene activation (c-Myc, Ras, Bcr-Abl), and loss of p53 [253]. In order to compensate for high levels of ROS, some cancer cells activate redox adaptive mechanisms [264]. Many anti-cancer regimens work at least in part through the generation of ROS, and thus may be rendered ineffective by redox adaptation. Chemotherapies including the anthracyclines (doxorubicin), taxanes (paclitaxel, docetaxel), alkylating agents, and platinum compounds (cisplatin, carboplatin) as well as radiation therapy all rely heavily on the induction of oxidative stress-induced apoptosis for their anti-tumor activities [235, 253, 265]; thus, redox adaptation confers resistance to many breast cancer therapies.

1.3.4.1 Redox adaptation through increased ROS detoxification

The ability to increase antioxidant function is essential for cancer cells with high ROS levels to return cellular redox status to normal. The concurrent elevation of markers of oxidative stress and increased expression and activity of antioxidants in breast cancer indicates redox adaptation. Due to their highly reactive nature, ROS are difficult to measure in tissue samples; as such, oxidative stress in tissue is often measured through quantification of oxidized cellular constituents including MDA, lipid hydroperoxides, and conjugated dienes (products of lipid peroxidation) [266] and 8-OHdG (a base lesion that results from DNA oxidation) [267].

Several groups observed increased levels of oxidative stress indicators accompanied by augmentation of SOD1/2, GSH, GPx, glutathione S-transferase (GST), and catalase expression and activity in breast cancer patient tissue in comparison to healthy controls [268-273]. Interestingly, the degree of increase in oxidative stress and antioxidant levels correlated with advanced disease, with greater increases in both observed in Stage III samples than in Stage I and II samples [271]; these findings support the role redox adaptive mechanisms in tumor progression. One study determined that GSH levels were increased by two fold in breast cancer tissue relative to normal breast, while tissue from lymph node metastases showed a four-fold increase in GSH over normal tissue [274]. Similarly, breast cancer brain metastases showed significant upregulation of GSH-associated enzymes glutathione reductase (GSR) and GST, which help them maintain a reduced cellular environment [275]. These observations indicate that redox adaptation is crucial for metastatic breast cancer, as metabolic pressures associated with a foreign environment can promote oxidative stress [276].

GSH has long been recognized as having an important role in cancer drug resistance [277]; alterations in ROS-scavenging systems can have significant effects on the metabolism of alkylating agents and platinum compounds, inactivating electrophilic intermediates [235, 253]. Introduction of exogenous antioxidants GPx or SOD to MCF7 cells is sufficient to induce therapeutic resistance to doxorubicin [278], and GPx mRNA and activity were also increased in MCF7 cells with acquired doxorubicin resistance

[279]. Antioxidants GST and SOD were also found to be elevated in tamoxifen-resistant MCF7 tumors in a xenograft study, indicating a role for antioxidants in resistance to targeted therapies [280]. Increased GSH was also associated with resistance to ROS-inducing drugs in a mouse model of breast cancer brain metastasis; upregulation of GSH in response to bortezomib resulted in a 60-fold reduction in sensitivity of metastatic cells compared to parental cells [275]. Thus, redox adaptation via enhanced antioxidant capacity plays a vital role in mediating resistance to anti-cancer regimens, affecting both tumor response and patient prognosis.

1.3.4.2 Redox adaptation through activation of redox-sensitive transcription factors

Redox sensitive TFs including NF-κB, Nrf2, AP-1, and HIF-1α promote the expression of antioxidant molecules [253], and thus promote redox adaptation through the mechanisms described in Section 1.3.4.1. Some redox-sensitive TFs also induce expression of pro-survival and anti-apoptotic genes, which are also protective against oxidative stress [253, 281].

The Nrf2 TF is an important regulator of the oxidative stress response, modulating the transcription of genes with an antioxidant response element (ARE) [282] including antioxidants and phase II detoxifying enzymes [NADPH quinone oxidoreductase (NQO1), heme oxygenase 1 (HO-1), peroxiredoxin (Prx), Trx, GST, and GSH synthesis enzymes] and proteasomal and heat shock protein (HSP) genes, which prevent apoptosis via the misfolded protein response [283]. The GSH synthesis system is

under the transcriptional control of Nrf2, and tumor cell lines with acquired resistance to chemotherapeutic drugs often display abundant levels of GSH and Nrf2 activation [284, 285]. In MCF7 cells, ROS induction and depletion of GSH activates Nrf2; upregulation of ARE genes restores cellular pools of GSH and protects against oxidative stress [286]. Nrf2 is an important prognostic factor in determining drug response in a number of cancer types [287]. In a panel of breast cancer cell lines, paclitaxel sensitivity correlated negatively with antioxidant capacity, and co-treatment with a Nrf2 inhibitor enhanced sensitivity [225]. Stabilization of Nrf2 in MCF7 cells resulted in resistance to H_2O_2, paclitaxel, and doxorubicin [288], and acquired resistance to doxorubicin in MCF7 cells was associated with high expression of Nrf2 and its target proteins [289]. Activation of Nrf2 in MCF7 cells with acquired tamoxifen resistance resulted in upregulation of antioxidants and was associated with reduced ROS production in resistant cells [290].

NF-κB activity is induced by oxidative stress [35, 37], and transcriptional target genes include antioxidants (SOD1/2, Trx, and the GSH-associated enzymes GPx, GST-pi, and γ glutamylcysteine synthetase) and anti-apoptotic proteins (Bcl-2, Bcl-xL, cIAP1/2, and XIAP) [35, 37]. These detoxify intracellular ROS and block oxidative stress-induced apoptosis, regulating the cellular response to an altered redox state at multiple levels. Constitutive activation of NF-κB is observed in many types of cancer [291] and can inhibit apoptosis induced by chemotherapy and ionizing radiation [285, 292]. Taxane-resistant MCF7 cell line variants revealed consistitutive NF-κB activation, and inhibition

of NF-κB signaling reestablished sensitivity [293]. Constitutive activation of NF-κB is also associated with resistance to ER-targeting by tamoxifen and AIs [294, 295]. A cytoprotective stress response mediated by NF-κB subunit p65/RelA was found in breast cancer cell lines with acquired resistance to lapatinib, and these results were corroborated by analysis of biopsies from ErbB2 positive breast cancer patients receiving lapatinib monotherapy. Responders showed a median 40% decrease in p-RelA after 28 days of treatment, while non-responders showed ~75% increase, supporting a central role for NF-κB in response to lapatinib therapy [111]. Examination of radioresistant variants of MCF7 cells revealed NF-κB-mediated upregulation of SOD2 and other genes that participate in radiation-induced adaptive responses; inhibition of NF-κB signaling decreased expression of target genes and sensitized cells to radiation [296]. Together, these data indicate that redox-sensitive TFs can induce a redox adapted state that promotes resistance to chemo-, targeted, and radiotherapies in breast cancer.

1.3.4.3 Redox adaptation through activation of survival signaling and upregulation of anti-apoptotic factors

Sustained oxidative stress promotes constitutive activation of survival signaling and upregulation of anti-apoptotic molecules; this promotes cell survival in response to oxidative stress such as that induced by anti-cancer drugs and radiotherapy. The PI3K/Akt pathway is activated in times of oxidative stress [226, 229] and promotes cell cycle progression and proliferation by modulating cell cycle regulators and controls cell death by inducing anti-apoptotic proteins and inhibiting pro-apoptotic molecules [256].

In a study of breast cancer cell lines, constitutive Akt activation was associated with cell survival, while treatment with a PI3K inhibitor enhanced sensitivity to a myriad of therapies including doxorubicin, paclitaxel, trastuzumab, and etoposide. Ectopic expression of constitutively active Akt renders MCF7 breast cancer cells insensitive to tamoxifen treatment [297] through Akt-mediated activation of NF-κB [298]. p-Akt positivity was associated with poor disease-free survival in breast cancer cases where patients received post-operative hormonal therapy [299]. Trastuzumab-mediated activation of the phosphatase PTEN is required for drug sensitivity, rendering PTEN null cells resistant in *in vitro* and *in vivo* models. Response to trastuzumab was also poorer in patients with PTEN-deficient breast cancers than those with functional PTEN [95]. Introduction of constitutively active Akt confers radioresistance on MCF7 cells [300], and endogenous constitutive activation of the PI3K/Akt pathway in BT-474 cells is associated with resistance to radiation, supporting the importance of PI3K/Akt signaling in the determination of breast cancer susceptibility to therapy [301].

ERK signaling promotes survival through upregulation of anti-apoptotic proteins and inhibition of pro-apoptotic molecules [258]. Evaluation of the activity of Raf-1, an upstream activator of the ERK cascade, in a panel of cancer cell lines revealed an inverse correlation between Raf-1 activity and doxorubicin sensitivity [302], while expression of constitutively active Raf-1 in MCF7 cells conferred resistance to doxorubicin and paclitaxel [295]. In a study of 109 patients with TN breast cancer,

overexpression of ERK correlated with anthracycline resistance and poor survival [302]. The ERK signaling pathway also plays a role in resistance to targeted therapies; in an MCF7-derived cell line model, acquired tamoxifen resistance was linked to increased ERK phosphorylation [290]. Tamoxifen inhibits ERK phosphorylation in parental cells, while cells with acquired resistance show increased ERK phosphorylation in response to treatment [303]. A clinical study found that patients with >1% ERK1/2 phosphorylation did not respond to tamoxifen, while patients without ERK1/2 phosphorylation did [304].

Upregulation of anti-apoptotic factors can mediate resistance against a wide variety of therapeutic mechanisms including oxidative stress; the Bcl-2 family has been implicated in resistance to a number of anti-cancer drugs. Bcl-2 modulation of mitochondrial respiration enhances GSH turnover in the cell to combat exogenous increases in ROS [305]. A study in breast cancer cell lines revealed that sensitivity to cisplatin and paclitaxel could be induced by knockdown of Bcl-2 or pre-treatment with a small molecule inhibitor. XIAP is the most potent member of the IAP family and has been linked with poor prognosis and therapy resistance in several cancer types [201, 207, 208, 210-215]. In cell line models of TRAIL-resistant breast cancer, XIAP depletion overcame resistance; XIAP targeting with siRNA or a Smac mimetic also enhanced therapeutic response to ErbB antagonists trastuzumab, lapatinib, and gefitinib [306]. Another study in MCF7 cells revealed that Smac mimetics enhanced the apoptotic response to paclitaxel, doxorubicin, etoposide, and tamoxifen [307]. These data indicate

that increases in the expression and activity of anti-apoptotic proteins can protect breast cancer cells from therapeutic apoptosis induced by anti-cancer drugs.

1.3.4.4 Interplay of redox adaptive mechanisms in therapeutic resistance

While these redox adaptive mechanisms have each been discussed separately as mediators of therapeutic resistance, these factors interact with and modulate one another in many ways. The crosstalk between them results in greater resistance to oxidative stress than could be achieved by any one factor alone; indeed, some of these mechanisms could not function without the others. Activation of survival signaling pathways such as PI3K/Akt and ERK1/2 via H_2O_2 can activate redox-sensitive TFs such as Nrf2 and NF-κB. Many of the antioxidants discussed above are under the control of redox-sensitive TFs, and many anti-apoptotic proteins are also controlled by those same TFs [35-37, 308]. Enhancement of cellular antioxidant capacity likely could not occur without modulating the activities of the TFs upstream from them. Increased transcriptional activity of Nrf2 and NF-κB has also been linked with upregulation of survival pathway components, culminating in the activation of those pathways; for example, activation of NF-κB promotes the phosphorylation of Akt [309]. Additionally, some targets of the redox-sensitive TFs can modulate the transcriptional activity of their activators. Because IκB kinase (IKK) is a substrate of Akt, Akt activation can stimulate NF-κB activity, promoting a feedback loop between the two [197, 198, 310, 311]. It has also been shown that the anti-apoptotic protein XIAP, a target of NF-κB-mediated

transcription, can modulate the transcriptional activity of NF-κB via interaction with the TAB1 adaptor protein and TAK1 kinase [198].

Thus, redox adaptive mechanisms work in concert to regulate one another and participate in feedback loops, resulting in reduction of oxidative stress sensitivity. This confers resistance to drugs whose mechanism of action involve the generation of ROS and promotes the development of tumors that are highly refractory to therapeutic intervention. As such, redox adaptation represents a powerful therapeutic target for the development of new anti-tumoral agents for breast cancer.

1.4 IBC Cell Line Models

1.4.1 Patient-derived IBC models: SUM149, SUM190, and MDA-IBC-3

Three primary patient-derived IBC cell lines were used in this dissertation: SUM149, SUM190, and MDA-IBC-3 (Fig. 1.2). SUM149 is a basal type cell line with EGFR/ErbB1 activation; absence of ER, PR, and ErbB2/Her2 qualify it as TN breast cancer [312, 313]. SUM149 cells have a short doubling time of 14-21 h and are enriched for cells with a CD44+/CD24-/low phenotype, which is associated with stem cell-likeness [114, 313]. SUM190 belongs to the Her2-overexpressing subtype and is also negative for ER and PR. SUM190 has a much slower doubling time than SUM149, at ~42 h and does not express a CD44+/CD24-/low population [312, 313]. Both SUM149 and SUM190 are characterized by p53 mutation [41]. MDA-IBC-3 is a cell line recently isolated from primary tumor cells in the pleural effusion of an IBC patient [314]. As a newer cell line,

less is known about MDA-IBC-3 cells; however, they are known to be Her2-overexpressing and negative for ER and PR expression. They also have a very slow doubling time of approximately 76 h and, similar to SUM190, do not express a CD44+/CD24-/low population [313]. SUM149, SUM190, and MDA-IBC-3 cell line models represent the two most common subtypes of IBC: the basal, ErbB1/EGFR-activated subtype (SUM149), and the ErbB2/Her2-overexpressing subtype (SUM190, MDA-IBC-3).

1.4.2 Models of acquired resistance in IBC: rSUM149 and rSUM190

The rSUM149 and rSUM190 models of acquired therapeutic resistance were generated by Dr. Katherine Aird through continued exposure of parental SUM149 and SUM190 IBC cells to increasing concentrations of an analog of the ErbB1/2 inhibitor lapatinib analog (GW583340; Fig. 1.2). Initially, exposure of the parental lines to GW583340 resulted in massive cell death, but a few cells survived and grew out into colonies over a period of weeks following each increase in drug concentration. GW583340 concentration was continually increased over a period of ~3 months, after which the resistant lines- rSUM149 and rSUM190- were maintained in regular growth media supplemented with 7.5 and 2.5μM GW583340 respectively [114].

Examination of ErbB1/2 phosphorylation in the resistant rSUM149 and rSUM190 cell lines revealed that the primary mechanism of action of lapatinib, inhibition of ErbB1/2 signaling, remained intact in these cells. Both p-ErbB1 (in rSUM149) and p-ErbB2 (in rSUM190) levels, as well as downstream p-Akt, were reduced in the resistant

cells, similar to results in the parental SUM149 and SUM190 cells. Acquisition of resistance to lapatinib in the rSUM149 and rSUM190 cell lines was determined to be the result of overexpression of XIAP through an increase in IRES-mediated translation. Lentivirus-mediated overexpression of XIAP in parental SUM149 cells was protective against lapatinib-induced cell death, and targeting of XIAP with a small molecule inhibitor in rSUM149 and rSUM190 enhanced lapatinib response [114]. These studies reveal that apoptotic dysregulation via enhancement of XIAP translation/expression is a novel mechanism of lapatinib resistance in IBC and indicate that targeting of XIAP may be a rational strategy to enhance apoptosis and prevent or reverse lapatinib resistance.

Further studies of the resistant cell lines revealed a novel mechanism of lapatinib-mediated cell death: the induction of oxidative stress. While lapatinib induced ROS at levels similar to the classical ROS-inducing agents paraquat and H_2O_2 in parental SUM149 and SUM190 cells, rSUM149 and rSUM190 cells maintained low levels of ROS in the presence of lapatinib. Additionally, the resistant cell lines were insensitive to ROS induction by H_2O_2 and paraquat and associated cell death. rSUM149 and rSUM190 cells showed a lack of AMP-activated protein kinase (AMPK) phosphorylation, a marker of oxidative stress [315] that was observed in the parental lapatinib-treated cells, in response to lapatinib. Interrogation of cellular antioxidant capacity revealed a redox adaptive mechanism mediated by upregulation of SOD1 and SOD2 in the resistant cells, as well as an increase in the cellular pool of GSH. Redox modulation with an SOD

inhibitor or pro-oxidant reversed the resistance of rSUM149 and rSUM190 to ROS-mediated apoptosis, and addition of an exogenous antioxidant was protective against lapatinib in the parental SUM149 and SUM190 cells, confirming the importance of ROS generation for lapatinib-induced cell death [78]. These studies reveal a new mechanism for lapatinib-induced apoptosis and highlight a novel, redox adaptive response in rSUM149 and rSUM190 cells that is protective against cell death associated with the induction of ROS by a number of agents.

Taken together, these studies indicate a multifactorial resistance mechanism in rSUM149 and rSUM190 cells by which apoptotic dysregulation and redox adaptation both contribute to reduced cell death in response to treatment. Identification of these mechanisms enhances the current understanding of lapatinib resistance in IBC and opens the door for new therapeutic strategies targeting these resistance mediators as a way to prevent or reverse resistance to therapy-mediated apoptosis.

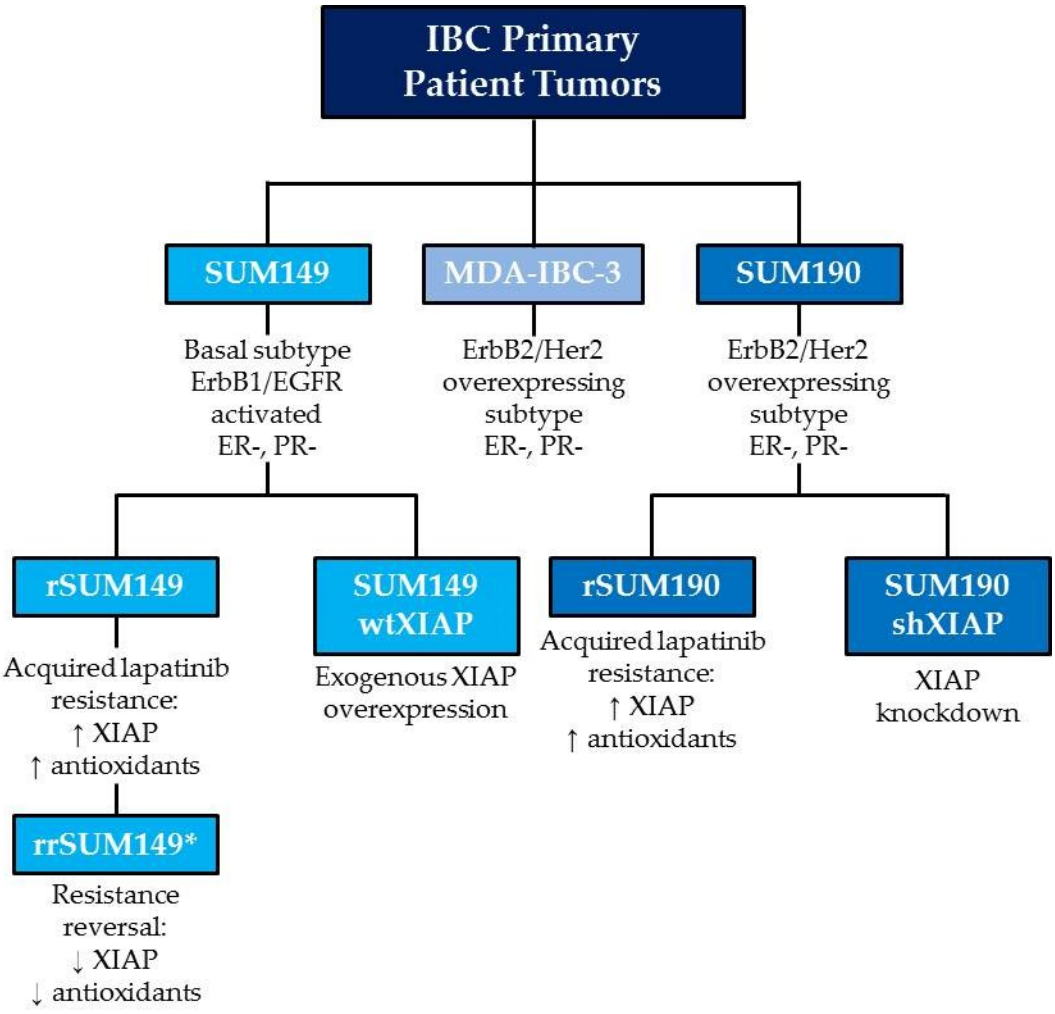

Figure 1.2: IBC cell line models used in this dissertation

*Generation and characterization of the rrSUM149 isogenic-derived cell line is detailed in Chapter 3.

1.5 Research Objectives

The studies outlined here are intended to address our hypothesis that apoptotic dysregulation and redox adaptive mechanisms mediate the drug resistant phenotype in IBC cells (Fig. 1.3), and thus, targeting of these mechanisms can overcome therapeutic resistance.

1.5.1 Objective 1

Development and characterization of an isotype-matched IBC cellular model to investigate the mechanisms of acquired therapeutic resistance (discussed in Chapter 3)

1.5.2 Objective 2

Characterization of IAP-specific small molecule inhibitors as a means of targeting the mechanism of apoptotic dysregulation in IBC therapeutic resistance (discussed in Chapters 4 and 5)

1.5.3 Objective 3

Characterization of a novel redox modulatory combination as a means of targeting redox adaptive mechanisms of therapeutic resistance in IBC (discussed in Chapter 6)

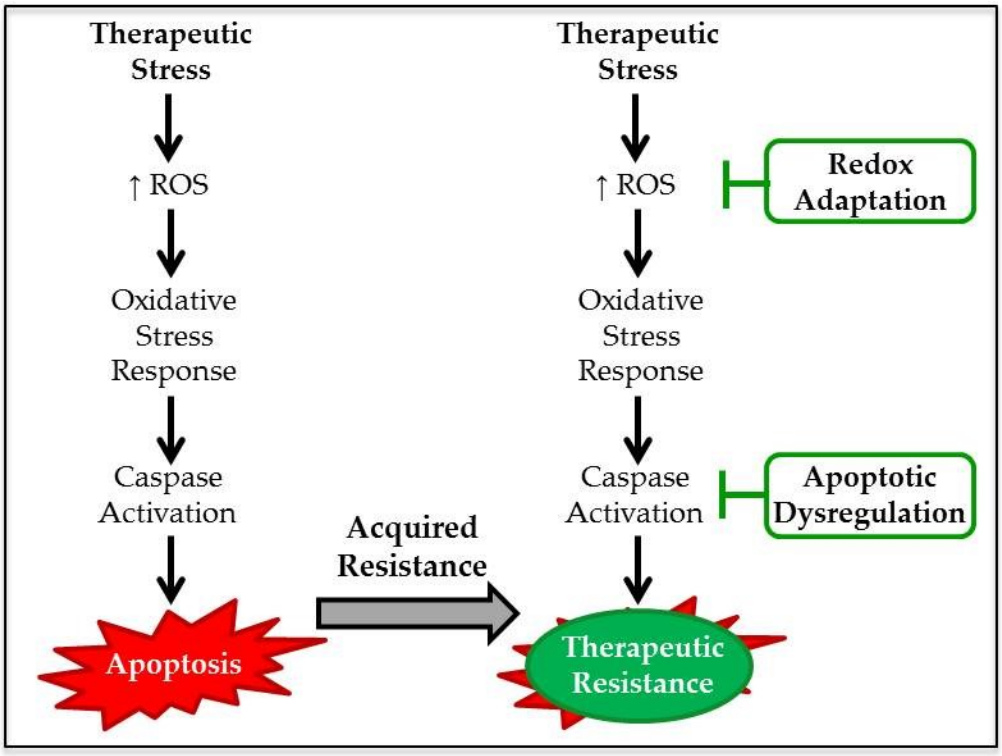

Figure 1.3: Hypothesis

We hypothesize that apoptotic dysregulation and redox adaptive mechanisms mediate the drug resistant phenotype in IBC cells.

2 Materials and Methods

2.1 Cell Culture

2.1.1 Cell lines and reagents

SUM149 and SUM190 cells were obtained from Asterand, Inc. (Detroit, MI). MDA-IBC-3 cells were provided by Wendy Woodward at MD Anderson Cancer Center [314]. SUM149 and SUM190 cells with acquired resistance to lapatinib analog GW583340 (referred to as rSUM149 and rSUM190) were selected by Dr. Katherine Aird by culturing cells in normal growth medium supplemented with increasing concentrations of GW583340 (0.25–7.5 and 0.25–2.5 μM, respectively) [114]. Initially, marked cell death and decrease in cell growth were observed in the cells. However, after 2 weeks of each increase in drug concentration, small colonies of viable cells were observed, which were cultured until confluence before the next increase in drug concentration. This was continued for a minimum of 3 months. From then on, both rSUM149 and rSUM190 cells were routinely cultured in normal media with addition of 7.5 and 2.5 μM GW583340, respectively. Stable SUM149 cells overexpressing wild-type XIAP (SUM149 wtXIAP) and SUM190 cells with XIAP knockdown via shRNA (SUM190 shXIAP) were also generated by Dr. Aird. A detailed account of their creation can be found in [114, 316].

Ham's F-12 nutrient mixture was purchased from Gibco (Carlsbad, CA). DMEM was purchased from Mediatech (Herdon, VA). Insulin, hydrocortisone, HEPES, penicillin, streptomycin, ethanolamine, transferrin, sodium selenite, and epidermal

growth factor (EGF) were all purchased from Sigma Aldrich. (St. Louis, MO). FBS was from Thermo Fisher Scientific (Hyclone Labs, Logan, UT). SUM149 cells were routinely cultured in Ham's F-12 nutrient mixture supplemented with 5 μg/mL insulin, 1 μg/mL hydrocortisone, 10 mM HEPES, 10 units/mL penicillin, 10 μg/ml streptomycin, and 5% fetal bovine serum. SUM190 cells were routinely cultured in Ham's F-12 nutrient mixture supplemented 5 μg/mL Insulin, 1 μg/mL hydrocortisone, 5 mM ethanolamine, 10 mM HEPES, 5 μg/mL transferrin, 10 nM triiodo thyronine, 50 nM sodium selenite, 10 units/mL penicillin, 10 μg/mL streptomycin and 2% fetal bovine serum. 24 h after splitting, media was changed to serum-free conditions. MDA-IBC-3 cells were cultured in Ham's F12 nutrient mixture supplemented with 10% FBS, 5 μg/mL insulin, 1 μg/mL hydrocortisone, 10 units/mL penicillin, and 10 μg/mL streptomycin.

Research-grade lapatinib analog GW583340 was obtained from Tocris Bioscience (Bristol, UK), and TRAIL was obtained from Enzo Life Sciences (Farmingdale, NY). Dimethyl sulfoxide (DMSO), embelin, paraquat, TNF-α, disulfiram (DSF), copper sulfate, bathocuproine sulfonate (BCS), and tetrathiomolybdate (TM) were obtained from Sigma Aldrich (St. Louis, MO). The SOD mimic (MnTnHex-2-PyP^{5+}) was obtained from Dr. Ines Batinic-Haberle at Duke University [317]. The Smac mimetics Birinapant and GT13402 were obtained from TetraLogic Pharmaceuticals (Malvern, PA). The MEK1/2 inhibitor U0126 was obtained from Cell Signaling Technologies (Danvers, MA). A TNF-α neutralizing antibody was purchased from R&D Systems (Minneapolis, MN),

and Q-VD-OPh pan-caspase inhibitor was purchased from Cal Biochem (Billerica, MA). All cell culture plates were acquired from Corning Incorporated (Corning, NY) unless indicated otherwise. The chemical structures for lapatinib, paraquat, Birinapant, embelin, and DSF can be found in Figure 2.1.

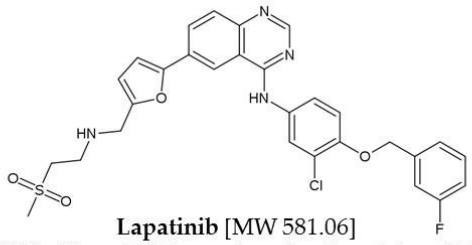

Lapatinib [MW 581.06]
(*N*-[3-chloro-4-[(3-fluorophenyl)methoxy]phenyl]-6-[5-[(2-methylsulfonylethylamino)methyl]-2-furyl] quinazolin-4-amine)

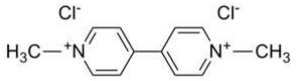

Paraquat [MW 257]
(1,1'-Dimethyl-4,4'-bipyridinium dichloride)

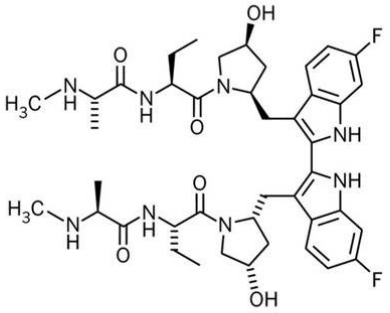

Birinapant [MW 806.94]
(2S,2'S)-*N*,*N*'-((2S,2'S)-((3S,3'S,5R,5'R)-5,5'-((6,6'-difluoro-1H,1'H-[2,2'-biindole]-3,3'-diyl)bis(methylene))bis(3-hydroxypyrrolidine-5,1-diyl))bis(1-oxobutane-2,1-diyl))bis(2-(methylamino)propanamide)

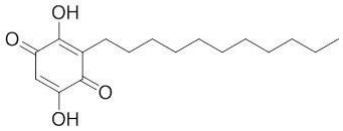

Embelin [MW 294]
(2,5-Dihydroxy-3-undecyl-1,4-benzoquinone)

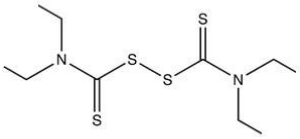

Disulfiram [MW 296.54]
(1,1',1'',1'''-[disulfanediylbis (carbonothioylnitrilo)]tetraethane)

Figure 2.1: Chemical structure of drugs used in this thesis

2.1.2 Generation of resistance reversal IBC cell line model

In order to generate the rrSUM149 cells (resistance reversal model), rSUM149 cells were transferred to regular SUM149 growth media without GW583340 lapatinib analog, and cells were maintained in GW583340-free media for an extended period (~2 months) prior to use in these studies. Cells were tested on a weekly basis for sensitivity toward GW583340 by trypan blue exclusion and 3-[4, 5-dimethylthiazol-2yl]-2, 5 diphenyl tetrazolium bromide (MTT) assay, and interrogation of previously discovered resistance-associated proteins was performed by western immunoblot.

2.1.3 shRNA-mediated knockdown of XIAP

rSUM149 cells were seeded at 30,000 cells per well into a 12 well plate and allowed to adhere overnight. After 24 h, cells were transfected with a plasmid containing XIAP-targeting shRNA using Mirus TransIT-2020 transfection reagent (Mirus Biosciences, Madison, WI) according to manufacturer's instructions. Treatments were applied 48 h post transfection for 24 h, and then cells were harvested for trypan blue exclusion assay. Effective knockdown was confirmed by western immunoblot analysis.

2.1.4 shRNA-mediated knockdown of TNFR1

SUM190 cells were seeded in 6 well plates at 150,000 cells per well and allowed to adhere overnight. After 24 h, either scramble control siRNA or TNF-α receptor 1 (TNFR1) targeting siRNA at 100 nM was applied in the presence of Dharmafect transfection reagent (Thermo Scientific, Waltham, MA). Treatments were added the day

after transfection, and cells were harvested after 24 h for trypan blue viability staining and western immunoblotting to confirm knockdown.

2.2 Determination of cell viability and proliferation

2.2.1 Trypan blue exclusion assay

Cell viability was determined by trypan blue exclusion assay. Cells were seeded in 6 well plates at 75,000 (SUM149 and derivatives) or 150,000 (SUM190 and derivatives, MDA-IBC-3) cells per well and allowed to adhere overnight. Cells were treated with the agents described for 24 h unless otherwise indicated. Then cells were trypsinized and resuspended in 1x DPBS. 10 μL of cell suspension was added to 10 μL 0.4% trypan blue, and 10 μL of the mixture was loaded onto a hemocytometer; cells were counted, and live and dead cell numbers were recorded. Percent viability was calculated as the number of live cells over the total number of cells.

2.2.2 MTT assay

Proliferation was determined via MTT (Sigma Aldrich, St. Louis, MO) assay. Cells were seeded in a 96-well plate and allowed to reach 70% confluence. Culture medium was aspirated and changed the day of treatment. After treatment with indicated agents, culture media was aspirated and MTT was added at a concentration of 5 mg/mL. Cells were incubated at 37°C until the MTT reaction caused the formation of granulated purple coloration. DMSO was added to each well, and absorbance was read at 550 nm in a BioRad plate reader (Hercules, CA).

2.2.3 High-throughput MTT assay

An automated method developed and conducted by Shalonda P. Ingram and Dr. Kevin P. Williams at North Carolina Central University was used to measure cell proliferation by MTT [318] adapted from a manual version of the assay previously described by us [319] in which cells were seeded into a 96-well plates and reagent additions were made utilizing multichannel pipettors. More details on this method can be found in Ms. Ingram's graduate thesis and in this publication [320]. For the fully automated procedure, SUM149 or SUM190 cells were seeded at a density of 800 or 1000 cells per well respectively (40 μL) in columns 3-24 of clear 384-well tissue culture plates using a Multidrop 384 (Thermo Fisher, Waltham, MA) bulk dispenser and allowed to adhere for 24 h. For quantitative high throughput screening (qHTS) drug screening studies, media alone was added to columns 1 and 2 as minimum signal controls. All subsequent aspiration and reagent addition steps were carried out using the Biomek NX workstation which was equipped with a plate stacker, bar code reader, and wash station. Intermediate dose response compound plates were generated separately and added to the cell plates, allowing dilution of compounds directly in 100% DMSO prior to adding media and avoiding potential solubility issues with carrying out serial dilutions in aqueous cell culture media. Culture medium was aspirated and the drugs from the intermediate plates added (20 μL) to the cell plate. Cells were then incubated for 72 h unless otherwise stated.

After incubation, culture media was aspirated and MTT (5 mg/mL) added to each well using the Biomek NX. Cells were incubated at 37°C for 4 h to allow formation of the colored formazan product. The reagent was aspirated using the Biomek NX and DMSO was added using the Multidrop. Plates were incubated for a further 2 h and then absorbance was read at 550 nm in a SpectraMax Plus 384 plate reader (Molecular Devices, Sunnyvale, CA).

2.2.4 TMRE flow cytometric staining

Viability and cell injury were assessed using the mitochondrial membrane potential marker tetramethylrhodamine, ethyl ester, perchlorate (TMRE). Cells were treated with the indicated concentrations for 1 h, then harvested and incubated for 30 min with 500 nM TMRE (Molecular Probes, Life Technologies, Grand Island, NY). Cells were washed twice with 1% BSA/PBS and analyzed for fluorescence by flow cytometry.

2.2.5 Clonogenic growth assay

Cells were plated in triplicate in 6 well plates at 250-500 cells/well (SUM149) or 500-1000 cells/well (SUM190) and allowed to adhere overnight. Cells were treated with the indicated agents or combinations for 24 h, after which the cells were washed twice with PBS and regular growth media was added. The cells were allowed to grow for 5-14 days, with the addition of fresh media every 4-5 days. Once colonies of at least 50 cells were observed, the cells were washed with PBS, fixed, stained with 0.4% crystal violet, then rinsed in cold water and left to dry overnight. Colonies were counted and imaged

using a ColCount (Oxford Optronix, Oxford, UK), and colonies formed per cells plated was calculated. Numbers were normalized to the untreated sample.

2.3 Determination of apoptosis

2.3.1 Annexin-V flow cytometric staining

Cells were seeded in 6 well plates at 75,000 (SUM149 and derivatives) or 150,000 (SUM190 and derivatives) cells per well and allowed to adhere overnight. Cells were treated with the indicated agents for the indicated time. Cells were harvested with 0.25% trypsin (- EDTA), washed with PBS, and resuspended in biotin-conjugated Annexin-V (Beckman Coulter, Brea, CA) for 5 min at room temperature (RT). Cells were washed again with PBS and resuspended in streptavidin-conjugated FITC (Life Technologies, Grand Island, NY) and 7-AAD (BD Pharminogen, San Jose, CA) dyes for 15 min on ice. Cells were washed and resuspended in PBS, and then at least 25,000 events were collected on a BD FACSCalibur flow cytometer. Results were analyzed using FlowJo software (Tree Star, Inc., Ashland, OR).

2.3.2 Caspase activity assay

Cells were seeded in 6 well plates, and the next day cells were treated for 4 h in regular growth media. After incubation, an equal volume of Caspase-3/7-Glo reagent (Promega, Madison, WI) was added to the wells, and plates were incubated for 30 min at RT. Luminescent signal was measured on a Veritas microplate luminometer (Turner

BioSystems, Sunnyvale, CA) with a 1 s integration time. Caspase activity was normalized to the untreated sample.

2.4 Assessment of Smac mimetics

2.4.1 Determination of Smac mimetic binding affinities by fluorescence polarization assay

Fluorescence polarization assays were conducted by Chris Benetatos and the TetraLogic Pharmeceuticals research team. The binding affinities of compounds to XIAP and cIAP1 were determined as described previously [321] using a fluorogenic substrate and are reported as K_d values. Initially, the dissociation constant (K_d) for the fluorescently labeled modified Smac peptide (AbuRPF-K(5-Fam)-NH2; FP peptide) was determined by using a fixed concentration of peptide (5 nM) and titrating varying concentrations of protein (0.075 μM – 5 μM in half log dilutions). The dose-response curves were produced by a non-linear least squares fit to a single-site binding model using GraphPad Prism (Graphpad Software, La Jolla, CA; data not shown), with 5 nM of FP peptide and 50 nM of XIAP used in the assay. Various concentrations of Smac mimetics (100 μM – 0.001 μM in half log dilutions) were added to FP peptide:protein binary complex for 15 minutes at RT in 100 μL of 0.1 M potassium phosphate buffer, pH 7.5, containing 100 mg/mL bovine γ-globulin. Following incubation, the polarization values were measured on a Perkin-Elmer Victor^{2}V multi-label plate reader using a 485 nm excitation filter and a 520 nm emission filter. IC_{50} values were determined from the plot using non-linear least squares analysis in Graphpad Prism. Calculations were based

on a maximum signal (protein BIR:FP peptide complex treated with DMSO alone) after subtraction of background.

2.4.2 TNF-α measurement of Smac mimetic-treated cells

Measurement of TNF-α was conducted by Chris Benetatos and the TetraLogic Pharmeceuticals research team. TNF-α protein levels were measured in cell culture supernatants using the BD OptEIA TNF-α ELISA kit II according to the manufacturer's instructions. Briefly, 200 μL of culture supernatants were tested in triplicate. A standard curve was generated using the manufacturer supplied standard. Absorbance was read at 450 nm on a Perkin-Elmer Victor^2 multi-label plate reader (Waltham, MA). The 570 nm background correction was subtracted from 450 nm values to yield the final results.

2.5 Western immunoblotting

Cells were harvested and immediately lysed in cell lysis buffer containing NP40 with fresh protease inhibitor cocktail (Sigma Aldrich) and 1 mM PMSF or Halt Protease/ Phosphatase Inhibitor Cocktail and 2 mM DTT (Thermo Scientific). Protein concentration was determined by the Pierce BCA Protein Assay Kit (Rockford, IL) or the Pierce 660nm Protein Assay (Thermo Scientific). Equal amounts of cell lysates were then subjected to SDS-PAGE under reducing conditions. Before loading onto the gel, all lysates were boiled for 5 min and immediately cooled on ice. The protein was transferred onto Immobilon-P PVDF membrane (Millipore, Billerica, MA) previously soaked in methanol and transfer buffer by the TRANS-BLOT SD semi-dry transfer cell

(BioRad). After the transfer process was complete, membranes were incubated with blocking buffer (5% dry nonfat milk in 1 X TBS-0.1% Tween 20) for 1 h at RT. Membranes were incubated with primary antibodies at the indicated dilution overnight at 4°C; a list of antibodies used in this dissertation can be found in Table 2.1. The next day, membranes were washed three times with wash buffer (1 X TBS-0.1% Tween 20) for 5 min each and subsequently incubated with appropriate secondary antibody conjugated with horseradish peroxidase (rabbit 1:1000, mouse 1:2000 dilution) for 1 h at RT. Membranes were again washed three times in wash buffer for 5 min each, and then bands were visualized using SuperSignal West Pico Chemiluminescent Substrate (Thermo Scientific). Signals were developed after exposure to Kodak BioMax XAR X-ray film (X-Omat films, Eastman Kodak Co., Rochester, NY). Actin or GAPDH immunodetection was conducted as a loading control. This was done by stripping the membrane in stripping buffer [100 mM 2-mercaptoethanol, 2% SDS, 62.5 mM Tris-HCl (pH 6.7)] at 50°C for 30 min followed by washing and blocking procedure as described above. Densitometric analysis was performed using the NIH ImageJ software.

Table 2.1: Antibodies used in this dissertation

Antibody	Company	Catalog #	Dilution	2° Ab	MW (kDa)
Actin	Santa Cruz	sc-1615R	1:1000	rabbit	43
AMPK	Cell Signaling	2532	1:1000	rabbit	62
Bcl-2	Santa Cruz	sc-7382	1:1000	mouse	26
c-FLIP	Cell Signaling	8510	1:1000	rabbit	55
Caspase-3	Cell Signaling	9662	1:1000	rabbit	17, 19, 35
Caspase-8	Cell Signaling	9746	1:1000	mouse	18, 43, 57
Catalase	Abcam	ab16731	1:2000	rabbit	60
cIAP1	Cell Signaling	4952	1:1000	rabbit	62
cIAP2	Cell Signaling	3130	1:1000	rabbit	70
DR4	Santa Cruz	sc-6823	1:2000	goat	56
DR5	Cell Signaling	3696	1:1000	rabbit	40, 48
eIF4G1	Cell Signaling	2469	1:1000	rabbit	220
ERK1/2 (p44/42)	Cell Signaling	9102	1:1000	rabbit	42, 44
GAPDH	Santa Cruz	sc-47724	1:2000	mouse	37
JNK	Cell Signaling	9252	1:1000	rabbit	46, 54
NF-κB (p65)	Cell Signaling	8242	1:1000	rabbit	65
PARP	Cell Signaling	9532	1:1000	rabbit	89, 116
p38	Cell Signaling	9212	1:1000	rabbit	43
p-AMPK (Thr172)	Cell Signaling	2531	1:1000	rabbit	62
p-ERK1/2 (Thr202/Thr204)	Cell Signaling	9101	1:1000	rabbit	42,44
p-JNK (Thr183, Tyr185)	Cell Signaling	9251	1:1000	rabbit	46, 54
p- NF-κB (Ser536)	Cell Signaling	3031	1:1000	rabbit	65
p-p38 (Thr180, Tyr182)	Cell Signaling	9211	1:1000	rabbit	43
Smac/DIABLO	Cell Signaling	2954	1:1000	mouse	21
SOD1	Cell Signaling	2770	1:1000	rabbit	18
SOD2	BD Biosciences	611580	1:1000	mouse	25
Survivin	Cell Signaling	2808	1:1000	rabbit	16
TNFR1	Cell Signaling	3736	1:1000	rabbit	55
XIAP	BD Biosciences	610762	1:2000	mouse	57

2.6 Measurement of intracellular reactive oxygen species

Cells were cultured in 6-well plates in regular growth media until reaching 70–80% confluence and then treated for 24 h. Cells were harvested and incubated for 30 min with 10 μM dyes to detect ROS. 2',7'-dichlorodihydrofluorescein diacetate (H_2DCFDA), dihydroethidium (DHE), and MitoSOX Red (Molecular Probes, Carlsbad, CA) were used to detect hydrogen peroxide-derived radicals, cytoplasmic superoxides, and mitochondrial superoxides respectively. Cells were washed twice with 1% BSA/PBS and analyzed for fluorescence by flow cytometry. At least 25,000 events were collected on a FACScalibur flow cytometer (Beckton Dickinson, Rockville, MD) and analyzed using FlowJo software (Tree Star, Inc., Ashland, OR). For DHE and H_2DCFDA staining, high fluorescence was calculated by setting a gate on the control cells where the peak reached a minimum, and all experimental samples were compared to this control gate. For MitoSOX Red staining, fold induction of ROS was calculated relative to the untreated sample.

2.7 Measurement of antioxidant capacity and signaling

2.7.1 Measurement of reduced glutathione

Reduced glutathione levels were assessed using the GSH-Glo™ Glutathione Assay (Promega, Madison, WI) as per the manufacturer's instructions. Briefly, 3 μg total cell lysates were incubated at RT for 30 min with 50 μL of prepared GSH-Glo™ Reagent 2X. Then, 100 μL of reconstituted Luciferin Detection Reagent was added, plates were

mixed and incubated at RT for 15 min, and luminescence was read using a Veritas 96-well luminometer with a 1 s integration time.

2.7.2 Measurement of Nrf2 activity

Cells were seeded at 4,000 cells/well in a white 96 well plate (Greiner Bio-One, Monroe, NC) and allowed to adhere overnight. Cells were then transfected with pGL4.37 (ARE firefly luciferase reporter, Promega) and pGL4.75 (Renilla luciferase control, Promega) plasmids using a 3:1 ratio of XTremeGene HP (Roche Applied Science) transfection reagent to DNA. The next day cells were treated for 24 h, after which an equal volume of Dual-Glo reagent (Promega) was added to the cells and firefly luminescence was read on a Veritas microplate luminometer. Then an equal volume of Dual-Glo Stop & Glo reagent (Promega) was added to the cells, and Renilla luminescence was read. Firefly luminescence was normalized to Renilla luminescence to account for differences in transfection efficiency or viability, and this value was normalized to the untreated sample.

2.8 Copper assays

2.8.1 Complementation of Ctr1/Ctr3-deficient yeast cells with copper ionophores

SEY6210 (wildtype for Ctr1/3) [322] and Ctr1/Ctr3 deletion mutant MPY17 [323, 324] *Saccharomyces cerevisiae* cells were grown in YPEG media (3% ethanol, 3% glycerol, 1% yeast extract, 2% Bacto Peptone, 2% agar) with or without the addition of known copper ionophore zinc pyrithione (ZPT) [325] or DSF at 0-50 μM. Cells were allowed to

grow at 30°C for 3 days, after which absorbance at 600nm was measured on a Spectramax Plus 384 plate reader (Molecular Devices) as an indicator of growth.

2.8.2 Measurement of intracellular copper

SUM149 and rSUM149 cells were treated with DSF, copper, or DSF-Cu for 24 h, and lysates were prepared as described in Section 2.5. Lysates were analyzed for copper content using a Thermo Scientific Element2 inductively coupled plasma high resolution mass spectrometer (ICP-HRMS) at the W.M. Keck Elemental Geochemistry Laboratory (University of Michigan, Ann Arbor, MI) by Ted Huston, and copper content of the lysis buffer was subtracted from each sample. Values were normalized to protein concentration for reporting as ng Cu/mg protein.

2.9 Assessment of anchorage-independent growth potential

Cells were plated in 6 well plates at 75,000 (SUM149 and derivatives) or 150,000 (SUM190 and derivatives) cells/well and allowed to adhere overnight. Treatments were applied for 24 h, after which cells were harvested and counted with trypan blue viability stain. A base layer of 0.7% agarose in regular growth medium was poured into wells of a 12 well plate and allowed to solidify at 4°C. Then 12,500 cells/well from each treatment were plated in triplicate in 0.45% agarose in regular growth medium on top of the base layer and allowed to solidify at 4°C. Plates were then transferred to a 37°C incubator with 5% CO_2 and allowed to grow for 14 to 21 days. Once visible colonies had formed, they were counted under a microscope, and colony counts were normalized to the

untreated sample. Images of representative fields were taken with 5x magnification using a Zeiss Axio Observer A1 microscope (Thornwood, NY), Hamamatsu Orca ER digital camera (Bridgewater, NJ), and MetaMorph software (Molecular Devices).

2.10 Examination of intracellular ALDH activity

The ALDEFLUOR kit (Stem Cell Technologies, Durham, NC) was used to identify cells with high aldehyde dehydrogenase (ALDH) enzymatic activity according to the manufacturer's instructions. Briefly, SUM149 cells were suspended in ALDEFLUOR assay buffer containing ALDH substrate (1 μM, 1×10^6 cells) and incubated for 35 minutes at 37°C. For each treatment, a sample of cells was incubated with 50 mM of the specific ALDH inhibitor diethylaminobenzaldehyde (DEAB) as negative control. Flow cytometric analysis was conducted using a FACSCalibur flow cytometer (Beckton Dickinson, Franklin Lakes, NJ) and analyzed using Cellquest (Beckton Dickinson). ALDEFLUOR fluorescence was excited at 488 nm, and fluorescence emission was detected using a standard fluorescein isothiocyanate (FITC) 530/30 band pass filter. The sorting gates were established using the 7-AAD stained cells for viability and the ALDEFLUOR-stained cells treated with DEAB as negative controls. Dot plots from a representative experiment are shown with mean ± SEM from a total of four experiments.

2.11 Analysis of drug interactions

Analysis of drug interactions was performed using Calcusyn software (Biosoft, Cambridge, UK), which uses the Chou-Talalay method [326] where a combination index (CI) <1 indicates synergism.

2.12 Statistical analysis

Statistical analyses were performed using Graphpad InStat (Graphpad Software, Inc., La Jolla, CA) and the Student's two-tailed t-test. Differences were considered significant at $p<0.05$.

3 Development and characterization of a model to investigate the reversibility of acquired therapeutic resistance in IBC

3.1 Introduction

Despite the improvements gained from multidisciplinary management and anthracycline- and taxane-based polychemotherapy regimens [327], women with IBC continue to have worse survival outcomes than those with LABC [328]. There is no standard IBC-specific treatment for patients with advanced disease, and enrollment in clinical trials has been strongly recommended [3]. Patients with IBC of the TN subtype are consistently associated with the worst outcomes [15]. Since endocrine and Her2-targeting therapies are ineffective in TN IBC, EGFR inhibitors such as gefitinib and erlotinib and an anti-EGFR antibody (cetuximab) are in clinical trials; however, recent results from the cetuximab trials have been disappointing in EGFR-overexpressing TNBC patients [329].

For IBC tumors with ErbB1/EGFR of ErbB2/Her2 overexpression, ErbB1/2 targeting agents including the Her2-targeting antibody trastuzumab and the dual ErbB1/2 tyrosine kinase inhibitor lapatinib are approved for treatment. Although the CR rate of patients receiving lapatinib monotherapy has been remarkable (50% CR rate in ErbB2-overexpressing IBC patients) [79], a significant number of patients are unresponsive to lapatinib, and acquired resistance is frequent [81, 330].

A major unmet clinical challenge in IBC that affects patients regardless of subtype is the rapid development of chemo- and radiotherapy resistance [287]. Efficacy of many therapeutics is largely influenced by induction of ROS, which induce cell death in response to therapy [253]. Previous identification of IBC cells with acquired therapeutic resistance to lapatinib revealed adaptation to oxidative stress induced by lapatinib, resulting in insignificant ROS accumulation [78]; this inhibits apoptosis and enhances cancer cell survival. The therapy-resistant IBC cells overexpress XIAP [114], which is correlated with redox adaptation in these models, with increased expression of the antioxidants SOD1/2 and GSH leading to enhanced ROS detoxification [78].

Few profiling studies have looked specifically at linking tumor cell drug responses to drug resistance. In this study, a qHTS approach was employed to profile the NCI Developmental Therapeutics Program (NCI-DTP) Approved Oncology Drug Set II in an IBC model established from a patient tumor [312] and its isogenic derivatives. To obtain pharmacological information from the screening data, compounds were screened at multiple concentrations. The study's primary objective was to determine whether the development of resistance to lapatinib has any effect on sensitivity to other chemo- and targeted drugs. Secondly, we investigated whether removal of lapatinib as a selective pressure from rSUM149 would impact sensitivity to lapatinib and other anti-cancer agents. Therefore, efficacy of the NCI-DTP Approved Oncology Drug Set II was characterized in parental SUM149; rSUM149, an isogenic

derived line from SUM149 wherein a clonal population of cells was selected for acquired resistance to lapatinib [114]; and an isogenic derivative generated by removal of lapatinib from rSUM149 for an extended period of time (rrSUM149, resistance reversal model). Lapatinib sensitivity and resistance was confirmed for each cell line in the qHTS MTT format (Fig. 3.1). Analysis of the parental and isogenic-derived IBC cell lines provides a unique model system through which we can enhance our understanding of acquired therapeutic resistance and the effects of redox adaptation on anti-cancer drug efficacy.

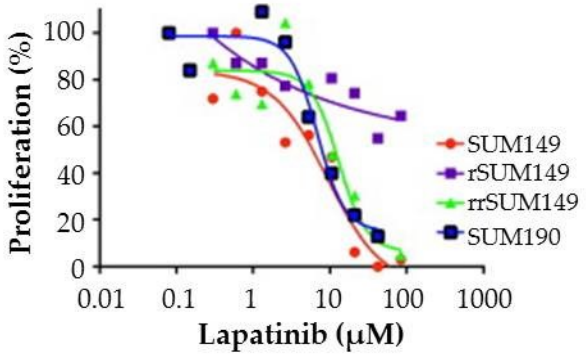

Figure 3.1: Validation of qHTS and isogenic-derived IBC cell line models

Representative qHTS dose response curves for lapatinib in SUM190, SUM149, and isogenic-derived rSUM149 and rrSUM149 cell lines.

3.2 Lapatinib-resistant rSUM149 cells are cross-resistant to multiple chemo- and targeted therapies

A qHTS strategy developed by Shalonda M. Ingram and Kevin P. Williams at North Carolina Central University was used generate representative heat map profiles of proliferation in response to the complete 89 drug set, screened in dose response, in the SUM149 cells. Proliferation data was normalized to in-plate controls in order to generate a heat map for each drug response (Fig. 3.2A). Drugs were grouped in the heat map based on their mechanism of action. Analysis of the qHTS data identified potent drugs that consistently demonstrated IC_{50} values <15 μM for inhibition of proliferation in SUM149 (Table 3.1). In addition to lapatinib, the most efficacious drugs included anti-metabolites, anti-neoplastic antibiotics, anthracyclines, tyrosine kinase inhibitors, an HDAC inhibitor, and a proteasome inhibitor. Alkylating agents (Fig. 3.2A, group 6) and platinum compounds (group 8) were generally ineffective in SUM149. Gemcitabine, the vinca alkaloids, and mTOR inhibitors rapamycin and everolimus demonstrated modest micromolar activity but were not amongst the top 15 drugs in SUM149 cells (Fig. 3.2A, Table 3.1). A number of approaches were undertaken to confirm the top 15 anti-cancer drugs identified from the primary qHTS; these are detailed in [320].

Table 3.1: IC_{50} values for the 15 most efficacious drugs in the SUM149 cell line from the NCI-DTP library

Drug	qHTS MTT IC_{50} (μM)	Drug Class
Dactinomycin	<0.02	Anti-neoplastic antibiotic
Plicamycin	<0.02	Anti-neoplastic antibiotic
Bortezomib	<0.02	Proteosome inhibitor
Doxorubicin	<0.02	Anthracycline
Daunorubicin	<0.02	Anthracycline
Fludarabine	2.1 ± 1.1	Anti-metabolite
Mitoxantrone	2.5 ± 0.6	Anti-neoplastic antibiotic
Sorafenib	4.5 ± 0.4	Kinase inhibitor
Sunitinib	5.0 ± 0.8	Kinase inhibitor
Gefitinib	6.2 ± 2.3	Kinase inhibitor
Vorinostat	8.9 ± 4.9	HDAC inhibitor
Lapatinib	9.0 ± 0.3	Kinase inhibitor
Mitomycin	9.1 ± 0.4	Anti-neoplastic antibiotic
Bleomycin	13.8 ± 2.0	Anti-neoplastic antibiotic
Capecitabine	15.0 ± 9.5	Anti-metabolite

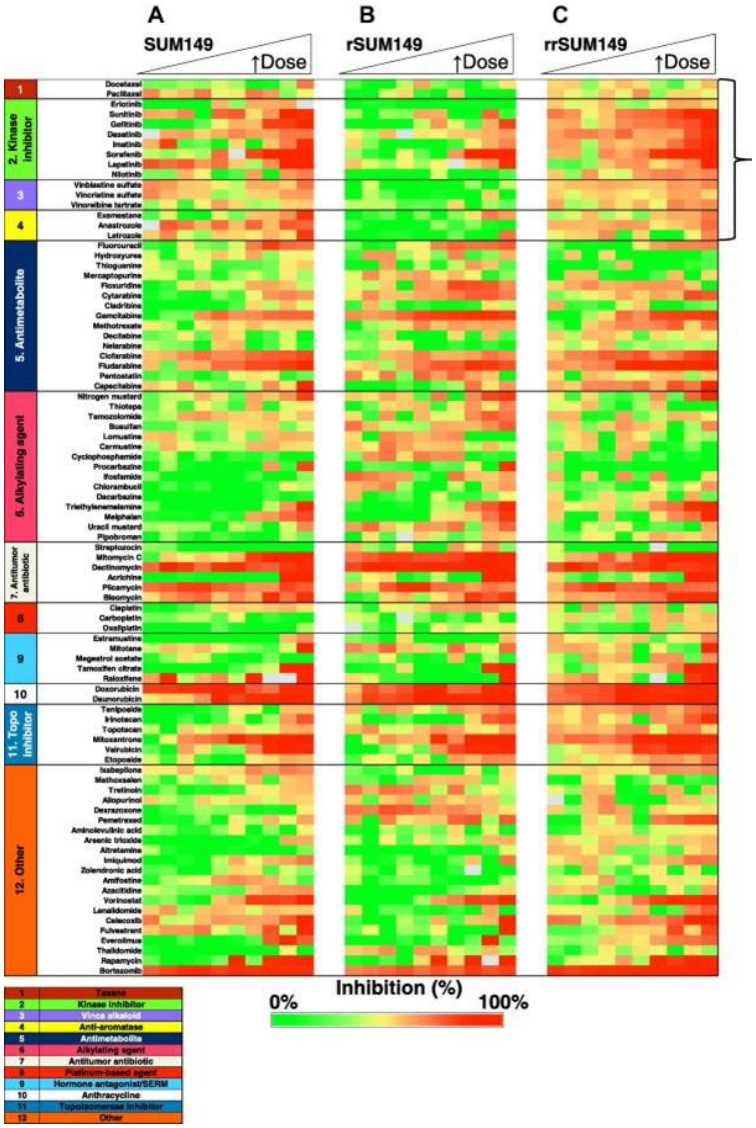

Figure 3.2: Comparative efficacy profiling of the NCI-DTP 89 oncology drug set in parental SUM149 and isogenic-derived rSUM149 and rrSUM149 cell lines

Heat map profile for proliferation inhibitory effects of the NCI approved oncology set in SUM149 (A), rSUM149 (B) and rrSUM149 (C) cells. Cells were incubated with drugs in a 10-point two-fold dilution series dose curve for 72 h; cell proliferation assessed by qHTS MTT assay. Each row represents dose response data for a single drug. Percent inhibition values were calculated for each concentration and data normalized to vehicle and no cell controls. The heat map key indicates red for 100% inhibition to green for 0% inhibition. Outlier values are shown as grey. Drugs are listed on the vertical axis and grouped for drug class. A representative experiment is shown. Each cell line was profiled for a minimum of two independent screens.

Next, responses to the drugs which were identified as most potent in SUM149 were profiled in the resistant rSUM149 cells; heat maps for dose effects in this cell line can be found in Figure 3.2B. Doxorubicin, bortezomib, dactinomycin, plicamycin and daunorubicin, which were previously identified as inhibiting proliferation in SUM149 cells at all concentrations tested, were equally effective in the rSUM149 cells, with IC_{50}s of <0.2 μM. In addition to those drugs, fludarabine and vorinostat were highly potent in the acquired resistance model as well as in the parental line (Fig. 3.2, Table 3.2).

Table 3.2: IC_{50} values for drugs most efficacious in SUM149 cells for the three isogenic-derived IBC models*

Drug	Mechanism of Action	Primary IC_{50} ± SD (μM)		
		SUM149	***rSUM149***	***rrSUM149***
Fludarabine	Anti-metabolite	2.1 ± 1.1	1.7 ± 0.8	1.4 ± 0.9
Mitoxantrone	Anti-neoplastic antibiotic	2.5 ± 0.6	11.4 ± 1.3	3.8 ± 3.4
Sorafenib	Kinase inhibitor	4.5 ± 0.4	14.6 ± 3.1	7.8 ± 1.6
Sunitinib	Kinase inhibitor	5.0 ± 0.8	>25	7.05 ± 6.3
Gefitinib	Kinase inhibitor	6.2 ± 2.3	>50	2.8
Lapatinib	Kinase inhibitor	9.0 ± 0.3	>50	9.1
Vorinostat	HDAC inhibitor	8.9 ± 4.9	6.2 ± 0.6	2.75 ± 2.1
Mitomycin	Anti-neoplastic	9.1 ± 0.4	18.5 ± 0.8	6.2 ± 0.4
Bleomycin	Anti-neoplastic antibiotic	13.8 ± 2.0	>50	9.5
Capecitabine	Anti-metabolite	15.0 ± 9.5	>50	26 ± 1.4

*Doxorubicin, bortezomib, dactinomycin, plicamycin, and daunorubicin all had IC_{50} values of >0.2 μM in all three isogenic cell lines.

Compared to the parental SUM149 cells, the lapatinib-resistant rSUM149 cells exhibited cross-resistance to multiple targeted- and chemo-therapeutic agents amongst the 15 most potent drugs identified in SUM149, as well as other lower potency drugs. Cross-resistance generally applied to drugs from four of the classes (highlighted by a bracket in Fig. 3.2) including the taxanes (Fig. 3.2B, group 1), a subset of the kinase inhibitors (group 2), vinca alkaloids (group 3), and aromatase inhibitors (group 4). A shift in the IC_{50} values from the parental to resistant SUM149 cells was observed for several of the drugs tested. From the initial top 15 drugs that were efficacious in the parental SUM149 cells, the tyrosine kinase inhibitors, capecitabine, mitomycin, mitoxantrone, and bleomycin were characterized by a dramatic reduction in potency in rSUM149, in addition to previously published lapatinib resistance (Table 3.2, Fig. 3.2B). IC_{50}s for some of the most potent drugs in SUM149 (white bars) and their comparative efficacy in rSUM149 (black bars) is displayed graphically in Figure 3.3.

3.3 Reversal of resistance to lapatinib resensitizes rrSUM149 cells to a number of agents to which rSUM149 is insensitive

We then sought to profile the entire drug panel in the resistance reversal (rrSUM149) cell line model. rrSUM149 is a unique isogenic cell line which was generated through the removal of lapatinib from rSUM149 culture conditions for a period of >2 months, which allowed for outgrowth of a population of cells which were resensitized to lapatinib treatment. A comparative heat map profile for all 89 drugs in parental SUM149 and its two isogenic derived cell lines rSUM149 and rrSUM149 is shown in Fig. 3.2A-C.

Doxorubicin, bortezomib, dactinomycin, plicamycin, and daunorubicin, which inhibited proliferation in SUM149 and rSUM149 cells at all concentrations tested, were highly efficacious in the rrSUM149 cells. Table 3.2 details other drugs from the top 15 identified from the NCI-DTP oncology set in SUM149 cells and the corresponding IC_{50} values in the rSUM149 and rrSUM149 cells; IC_{50} data is represented graphically for a selection of the top compounds in SUM149 for SUM149 (white bars), rSUM149 (black bars), and rrSUM149 (gray bars) in Figure 3.3. Interestingly, data in Table 3.2 and Figures 3.2 and 3.3 indicate that the rrSUM149 cells regained sensitivity and potency comparable to the parental SUM149 cells not only in response to lapatinib, but also upon treatment with other targeted- and chemotherapeutic agents in the top 15 panel, indicating cross-resensitization.

Thus, comparative efficacy profiling of the approved oncology drug set in SUM149 parental and isogenic derived models of acquired resistance and re-sensitization demonstrates that lapatinib-resistant IBC cells are cross-resistant to multiple oncology drugs, while resensitization to lapatinib is accompanied by increased sensitivity to other therapeutic agents.

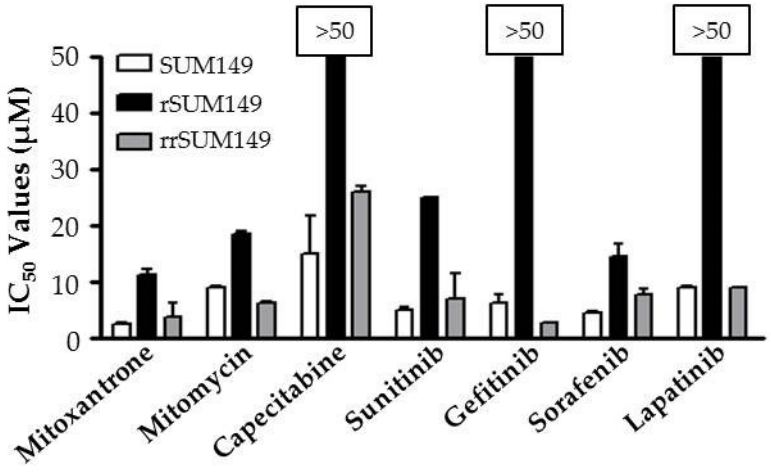

Figure 3.3: Comparative IC_{50} values for drugs displaying cross-resistance and cross-resensitization in SUM149 and isogenic-derived rSUM149 and rrSUM149 cell line models

Mean and SD values based on a minimum of three independent qHTS MTT experiments. IC_{50} values determined with GraphPad Prism 5.0.

3.4 Mechanism of resistance reversal: the rrSUM149 model behaves similarly to parental SUM149 cells in response to oxidative stress

To further characterize the resistance reversal model and understand the mechanisms behind their cross-resensitization, the rrSUM149 cells were compared to rSUM149 and SUM149 cells using several important factors associated with acquired resistance in the rSUM149 model [78, 114]. Measurement of ROS (cytoplasmic superoxides and hydrogen peroxide-derived radicals) at two distinct time points during the generation of the resistance reversal model showed that after one month of growth in GW583340 (research grade lapatinib analog)-free media, at which time the cells were still resistant to lapatinib-induced cell death, the rrSUM149 cells (Fig. 3.4A and 3.4B, gray bars- One) remained insensitive to the induction of ROS accumulation by lapatinib; their response is consistent with the rSUM149 cells (Fig. 3.4A and 3.4B, black bars) which are constantly growing in lapatinib. However, after two months of growth in lapatinib-free media, at which time the cells were resensitized to lapatinib, the rrSUM149 cells (Fig. 3.4A and 3.4B, gray bars- Two) regained the ability to accumulate ROS, showing levels comparable to the parental SUM149 cells in response to challenge with lapatinib.

We previously showed that SUM149 cells treated with lapatinib exhibit increased phosphorylation of AMPK, which serves as a marker of oxidative stress, but that rSUM149 cells, which are maintained in media with lapatinib, do not show an increase in p-AMPK; this indicates a partial loss of stress responsive signaling to lapatinib [78].

Thus, the phosphorylation status of AMPK in the resistant reversal cell line rrSUM149 following lapatinib treatment was examined. Following one month of growth in lapatinib-free media, at which time the cells maintained resistance to lapatinib, the cells showed only a very minimal increase in p-AMPK levels upon treatment with lapatinib (Fig. 3.4C, One). However, after a period of two months of growth in lapatinib-free media, treatment of rrSUM149 cells with lapatinib induced approximately a two-fold increase in AMPK phosphorylation, indicating that the cells are experiencing significant oxidative stress (Fig. 3.4C, Two).

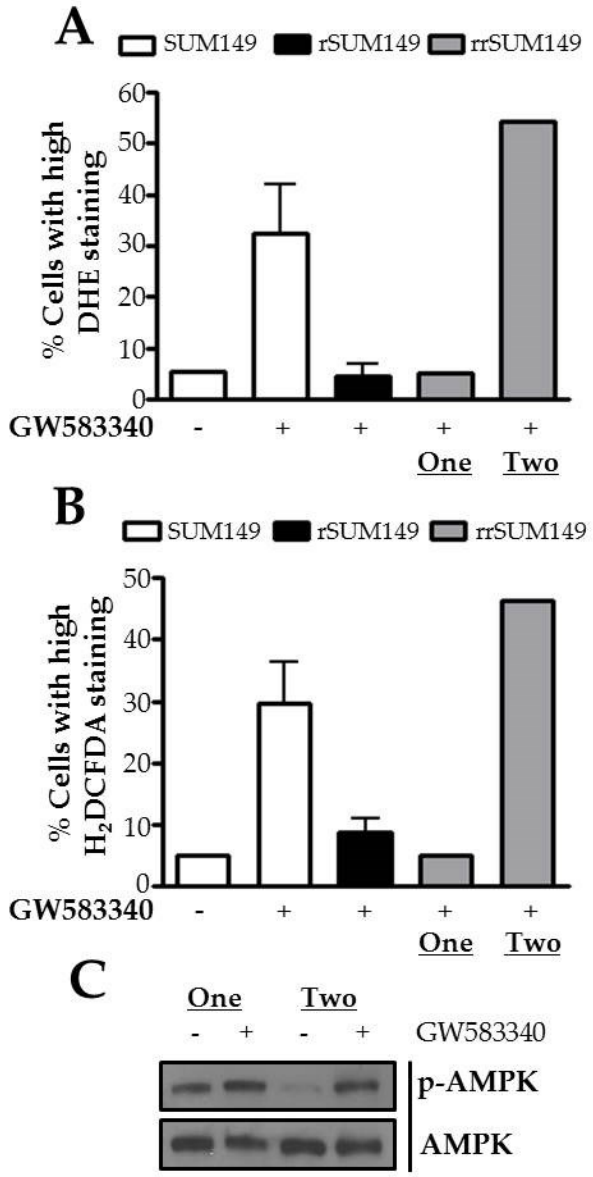

Figure 3.4: Resistance reversal in the rrSUM149 cell line is associated with enhanced ROS accumulation and activation of the AMPK stress response

(A) Cytoplasmic superoxides and (B) H_2O_2-derived radicals as measured by flow cytometric staining with DHE and H_2DCFDA in parental SUM149 cells (white bars) untreated and treated with 7.5 μM lapatinib, rSUM149 cells (black bars) growing in 7.5 μM lapatinib, and rrSUM149 cells following removal of drug for one or two months (gray bars) treated with 7.5 μM lapatinib. (C) Western immunoblot analysis of AMPK expression and phosphorylation in rrSUM149 cells treated with 7.5 μM lapatinib following one or two months of growth in lapatinib-free media.

3.5 Resistance reversal rrSUM149 cells have reduced expression of anti-apoptotic and antioxidant molecules compared to rSUM149 cells

Acquired resistance in the rSUM149 model was previously correlated with upregulation of XIAP expression relative to the parental SUM149 cells [331]. To further investigate the mechanisms that mediate the reversal of resistance in rrSUM149 cells, the levels of XIAP and several other anti-apoptotic proteins, as well as Smac/DIABLO, a negative regulator of XIAP, were examined in the panel of SUM149, rSUM149, and rrSUM149 cells. Data in Fig. 3.5A show that, consistent with previous results, XIAP expression was upregulated approximately two-fold in rSUM149, and interestingly, XIAP expression in the rrSUM149 cells was significantly reduced compared to rSUM149 to levels comparable with the parental SUM149 cells. In addition, cIAP1 and Bcl-2 were both increased to some degree in rSUM149 cells, a further indication of their high degree of apoptotic dysregulation. While cIAP2 and survivin levels were unchanged in rSUM149 cells compared to SUM149, there was a decrease in all anti-apoptotic proteins that were examined in the rrSUM149 cells; expression either returned to parental SUM149 levels or in some cases was even lower (cIAP1/2, survivin). Levels of the IAP inhibitor Smac/DIABLO were unchanged across the panel of cell lines.

As there is a significant difference in ROS accumulating abilities across the cell lines (Fig. 3.4A and 3.4B) and because increased antioxidant expression in the rSUM149 cell line has been observed [332], the expression of SOD2 and catalase, two important

intracellular antioxidants was examined. Catalase expression did not show any significant changes across the cell lines (Fig. 3.5B). In contrast, SOD2 was significantly upregulated in the rSUM149 cells as observed previously, and expression was markedly reduced in the rrSUM149 resistance reversal model (Fig. 3.5B).

Together, these data indicate that rrSUM149 cells are more susceptible to ROS-mediated cell death than the rSUM149 cells due to reduced expression of anti-apoptotic and antioxidant proteins.

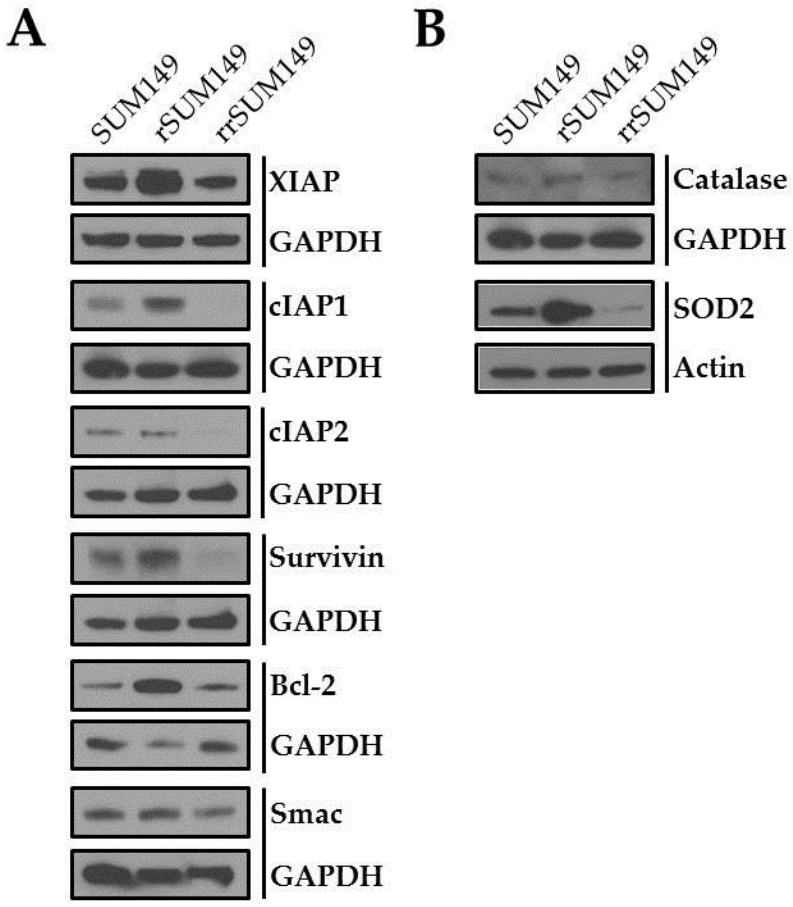

Figure 3.5: The resistance reversal rrSUM149 cell line model is characterized by downregulation of anti-apoptotic proteins and reduced antioxidant capacity

(A) Western immunoblot analysis of basal anti-apoptotic proteins XIAP, cIAP1, cIAP2, survivin, Bcl-2, and Smac expression in untreated SUM149, rSUM149, and rrSUM149 cells. GAPDH was used as a loading control. (B) Western immunoblot analysis of basal catalase and SOD2 expression in untreated SUM149, rSUM149, and rrSUM149 cells. GAPDH and β-actin were used as loading controls.

3.6 Discussion

IBC is characterized by rapid progression from onset of disease, therefore early and aggressive multimodal therapy is essential to improve patient outcomes. IBC tumors are frequently either EGFR/ErbB1- or ErbB2/Her2-positive, and clinical strategies using trastuzumab and lapatinib have yielded some success; however, intrinsic and acquired resistance to these agents is a significant challenge. Adding to these barriers to successful treatment, there is paucity of IBC cellular models in which to study the molecular basis for the disease and potential therapeutic regimens. In the present study, we have characterized a novel isogenic-derived model of disease progression to drug resistance and subsequent resistance reversal. A set of IBC cell lines (SUM149, rSUM149, and rrSUM149) representing the basal subtype was profiled in a qHTS format in order to identify drugs from the NCI-DTP 89 approved oncology drug library that can potently inhibit IBC cell proliferation.

High throughput profiling and screening have utilized a range of different endpoints including cytotoxicity, viability [333], survival [334], growth inhibition [335], and proliferation [336]. In this study, the MTT cell proliferation assay was chosen as the basis for qHTS screening due to its ease of automation, widespread use, and economical cost per well. Using this approach, a subset of drugs exhibiting efficacy in these cell line models was rapidly identified and confirmed.

As a result of our profiling efforts, we have identified several drug classes including anti-metabolites, anti-neoplastic antibiotics, anthracyclines, and a subset of tyrosine kinase inhibitors as displaying potency in the SUM149 cell line, a well-established model of basal type, EGFR-activated IBC [337-341]. In addition, a subset of the drugs tested was highly potent even in the acquired lapatinib resistance model rSUM149. These agents include dactinomycin, plicamycin, bortezomib, doxorubicin, daunorubucin, fludarabine and vorinostat. However, while certain drugs remained efficacious in the resistant cell line model, the rSUM149 cells were cross-resistant to a number of drugs which were previously found to be efficacious in the parental cells, including some tyrosine kinase inhibitors (sorafenib, sunitinib, and gefitinib), capecitabine, mitoxantrone, mitomycin, and bleomycin. The results of oncology drug profiling in parental and resistant SUM149 cells indicates a mechanism of lapatinib-induced acquired resistance that promotes cross-resistance to other tyrosine kinase inhibitors as well as a subset of drugs that target DNA synthesis and repair.

The present study shows that removal of lapatinib, the primary drug against which resistance was developed in rSUM149 cells, for an extended period led to development of a population of cells (rrSUM149) that are resensitized to multiple drugs in addition to lapatinib (sorafenib, sunitinib, gefitinib, capecitabine, mitoxantrone, mitomycin, and bleomycin; Fig. 3.2 and 3.3, Table 3.2), behaving in a manner similar to the parental SUM149 cells. Resensitization was associated with a decrease in expression

of anti-apoptotic proteins including XIAP, cIAP1, cIAP2, survivin, and Bcl-2 (Fig. 3.5A) as well as the antioxidant SOD2 (Fig. 3.5B) and increased capacity for ROS accumulation (Fig. 3.4A and 3.4B).

In addition, the rrSUM149 cells regained the ability to activate AMPK, a cellular metabolic regulator that also acts as a sensor for oxidative stress [342], in response to lapatinib exposure (Fig. 3.4C). Thus, the mechanistic phenotype of redox adaptation in the rSUM149 cells (Fig. 3.6) supports the observation of cross-resistance to multiple drugs, which also occurs commonly in patients; further, decreased expression of survival factors and antioxidant mechanisms restored ROS accumulating capabilities in the rrSUM149 cell line, leading to resensitization of the cells to a wide variety of treatments (Fig. 3.6).

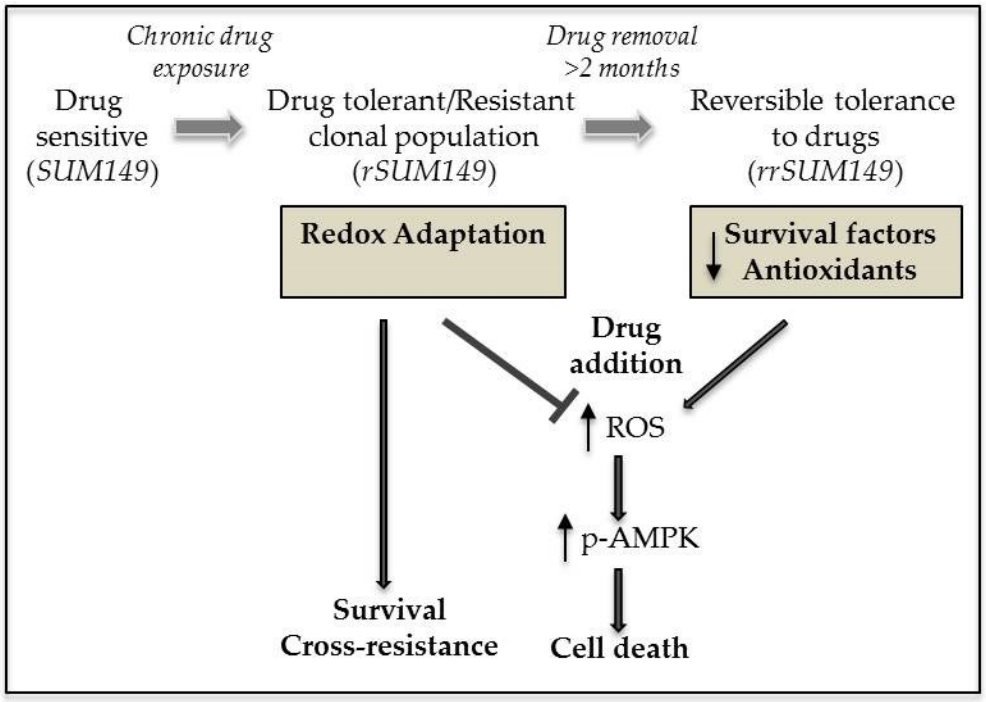

Figure 3.6: Schematic representation of drug sensitivity and tolerance in isogenic SUM149-derived IBC models

Cancer cells have inherently high levels of ROS due to oncogenic signals and altered metabolism compared to normal cells. Presence of therapeutic insults/cellular stress can cause further increase in ROS, which in the absence of adaptive mechanism is associated with drug sensitivity and induction of cell death (SUM149). However, chronic stress leads to redox adaptive mechanisms such as increases in survival factors and antioxidants/ROS scavenging systems. These cells can suppress therapy-mediated ROS induction and/or rapidly clear ROS, which selects for a phenotypically distinct drug tolerant subpopulation of cells (rSUM149) that are drug tolerant due to their ROS protective mechanisms and contributes to multidrug resistance. Drug tolerance in this population of cells can be reversed by removal of the therapeutic stress for an extended period; loss of their redox adaptive mechanisms renders the resistant reversal cells (rrSUM149) highly therapy-sensitive.

From these studies, it appears that mechanisms involving the activation of pro-survival pathways and redox adaption contribute to the observed therapeutic resistance to lapatinib and cross-resistance to other drugs. The reversibility of this resistance to a re-sensitized state after removal of drug is intriguing mechanistically. In a recent study, the existence of a drug-tolerant sub-population of cells (persisters) termed DTPs has been proposed based on observations of acquired drug resistance [343]. The theory suggests that within a heterogeneous population of cells, there exists a subpopulation of reversibly drug tolerant cells that are dormant until dosed with high concentrations of drugs, at which time a subset of DTPs that is able to tolerate growing in the presence of drug gives rise to drug-tolerant expanded persisters (DTEPs) [343]. There is some evidence that these drug tolerant clones exist *de novo* and may share some properties with cancer stem cells [343]. This DTEP population may be analogous to the rSUM149 cells in our isogenic model. Indeed, SUM149 cells show significant ALDH positivity [344-346], a characteristic that is associated with cancer stem cells, and thus may also contain a subpopulation of DTPs. Hence, it may be possible to eliminate the emergence of drug tolerant cells from the SUM149 isogenic model by treatment of the parental cells with lapatinib in combination with drugs that target the adaptive mechanisms described here. These results emphasize the central roles that apoptotic dysregulation and redox adaptation play in therapeutic resistance not only to lapatinib, but to a wide range of anti-tumoral agents. Thus, the potential therapeutic targets identified in previous studies

[78, 114] are confirmed by their loss in the resistance reversal model, strengthening the need for novel strategies to relieve apoptotic dysregulation and modulate cellular redox to prevent and overcome drug resistance in IBC.

In conclusion, we report the first description of drug efficacy profiles in isogenic-derived IBC cells with differential sensitivity phenotypes by screening approved drugs that can act as potent inhibitors of IBC cell proliferation. These experiments have the potential to identify potent anti-tumoral combinations and facilitate their inclusion in clinical trials immediately. Our findings in combination with the currently available database of IBC gene signatures facilitate a significant step toward improved treatment protocols for patients with IBC and support the idea that anti-apoptotic mechanisms and redox adaptation are potential targets for therapeutic intervention that merit further investigation as a means of enhancing therapeutic apoptosis and overcoming resistance in IBC.

4 Targeting IAPs with Smac mimetics with differential IAP specificity

4.1 Introduction

Acquired therapeutic resistance due to tumor cell adaptation to persistent stress is an unmet challenge in IBC [3]. We have identified XIAP overexpression via post-transcriptional mechanisms as a dominant feature of apoptotic dysregulation involved in acquired resistance to the ErbB1/2 tyroskine kinase inhibitor lapatinib, which is associated with cross-resistance to other anti-cancer drugs [114, 320]. The importance of this resistance mechanism is supported by other studies that have shown consistent differences in phenotype at the molecular level between IBC and locally advanced non-IBC tumors, where IBC is characterized by a hyperproliferative state and apoptotic dysregulation [46, 78, 81, 103, 114, 222-224, 347-349]. Further studies revealed upregulation of many anti-apoptotic factors in addition to XIAP in the rSUM149 model of therapeutic resistance, including cIAP1, cIAP2, survivin, and Bcl-2. Expression of these factors was also reduced in a model of resistance reversal (rrSUM149), indicating their importance in maintaining the drug resistant phenotype [320]. Thus, the development of novel therapeutic strategies targeting the anti-apoptotic axis is highly relevant in IBC.

The IAPs are a highly conserved family of endogenous apoptosis inhibitors that have been shown to inhibit apoptosis induced by both extrinsic and intrinsic stimuli; their BIR domains are important for anti-apoptotic function and mediate interactions with other

proteins. cIAP1 and cIAP2, which were originally identified as components of the TNF-α receptor (TNFR) complex, are increasingly recognized as modulators of diverse extrinsic signals. By regulating the ubiquitination states of key substrates via their *C*-terminal RING E3 ligae domains, they promote survival signaling. XIAP, in addition to having a *C*-terminal RING domain, is a direct caspase inhibitor which can bind to activated caspases-3, -7, and -9, inhibiting their proteolytic activity [350].

While XIAP is not a classical oncogene, it has been detected at elevated levels in tumors resistant to chemotherapy and is associated with poor outcome in many cancers [215, 319, 351, 352]. Currently, two approaches have been taken in the development of clinical XIAP inhibitors: anti-sense oligonucleotides that reduce XIAP expression, and small molecule inhibitors that antagonize XIAP's caspase inhibitory function. These molecules are currently being evaluated in preclinical and clinical Phase 1/2 studies [353, 354]. One class of XIAP inhibitors under development is the Smac mimetics, which are modeled after the AVPI tetrapeptide IAP binding motif (IBM) of the endogenous IAP inhibitor Smac/DIABLO [355]. Smac/DIABLO is one of the main antagonists of IAPs through its ability to bind the BIR3 region of IAP proteins via its *N*-terminal AVPI tetrapeptide. XIAP overexpression can inhibit the release of endogenous Smac from the mitochondria, highlighting its importance in the apoptotic process [356]. Recently, Smac/DIABLO expression was assessed in 62 breast cancer patient specimens by flow cytometry and found to correlate inversely with tumor stage [357].

Smac mimetics are potent pro-apoptotic agents, with mechanisms that include: 1. steric hindrance and/or competitive occlusion of the XIAP caspase binding sites; 2. degradation of XIAP; 3. induction of TNF-α-mediated cell death (the predominant mechanism of many of the Smac mimetics is recognized as being TNF-α dependent [358, 359]); and 4. inhibition and degradation of other IAP family members. Multiple IAP targeting is important due to the fact that in many cases when XIAP is inhibited, other IAPs suppress apoptosis by compensatory mechanisms [358, 360-363]. Because Smac is known to act as a dimer, bivalent Smac mimetics were introduced with the idea that they would be more efficacious than their monovalent counterparts; this has since been demonstrated to be true. Currently, Smac mimetics including bivalent Birinapant (formerly TL32711) are in clinical trials [364]. While only a subset of tumor cell lines is sensitive to single agent Smac mimetic treatment, their combination with different therapeutic agents has been shown to increase the potency of those agents [137, 365-369].

In this study, the effects of Smac mimetics as single agents and in combination with TRAIL were examined. TRAIL is classical apoptosis-inducing ligand whose binding to DR4 and DR5 on the cell surface results in receptor aggregation, recruitment of FADD, DISC formation, and activation of caspase-8, leading to apoptosis [370]. Since TRAIL induces tumor cell death via the extrinsic pathway, the status of intracellular sensors such as p53 is less relevant, making it attractive as an anti-cancer agent [371]. While TRAIL is a promising therapeutic due to its cancer cell specificity and low toxicity

to normal tissue [372], there is a considerable amount of intrinsic resistance to TRAIL, and acquired resistance is common after repeated exposure [373]. Mechanisms of resistance include: downregulation of death receptors; constitutive activation of Akt and/or NF-κB; overexpression of cFLIP; mutations in the *Bax* and *Bak* genes; overexpression of anti-apoptotic proteins including the Bcl-2 family and IAPs; and defects in the release of mitochondrial proteins [373-377]. Agents that sensitize cells to TRAIL-induced apoptosis are attractive candidates for combination cancer therapy; thus, IAP-targeting with Smac mimetics is a promising strategy to sensitize resistant cells to TRAIL.

4.2 IAP binding affinity of novel bivalent Smac mimetics

A fluorescence polarization assay was used to determine the dissociation constants (K_d) of Smac mimetics Birinapant and GT13402 for XIAP and cIAP1 by monitoring the decrease in fluorescence polarization signal due to competitive displacement of an FP peptide from the BIR3/FP peptide binary complex. Both Smac mimetic compounds induced a dose-dependent decrease in the fluorescence signal; the K_d of Birinapant for XIAP and cIAP1 were determined to be 45 nM and <1nM respectively (Table 4.1). In contrast, GT13402 has lower affinity for XIAP, with a K_d close to 1 μM, but similar affinity for cIAP1 (K_d <1 nM).

Table 4.1: Binding constants (K_d) of Smac mimetics for IAPs as determined by fluorescence polarization assay

Compound	XIAP K_d (nM)	cIAP1 K_d (nM)
Birinapant	45	<1
GT13402	997	<1

4.3 Smac mimetics enhance TRAIL potency in TRAIL-sensitive SUM149 IBC cells

The basal-type IBC cell line SUM149 has been observed to be TRAIL-sensitive [378, 379], which was supported by data in Figure 4.1A displaying a dose-dependent decrease in viability following TRAIL treatment (0-100 ng/mL). Characterization of the Smac mimetic compounds as single agents in SUM149 cells revealed that neither Birinapant nor GT13402 induced cell death as measured by trypan blue exclusion assay, even at the highest concentrations tested (1000 nM Birinapant, 10,000 nM GT13402- Fig. 4.1A). However, combinations of TRAIL (10-50 ng/mL) and Birinapant (0-1000 nM) enhanced TRAIL potency in SUM149 cells, with a statistically significant ~25% reduction in viability achieved with as low as 25 ng/mL TRAIL + 30 nM Birinapant (Fig. 4.1B). GT13402, which has low affinity for XIAP compared to Birinapant, did not significantly enhance TRAIL potency, even at the highest concentration tested (10,000 nM, Fig. 4.1B).

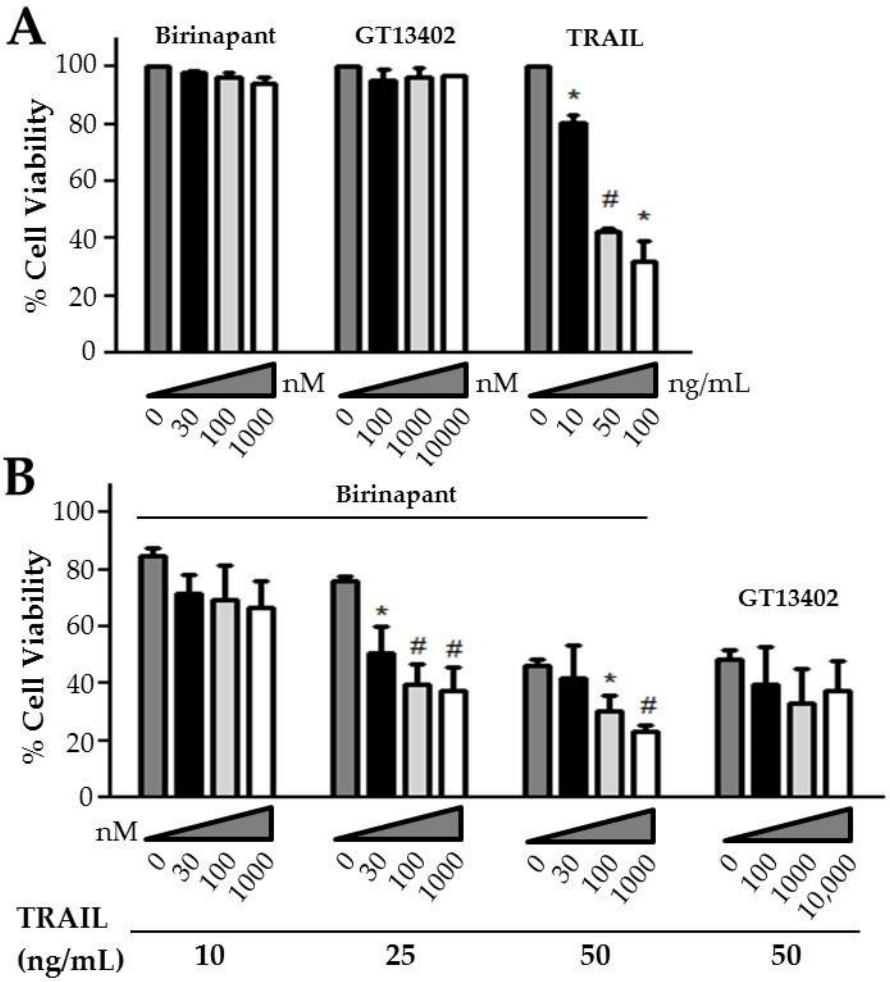

Figure 4.1: Smac mimetics enhance TRAIL-induced cell death in SUM149 cells

A, Viability as determined by trypan blue exclusion assay of SUM149 cells treated with Birinapant (0-1000 nM), GT13402 (0-10,000 nM), and TRAIL (0-100 ng mL^{-1}) alone. Bars represent mean±SEM viable cells taken as a percentage of total cells (n=2-3; **P*<0.05, #*P*<0.005, all comparisons made to untreated). **B**, Viability as determined by trypan blue exclusion assay of SUM149 cells treated with TRAIL (10-50 ng mL^{-1}) alone or in combination with Birinapant (0-1000 nM) or GT13402 (0-10,000 nM). Bars represent mean±SEM viable cells taken as a percentage of total cells (n=3-5; **P*<0.05, #*P*<0.005, all comparisons made between TRAIL+Smac mimetic and same concentration of TRAIL alone).

Birinapant as a single agent caused significant degradation of cIAP1 and 2, which was not enhanced by addition of TRAIL (Fig. 4.2A). While a slight decrease in XIAP expression can be seen following TRAIL treatment, no significant decrease in XIAP was observed following combinatorial treatments (Fig. 4.2A). However, Birinapant+TRAIL-treated cells showed increased levels of active caspases-8 and -3, as well as poly-ADP ribose polymerase (PARP) cleavage, over single agents within 4 h of treatment, indicative of apoptosis-mediated cell death (Fig. 4.2A). Annexin-V/7-AAD flow cytometric staining further confirmed the mechanism of death to be apoptosis, with a dose-dependent increase in cells staining positive for Annexin-V (white+gray bar) from approximately 30% with TRAIL alone to 50-55% following treatment with TRAIL+ Birinapant after 12 h (Fig. 4.2B).

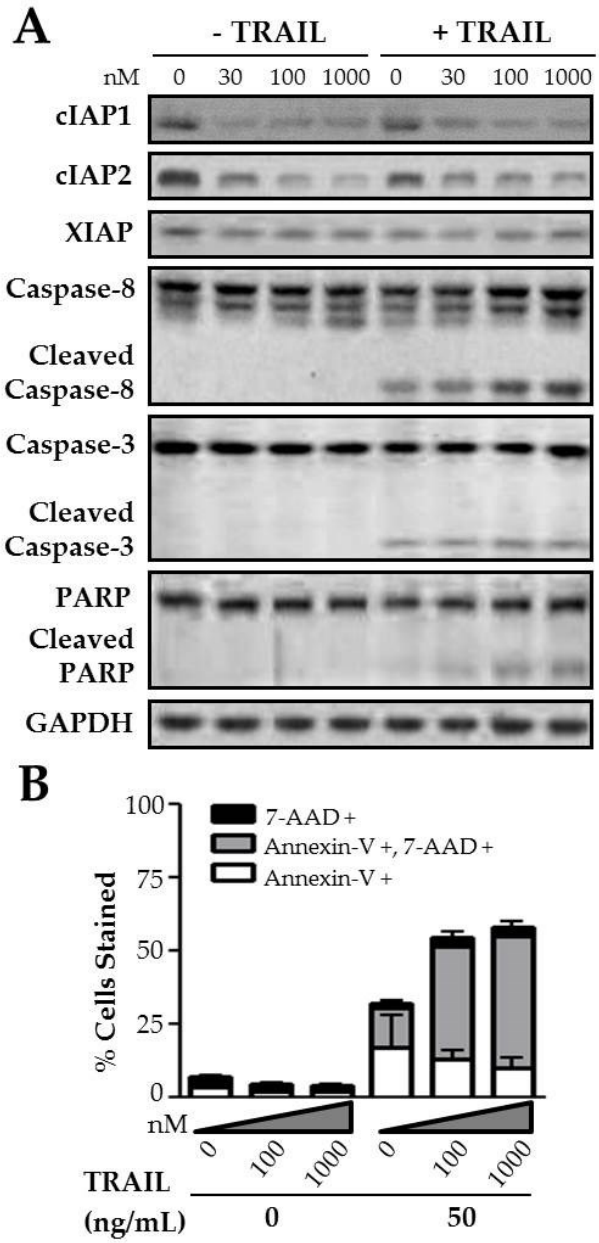

Figure 4.2: Birinapant reduces cIAP1/2 expression and induces caspase cleavage to enhance TRAIL-mediated apoptosis in SUM149 cells

A, Western immunoblot analysis of cIAP1, cIAP2, XIAP, caspase-3, caspase-8 and PARP expression in SUM149 cells treated with Birinapant (0-1000 nM) ± TRAIL (50 ng/mL). GAPDH was used as a loading control. **B**, Annexin-V/7-AAD flow cytometric staining of SUM149 cells treated with Birinapant (0-1000 nM) ± TRAIL (50 ng/mL) (n=2).

Because XIAP overexpression has been identified as a critical factor in TRAIL resistance [319, 376, 380], we wanted to delineate the role of XIAP expression in sensitivity to Smac mimetics. To do this, we characterized both Birinapant and GT13402, which have differential affinity for XIAP, in SUM149 wtXIAP, a SUM149-derived isogenic cell line with stable exogenous XIAP overexpression [114]. Data in Figure 4.3 show that Birinapant was more effective in increasing TRAIL potency than GT13402 in SUM149 wtXIAP. This reveals the IAP specificity of the Smac mimetics and the importance of targeting XIAP along with cIAP1 and 2 in this model. Neither Birinapant nor GT13402 affected viability of SUM149 wtXIAP cells as a single agent (data not shown).

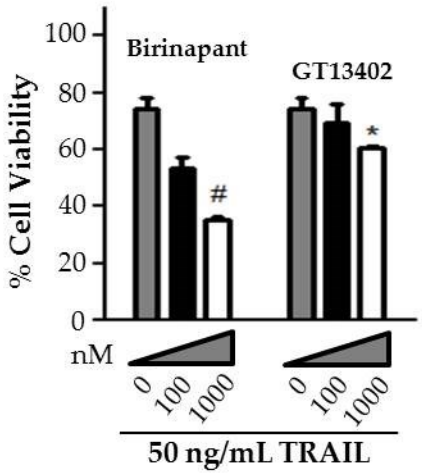

Figure 4.3: Birinapant is more effective than GT13402 at sensitizing SUM149 wtXIAP cells to TRAIL-mediated cell death

Viability as determined by trypan blue exclusion assay of SUM149 wtXIAP cells treated with TRAIL (50 ng/mL) and Birinapant or GT13402 (0-1000 nM). Bars represent mean±SEM viable cells taken as a percentage of total cells (n=2-3; *P<0.05, #P<0.005, all comparisons made to untreated).

4.4 Smac mimetics induce apoptosis as single agents in TRAIL-resistant SUM190 cells

In order to evaluate the efficacy of the Smac mimetics in a TRAIL-resistant cell line, we characterized Birinapant and GT13402 in SUM190, a cell line isolated from a patient IBC tumor with ErbB2-overexpression and insignificant DR4 expression (a factor that can contribute to TRAIL resistance) as shown in Figure 4.4A. SUM190 cells were only moderately sensitized to TRAIL (Fig. 4.4C) when XIAP was stably downregulated using an XIAP-targeting shRNA lentiviral construct (SUM190 shXIAP, Fig. 4.4B).

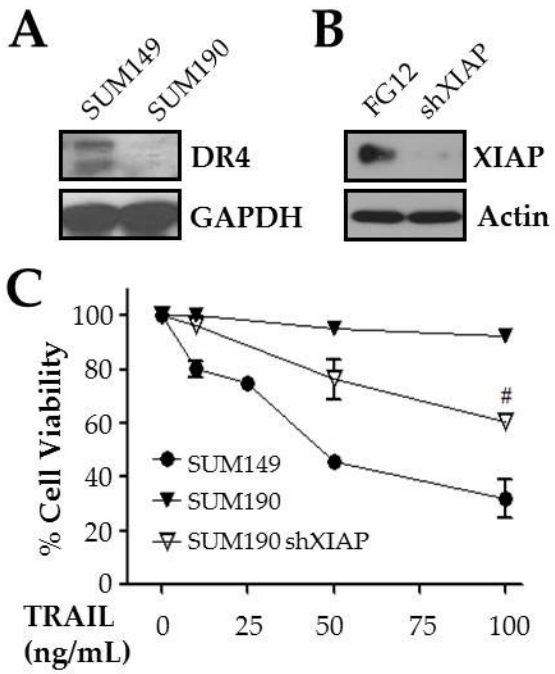

Figure 4.4: TRAIL resistance in SUM190 is mediated in part by XIAP

A, Western immunoblot analysis showing TRAIL receptor DR4 expression in SUM190 and SUM149 cells. GAPDH was used as a loading control. **B**, XIAP expression in SUM190 FG12 vector control and SUM190 shXIAP cells. Actin was used as a loading control. **C**, Viability as determined by trypan blue exclusion assay of SUM149, SUM190 and SUM190 shXIAP after treatment with TRAIL (0-100 ng/mL) at 24 h. Data represent mean±SEM viable cells taken as a percentage of total cells (n=3-5; #P<0.005, all comparisons made between SUM190 and SUM190 shXIAP at the same concentration of TRAIL).

In contrast, Birinapant, which targets cIAP1, cIAP2, and XIAP with high affinity, significantly decreased the viability of SUM190 cells in a dose-dependent manner. Data in Figure 4.5A show approximately 50% cell death at 300 nM as measured by trypan blue exclusion assay. The requirement of pan-IAP antagonism is supported by the observations: 1. Treatment with GT13402 (lower affinity for XIAP) also reduces SUM190 cell viability as a single agent (Fig. 4.5A); 2. Birinapant (high affinity for cIAP1/2 and XIAP) is more potent (20% viability at 1000 nM) than GT13402 (60% viability at 1000 nM) in this assay (Fig. 4.5A); 3. Birinapant treatment in the XIAP knockdown cell line (SUM190 shXIAP, Fig. 4.5B) caused an overall reduction in viability at lower doses (30-300 nM) compared to the parental SUM190 cells at the corresponding doses; 4. The difference in potency between the two compounds with differential affinity for XIAP was attenuated in the XIAP-knock down cell line (Fig. 4.5B).

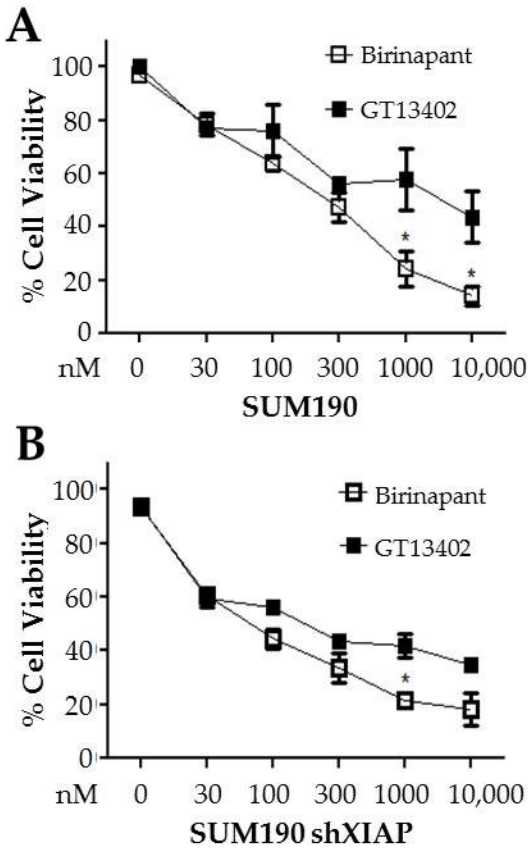

Figure 4.5: Smac mimetics induce death as single agents in SUM190 cells, and Birinapant is more efficacious than GT13402 due to its high affinity for XIAP

A, SUM190 cell viability as determined by trypan blue exclusion assay when treated with Birinapant or GT13402 (0-10,000 nM). **B**, Viability of SUM190 shXIAP cells as determined by trypan blue exclusion assay treated with Birinapant or GT13402 (0-10,000 nM). Data represent mean±SEM viable cells taken as a percentage of total cells (n=3-5; **P*<0.05, all comparisons made between Birinapant and GT13402 at the same concentration).

To confirm apoptotic cell death with Birinapant treatment, immunoblot analysis was conducted, and data in Figure 4.6A show a significant decrease in cIAP1 levels and enhanced PARP cleavage. However, no decrease in XIAP expression or change in JNK phosphorylation levels was observed (Fig. 4.6A). In addition, Annexin-V/7-AAD staining by flow cytometric analysis was carried out at 12 h. Data in Figure 4.6B show an increase in Annexin-V positive cells (white+gray bar) with no change in 7-AAD single positive cells (black bar), further supporting an apoptotic mechanism of cell death.

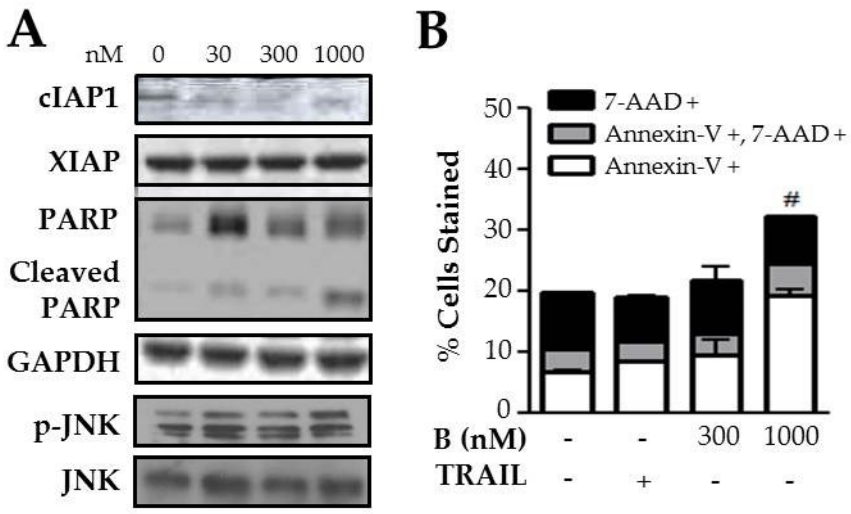

Figure 4.6: Birinapant induces apoptosis as a single agent in SUM190 cells

A, Western immunoblot analysis of cIAP1, XIAP, and PARP expression, and JNK phosphorylation status in SUM190 cells treated with Birinapant (0-1000 nM) for 4 h. GAPDH and total JNK were used as loading controls. **B**, Annexin-V/7-AAD flow cytometric staining of SUM190 cells treated with Birinapant (B; 0-1000 nM) or TRAIL (100 ng/mL) (n=2; #P<0.005; all comparisons made to the untreated sample based on total Annexin-V staining).

Because pro-survival NF-κB signaling can interfere with cell death, we conducted a time course study to evaluate its activation post-Birinapant treatment. Data in Figure 4.7 show that there is an initial increase in p-NF-κB at 4 h with no change in total protein levels. However, at 8-12 h time points, a time-dependent decrease in both total and phosphorylated NF-κB is observed. By 24 h, expression of both total and phosphorylated protein returns to untreated levels. Thus, NF-κB-mediated protection from cell death is unlikely, and Smac mimetics are effective as single agents in the SUM190 IBC cellular model.

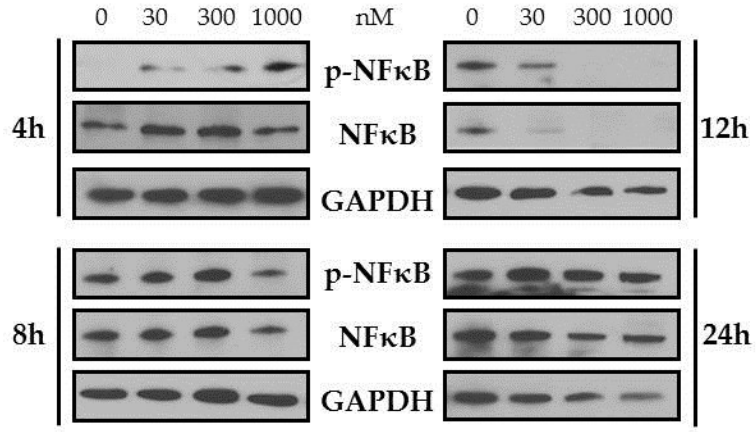

Figure 4.7: Birinapant does not activate NF-κB signaling

Western immunoblot analysis of total NF-κB and phosphorylation status in SUM190 cells treated with Birinapant (0-1000 nM) for 4, 8, 12, or 24 h, as indicated. GAPDH was used as a loading control.

4.5 Smac mimetics inhibit clonogenic growth capacity in combination with TRAIL and as single agents

To determine the effect of Smac mimetics on the growth characteristics of IBC cells, clonogenic growth potential was assessed. Data in Figure 4.8A show that in TRAIL-sensitive SUM149 cells, Birinapant+TRAIL significantly reduces clonogenic potential even at lower doses (40% decrease in colony formation at 30 nM Birinapant + 10 ng/mL TRAIL compared to 10 ng/mL TRAIL). Representative images show the decrease in colonies formed with Birinapant+TRAIL vs. TRAIL alone. Further, Birinapant was more potent than GT13402 in increasing TRAIL efficacy, with only 8% colony formation efficiency at 100 nM Birinapant + 50 ng/mL TRAIL, compared to 32% with 100 nM GT13402 + 50 ng/mL TRAIL (Fig. 4.8B). Similar to our results from the trypan blue exclusion assay in Figure 4.1A, neither Birinapant nor GT13402 caused any change in SUM149 colony formation as single agents (data not shown).

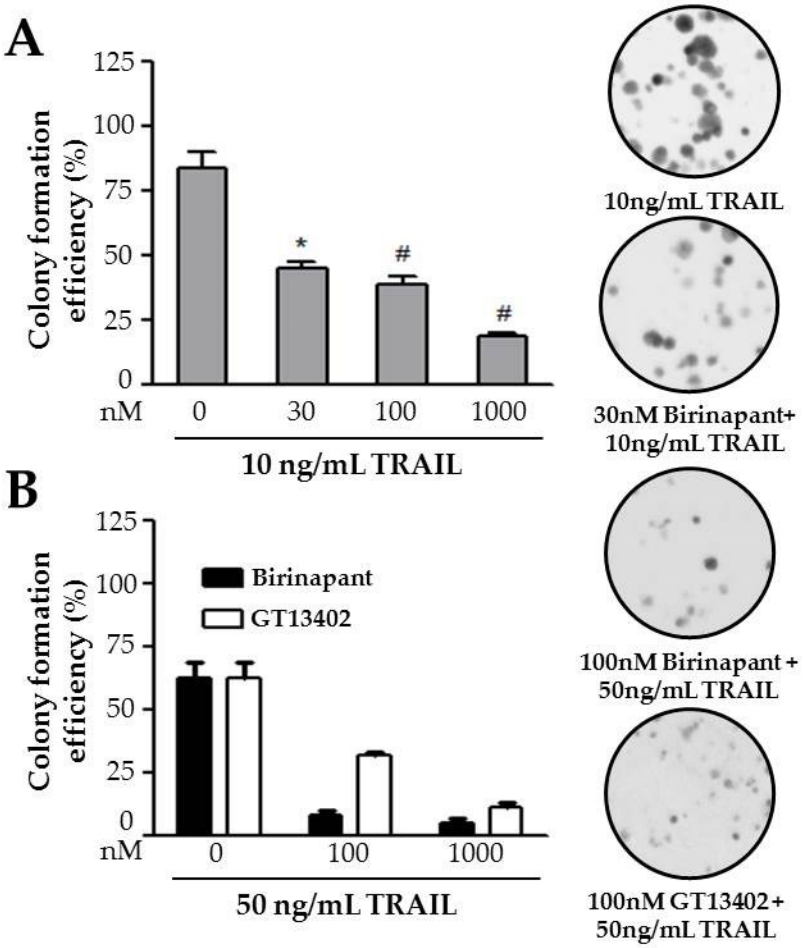

Figure 4.8: Smac mimetics inhibit clonogenic growth potential in combination with TRAIL in SUM149 cells

A, Clonogenic growth assay in SUM149 cells treated with TRAIL (10 ng/mL) alone or in combination with Birinapant (0-1000 nM). Bars represent mean±SEM colonies formed/cells plated as a percentage of the untreated sample. Representative images are shown on the right. **B**, Clonogenic growth assay in SUM149 cells treated with TRAIL (50 ng/mL) alone or in combination with Birinapant or GT13402 (0-1000 nM). Bars represent mean±SEM colonies formed/cells plated as a percentage of the untreated sample. Representative images are shown on the right.

Unlike in SUM149 cells, both Smac mimetics were similarly effective at inhibiting the clonogenic growth potential of TRAIL-resistant SUM190 as single agents (Fig. 4.9). Representative images show a decrease in SUM190 colony formation following treatment with Birinapant and GT13402.

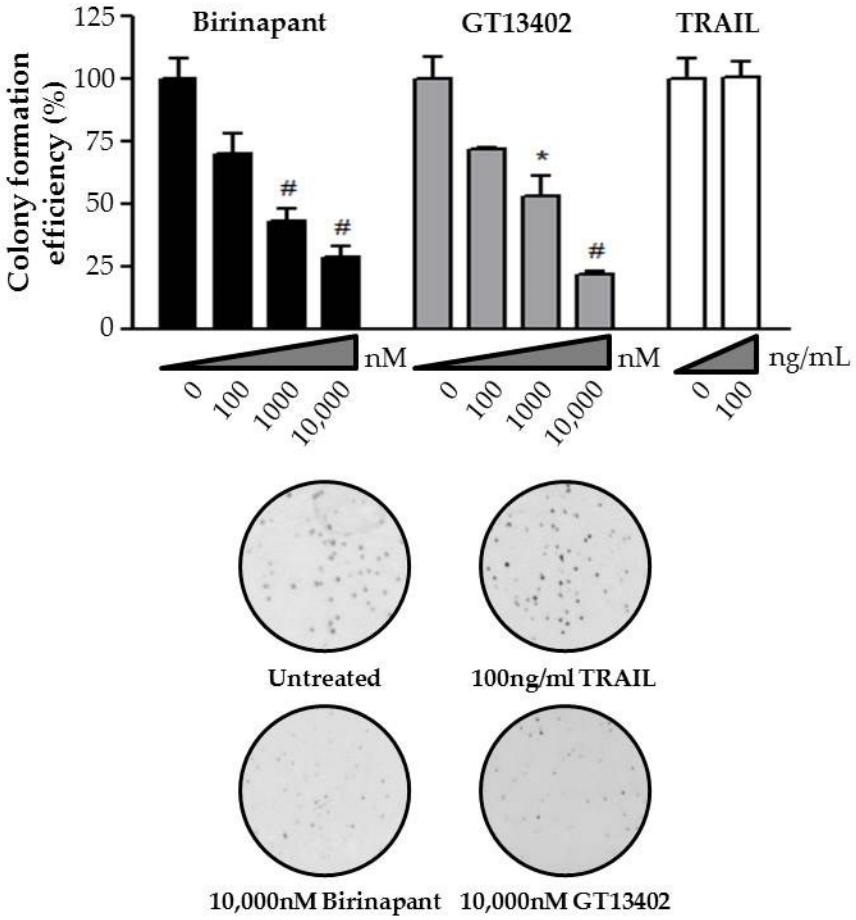

Figure 4.9: Smac mimetics inhibit clonogenic growth potential as single agents in SUM190 cells

Clonogenic growth assay in SUM190 cells treated with Birinapant, GT13402 (0-10,000 nM) or TRAIL (0-100 ng/mL). Bars represent mean±SEM colonies formed/cells plated as a percentage of the untreated sample (*P<0.05, #P<0.005; all comparisons made to the untreated sample). Representative images are shown below.

4.6 Smac mimetics inhibit anchorage-independent growth potential in combination with TRAIL and as a single agent

Anchorage-independent colony formation in soft agar has been widely used as an *in vitro* model to assess cancer cell tumorigenic potential and is considered to be a reasonably good predictor of *in vivo* activity [381, 382]. Data in Figure 4.10A reveal that Birinapant+TRAIL (black bar) causes a 55% reduction in the number of colonies formed while TRAIL alone (white bar) causes a 20% decrease relative to untreated. Representative images of colonies formed in soft agar show similar sized colonies in all treatment groups but a significant reduction in colony number of the Birinapant+TRAIL combination. Analysis of AIG in SUM190 cells revealed a dose-dependent decrease in AIG following treatment with Birinapant (100-10,000 nM, Fig. 4.10B). Data show a significant ~50% decrease in the number of colonies formed with 100 nM Birinapant treatment relative to untreated (Fig. 4.10B). Representative images of colonies formed in soft agar show a reduction in colony number with increasing dose of Birinapant.

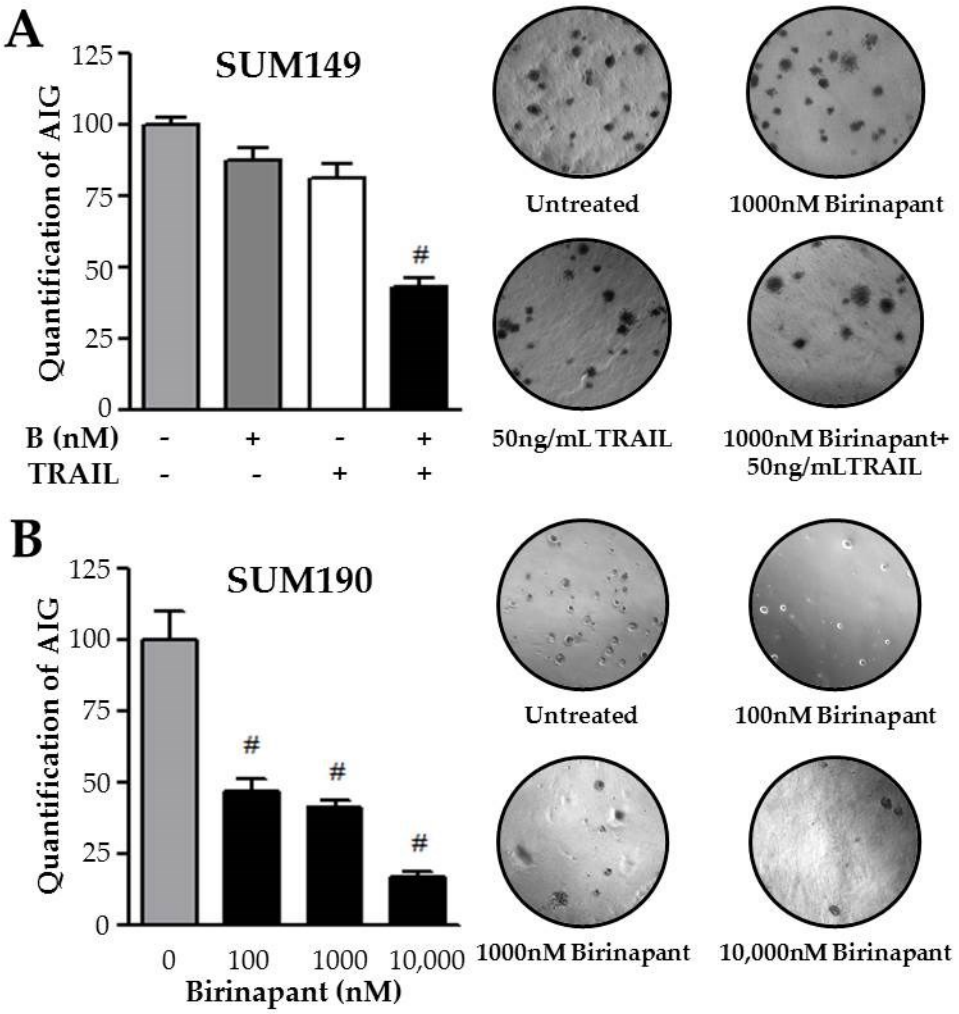

Figure 4.10: Birinapant inhibits anchorage-independent growth in combination with TRAIL and as a single agent in SUM149 and SUM190 cells respectively

A, Anchorage-independent growth assay in SUM149 cells treated with TRAIL (50 ng/mL), Birinapant (1000 nM), or the combination. Bars represent mean±SEM colonies formed in soft agar as a percentage of the untreated sample (#*P*<0.005; comparisons made to TRAIL alone). Representative images are shown on the right. **B**, Anchorage-independent growth assay of SUM190 cells treated with Birinapant (0-10,000 nM). Bars represent mean±SEM colonies formed in soft agar as a percentage of the untreated sample (#P<0.005; all comparisons made to the untreated sample). Representative images are shown on the right.

4.7 Smac mimetic efficacy in SUM149 and SUM190 cells is TNF-α-independent and caspase-dependent

Studies were then conducted to evaluate whether TNF-α influences Smac mimetic efficacy in IBC cellular models. Since Smac mimetics, in addition to binding IAPs, have been shown to induce TNF-α production in sensitive cells, we measured TNF-α levels in the conditioned media of Birinapant-treated SUM149 and SUM190 cells by ELISA. Data in Figure 4.11A reveal insignificant TNF-α secretion in SUM149; SUM190 cells, which are sensitive to Smac mimetics as single agents, produce autocrine TNF-α in a dose-dependent fashion in response to Birinapant treatment, although it should be noted that the levels were in the low picogram/mL range. Addition of exogenous TNF-α (50 ng/mL) in combination with Birinapant in SUM190 cells had no additive effect on cell death compared to Birinapant alone as measured by trypan blue exclusion (Fig. 4.11B) and assessment of clonogenic growth capacity (Fig. 4.11C).

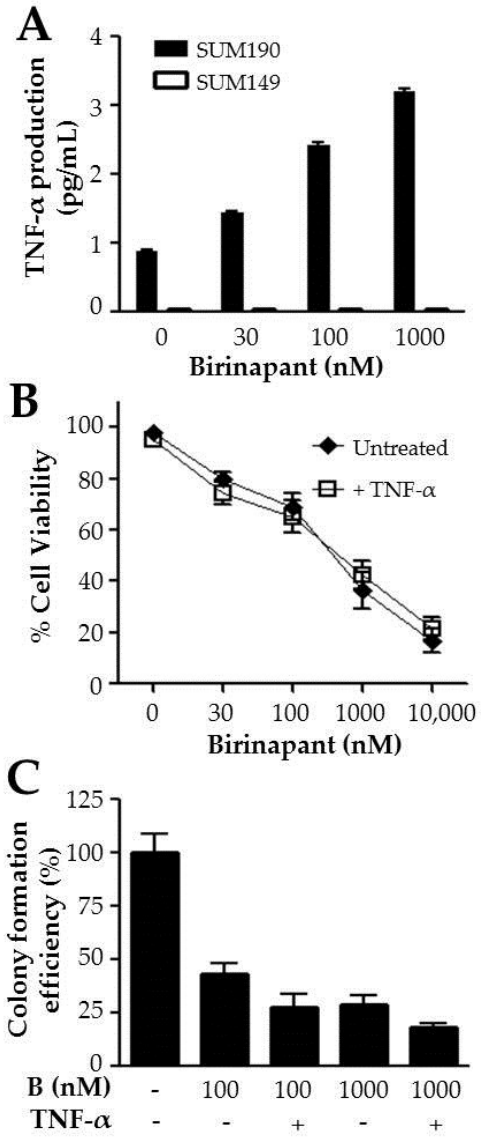

Figure 4.11: SUM190 cells produce low levels of autocrine TNF-α after treatment with Birinapant, but exogenous TNF-α does not sensitize SUM190 cells to Birinapant

A, TNF-α production as determined by ELISA in conditioned media from SUM149 and SUM190 cells treated with Birinapant (0-1000 nM). Bars represent mean±SEM (n=3). **B**, Viability as determined by trypan blue exclusion assay of SUM190 cells treated with Birinapant (0-1000 nM) alone or in combination with TNF-α (50 ng/mL). Data represent mean±SEM viable cells taken as a percentage of total cells (n=2-4). **C**, Clonogenic growth assay of SUM190 cells treated with Birinapant (B; 0-1000 nM) alone or in combination with TNF-α (50 ng/mL). Bars represent mean±SEM colonies formed/cells plated as a percentage of the untreated sample.

Next, the effect of TNF-α receptor (TNFR1) knockdown was evaluated in SUM190 cells using TNFR1-targeting siRNA and control scrambled siRNA at 24 h. Birinapant-induced cell death was not reversed (Fig. 4.12A) by specific TNFR1 downregulation (Fig. 4.12B).

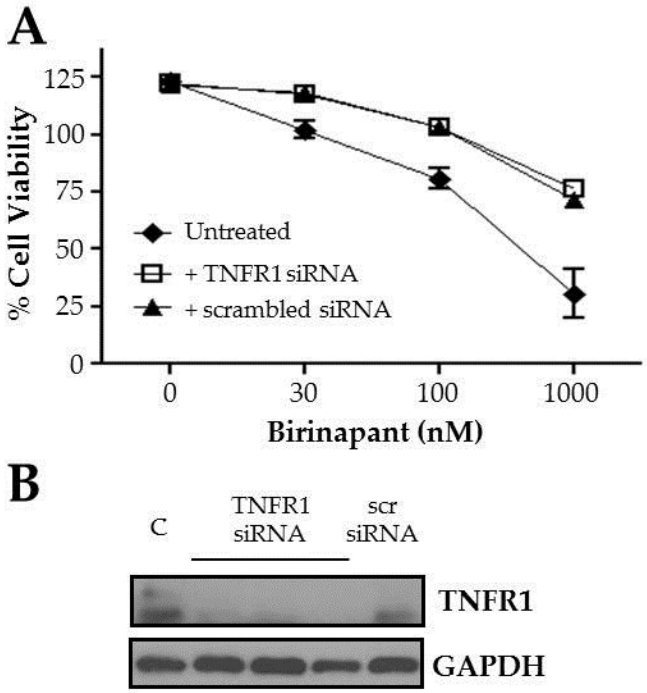

Figure 4.12: Inhibition of TNF-α signaling through knockdown of TNFR1 does not inhibit Birinapant-induced cell death in SUM190 cells

A, Viability as measured by trypan blue exclusion assay of SUM190 cells with TNFR1 knockdown via siRNA or control siRNA treated with Birinapant (0-1000 nM). Data represent mean±SEM viable cells taken as a percentage of total cells (n=1-4). **B**, Western immunoblot analysis of TNFR1 in control SUM190 cells (C) and those transfected with TNFR1-targeting siRNA or scrambled siRNA (scr). GAPDH was used as a loading control.

Further, addition of a TNF-α neutralizing antibody (10 μg/mL) as in a method described previously [383] to SUM149 (Fig. 4.13A and 4.13B) or SUM190 (Fig. 4.13C and 4.13D) cells did not reverse the decrease in viability or colony formation caused by Birinapant in combination or as a single agent.

In contrast to the TNF-α studies, the apoptosis-inducing effect of Birinapant+TRAIL in SUM149 is potently reversed in the presence of pan-caspase inhibitor Q-VD-OPh, as evidenced by trypan blue exclusion assay and clonogenic growth assay (Fig. 4.13A and 4.13B). Similar reversal using Q-VD-OPh is observed in Birinapant-treated SUM190 cells (Fig. 4.13C and 4.13D). Together, these results reveal a TNF-α-independent but IAP- and caspase-dependent mechanism of action of Birinapant +TRAIL in SUM149 cells and Birinapant as a single agent in SUM190 cells.

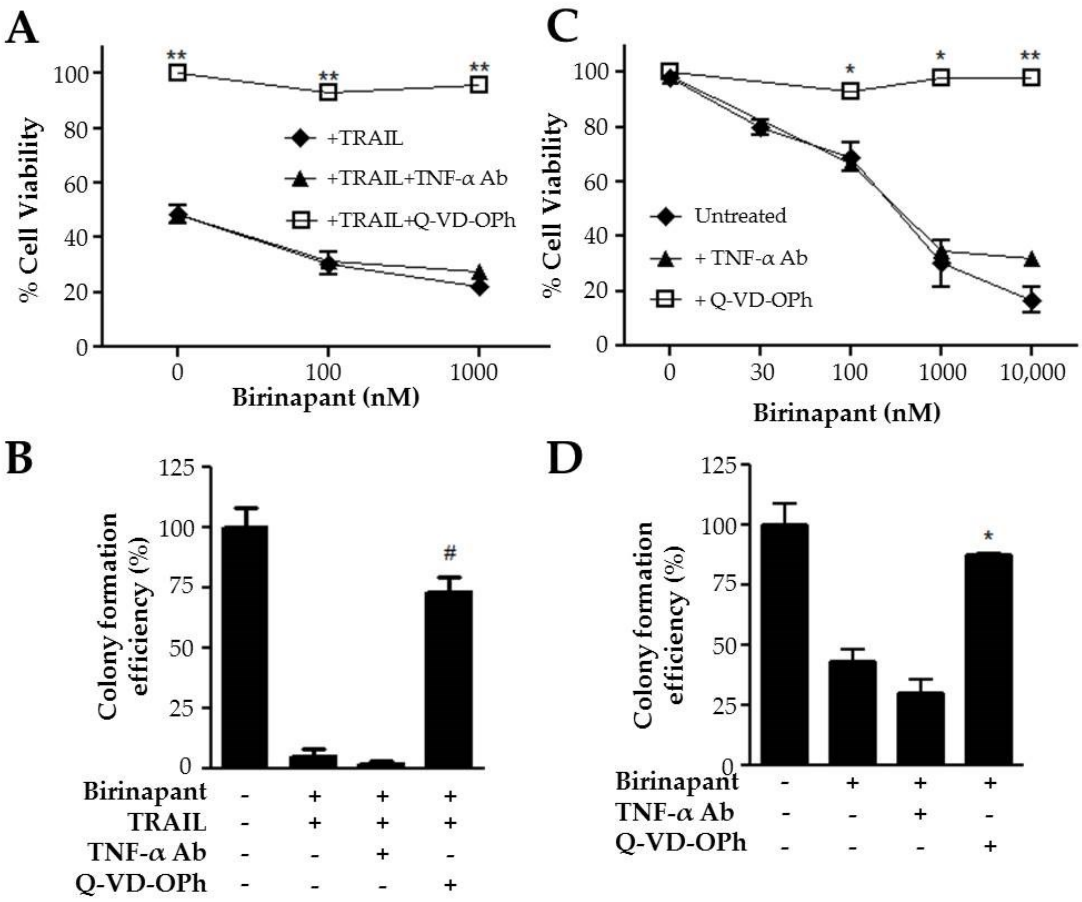

Figure 4.13: Birinapant acts in a TNF-α-independent, caspase-dependent manner to kill SUM190 cells as a single agent and sensitize SUM149 cells to TRAIL

A, Viability of SUM149 cells treated with TRAIL (50 ng/mL) + Birinapant (0-1000 nM) ± a TNF-α neutralizing antibody (10 μg/mL) or pan-caspase inhibitor Q-VD-OPh (20 μM). Data represent mean±SEM viable cells as a percentage of total cells (n=2-4, ***P*<0.01; comparisons made between Birinapant+TRAIL and Birinapant+TRAIL+TNF-α Ab or Q-VD-OPh). **B**, Clonogenic growth assay of SUM149 cells treated with TRAIL (50 ng/mL) + Birinapant (1000 nM) ± TNF-α Ab (10 μg/mL) or Q-VD-OPh (20 μM). Bars represent mean±SEM colonies formed/cells plated as a percentage of untreated. (#*P*<0.005; comparisons made between Birinapant+TRAIL and Birinapant+TRAIL+TNF-α Ab or Q-VD-OPh). **C**, Viability of SUM190 cells treated with Birinapant (0-1000 nM) ± TNF-α Ab (10 μg/mL) or Q-VD-OPh (20 μM). Data represent mean±SEM viable cells as a percentage of total cells (n=2-4, **P*<0.05, ***P*<0.01; comparisons made between Birinapant and Birinapant+Q-VD-OPh). **D**, Clonogenic growth assay of SUM190 cells treated with Birinapant (1000 nM) ± TNF-α Ab (10 μg/mL) or Q-VD-OPh (20 μM). Bars represent mean±SEM colonies formed/cells plated as a percentage of untreated. (**P*<0.05; comparisons made between TNF- α Ab or Q-VD-OPh-treated).

4.8 Discussion

We report herein IAP binding affinities of Birinapant and GT13042, two bivalent Smac mimetics, and their efficacy in IBC cellular models with differential TRAIL sensitivity and XIAP expression. IBC is a particularly aggressive subset of breast cancer that is characterized by apoptotic dysregulation, which has been observed in IBC cells and patient tumors [46, 78, 81, 103, 114, 224, 349]. Generation of isogenic IBC cell models with therapeutic resistance to lapatinib revealed upregulation of several anti-apoptotic proteins, and overexpression of XIAP correlated directly with therapeutic resistance [78, 114, 320]. Thus, it is of particular interest to identify inhibitors of XIAP, as well as other members of the IAP family, in order to prevent or reverse acquired therapeutic resistance in IBC. It may be possible to treat IBC with an IAP inhibitor alone, or to sensitize these tumors to other drugs as part of a combination regimen. One way to inhibit the IAP family of proteins is through the use of Smac mimetics, which act similarly to Smac/DIABLO, a known endogenous mediator of IAP degradation that promotes initiation of apoptosis.

In the present study, parental SUM149 and SUM190 IBC cell lines and their isogenic derivatives with differential XIAP expression (SUM149 wtXIAP and SUM190 shXIAP) were characterized for Smac mimetic sensitivity. These multiple lines were treated with Birinapant (pan-IAP antagonist with high affinity for cIAP1/2 and XIAP) and GT13402, which has lower affinity for XIAP. The differential binding of these two Smac mimetics

provides a molecular approach by which to investigate which IAPs are important for efficacy of Smac mimetics in IBC. Both Birinapant and GT13402 caused degradation of cIAP1 and cIAP2 but did not affect XIAP levels. Birinapant was more efficacious than GT13402 in both cell lines, emphasizing the importance of targeting XIAP in these models. It has been recently reported that bivalent Smac mimetic BV6 degrades both cIAP1 and XIAP but not cIAP2 in glioblastoma cells, revealing mechanistic differences associated with different cell models [369]. In general, Smac mimetic compounds are more efficacious in increasing potency of other drugs than as single agents [355]; a similar phenomenon was observed in the SUM149 cells, which were insensitive to Birinapant and GT13402 alone. However, the addition of Birinapant significantly enhanced TRAIL efficacy.

The single agent efficacy of Birinapant in the SUM190 cell line was a significant finding. SUM190 does not express the DR4 death receptor and is insensitive to TRAIL treatment, which was found to be due at least in part to high XIAP expression. Previous studies have shown that Smac mimetics can cause paradoxical activation of pro-survival NF-κB signaling by autocrine TNF-α production, which can blunt the efficacy of Smac mimetics [358, 359, 363, 384-386], particularly in an *in vivo* setting. However, Birinapant efficacy may not be affected by NF-κB activation in SUM190 cells since only transient changes were observed, with slight activation and downregulation at earlier time points, while activated and total NF-κB returned to basal levels by 24 h. This is further

supported by the observation that Birinapant efficacy is not dependent on TNF-α production. The SUM190 cells showed only a modest increase in TNF-α levels in the picogram/mL range in culture supernatants from Birinapant-treated cells. This is unique in that pro-apoptotic activity of other Smac mimetics is usually associated with significant autocrine production of TNF-α and subsequent interaction with death receptors [358, 359, 385]. While a recent study in pancreatic cells with another Smac mimetic reported that inhibition of TNF-α by a neutralizing antibody reduced activation of caspases [386], addition of a neutralizing TNF-α antibody or silencing of TNFR1 using siRNA failed to prevent Birinapant-induced cell death in SUM190 cells. A similar result was observed in Birinapant+TRAIL-treated SUM149 cells, where addition of a neutralizing TNF-α antibody failed to inhibit cell death. Furthermore, addition of exogenous TNF-α did not enhance Smac mimetic-mediated cell death in the SUM190 model, supporting a TNF-α-independent mechanism for Birinapant in the IBC cells.

Additionally, the effect of Birinapant was further characterized using anchorage-independent growth as a predictor of *in vivo* behavior. The ability of cells *in vitro* to grow in the absence of anchorage has been shown to correlate directly with cancer cell tumorigenicity in multiple mouse models [381, 387]. Thus, the reduction in anchorage-independent growth observed in Birinapant+TRAIL-treated SUM149 cells and Birinapant-treated SUM190 cells highlights Birinapant's ability to target tumorigenic cells and indicates the potential for *in vivo* efficacy.

The present study shows that Birinapant efficacy corresponded with cIAP1/2 degradation, apoptotic parameters, and was reversed by addition of a caspase inhibitor. In a recent study, a monovalent Smac mimetic (LBW242) similarly induced cell death in a TNF-α-independent, caspase-dependent manner in neuroblastoma cell lines without degradation of cIAP1/2 [388]. However, IC_{50} values for LBW242 as a single agent in neuroblastoma cells were in the 50 μM concentration range, which caused significant toxicity in matched normal cells. Birinapant, however is efficacious at lower nanomolar concentrations in the cells tested here and is well tolerated at up to the highest dose tested in animals (60 mg/kg) [364].

At the present, there is no standard IBC-specific treatment plan for patients with advanced disease [3]. A Phase 1a dose escalation study of Birinapant was recently completed in patients with refractory solid tumors and lymphoma, and a Phase1b/2a trial is ongoing in which Birinapant will be combined with standard of care chemotherapies [364]. Through the use of IBC cell lines with differential XIAP expression and Smac mimetics with different affinities for XIAP, this study substantiates findings from previous work identifying XIAP is an important resistance factor and therapeutic target in IBC. By demonstrating that inhibition of XIAP in combination with cIAP1/2 using the Smac mimetic Birinapant effectively induces death in a panel of IBC cell lines, this study strengthens the feasibility of developing clinical trials for Birinapant in IBC.

5 Targeting XIAP with the small molecular functional inhibitor embelin

5.1 Introduction

IBC is often characterized by the acquisition of resistance to chemo-, targeted- and radiotherapies, resulting in poor prognosis compared to LABC [3, 12]. Many therapeutic agents induce therapeutic apoptosis through increases in ROS [389, 390]; however, continuous treatment promotes selection for cells that develop mechanisms to cope with increased ROS, resulting in drug resistance [253]. We previously reported that overexpression of XIAP is a key feature in acquired resistance to ErbB1/EGFR- and ErbB2/Her2-targeting agents in SUM149- and SUM190-derived IBC cell models [103, 114]. The clonal population of IBC cell lines with acquired therapeutic resistance is also characterized by redox adaptation via upregulation of antoxidants SOD1/2 and GSH [78]. Together, these characteristics were associated with cross-resistance to oxidative stressors such as H_2O_2 and paraquat [78] as well as a number of targeted and chemotherapeutics [320]. Therefore, it is clear that XIAP overexpression and enhanced ability to detoxify ROS can contribute to the development of resistance in IBC therapy. While it has been found that XIAP expression is key determinant of TRAIL sensitivity in the parental SUM149 and SUM190 cells as well as in other cell line models [316, 319, 352, 353], it is unknown how the altered profile of anti-apoptotic and antioxidant proteins in the acquired resistant IBC cell line models will affect the response to TRAIL and whether this can be modulated by ROS accumulation.

Embelin, a natural plant-derived agent, is a cell permeable, small molecule inhibitor of XIAP specifically that was identified through structure-based computational screening of a database of traditional herbal medicines [321]. It binds to the BIR3 domain of XIAP with affinity similar to natural Smac/DIABLO, blocking XIAP's interaction with caspases and promoting apoptosis. In addition to targeting XIAP, embelin has been reported to inhibit NF-κB signaling and to have anti-tumor, anti-inflammatory, and analgesic properties [391, 392]. In the present study, we observed that in addition to blocking XIAP's caspase-inhibitory function, embelin suppressed key antioxidants and promoted the accumulation of ROS to potentiate TRAIL efficacy, revealing a new mechanism of embelin action.

5.2 XIAP overexpression inversely correlates with TRAIL sensitivity in IBC cells

In this study, the role of XIAP in TRAIL sensitivity was evaluated in SUM149 cells (TN, EGFR-activated cell line [312]. Isogenic cells with differential XIAP expression derived from SUM149 were characterized for TRAIL sensitivity (10-1000 ng/mL) at a 24 h time period. These include parental SUM149, SUM149 wtXIAP (stable XIAP overexpression via a lentiviral construct) and its vector-control counterpart SUM149 FG9 [114], rSUM149 [114], a model of acquired resistance to an ErbB1/2 targeting agent with endogenous high XIAP expression, and rSUM149 with XIAP knockdown (rSUM149 shXIAP). Cell viability determined by trypan blue exclusion assay shows that parental SUM149 cells are significantly more sensitive to TRAIL than rSUM149 (Fig. 5.1A) and

SUM149 wtXIAP cells (Fig. 5.1B). Calculated IC_{50} for cell viability in the presence of TRAIL was approximately 770 ng/mL in SUM149wtXIAP cells, 530 ng/mL in endogenously XIAP overexpressing rSUM149 cells, and 45 ng/mL ($p<0.005$) in vector control SUM149 cells. To further investigate the role of XIAP in sensitivity to TRAIL, we characterized TRAIL efficacy in rSUM149 cells with XIAP knockdown through transfection of a plasmid expressing shRNA directed against XIAP (rSUM149 shXIAP). Immunoblot analysis is shown in the inset of Figure 5.1C. Data in Figure 5.1C show that XIAP knockdown in the rSUM149 cells results in higher sensitivity to TRAIL-induced cell death. Knockdown of XIAP in the rSUM149 cells caused a pronounced decrease in IC_{50} from 530 ng/mL in rSUM149 cells to approximately 30 ng/mL in the rSUM149 shXIAP cells. XIAP knockdown caused the rSUM149 shXIAP cells to become even more sensitive to TRAIL than the parental SUM149 cells, which have some basal level of XIAP expression; rSUM149 shXIAP cell viability drops to ~60% upon treatment with 10 ng/mL TRAIL, while SUM149 cell viability is about 80% with the same treatment.

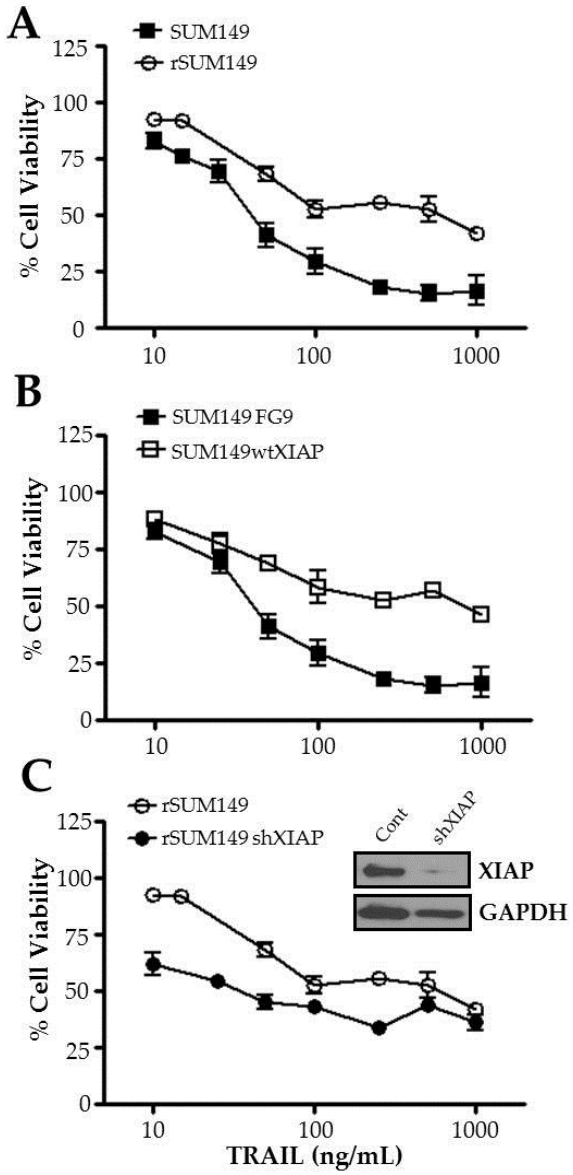

Figure 5.1: Effect of TRAIL expression on viability of isogenic-derived SUM149 cell line models

A, SUM149 and rSUM149 cells were treated with TRAIL for 24 h, and viability was assessed. **B**, SUM149 wtXIAP and vector control SUM149 FG9 cells were treated with TRAIL for 24 h, and viability was assessed. **C**, rSUM149 and rSUM149 cells with knockdown of XIAP expression (rSUM149 shXIAP) were treated with TRAIL for 24 h, and viability was assessed. Bars represent mean±SEM viable cells taken as a percentage of the untreated control (n=2-4). Inset: XIAP expression in rSUM149 cells and rSUM149 shXIAP cells. GAPDH was used as a loading control.

Cell viability differences were consistent with XIAP downregulation post TRAIL treatment in the SUM149 cells compared to the rSUM149 and SUM149wtXIAP cells (Figure 5.2A). In addition, a functional assay was used to measure the activity of caspases during the apoptotic process; this assay was performed after 4 h of TRAIL treatment to ensure that cells were dying but not yet dead, at which point caspase activity would be unreadable. XIAP decrease following treatment in the TRAIL-sensitive SUM149 cells corresponded with increased caspase-3/7 activity (Figure 5.2B, $p<0.005$) compared to limited caspase activity post-TRAIL treatment in the rSUM149 and SUM149wtXIAP cells. These results demonstrate that SUM149 wtXIAP and rSUM149 cells with XIAP overexpression compared to SUM149 show significantly reduced sensitivity to TRAIL-mediated apoptosis.

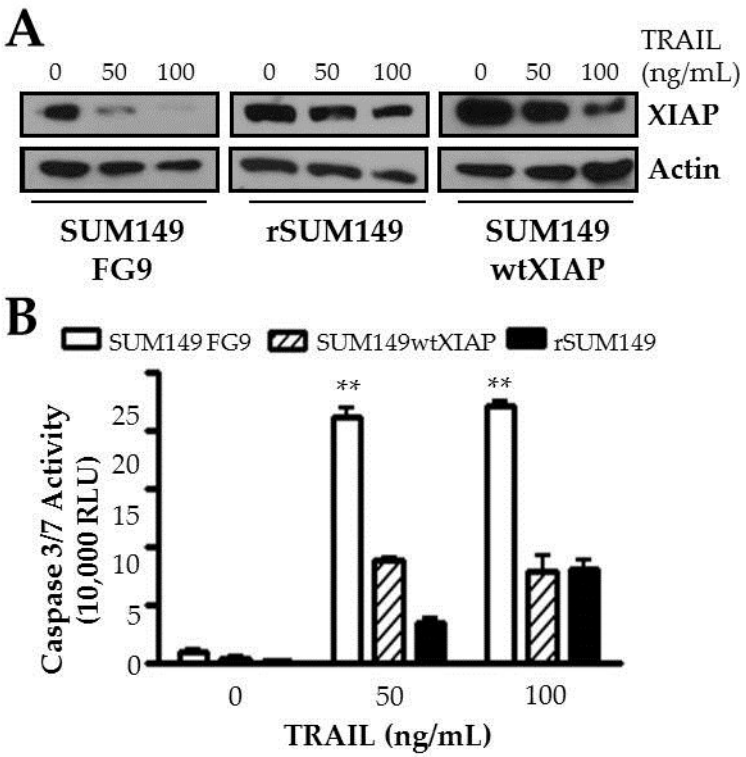

Figure 5.2: TRAIL sensitivity in SUM149 is associated with downregulation of XIAP and caspase activation

A, XIAP immunoblot analysis of rSUM149, SUM149 wtXIAP, and SUM149 FG9 vector control cells treated with TRAIL for 24 h. Treatments are compared to untreated cells. Actin was used as a loading control. **B**, Caspase-3/7 activity in rSUM149, SUM149 wtXIAP, and SUM149 FG9 vector control cells after treatment with TRAIL for 3 h. Bars represent mean±SEM RLU (n=3). **$p<0.005$.

5.3 The XIAP inhibitor embelin enhances TRAIL sensitivity

Since XIAP overexpression and activity corresponds with decreased TRAIL sensitivity in the SUM149 model, we evaluated the effects of embelin, a small molecular inhibitor of XIAP, in combination with TRAIL. Combination studies with TRAIL and embelin were conducted at 24 h, and viability was assessed by trypan blue exclusion assay. Data in Figure 5.3A-C show that embelin at 24 h alone at three concentrations (12.5, 25, 50 μM) induced a modest decrease (10-25%) in viability in the three cell lines. TRAIL (50 ng/mL) alone at 24 h as described in Figure 5.1, shows higher sensitivity in the parental SUM149 cells (Fig. 5.3A) compared to the XIAP overexpressing SUM149wtXIAP (Fig. 5.3B) and rSUM149 (Fig. 5.3C) isogenic lines. Combining increasing concentrations of embelin with TRAIL (50 ng/mL) at 24 h caused a significant decrease in cell viability in all three cell lines. Increasing concentrations of TRAIL up to 100 ng/mL in combination with 25 μM or 50 μM embelin did not have any significantly enhanced response over that seen in Figure 5.3 (data not shown).

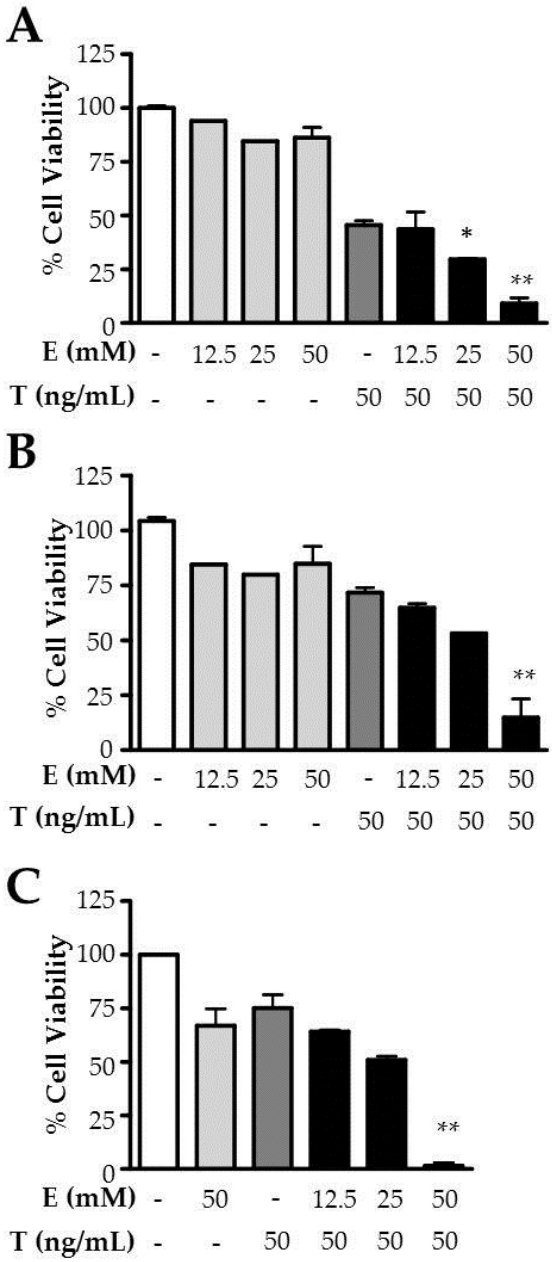

Figure 5.3: Embelin enhances the pro-apoptotic effects of TRAIL in SUM149, SUM149 wtXIAP, and rSUM149

A, SUM149 FG9 vector control, **B**, SUM149 wtXIAP, and **C**, rSUM149 cells were treated with embelin (12.5-50 μM) and TRAIL (50 ng/mL) alone or in combination for 24 h, and viability was assessed by trypan blue exclusion. Bars represent mean±SEM of viable cells (n=2-8). *$p<0.05$, **$p<0.005$.

In order to characterize the interaction of these two agents, we analyzed the results in Figure 5.3 with Calcusyn (Biosoft, Cambridge, UK), a program that employs the Chou-Talalay Method, a derivation of the mass-action law principle [326]. When experimental data is entered into the program, it produces graphs in which the X axis represents the dose of each drug alone or in combination, and the Y axis represents treatment efficacy, with an effect of 1.0 meaning 100% cell death, while 0.5 is equal to 50% cell death. From these graphs (Figure 5.4A-C), the program calculates a combination index (CI) that is a quantitative measurement of the relationship between two agents; a CI greater than 1 indicates antagonism, while a CI of one indicates an additive interaction and a CI less than one indicates synergism. The CI values for the interaction between embelin and TRAIL in SUM149, SUM149 wtXIAP and rSUM149 cells were all calculated to be well below one (Table 5.1, Fig. 5.4), which is indicative of strong synergism in all three cell lines.

Table 5.1: Combination indices (CI) for the interactions between embelin and TRAIL in SUM149-derived isogenic cell lines

Cell Line	Combination Index (CI)
SUM149	0.077
SUM149 wtXIAP	0.041
rSUM149	0.122

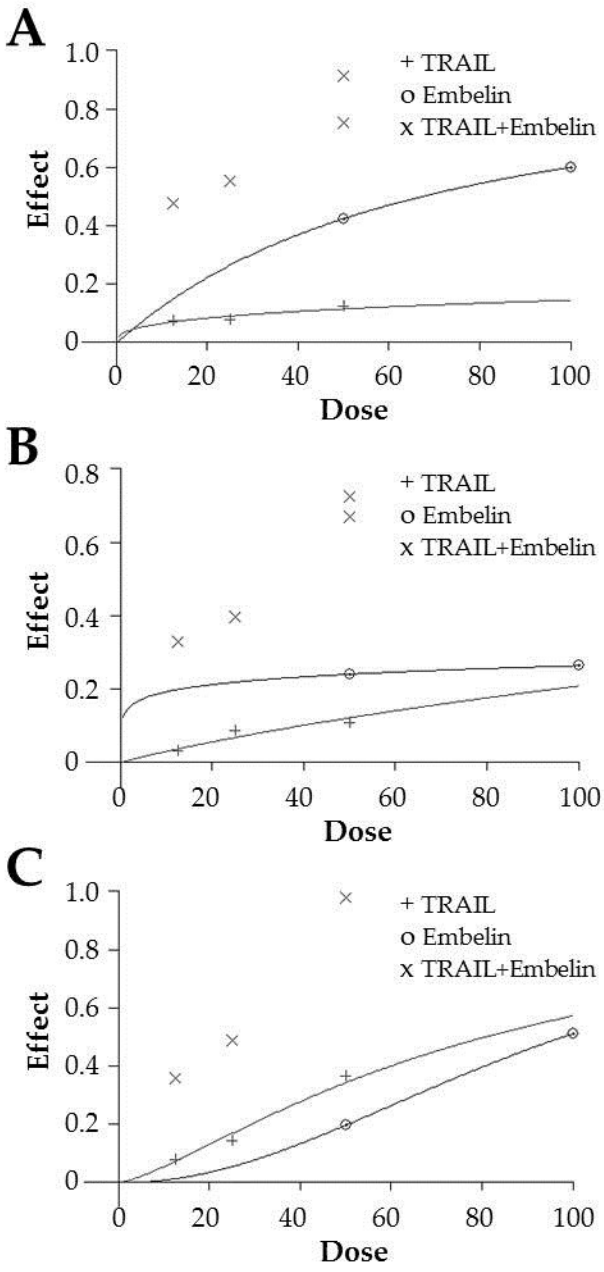

Figure 5.4: Combinatorial analysis reveals synergy between embelin and TRAIL

Dose effect curves for **A**, SUM149, **B**, SUM149 wtXIAP, and **C**, rSUM149 treated with embelin and TRAIL alone as well as the combination created using Calcusyn software.

The effects of embelin, TRAIL, or embelin+TRAIL on downstream TRAIL signaling pathway proteins in treated lysates were analyzed by western immunoblot. Immunoblot analysis of death receptors DR4 and DR5 (Figure 5.5A,B) in SUM149 cells revealed no significant upregulation of death receptor expression in response to treatment. The same results were seen in the SUM149 wtXIAP cells upon treatment with embelin and/or TRAIL (data not shown).

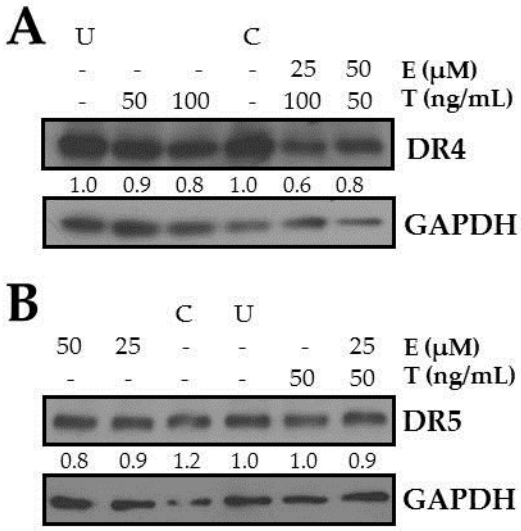

Figure 5.5: Embelin does not effect death receptor expression in SUM149 cells

Western immunoblot analysis of **A**, DR4 and **B**, DR5 expression in SUM149 cells treated with embelin, TRAIL, or embelin+TRAIL for 24 h. Treatments were compared to untreated cells (U) or DMSO vector control (C). Numbers represent densitometric analysis of protein normalized to GAPDH.

A decrease in cFLIP, a caspase-8 homolog that binds to the DISC to block caspase activation, was observed following treatment with embelin and TRAIL alone as well as in combination in the parental SUM149 cells (Figure 5.6A). However, cFLIP levels remain unchanged in the XIAP overexpressing cells (Figure 5.6B) treated with embelin, TRAIL or embelin+TRAIL, although cell death was significantly increased (Figure 5.3). Examination of lysates from SUM149 wtXIAP cells treated with embelin or embelin+TRAIL reveal XIAP downregulation upon treatment with embelin compared to control. In addition, an XIAP cleavage product (30 kDa) and potent inhibition of full length XIAP levels are detected in cells treated with embelin+TRAIL (Figure 5.6C). In summary, embelin and TRAIL synergize to increase cell death in the TN IBC cell model.

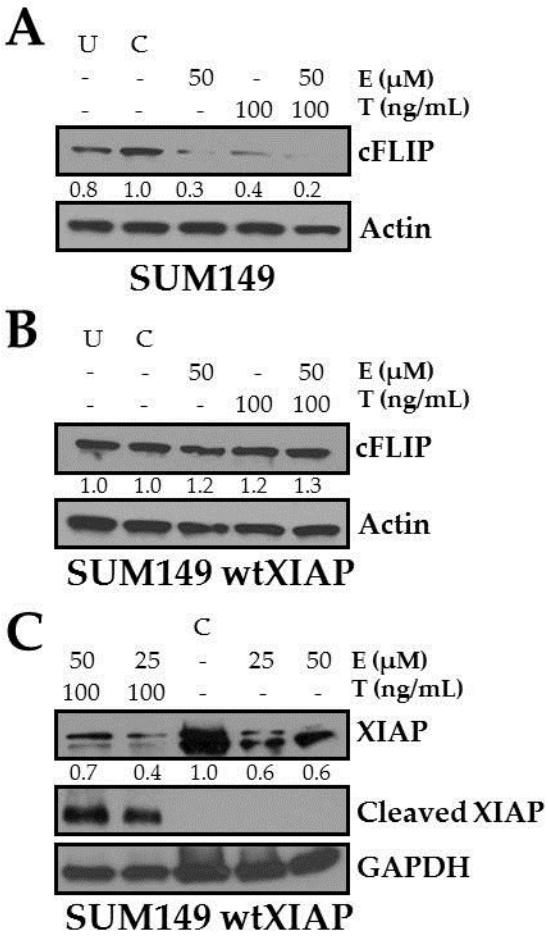

Figure 5.6: Sensitization to TRAIL by embelin is associated with reduced XIAP expression

cFLIP western immunoblot analysis of **A**, SUM149 and **B**, SUM149 wtXIAP cells treated with embelin, TRAIL, or embelin+TRAIL for 24 h. **C**, XIAP immunoblot analysis of SUM149 wtXIAP cells treated with embelin, TRAIL, or embelin+TRAIL for 24 h; full length XIAP and its cleavage product are shown. Treatments were compared to untreated cells (U) or DMSO vector control (C). Numbers represent densitometric analysis of protein normalized to β-actin or GAPDH.

5.4 Embelin modulates the ERK signaling pathway

To further study the mechanisms behind the combinatorial synergism, signaling pathways that are linked to apoptosis were examined in response to treatment. For this purpose, SUM149 and SUM149 wtXIAP cells were treated with embelin, TRAIL, or embelin+TRAIL at the indicated concentrations for 24 h and then examined for the phosphorylation status of extracellular signaling regulated kinase (ERK1/2) and the stress-activated protein kinase (SAPK) JNK (Figure 5.7). In SUM149 cells, cell death associated with embelin or embelin+TRAIL correlated with a decrease in p-ERK1/2 (Figure 5.7A). Interestingly, in the SUM149 wtXIAP cells with exogenous XIAP overexpression, the basal levels of ERK1/2 phosphorylation were lower than the parental SUM149 cells. Further, an increase in p-ERK1/2 was observed in embelin- and embelin+TRAIL-treated SUM149 wtXIAP cells compared to vehicle- or TRAIL-treated cells (Figure 5.7B). To interrogate the nature of ERK1/2 signaling in this system, we added the MEK1/2 inhibitor U0126 to the embelin+TRAIL combination in SUM149 wtXIAP cells to block ERK1/2 phosphorylation. This resulted in further reduction of cell viability from approximately 25% with embelin+TRAIL treatment to less than 1% viable cells in the presence of embelin+TRAIL+U0126 (Figure 5.7C). No specific change in p-JNK levels was observed in the various treatments as compared to vehicle control in the SUM149 or SUM149 wtXIAP cells (data not shown).

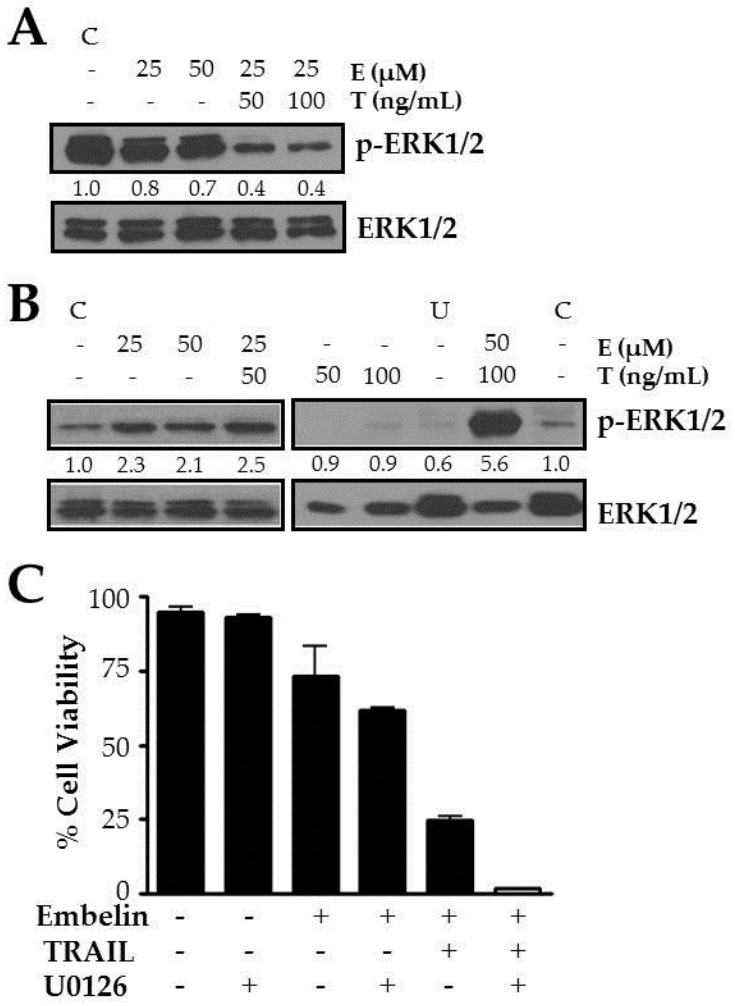

Figure 5.7: Embelin+TRAIL has differential effects on ERK signaling in SUM149 and SUM149 wtXIAP cells

A, Phospho-ERK1/2 (MAPK p44/42) western immunoblot analysis of SUM149 cells treated with embelin or embelin+TRAIL for 24 h. **B**, Phospho-ERK1/2 western immunoblot analysis of SUM149 wtXIAP cells treated with embelin, TRAIL, or embelin+TRAIL. Treatments were compared to untreated cells (U) or DMSO vector control (C). Numbers represent densitometric analysis of p-ERK1/2 normalized to total ERK1/2 protein. **C**, Cellular viability as determined by trypan blue viability assay for SUM149 wtXIAP cells treated with 50 μM embelin, 50ng/ mL TRAIL, or combination, and the combination with the addition of 10 μM U0126 MEK1/2 inhibitor.

5.5 Embelin induces generation of intracellular ROS by downregulation of SOD1 and oxidation of glutathione

Recently we reported [78] that the XIAP overexpressing rSUM149 cells which have acquired resistance to therapeutic apoptosis mediated by lapatinib have lost the ability to accumulate ROS in the presence of oxidizing agents like paraquat and hydrogen peroxide; they also have high expression of key antioxidants SOD1/2 and GSH. Interestingly, embelin treatment downregulates SOD1 (Figure 5.8A) and consumes GSH (Figure 5.8B, $p<0.05$) in the rSUM149 cells, inhibiting the detoxification of damaging oxidative species. Decrease in antioxidant expression corresponds with an increase in mitochondrial superoxides as measured by flow cytometry compared to paraquat, a classical ROS generating agent which we have previously reported [78] to have insignificant effects on ROS generation in the rSUM149 cells (Figure 5.8C). Embelin also decreases mitochondrial membrane potential as measured by TMRE staining, which the classical ROS-inducer paraquat fails to do in the rSUM149 cells (Fig. 5.8C).

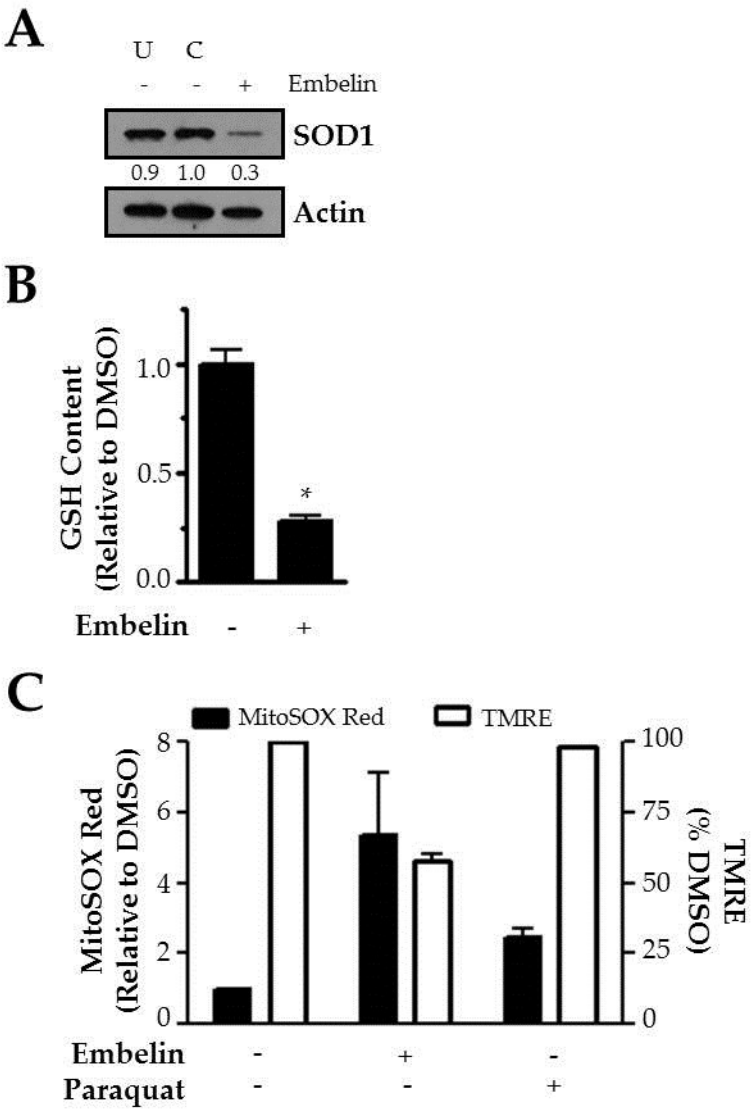

Figure 5.8: Embelin reduces cellular antioxidant capacity and generates ROS in rSUM149 cells to induce cell death

A, Western immunoblot analysis of SOD1 in rSUM149 cells treated with 50 μM embelin or vector control (C). Numbers represent densitometric analysis of protein normalized to β-actin. **B**, Glutathione content of cells treated with 50 μM embelin or a vector control. * $p < 0.05$. **C**, Left axis displays accumulation of mitochondrial superoxide in cells treated with 50 μM embelin for 1 h or 5 mM paraquat for 24 h as measured by fold increase in MitoSOX Red staining via flow cytometry. Right axis displays decrease in mitochondrial membrane integrity, measured by percent of cells with high TMRE staining via flow cytometry.

5.6 SOD mimetic/antioxidant reverses efficacy of the Embelin+TRAIL combination

To determine whether the generation of ROS by embelin is specifically contributing to enhanced cell death observed with embelin+TRAIL treatment, we tested the effect of an SOD mimic (MnTnHex-2-PyP^{5+}) [78, 317], which acts as a potent antioxidant both *in vitro* and *in vivo* and was simultaneously added to the combination at increasing concentrations. Addition of the SOD mimic to embelin+TRAIL provided protection against ROS and resulted in a dose-dependent increase in cellular viability (Figure 5.9). Together, these results indicate that the concurrent inhibition of XIAP along with modulation of antioxidant molecules and ROS generation by embelin sensitizes resistant cells to TRAIL-induced apoptosis.

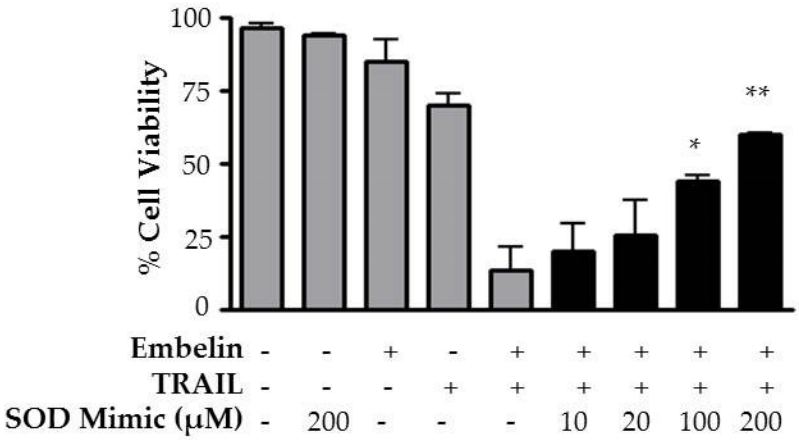

Figure 5.9: Addition of an exogenous antioxidant (SOD mimetic) partially rescues embelin+TRAIL-induced cell death in SUM149 wtXIAP cells

Cellular viability as determined by trypan blue exclusion assay for SUM149 wtXIAP cells treated with 50 μM embelin, 50ng /mL TRAIL, or combination (gray bars) and the combination with the addition of an SOD mimic (MnTnHex-2-PyP^{5+}) at 10-200 μM (black bars). *$p<0.05$, **$p<0.005$.

5.7 Discussion

We report herein an inverse correlation between XIAP expression and TRAIL sensitivity in isogenic cell lines developed from the primary patient tumor-derived SUM149 cell line [312]. Endogenous and exogenous overexpression of XIAP in SUM149 cells (rSUM149 and SUM149 wtXIAP) resulted in increased resistance to TRAIL-induced apoptosis and reduced caspase activation relative to the parental TRAIL-sensitive SUM149 cells. Conversely, knockdown of XIAP in the rSUM149 cells enhanced TRAIL efficacy; the knockdown rendered the rSUM149 shXIAP cells even more sensitive to TRAIL-induced apoptosis than the parental SUM149 cells, which express basal levels of XIAP. In addition, the XIAP inhibitor embelin synergizes with TRAIL to induce apoptosis in XIAP-overexpressing IBC cell lines (SUM149 wtXIAP and rSUM149) and enhances the potency of TRAIL in the isogenic TRAIL-sensitive counterpart (SUM149), the first report of this phenomenon in IBC. Embelin also activated ERK1/2 in SUM149 wtXIAP cells, and this effect was amplified and accompanied by increased cell death when combined with TRAIL. Embelin treatment reversed high SOD1 expression and inhibited the increased GSH detoxification capacity in the redox adapted IBC resistance model; this led to the accumulation of ROS, identifying a potential new mechanism of action for embelin.

Previous studies evaluating therapeutic agents (such as gossypol, perifosine, and zerumbone) and chemotherapies that can potentiate TRAIL efficacy have reported

upregulation of TRAIL-specific death receptors as an important mechanism of TRAIL sensitization [393-395]. However, no increase in DR expression was observed in the embelin-treated cells, indicating that this mechanism was not responsible for sensitization of the IBC lines. The caspase-8 homolog cFLIP has previously been reported to block apoptosis induced by ligand binding to Fas/CD95, TRAIL, and TNF receptors [373, 396, 397]. In certain contexts, inhibiton or downregulation of cFLIP sensitizes resistant cells to TRAIL-induced apoptosis [398-403]. In the current study, cFLIP protein levels decreased significantly in TRAIL- or embelin+TRAIL-treated parental SUM149 cells; however, cFLIP levels were unchanged in embelin+TRAIL-treated XIAP overexpressing cells even though they underwent apoptosis in response to the combination. These observations indicate that cFLIP expression is not sufficient to determine TRAIL sensitivity in this model.

In the present study, single agent embelin treatment caused an increase in ERK1/2 phosphorylation in the XIAP overexpressing cell line (SUM149 wtXIAP), and this effect was amplified by combination with TRAIL, which corresponded with significant cell death. In contrast, treatment with embelin or embelin+TRAIL decreased ERK1/2 phosphorylation in SUM149 cells. Interestingly, SUM149 wtXIAP cells have very low basal levels of ERK1/2 phosphorylation compared to the parental SUM149 cells. This observation is consistent with a previous study in which knockdown of XIAP in a mouse model resulted in an increase in ERK1/2 phosphorylation [404]. ERK signaling is largely

proliferative [258] and promotes survival [405]; in some cases, downregulation or inhibition of ERK1/2 is necessary for apoptosis to occur in normal and cancerous cells. Studies in neuronal [406] and leukemia models [407, 408] have reported that concurrent activation of p38 MAPK and JNK in conjunction with inhibition of ERK is critical for the induction of apoptosis. However, there is also convincing evidence implicating the Ras/Raf/ERK pathway in pro-apoptotic signaling events such as the expression of death ligands and/or receptors [393], modulation of Bcl-2 family members resulting in disruption of the mitochondrial membrane, and suppression of anti-apoptotic signaling molecules [409]. In fact, the action of many apoptosis-inducing drugs including estradiol, tamoxifen, and cephalosporin is abrogated by Ras/Raf/ERK pathway inhibition [410]. In the parental SUM149 cells, which have basal levels of XIAP expression, treatment with embelin correlated with reduced ERK1/2 phosphorylation, indicating a pro-survival role of ERK signaling. In the SUM149 wtXIAP cells, which overexpress XIAP and have low basal ERK1/2 phosphorylation, treatment with apoptosis-inducing agents correlated with increased ERK1/2 phosphorylation, suggesting that ERK1/2 signaling may be a compensatory mechanism to oppose apoptosis. This is further supported by the observation that addition of U1026, a MEK1/2 inhibitor that blocks ERK phosphorylation, to embelin+TRAIL-treated SUM149 wtXIAP cells resulted in significant cell death beyond the embelin+TRAIL combination.

rSUM149 cells overexpress SOD1/2 and possess increased GSH levels, qualities which enhance their ability to detoxify ROS in the presence of oxidative agents [78]. Embelin caused a significant downregulation of SOD1 and GSH, increased superoxide levels, and sensitized rSUM149 cells to apoptosis, revealing an ROS-modulatory mechanism of embelin in IBC cells. Furthermore, addition of an SOD mimic (MnTnHex-2-PyP^{5+}) provided protection against ROS and reduced embelin+TRAIL-associated cell death in a dose-dependent manner. This is consistent with previous results in which treatment of parental SUM149 cells with an SOD mimic reversed the ability of these cells to accumulate ROS in the presence of oxidizing agents [78]. Together, these results indicate that embelin sensitizes IBC cells to TRAIL-mediated apoptosis through direct inhibition of XIAP's anti-caspase activity and by shifting the cellular redox balance toward oxidative stress-mediated apoptosis. Thus, the targeting of cellular redox adaptation through the use of ROS modulators may represent a promising new approach for enhancing therapeutic efficacy in IBC.

6 Targeting redox adaptation in IBC using the redox modulator disulfiram

6.1 Introduction

The altered redox status in cancer cells is a biochemical feature that is attractive for the development of selective therapeutic strategies [235, 411-413]. However, redox adaptive mechanisms including upregulation of ROS scavenging systems and antioxidant activity can confer drug resistance [264, 390]. The development of resistance to classic anti-tumoral therapies is a common occurrence and significant barrier to the successful treatment of IBC [3, 12]. Gene expression analyses indicate that IBC has higher expression of genes associated with NF-κB and related survival signaling pathways relative to non-IBC tumors [18, 32-34, 224, 414]. Additionally, redox adaptation through increased SOD1/2 expression and high levels of GSH was detected in acquired therapy-resistant IBC cell lines compared to therapy-sensitive parental cells. The increase in antioxidant defense mechanisms prevented the accumulation of ROS, significantly suppressed oxidative stress-associated cell death [78], and conferred drug resistance to various chemotherapeutics and targeted agents [320]. Reduction of antioxidant mechanisms by the XIAP inhibitor embelin was associated with ROS accumulation and sensitization of rSUM149 cells to therapeutic apoptosis [415]. These data indicate that redox modulators with pro-oxidant properties have the potential to promote ROS accumulation and induce oxidative stress in IBC cells as a strategy to

enhance cytotoxicity.

One such pharmacological agent is Disulfiram (DSF), a clinically utilized anti-alcoholism drug that can bind copper to form a complex (DSF-Cu). DSF is FDA-approved for the treatment of alcoholism and is safe even at high doses; the recommended dosage for alcoholic patients is currently 250-500 mg/day [416, 417]. DSF has been shown to be cytotoxic in cell line models of melanoma, colorectal, hematological, prostate, and breast cancer and is currently in Phase 1/2 clinical trials for the treatment of metastatic melanoma and refractory solid tumors of the liver [418]. Disulfiram's reported mechanisms of action include generation of ROS [419-421], proteasomal inhibition [422-424], DNA demethylation [425], and modulation of cell survival and death signaling pathways [419-422, 426].

In this study, DSF was assessed as a single agent and in combination with copper (DSF-Cu) in established patient tumor-derived models of IBC, isotype matched drug-resistant IBC cell lines, and an exogenous model of XIAP overexpression. DSF-Cu led to increased ROS accumulation accompanied by decreases in SOD1 expression and GSH levels, and addition of an SOD mimetic reversed cell death. Additionally, DSF-Cu blocked NF-κB activation, inhibited cancer stem cell-associated ALDH1 activity, prevented anchorage-independent cell growth, and induced apoptosis. Taken together,

this study provides a rationale for the repurposing of an old and safe drug for targeting IBC.

6.2 DSF induces death in IBC cells, and potency is enhanced by the addition of copper

In an effort to investigate the effects of DSF on IBC cell lines with different subtype and redox response status, we treated established patient-derived IBC tumor cell lines, isotype-matched cells selected for drug resistance, and a model of exogenous XIAP overexpression. The data in Figure 6.1 show treatment with a dose range of DSF alone or in the presence of 10 μM copper (DSF-Cu) in three established IBC cell lines: SUM149 (basal type, ROS sensitive), MDA-IBC-3 (Her2-overexpressing, ROS responsiveness unknown), and SUM190 (Her2-overexpressing, ROS sensitive) [312, 314]. DSF induces cell death at micromolar concentrations in all three cell lines, although SUM190 cells are much more sensitive than SUM149, and MDA-IBC-3 cells are relatively less sensitive (Fig 6.1A: SUM149-squares, IC_{50} of ~17 μM; Fig 6.1B: MDA-IBC-3- squares, IC_{50} >50 μM; Fig 6.1C: SUM190- IC_{50} of ~2.7 μM). DSF's potency was significantly enhanced by the addition of copper (DSF-Cu) in all three cell lines, with approximately a 100 fold or more decrease in IC_{50} values of SUM149 and MDA-IBC-3 (Fig 6.1A: SUM149- circles, IC_{50} of ~200 nM; Fig 6.1B: MDA-IBC-3- circles, IC_{50} of ~300 nM); SUM190 cells were so sensitive to the combination that 100% cell death was observed at the lowest concentration tested (50 nM DSF-Cu).

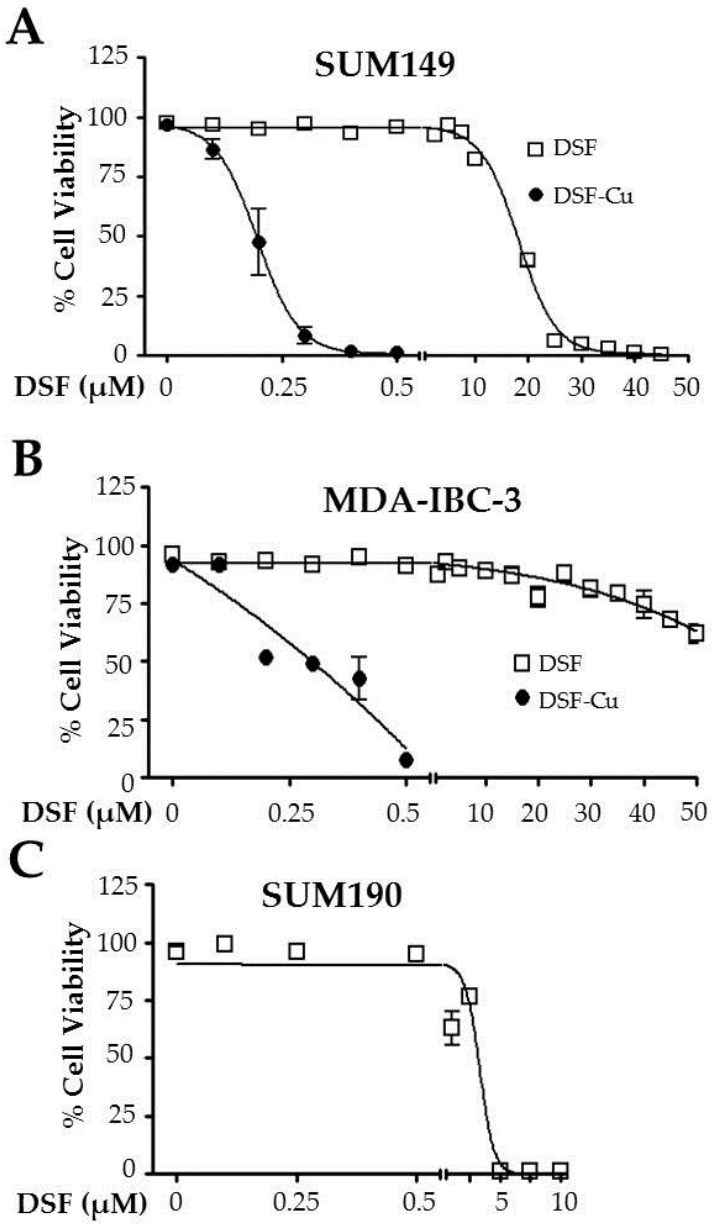

Figure 6.1: DSF induces cell death in patient-derived IBC cell lines, and potency is significantly enhanced by the addition of copper

Viability of **A**, SUM149, **B**, MDA-IBC-3, and **C**, SUM190 cells treated with DSF (0-50 μM, squares), copper (10 μM) or DSF-Cu (100-500 nM + 10 μM Cu, circles) as measured by trypan blue exclusion assay.

DSF and DSF-Cu were also tested in rSUM149 and rSUM190 (isogenic-derivatives of SUM149 and SUM190 selected for lapatinib resistance with increased SOD1/2 and GSH and reduced ROS-generating capability) and SUM149 wtXIAP cells with exogenous XIAP overexpression [78, 114]. The SUM149-derived models rSUM149 (Fig. 6.2A: squares) and SUM149 wtXIAP (Fig. 6.2B: squares) were somewhat less sensitive to disulfiram than the parental line, with IC_{50}s of ~25-30 μM compared to ~17 μM in SUM149 (Table 6.1). rSUM190 cells (Fig. 6.2A) also showed a slight decrease in sensitivity compared to the parental SUM190 model, with an IC_{50} of ~3.9 μM compared to ~2.7 μM in SUM190, and DSF-induced cell death was also enhanced by the addition of copper in the resistant rSUM149 (Fig. 6.2A: circles), SUM149 wtXIAP (Fig. 6.2B: circles), and resistant rSUM190 models, with IC_{50}s of ~230, and ~125 nM in rSUM149 and SUM149 wtXIAP (Table 6.1). Similar to their parental counterparts, rSUM190 cells were killed completely at the lowest DSF-Cu dose tested (50 nM).

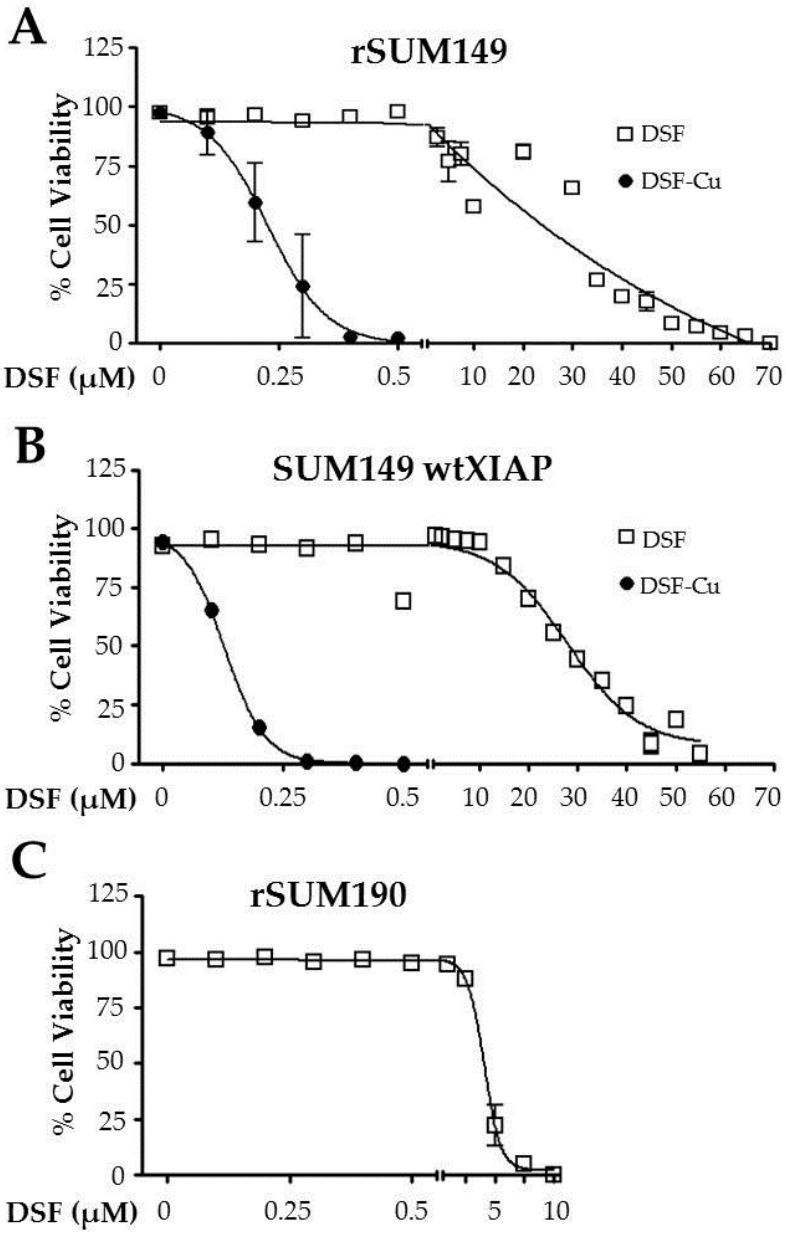

Figure 6.2: DSF induces cell death in isogenic-derived IBC models of therapeutic resistance, and potency is significantly enhanced by the addition of copper

Viability of **A**, rSUM149, **B**, SUM149 wtXIAP, and **C**, rSUM190 cells treated with DSF (0-70 μM, squares), copper (10 μM) or DSF-Cu (100-500 nM and 10 μM, circles) as measured by trypan blue exclusion assay.

Compared to previous reports of single agent efficacy in a panel of cancer cell lines, the IBC cell lines tested here, including SUM190 and rSUM190, are relatively insensitive to single agent DSF. The IC_{50} values for DSF alone and the combination of DSF-Cu in each IBC cell line is listed in Table 6.1, along with three non-IBC breast cancer, several prostate cancer, and three glioblastoma cell lines previously reported [420, 421, 427]. Interestingly, the addition of copper sensitizes the IBC cell lines to DSF-Cu at concentrations similar to or even lower than the other cancer cell lines (Table 6.1). Neither copper at the tested concentration nor DSF in the nanomolar range had an effect on cellular viability in any of the cell lines tested. As all cell lines were sensitive to DSF and DSF-Cu to some degree and the SUM190 models were too sensitive for any mechanistic studies with DSF-Cu, the remainder of the studies was performed in SUM149 and rSUM149 cells.

Table 6.1: IC_{50}s for DSF and DSF-Cu in cellular models of cancer

Cell Line	IC_{50}- DSF (nM)	SEM	IC_{50}- DSF-Cu (nM)	SEM	Cell Type	Reference
SUM149	17,620	1060	200.4	36.9	IBC	
SUM190	2,969	2,172	<50	NA	IBC	
MDA-IBC-3	>50,000	NA	300	100	IBC	
rSUM149	26,520	13,420	234.9	127.2	IBC	
rSUM190	3951	355	<50	NA	IBC	
SUM149 wtXIAP	29,710	5,670	126.7	7.3	IBC	
MCF7	456	62	211	23	BC	[421]
MDA-MB-231	495	49	476	48	BC	[421]
T47D	1100	87	443	62	BC	[421]
VCaP	94	19			PC	[427]
DuCaP	60	18			PC	[427]
LNCaP	170	36			PC	[427]
LNCaP C4-2	97	22			PC	[427]
PC-3	>1000	NA			PC	[427]
CU-145	>10,000	NA			PC	[427]
RWPE-1	>10,000	NA			PC	[427]
EP156T	>10,000	NA			PC	[427]
PrEC	>10,000	NA			PC	[427]
U251MG	>10,000	NA	464.9	236.4	GBM	[420]
U87MG	>10,000	NA	242.8	39.4	GBM	[420]
U373MG	>10,000	NA	119.7	38.7	GBM	[420]

To further investigate the necessity of copper in DSF's mechanism of action, we blocked DSF-Cu binding through the addition of potent copper chelators in molar excess. Addition of BCS (white bars), an extracellular copper chelator which cannot cross the cell membrane [428], or TM (gray bars), a cell permeable chelator [429], completely blocked DSF-Cu-induced cell death (black bars) in SUM149 (Fig. 6.3A) and rSUM149 (Fig. 6.3B) cells, highlighting the role of copper in enhancing the cytotoxic action of DSF. Neither the TM-Cu nor the BCS-Cu combinations caused any cytotoxicity in these studies, revealing the specific effect of the DSF-Cu complex in the cells tested.

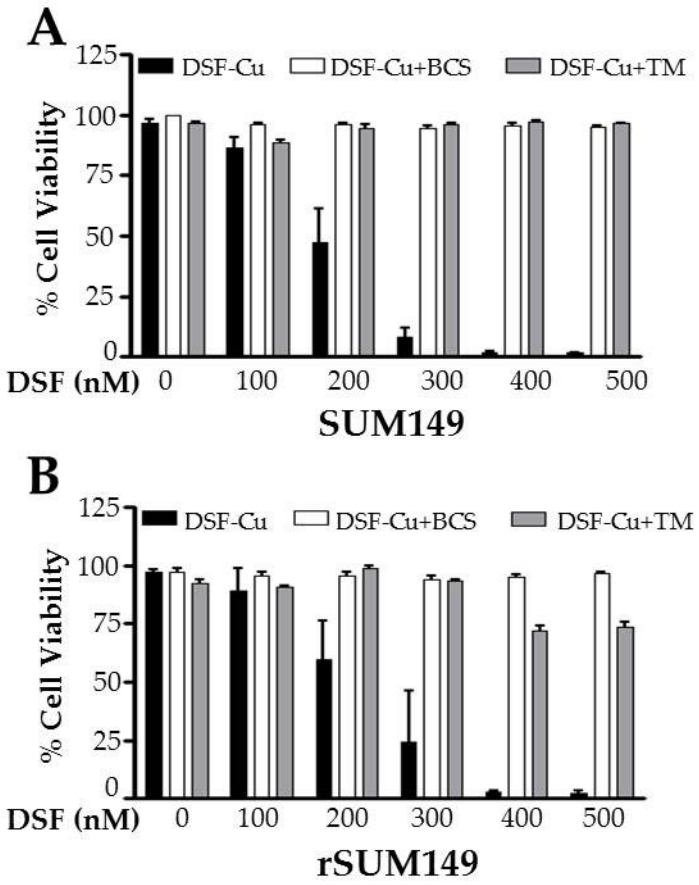

Figure 6.3: DSF-Cu-mediated cell death is potently reversed by the addition of copper chelators

Viability of **A**, SUM149 and **B**, rSUM149 cells treated with DSF-Cu (100-500 nM and 10 μM respectively), and the copper chelators bathocuproine disulphonate (BCS, 100 μM) or tetrathiomolybdate (TM, 10 μM) as measured by trypan blue exclusion assay.

6.3 DSF is a copper ionophore that induces Ctr1-independent copper uptake

DSF has been implicated as a copper ionophore with the ability to bring copper into cells independently of copper transporters due to its copper-binding ability and high lipophilicity; this would allow it to bypass the tightly regulated mechanisms that control intracellular copper levels [428, 430, 431]. However, it has not been explicitly proven that DSF can induce Ctr1-independent copper uptake. To test whether DSF can induce Ctr1-independent uptake of copper into cells, growth of Ctr1/3 wildtype SEY6210 *Saccharomyces cerevisiae* was compared to Ctr1/Ctr3 deletion mutant MPY17 cells [323, 324] in YPEG media; growth was measured by reading absorbance at 600 nm. Data in Figure 6.4 show that while SEY6210 cells (white bars) grow well in unsupplemented media, MPY17 cells (black bars) cannot grow in normal YPEG media. However, in the presence of low levels of the known copper ionophore ZPT [325], which brings enough copper into the cell for normal biological function, MPY17 cells grow similarly to the SEY6210 cells. At higher concentrations, ZPT increases cellular copper levels past those that support growth, indicated by the reduction in absorbance; SEY6210 cells, which take up normal levels of copper on their own, are more sensitive to ZPT-induced growth inhibition than MPY17 cells, showing a reduction in growth at 0.39 μM ZPT compared to 1.56 μM ZPT respectively (Fig. 6.4A). In this assay format, the addition of low concentrations of DSF to MPY17 cells enhanced their growth similar to ZPT treatment.

DSF also induced growth inhibition in both SEY6210 and MPY17 cells at concentrations of 6.25 μM and greater (Fig. 6.4B). These data indicate that DSF is able to act as an ionophore for copper, bringing copper into cells in a Ctr1/Ctr3-independent manner.

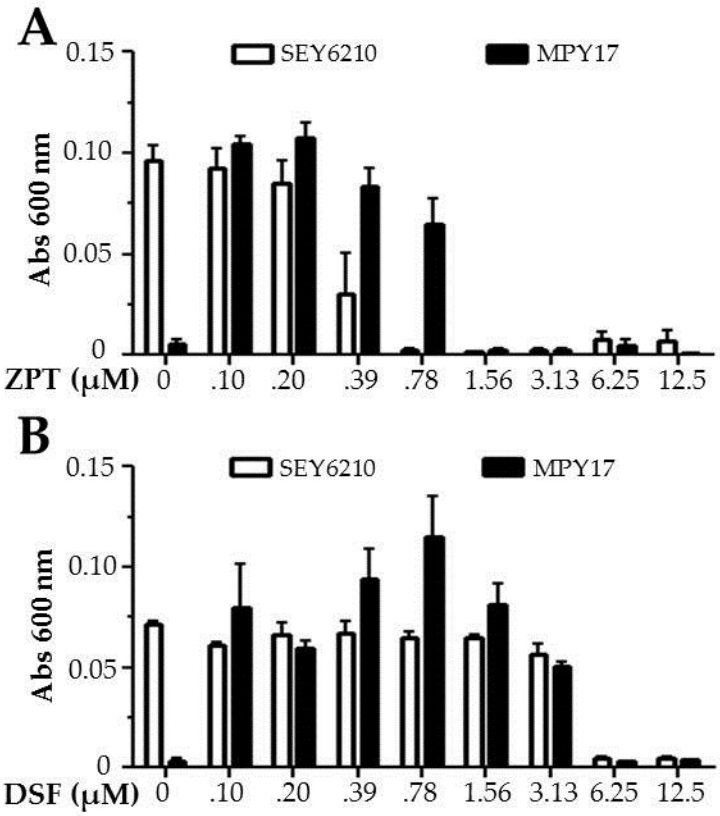

Figure 6.4: DSF acts as an ionophore to facilitate the uptake of copper into Ctr1/Ctr3 mutant yeast

Growth of Ctr1/Ctr3 wildtype SEY6210 or MPY17 Ctr1/Ctr3 deletion mutant yeast as measured by absorbance at 600 nm with the addition of a dose curve of **A**, known copper ionophore ZPT or **B**, DSF.

6.4 DSF strongly induces copper accumulation in IBC cells

DSF has been implicated as a copper ionophore with the ability to bring copper into cells independently of copper transporters due to its Cu-binding ability and high lipophilicity, thus bypassing the tightly regulated mechanisms in place to control intracellular copper levels [428, 430, 431]. Our results in Figure 6.4B support that claim. To determine whether DSF promotes the accumulation of copper in IBC cells, SUM149 and rSUM149 cells were treated with DSF, copper, or DSF-Cu for 24 h, and then copper content of cell lysates was determined by ICP-HRMS. A slight increase in intracellular copper concentration was observed upon treatment with 10 μM copper as a single agent, but there was a dramatic dose-dependent increase in intracellular copper upon treatment with DSF-Cu, up to 30 fold at the maximum DSF-Cu concentration tested (Fig. 6.5A).

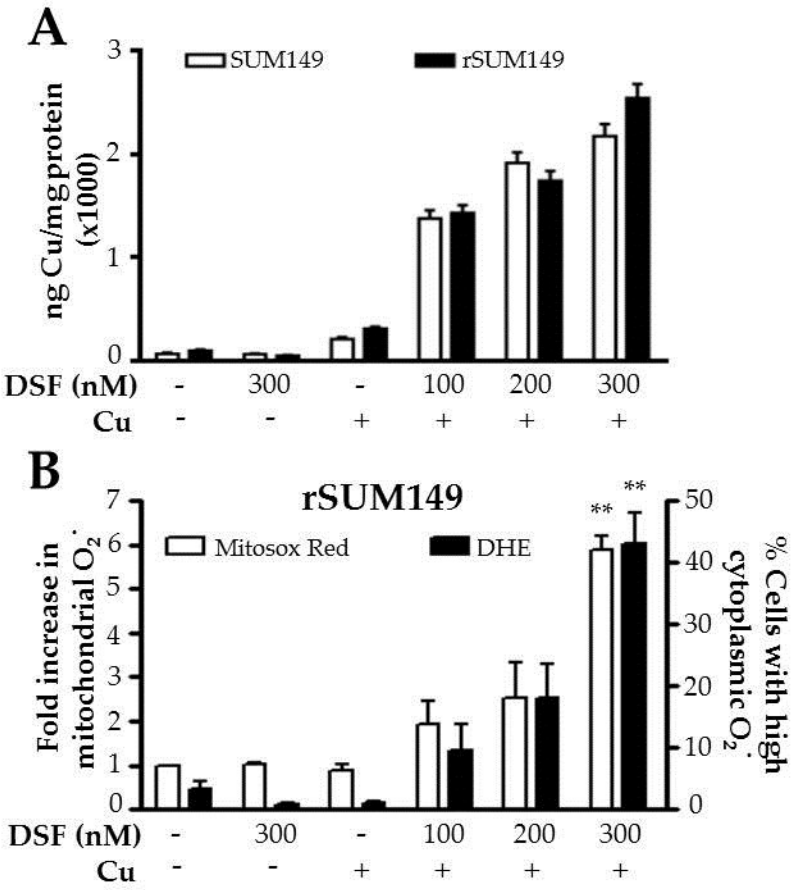

Figure 6.5: DSF strongly induces copper uptake in IBC cells, which is associated with significant accumulation of ROS

A, Copper content of SUM149 and rSUM149 cell lysates following 24 h treatment with DSF (300 nM), copper (10 μM), or DSF-Cu (100-300 nM, 10 μM) as measured by ICP-HRMS. Copper was normalized to protein content for each sample. **B**, Left axis shows fold induction of mitochondrial superoxides (lwhite bars), and right axis shows percentage of cells with high cytoplasmic superoxides (black bars) as measured by flow cytometric staining with MitoSOX Red or DHE respectively in rSUM149 cells treated with DSF (300 nM), copper (10 μM), or DSF-Cu (100-300 nM, 10 μM). **p<0.005.

6.5 DSF-Cu induces ROS accumulation and redox signaling in therapy-resistant rSUM149 cells

Since we observed that DSF-Cu induced cell death in the redox adapted rSUM149 cell line, we characterized the effects of DSF alone and DSF-Cu on ROS generation and downstream signaling. Flow cytometric dyes were utilized to measure relative levels of various ROS in rSUM149 cells. Data in Figure 6.5B show that while DSF and copper did not cause appreciable ROS accumulation as single agents at the concentrations tested, the DSF-Cu complex significantly induced the accumulation of mitochondrial (Mitosox Red, white bars) and cytoplasmic (DHE, black bars) superoxide radicals in rSUM149 cells, which are resistant to classical ROS generating agents such as paraquat and hydrogen peroxide, as well as multiple targeted and chemotherapeutics [78, 320, 415]. The increase in ROS corresponded with increased phosphorylation of the pro-apoptotic stress-related p38 MAPK as early as 4 h post treatment, with sustained activation 24 h post-treatment, as well as activation of redox-sensitive ERK1/2 (p44/42 MAPK) (Fig. 6.6).

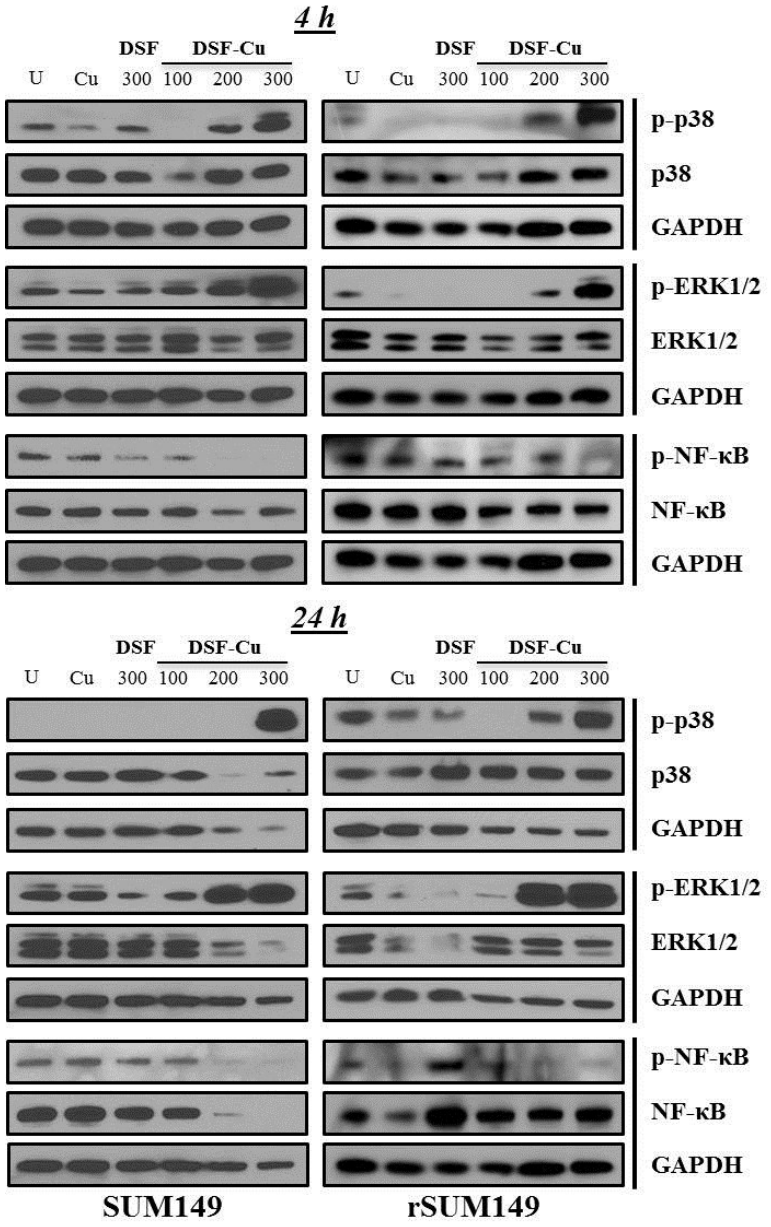

Figure 6.6: DSF-Cu activates redox-sensitive signaling and inhibits the pro-survival NF-κB pathway

Western immunoblot analysis of p38, ERK1/2, and NF-κB phosphorylation status in SUM149 and rSUM149 cells treated with DSF (300 nM), copper (10 μM), or DSF-Cu (100-300 nM, 10 μM) for 4 (above) or 24 (below) h. Total p38, ERK1/2, NF-κB, and GAPDH were used as loading controls.

NF-κB and Nrf2 are two important redox-responsive TFs that are activated by oxidative stress and promote the transcription of antioxidant genes and pro-survival molecules [36, 285]. DSF-Cu treatment resulted in downregulation of NF-κB phosphorylation as early as 4 h following treatment (Fig. 6.6), and this reduction was sustained 24 h post-treatment; total NF-κB expression was also reduced in SUM149 cells at 24 h (Fig. 6.6). Interrogation of Nrf2 transcriptional activity via an ARE luminescent reporter assay revealed that copper (10 μM) and high dose DSF (10-20 μM) induced Nrf2 transcriptional activity as single agents; however, the strongest Nrf2 induction was observed with low dose DSF-Cu treatment (150 nM, Fig. 6.7A). Interestingly, Nrf2 activation relative to untreated cells was higher in rSUM149 cells in response to reach treatment. In summary, DSF-Cu induces a strong oxidative stress response in the redox-adapted rSUM149 cells.

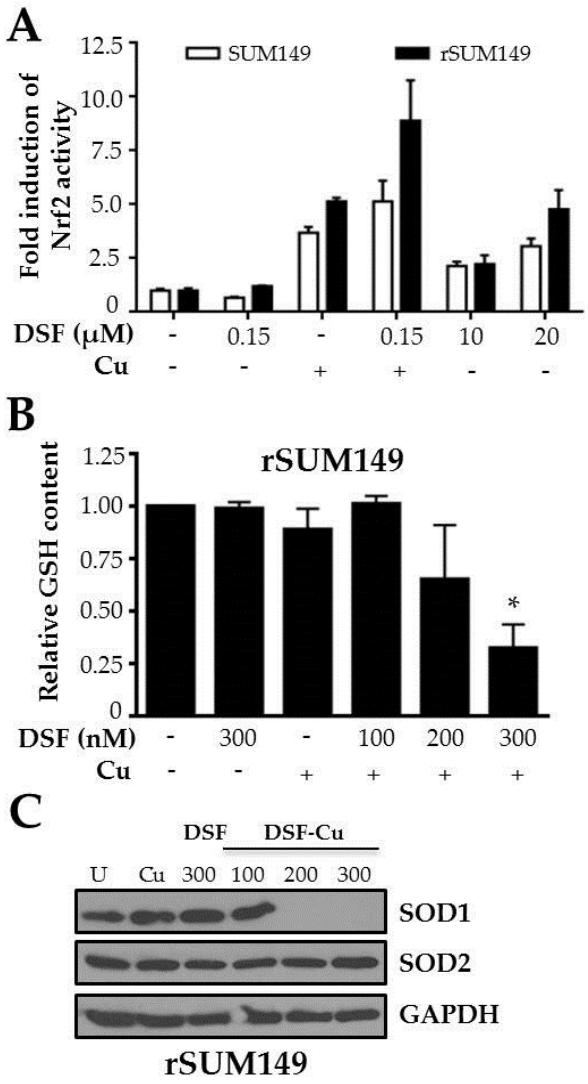

Figure 6.7: DSF-Cu activates the Nrf2 transcription factor but decreases cellular antioxidant capacity

A, Fold induction of Nrf2 activity as measured by ARE-responsive luciferase activity in SUM149 and rSUM149 cells treated with DSF (10-20 μM), copper (10 μM), or DSF-Cu (150 nM and 10 μM). **B**, Reduced glutathione content of rSUM149 cells treated with DSF (300 nM), copper (10 μM), or DSF-Cu (100-300 nM and 10 μM) relative to untreated cells as measured by Promega's GSH-Glo kit. **C**, Western immunoblot analysis of SOD1/2 expression in rSUM149 cells treated with DSF (300 nM), copper (10 μM), or DSF-Cu (100-300 nM, 10 μM). GAPDH was used as a loading control.

6.6 DSF-Cu inhibits intracellular antioxidants SOD1 and GSH

Since DSF-Cu increased ROS and redox signaling in the rSUM149 cells, which have high basal levels of antioxidants [78], we measured the expression of SOD1/2 and GSH in cells treated with DSF or DSF-Cu. The cellular pool of GSH was significantly reduced in rSUM149 cells following DSF-Cu treatment (Fig. 6.7B). Additionally, while SOD2 levels as measured by western immunoblot remained unchanged, SOD1 expression was strongly downregulated (Fig. 6.7C) following treatment with doses of DSF-Cu which are associated with cell death (Fig. 6.2B). Reduction of the cell's antioxidant defenses allows for the accumulation of ROS, which ultimately triggers oxidative stress-induced death as discussed in Section 1.3.2. Incubation of the cells with an exogenous SOD mimetic (MnTnHex-2-PyP^{5+}) with potent antioxidant activity effectively blocked cell death caused by DSF-Cu treatment (Fig. 6.8), confirming the pro-oxidant role of DSF-Cu.

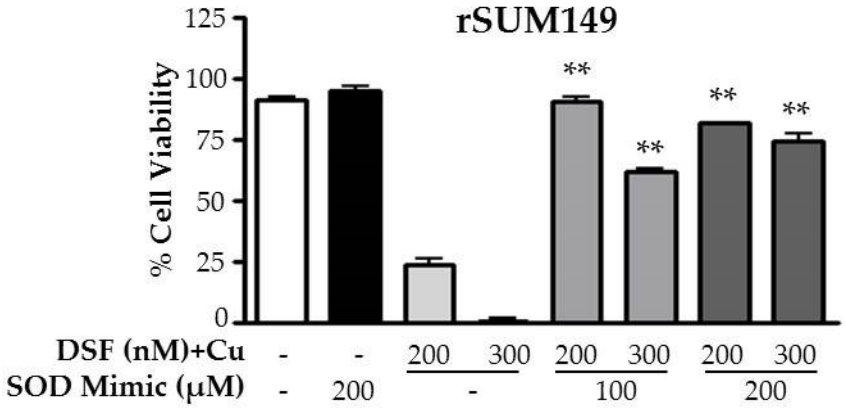

Figure 6.8: Addition of an SOD mimetic potently reverses DSF-Cu-mediated cell death in rSUM149 cells

Viability of rSUM149 cells treated with DSF-Cu (200-300 nM and 10 μM) ± an SOD mimetic (MnTnHexyl-2-Pyp^{5+}, 100-200 μM) as measured by trypan blue exclusion assay.

6.7 DSF-Cu downregulates XIAP and induces apoptosis in IBC cells

Following combination treatment with DSF-Cu and in association with cell death, there was a significant reduction in expression of XIAP, which is associated with therapeutic resistance in cell line models of IBC [78, 114], in both SUM149 and rSUM149 cells (Fig. 6.9). There was also an observed decrease in expression of the translation initiation factor eIF4G1 (Fig. 6.9), which has been reported to disappear during apoptosis due to its role as a substrate of activated caspases [432, 433]. Both of these findings indicate oxidative stress-induced apoptosis; an apoptotic mechanism of cell death was confirmed via western immunoblot analysis of PARP, which was cleaved in both cell lines (Fig. 6.9).

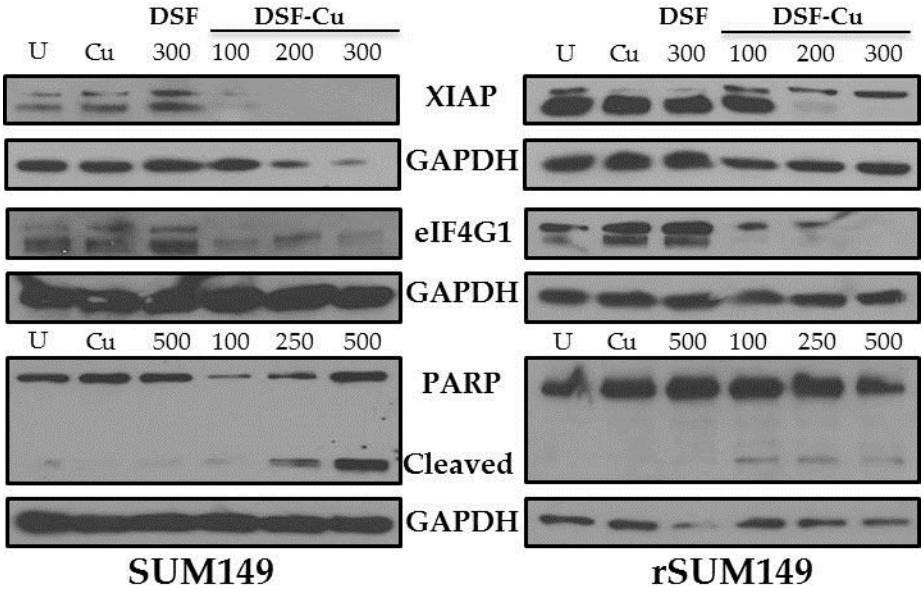

Figure 6.9: DSF-Cu reduces XIAP and eIF4G1 expression and induces apoptosis in SUM149 and rSUM149 cells

Western immunoblot analysis of XIAP and eIF4G1 expression and PARP cleavage in SUM149 (left) and rSUM149 (right) cells treated with DSF (300-500 nM), copper (10 μM), or DSF-Cu (100-500 nM, 10 μM). GAPDH was used as a loading control.

6.8 DSF-Cu inhibits ALDH1 activity in SUM149 IBC cells

Disulfiram is classically known as an inhibitor of aldehyde dehydrogenases; this mechanism is responsible for its anti-alcoholism activity, as it results in the build-up of toxic aldehydes when the patient consumes alcohol [434]. Since ALDH1 activity has been linked to stem cell-like properties [435] and is associated with increased growth capacity in 3D culture conditions and enhanced tumorigenic potential in xenograft studies [436-439], we characterized the effect of DSF and DSF-Cu on the ALDH+ stem cell-like population of SUM149 cells. SUM149 cells were treated for 24 h with a dose of DSF (100 nM) ± copper that induces minimal cell death and then analyzed for ALDH1 activity using the flow cytometric ALDEFLUOR assay; the specific ALDH inhibitor DEAB was used as a negative control for each sample. Data in Figure 6.10 show that while neither DSF nor copper as a single agent affected the ALDH+ population, the combination of DSF-Cu reduced the proportion of ALDH+ cells in the total population by approximately half (Fig. 6.10, $p < 0.05$).

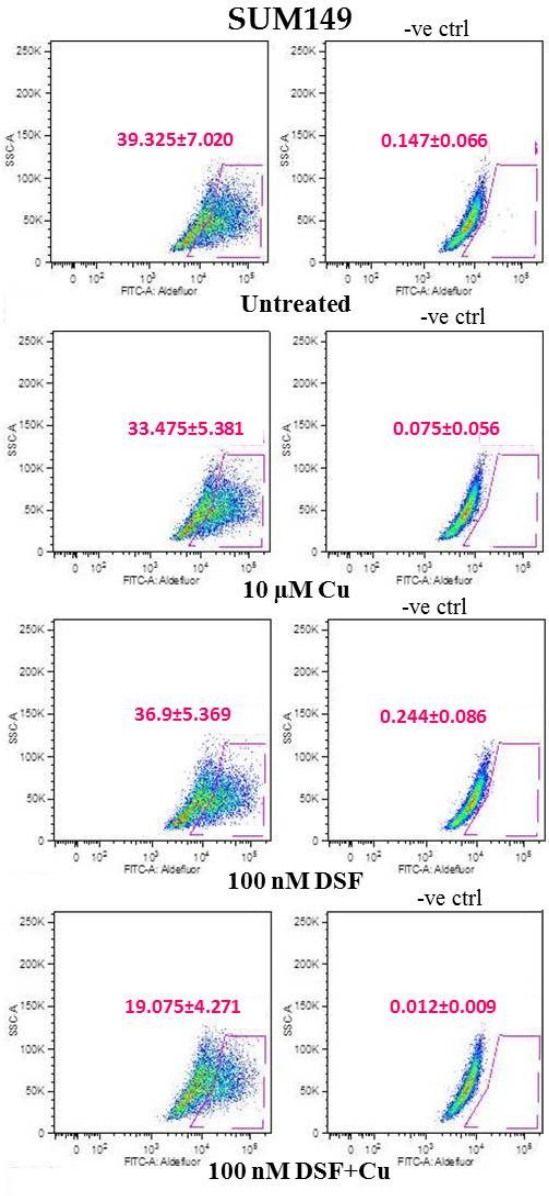

Figure 6.10: DSF-Cu inhibits ALDH activity in SUM149 cells

Representative flow cytometric analysis of ALDH activity in SUM149 IBC cells treated DSF (100 nM), copper (10 µM), or DSF-Cu (100 nM and 10 µM). Cells were incubated with ALDEFLUOR substrate (BAAA) and the specific inhibitor of ALDH, DEAB, was used to establish the baseline fluorescence of these cells and to define the ALDEFLUOR-positive region (gated population). Numbers shown are mean ± SEM of four separate experiments.

6.9 DSF-Cu potently inhibits anchorage-independent growth potential in SUM149 and rSUM149 cells

Anchorage-independent colony formation in soft agar is considered to be a reasonably good predictor of *in vivo* activity [381, 382]. Thus, we examined the effects of DSF and DSF-Cu on anchorage-independent growth (AIG) in SUM149 and rSUM149 cells; AIG was potently blocked by the combination of DSF in the nanomolar range (100-300 nM) in the presence of copper (Fig. 6.11). Additionally, DSF alone inhibited AIG in a dose-dependent manner in the 10-20 μM range in SUM149 cells (data not shown), similar to results in 2D culture in Figure 6.1A. Neither copper nor nanomolar doses of DSF had any measurable effect on the AIG potential of SUM149 or rSUM149 cells (Fig. 6.11). Representative images in Figure 6.11 show an abundance of large colonies growing in untreated or single treatment samples, but diffuse individual cells in the DSF-Cu samples.

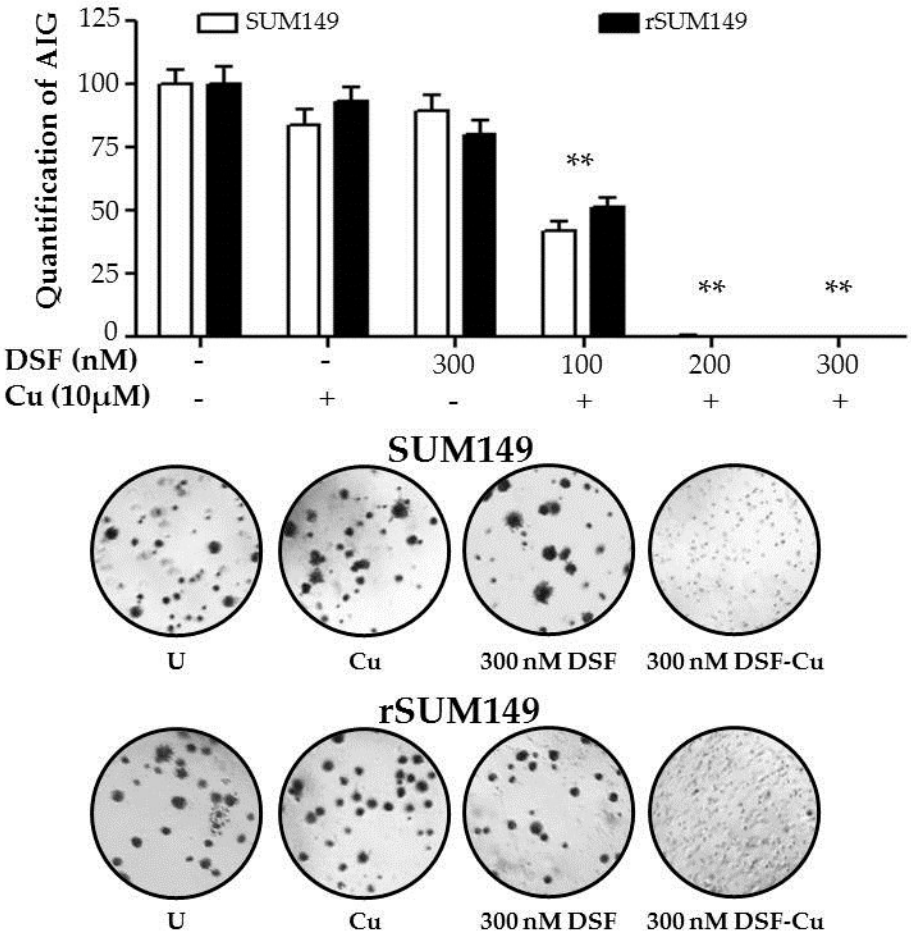

Figure 6.11: DSF-Cu potently inhibits anchorage-independent growth of SUM149 and rSUM149 cell lines

Quantification of anchorage-independent growth assay relative to untreated cells in SUM149 and rSUM149 cells treated with DSF (300 nM), copper (10 μM), or DSF-Cu (100-300 nM and 10 μM). Representative images of treated cells are shown below.

6.10 Discussion

We report herein the ability of a redox modulatory combination, DSF-Cu, to induce apoptotic cell death in IBC cells in a copper- and ROS-dependent manner. The combination is effective in patient-derived SUM149, MDA-IBC-3, and SUM190 cells, as well as SUM149 and SUM190-derived lapatinib-resistant cells (rSUM149, rSUM190) and a model of exogenous XIAP overexpression [78]. It is interesting to consider the differential sensitivity of the IBC models to DSF as a single agent; further studies to tease out the mechanisms behind this may reveal interesting data as to why the MDA-IBC-3 cell line, which has not been studied on the basis of redox responses, seems to be relatively insensitive to DSF alone. DSF potency was significantly enhanced in all lines by the addition of exogenous copper, and cell death was associated with intracellular copper accumulation and induction of ROS. Redox-sensitive signaling pathways p38, ERK1/2 (p44/42 MAPK), and Nrf2 were activated, while phosphorylation of the classical pro-survival factor NF-κB p65 was decreased. Examination of cellular antioxidant status revealed that a decrease in radical detoxifying capacity resulting from reduced SOD1 expression and loss of GSH activity caused the increased capacity for ROS accumulation. The cell death caused by DSF-Cu treatment was almost completely reversed by addition of an exogenous antioxidant (SOD mimetic), confirming the hypothesis that ROS induction is the mechanism of action responsible for DSF's efficacy in IBC cells. Cell

death was accompanied by a reduction in XIAP and eIF4G1 expression as well as PARP cleavage. Aldehyde dehydrogenase activity was inhibited by DSF-Cu, and anchorage-independent growth was negatively affected by the combination. The mechanisms by which DSF-Cu induces cell death are summarized in Figure 6.12.

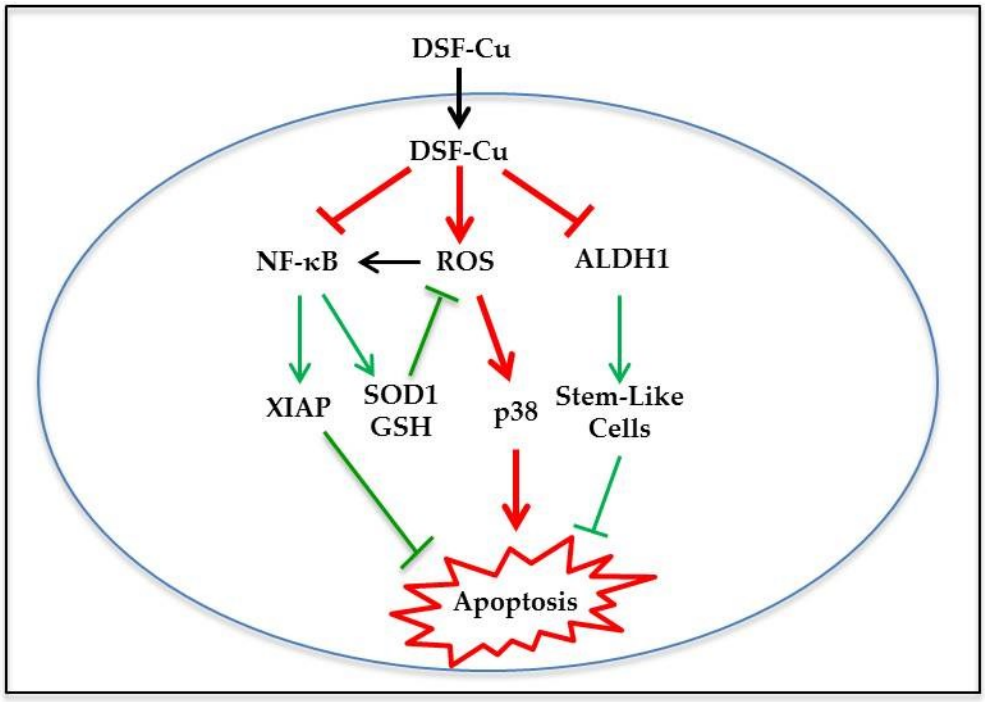

Figure 6.12: Mechanisms of DSF-Cu-induced cell death

DSF acts as an ionophore, bringing copper into cells in a Ctr1-independent manner. DSF-Cu generates a significant amount of ROS through influx of reactive copper ions and inhibition of cellular antioxidant capacity, possibly through inhibition of NF-κB, which regulates the transcription of many antioxidants as well as the anti-apoptotic protein XIAP. Downregulation of XIAP and activation of the pro-apoptotic p-38 pathway by ROS promote apoptotic cell death. Additionally, DSF-Cu inhibits ALDH activity, reducing the population of stem-like cells.

It is widely known that cancer cells often generate increased levels of ROS compared to normal cells, and that this increase in ROS can alter cell signaling pathways and induce further mutations to promote cell growth [253, 265, 440]. In order to compensate for increased oxidative stress, cancer cells activate redox adaptive mechanisms which enhance their ability to detoxify ROS; these changes can lead to therapeutic resistance [264]. As discussed in Sections 1.3.4 and 1.3.5, constitutive activation of the redox-sensitive TF NF-kB is observed in many cancer types [264, 291], and upregulation of antioxidant and ROS scavenging mechanisms have been associated with therapeutic resistance in cell line models including our own [78, 225, 441, 442]. The constitutive increase in ROS in these adapted cells theoretically makes them more sensitive toward therapies that inhibit ROS detoxification or further increase ROS above the apoptotic threshold [235, 253], supporting redox modulation as a promising strategy for therapeutic intervention.

Disulfiram is an old drug recently repurposed for cancer therapy, which is especially attractive due to the fact that extensive pharmacokinetics, clinical data, and FDA approval could facilitate its rapid incorporation into Phase 2 clinical trials. Many reports have cited an ROS-dependent mechanism of action for DSF [419-421, 443-445], making it an attractive agent for targeting redox adapation in IBC. Additionally, tumor cell toxicity has been reported to increase when DSF is used in conjunction with heavy

metals including copper, cadmium, and zinc [419, 420, 422-424, 426, 428, 446]. As cancer cells often accumulate copper at higher levels than normal tissue [447, 448], DSF's copper-mediated mechanism of action presents a potential method by which to target tumor cells preferentially, thus decreasing off target effects and increasing the therapeutic index.

As a single agent, DSF induced toxicity in the IBC cell lines only at concentrations in the micromolar range at doses that are not readily achievable in human plasma, where the accepted daily dosing of 250-500 mg per day yields a concentration of < 2 μM [449]. However, DSF's potency was significantly enhanced by the addition of copper, with IC_{50}s of 300 nM and below. So while these cell lines are relatively insensitive to DSF as a single agent compared to other breast cancer cell lines that have been tested (IC_{50}s of 400-1100 nM in MCF7, MDA-MB-231, and T47D) [421], they become equally or more sensitive than those cell lines upon the addition of copper, with cell death occurring at DSF concentrations well below those achievable *in vivo*.

Inhibition of antioxidant function has the potential to overcome redox adaptive therapeutic resistance. Sensitization of resistant pancreatic cancer cells has been achieved through knockdown of SOD2 [450], and downregulation of antioxidant capacity reversed paclitaxel resistance in models of bladder and breast cancer [225]. Analysis of DSF's proposed redox modulatory mechanism revealed that DSF-Cu not

only induces ROS, consistent with previous studies [419-421, 451], but also reduces SOD1 expression and GSH activity. Our results are consistent with previous reports that ROS induction by DSF is accompanied by oxidation of the intracellular pool of GSH [419, 451]; in contrast, Brar et al., who reported a different mechanism of action for DSF, did not detect ROS induction or GSH oxidation following treatment [452].

Whether these effects are mediated by DSF, copper, or the complex remains to be determined. It is possible that DSF merely acts as a transporter of copper into cancer cells, promoting the accumulation of reactive copper ions above levels that would be permitted by the tightly regulated cellular copper transport machinery; indeed, this view is supported by several studies including this one that have shown dramatic increases in intracellular copper levels following DSF treatment [428, 431]. Interestingly, Hothi et al. showed that DSF single agent efficacy was dependent on endogenous copper in the media (provided by fetal bovine serum), with the addition of BCS to DSF blocking its efficacy [453], while Navratilova et al. determined that insensitivity of densely plated cells to DSF compared to sparsely plated cells was due to rapid depletion of copper in the media, further supporting the role of copper in DSF 'single agent efficacy' [454]. Reversal of cell death in SUM149 and rSUM149 cells through copper chelation indicates that copper is indeed required for DSF-induced cell death. However, none of these results can firmly rule out the possibility that it is the reactive DSF-Cu

complex that is responsible for cell death rather than copper alone; determination of this requires further study.

Expression of XIAP, which we and others have previously correlated with therapeutic resistance in IBC and other cancer models, was down-regulated by DSF-Cu treatment. Reduction in this potent anti-apoptotic protein helps to tip the balance of pro- and anti-apoptotic factors in the direction of cell death. This may occur as a result of NF-κB inhibition or the increased copper levels within the cell; XIAP is regulated by direct binding of copper to its cysteine residues, which induces a conformational change that decreases XIAP stability and blocks its caspase inhibitory function [455]. Additionally, the combination of DSF-Cu reduced expression of the translation initiation factor eIF4G1, which is a known caspase substrate whose degradation is indicative of apoptotic cell death [432, 433]. As an important mediator of IRES-mediated cap-independent translation during times of cellular stress, eIF4G1 is essential to the pathogenesis of IBC tumors, promoting the formation of tumor emboli and passive metastasis through upregulation of p120 catenin, which anchors E-cadherin at tumor cell-cell adherens junctions [46]. The hypoxia/oxidative stress resistance factor VEGF is also under the translational control of eIF4G1, and XIAP, which is known to contain an IRES element, may also be regulated at least in part by eIF4G1 [50, 114]. Through its effects on these

proteins, DSF-Cu has the potential to reduce IBC pathogenicity and sensitize cells toward therapeutic apoptosis.

DSF-Cu potently activates the SAPK p38 MAPK, which is known to mediate apoptosis induced by external stimuli including oxidative stress [456]. Activation of p38 has been observed in response to many pro-oxidant agents [408, 457-461] as well as DSF or DSF-Cu [419-421]. Interestingly, the redox-sensitive ERK1/2 pathway is also activated in IBC cells exposed to DSF-Cu, while DSF-Cu has previously been reported to inhibit ERK1/2 signaling in AML cells [419]. While ERK1/2 generally promotes cell survival, the downstream effects of ERK1/2 signaling are known to be cell type- and stimuli-specific, and ERK1/2 phosphorylation can also promote apoptosis under certain circumstances [405, 410]. In a previous study, we observed ERK1/2 activation as a compensatory response to apoptotic stimuli in rSUM149 cells [415]; however, further investigation is required to determine the effects of ERK1/2 signaling in IBC cells in response to DSF-Cu.

NF-κB is a potent pro-survival TF that is activated by oxidative stress [36, 285]. NF-κB can protect cells from apoptosis induced by cytokines and chemotherapeutic agents through modulation of downstream genes including anti-apoptotic proteins such as Bcl-2, Bcl-xL, cIAP1/2, XIAP, and antioxidants including SOD and Trx2 [462]. NF-κB serves as a significant barrier to effective cancer treatment, and a number of tumor cell types have been reported to express high levels of constitutively active forms of NF-κB

[35, 426]. Interestingly, the anti-apoptotic protein XIAP can activate NF-κB signaling [197, 463], so targeting either of these molecules may negatively affect the other as well, amplifying the pro-apoptotic effects. The ability of DSF-Cu to inhibit NF-κB signaling while simultaneously inducing ROS and activating pro-apoptotic p38 signaling indicates the potential for strong anti-tumoral efficacy.

The Nrf2 TF is activated by alteration of cellular redox status due to elevated levels of ROS or reduction of antioxidant capacity. In times of oxidative stress, Nrf2 is released from its repressor Keap1, which undergoes oxidative modification, and activates genes with an ARE sequence [414]; in this way, Nrf2 serves as a sensor of oxidative stress, and its activation in SUM149 and rSUM149 cells (Fig. 3B) following DSF-Cu treatment indicates an oxidative intracellular environment. While downstream targets of Nrf2 include antioxidant enzymes such as SOD, NQO1, and GST [282, 308, 414], DSF-Cu treatment induced cell death (Fig. 6.1, 6.2) and decreased SOD and GSH (Fig. 6.7B, 6.7C), indicating that Nrf2 activation was not sufficient to overcome the massive amounts of ROS induced by DSF-Cu.

ALDH activity has been linked to cancer stem cells (CSCs) [464-466] and is associated with enhanced tumorigenic and metastatic potential [437, 439, 467] as well as resistance to chemo- and targeted therapies [468, 469]. Additionally, CSCs exhibit low basal levels of ROS [440, 470, 471], and some studies have shown that ALDH1A1 plays

an important role in protection again oxidative stress in multiple types of stem cells [472-474]. ALDH may be in part responsible for maintenance of low intracellular ROS in CSCs, and thus represents an important potential target for anti-tumoral therapy, particularly in redox adapted cells. Although DSF is known to be an ALDH inhibitor [475, 476], DSF alone did not show any effect on ALDH positivity at the concentrations tested, which are far below the IC_{50} for DSF in this model. However, the combination of DSF-Cu at a concentration associated with minimal cell death did inhibit ALDH activity in the IBC cells, which is consistent with previous results in glioblastoma [420] and breast cancer [421] cell lines where efficacy was observed only when DSF and Cu were used in combination. Further, the decrease in ALDH activity correlated with decreased tumorigenic properties. Because certain drugs can have differential effects in 2D and 3D cell culture models [382]and AIG is predictive of *in vivo* tumorigenicity [381], consistent induction of cell death in both model types provides strong evidence that the DSF-Cu combination may be efficacious *in vivo*. Ongoing studies in our laboratory to investigate the efficacy of DSF and DSF-Cu in murine xenograft models of IBC indicate that the combination is a potent inhibitor of tumor growth *in vivo*; completion of these studies will help to bolster the translational value of our work.

Together, these data demonstrate the efficacy of the DSF-Cu combination as an inducer of apoptosis in IBC models. DSF-Cu enhances ROS accumulation and apoptotic

signaling while inhibiting pro-survival pathways and antioxidant activity. This study indicates that DSF-Cu may be a successful therapeutic for IBC patients, including those with acquired therapeutic resistance due to redox adaptive mechanisms, and supports the translation of this FDA-approved drug into clinical trials for IBC.

7 Conclusions and Implications

In conclusion, the data presented in this dissertation demonstrate the reversibility of acquired therapeutic resistance in IBC and enhance the current understanding of the mechanisms behind therapeutic resistance and resistance reversal. While previous studies had identified potential therapeutic targets associated with resistance to the ErbB1/2 inhibitor lapatinib, the extent to which these mechanisms contributed to resistance, whether or not that resistance was specific to lapatinib or could mediate cross-resistance to other anti-cancer drugs, and the feasibility of targeting those resistance mechanisms had yet to be investigated. We determined that rSUM149 cells were cross-resistant to a multitude of targeted and chemo-therapeutic agents, and that resistance reversal was associated with a renewed ability to accumulate ROS and activate an oxidative stress response through AMPK, likely due to downregulation of protective antioxidants and anti-apoptotic proteins. Targeting of XIAP or redox adaptation in the IBC cells was able to overcome therapeutic resistance to apoptosis through both the extrinsic and the intrinsic pathways. Interestingly, several of the agents used modulated both apoptotic dysregulation and redox adaptive mechanisms to induce apoptosis; a schematic of their effects can be found in Figure 7.1. In this chapter, the implications of our work will be discussed, as well as new questions that have arisen from the results of these studies that will guide future investigations in this area.

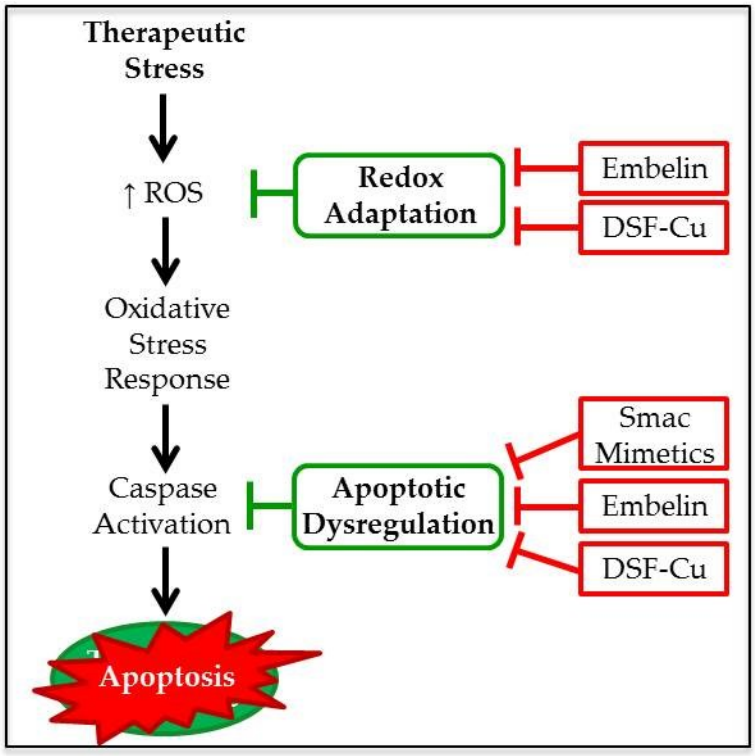

Figure 7.1: Schematic of IBC therapeutic resistance mechanisms and targeting of those mechanisms

Therapeutic resistance to activators of the intrinsic and extrinsic apoptotis pathways in cellular models of IBC is mediated through apoptotic dysregulation and redox adaptation. Enhanced expression of anti-apoptotic factors, especially the potent caspase inhibitor XIAP, as well as activation of pro-survival signaling such as NF-κB, which modulates transcription of the apoptotic program, contributes to apoptotic dysregulation. Redox adaptation is achieved through activation of redox-sensitive transcription factors and upregulation of the cell's antioxidant capacity. Targeting of apoptotic dysregulation using small molecule inhibitors of the IAPs including the Smac mimetic Birinapant and embelin overcomes therapeutic resistance to induce apoptosis; targeting of redox adaptation using the redox modulatory combination DSF-Cu also overcomes therapeutic resistance to induce apoptosis. Interestingly, the XIAP inhibitor embelin also reduces cellular antioxidant capacity, negatively affecting the redox adaptive mechanism; further, the redox modulatory combination DSF-Cu also negatively affects expression of XIAP, inhibiting the resistance mechanism of apoptotis dysregulation, indicating a potential link between the two.

The high throughput study investigating sensitivity of three progressive, isogenic-derived models of IBC was motivated by the observations that acquired therapeutic resistance in the rSUM149 and rSUM190 models was associated with distinct changes which reduced sensitivity toward classical ROS-inducing agents in addition to lapatinib. We questioned the reversibility of this resistance; were the changes involved the result of random mutations that were propagated due to a selective growth advantage, or were these features the result of some sort of stress response? In the event that the resistant cells were employing a stress responsive mechanism, it would be likely that resistance could be reversed by removal of the selective pressure, i.e. the stressor. The previous finding that XIAP overexpression in the resistant lines was the result of post-translational upregulation via an IRES element suggests the involvement of an inducible stress response, and the discovery that acquired resistance was reversible through lapatinib removal indicates a non-mutational mechanism, supporting this theory. Further interrogation of signaling including pro-survival NF-κB and the SAPKs JNK and p38 in the isogenic cell line models may help to determine the pathways that drive this response. Additionally, it is interesting to contemplate whether or not the IBC pathogenesis factor eIF4G1 might be involved in IRES-mediated upregulation of XIAP. eIF4G1 mediates cap-independent translation in times of cell stress and has been found to drive the translation of other IRES-containing mRNAs including p120 catenin and

VEGF in IBC [46, 50]; therefore, the upregulation of another IRES-containing protein in IBC cells in response to cellular stress raises the question of eIF4G1's potential involvement.

According to the DTP/DTEP concept, drug resistant cells may exist *de novo* in a heterogeneous population, but are selected for and allowed to grow out when sensitive cells are killed by treatment [477]. Indeed, these drug resistant cells may represent a subpopulation of cancer stem cells, which are known to exhibit reduced drug sensitivity [468, 469]. Measurement and comparison of stem cell markers including ALDH, CD24, and CD44 [478] in the parental cells and their resistant counterparts may help to determine whether this is the case. Interestingly, these two theories are not mutually exclusive; it may be that only cancer stem cells have the capability to combat cellular stress with an adaptive response, so that the resistant populations are the result of the expansion of a stem cell-like population when the drug resistant cells were killed off as a result of their inability to mount a protective response.

In addition to determining the reversibility of resistance in the rSUM149 cell line, the qHTS study confirmed a state of cross-resistance in those cells which was protective against the tyrosine kinase inhibitors sorafenib, sunitinib, and gefitinib as well as several chemotherapeutics that target DNA synthesis and repair (capecitabine, mitoxantrone, bleomycin, and mitomycin), all of which are known to induce oxidative stress [479-488].

These results make a very strong case for causal involvement of redox adaptation in therapeutic resistance in the rSUM149 cells. Further, reversal of resistance to lapatinib, associated with increased ROS-generating capabilities and reduced antioxidant and anti-apoptotic protein expression, was associated with resensitization to the same drugs. These results reiterate the importance of targeting the IAPs and/or the redox adaptive phenotype as a means of preventing or overcoming therapeutic resistance to a variety of anti-cancer agents and served as a rationale for the studies in Chapters 4, 5, and 6. An important future direction from this and previous studies is the validation of the resistance mechanisms observed in our cell line models in IBC patient tissue. Analysis of anti-apoptotic molecules and antioxidants at the protein level (because post-transcriptional modulation has been identied in these models) in matched pre- and post-treatment patient biopsies would enable us to evaluate the proposed resistance mechanisms *in vivo*; correlation of our *in vitro* findings with clinical data is an important step to substantiate the relevance of our work and determine whether our studies could translate to improved patient care.

Studies utilizing the Smac mimetics stemmed from the observed inverse correlation between IAP expression and drug sensitivity in rSUM190, rSUM149, and rrSUM149 cells. The use of two Smac mimetics with differential affinities for XIAP allowed us to tease out the involvement of XIAP specifically in resistance to TRAIL, a

highly clinically relevant agent. While the rSUM149 cells show increased expression of many anti-apoptotic factors, inhibition of cIAP1/2 alone by GT13042 was much less effective than inhibition of XIAP and cIAP1/2 by Birinapant in both SUM190 and SUM149. Interestingly, the SUM190 cells, which express high levels of XIAP mRNA and protein relative to SUM149 [103, 114] and are inherently resistant to TRAIL, were sensitive to the Smac mimetics as single agents, which is rather uncommon [365, 367-369]. These observations suggest a sort of 'IAP addiction' in the Her2-overexpressing SUM190 model, where the cells are highly dependent on IAP expression for survival. This phenomenon requires futher investigation, but determination of factors associated with increased reliance on the IAPs could be useful in predicting patient responses and choosing therapies. Studies in this chapter confirmed the utility of targeting the IAPs, XIAP in particular, and indicate that the Smac mimetics merit further study in animal models of IBC, which could pave the way for clinical trials.

While studies in Chapter 4 highlighted the importance of the IAPs in mediating drug resistance, the experiments in Chapter 5 confirmed the importance of redox modulation as a mechanism of therapeutic sensitization. While embelin effectively reduced the expression of XIAP, embelin+TRAIL-induced cell death was partially reversible through the addition of an exogenous antioxidant, indicating that ROS generation was a significant contributor to the combination's cytotoxicity. It is

interesting to contemplate whether embelin is an XIAP inhibitor *and* an ROS-inducing agent, or whether embelin induces ROS *through* its XIAP inhibitory function. XIAP expression and the levels of cellular antioxidants have correlated directly in all of the studies undertaken in this dissertation; XIAP, SOD1/2, and GSH are all overexpressed in the resistant cell lines, and XIAP and SOD1 were decreased in the resistance reversal cells (GSH levels were not tested, and SOD2 was not reduced in the rrSUM149 cells, data not shown). Treatment of rSUM149 cells with the XIAP inhibitor embelin downregulated SOD1 expression and decreased cellular GSH content, and targeting of the redox adapted state in rSUM149 with DSF resulted in decreases in both antioxidants SOD1 and GSH as well as XIAP. All of these data indicate that XIAP may modulate antioxidant capacity, and perhaps vice versa. There is evidence that XIAP can regulate the expression of certain antioxidants in a number of normal cell types [462, 489, 490]; one group tracked this function to modulation of NF-κB signaling [462]. Additionally, XIAP is known to promote SOD1 activity through activating ubiquitination of the copper chaperone CCS [455]. Conversely, studies in an animal model of transient focal cerebral ischemia determined that residues in XIAP undergo oxidation by ROS, which appears to negatively affect its anti-apoptotic functions; oxidation of XIAP was prevented by overexpression of SOD1 [491]. This study provides evidence that cellular redox status and antioxidant expression can also affect XIAP. Ongoing studies in our lab

utilizing the ectopic XIAP overexpression model SUM149 wtXIAP are aimed at determining whether XIAP does indeed play a role in regulating the redox capacity of IBC cells. We also plan to investigate whether these cells exhibit cross-resistance to other therapeutics as the rSUM149 cells do, and whether the same alterations in cellular redox capacity are involved.

The studies in Chapter 6, which were based on our understanding of the resistance and resistance reversal models of IBC, were focused on determining the feasibility of targeting the redox adaptive phenotype observed in rSUM149 and rSUM190 cells. Because therapeutic resistance is so common in IBC and this mechanism is associated with such a broad spectrum of resistance, strategies to overcome redox adaptation may be highly relevant to the IBC population. Although modulation of this axis using embelin was effective in rSUM149, embelin's reported effects on inflammation [392], hormone regulation [492], and antioxidant pathways [493] may blunt its efficacy or cause off target effects *in vivo*; thus, the development of other, more clinically relevant drugs is needed. DSF is an especially attractive redox modulator due to its multiple levels for cancer cell specificity; because its mechanism of action is copper-dependent, it is likely to preferentially target cells with high levels of copper. In fact, copper levels are elevated in a number of cancers, although copper measurement has never been performed on IBC patient tissue [447]; thus, analysis of copper levels in

IBC tissue merits future study. Further, the suggested 'threshold model' of ROS-induced apoptosis indicates that cancer cells, which often contain higher levels of ROS than normal cells, should be more vulnerable to additional oxidative insults because they are already near the threshold for apoptosis; it is suggested that their antioxidant defenses are already operating at maximum capacity to maintain homeostasis in the presence of high ROS, whereas normal cells with low ROS levels have a 'reserve' of antioxidants with which to combat exogenous oxidative stress [253].

Interestingly, DSF not only targeted the redox adaptive mechanism in IBC cells, inducing copper-dependent ROS accumulation in order to promote apoptotic cell death, but also reduced expression of XIAP, which we have now shown to be a potent mediator of therapeutic resistance through apoptotic dysregulation. This may occur through DSF-Cu-mediated inhibition of pro-survival NF-κB signaling, or perhaps the massive influx of copper into the cell caused by DSF facilitates copper binding to XIAP, promoting its destabilization and reduction in steady state levels [494]; additionally, XIAP may undergo oxidation by ROS [491]. Regardless of how the reduction in XIAP expression occurs, the effect is sensitization toward apoptotic cell death; it is interesting that the drug which was chosen for its redox modulatory abilities also negatively affects the other mechanism of therapeutic resistance identified by our studies. The fact that DSF-Cu inhibits both apoptotic dysregulation through downregulation of XIAP and redox

adaptation through reduction of the cell's antioxidant capacity may explain its very strong potency in the IBC cell lines, which is very promising from a therapeutic standpoint. The crosstalk between these two mechanisms and potential for modulation of antioxidant capacity by XIAP and vice versa merits further study.

In addition to downregulating XIAP and activating oxidative stress-induced apoptosis, DSF-Cu also inhibited the CSC-associated marker ALDH. This is intriguing in that if the original development of resistance in the rSUM149 and rSUM190 cell lines is due to the outgrowth of highly therapy-resistant stem cell-like cells, co-treatment with DSF-Cu could potentially prevent the development of resistance in the first place. Additionally, inhibition of NF-κB activity by DSF-Cu blocks the development of resistance through enhanced survival signaling, which is a common mechanism in many cancer types including IBC [35, 36]. DSF's efficacy in combination with copper at low concentrations that are readily achievable in humans suggests a promising future for this strategy; the incorporation of DSF or DSF-Cu into clinical trials for IBC in combination with standard therapeutics may prove to be beneficial for patients.

The development of biomarkers both for the rational selection of treatment regimens and as a measurement of therapeutic efficacy is important for improving CR rates. Due to the copper-dependent nature of DSF, intratumoral copper levels represent a potential biomarker for patients that might respond well to this sort of therapy, with

higher copper levels predicting a higher therapeutic index and increased tumor cell sensitivity. Since sensitivity to DSF-Cu-mediated cell death was associated with an increase in intracellular copper following treatment, copper levels could also potentially serve as a biomarker for treatment efficacy. The measurement of oxidative stress by non-invasive methods such as quantification of allantoins, F_2-isoprostanes, and 8-OHdG in the urine has recently come to light as a quick and easy way to monitor patient responses to ROS generating therapies [495, 496]. This technique represents a way to easily monitor oxidative stress and tumor response over time in order to determine whether DSF is effective in patients. The inclusion of biomarkers like these represents a step towards personalized medicine that could enhance our understanding of oxidative stress responses in patients; thus, these applications require further investigation.

The studies described here detail the first model of drug resistance reversal in IBC and provide mechanistic proof that XIAP and antioxidant overexpression are key mediators of therapeutic resistance in IBC cell line models. Further, these results provide evidence that XIAP may mediate cancer cell adaptation to oxidative stress through modulation of cellular antioxidant status, indicating yet another mechanism by which this potent IAP counteracts apoptosis. The utilization of clinical inhibitors of these resistance factors- Birinapant, which is in Phase 2 clinical trials for cancer, and DSF, which is FDA-approved for an alternate indication and currently in Phase 1, 2, and 3

clinical trials for the treatment of cancer- with promising results will hopefully facilitate the introduction of these agents into clinical trials targeting IBC and help to improve outcomes for this aggressive and deadly disease.

References

1. Hance KW, Anderson WF, Devesa SS, Young HA, & Levine PH (2005) Trends in inflammatory breast carcinoma incidence and survival: the surveillance, epidemiology, and end results program at the National Cancer Institute. *J Natl Cancer Inst* 97(13):966-975.

2. Gonzalez-Angulo AM, Hennessy BT, Broglio K, Meric-Bernstam F, Cristofanilli M, *et al.* (2007) Trends for inflammatory breast cancer: is survival improving? *Oncologist* 12(8):904-912.

3. Robertson FM, Bondy M, Yang W, Yamauchi H, Wiggins S, *et al.* (2010) Inflammatory breast cancer: the disease, the biology, the treatment. *CA Cancer J Clin* 60(6):351-375.

4. Yamauchi H, Woodward WA, Valero V, Alvarez RH, Lucci A, *et al.* (2012) Inflammatory breast cancer: what we know and what we need to learn. *Oncologist.* 17(7):891-899. doi: 810.1634/theoncologist.2012-0039. Epub 2012 May 1614.

5. Giordano SH & Hortobagyi GN (2003) Inflammatory breast cancer: clinical progress and the main problems that must be addressed. *Breast Cancer Res* 5(6):284-288.

6. Walshe JM & Swain SM (2005) Clinical aspects of inflammatory breast cancer. *Breast Dis* 22:35-44.

7. Dushkin H & Cristofanilli M (2011) Inflammatory breast cancer. *Journal of the National Comprehensive Cancer Network : JNCCN* 9(2):233-240; quiz 241.

8. Bonnier P, Charpin C, Lejeune C, Romain S, Tubiana N, *et al.* (1995) Inflammatory carcinomas of the breast: a clinical, pathological, or a clinical and pathological definition? *International journal of cancer. Journal international du cancer* 62(4):382-385.

9. Levine PH & Veneroso C (2008) The epidemiology of inflammatory breast cancer. *Semin Oncol* 35(1):11-16.

10. Wingo PA, Jamison PM, Young JL, & Gargiullo P (2004) Population-based statistics for women diagnosed with inflammatory breast cancer (United States). *Cancer Causes Control.* 15(3):321-328.

11. Chang S, Buzdar AU, & Hursting SD (1998) Inflammatory breast cancer and body mass index. *J Clin Oncol* 16(12):3731-3735.

12. Dawood S & Cristofanilli M (2011) Inflammatory breast cancer: what progress have we made? *Oncology (Williston Park).* 25(3):264-270, 273.

13. Mourali N, Muenz LR, Tabbane F, Belhassen S, Bahi J, *et al.* (1980) Epidemiologic features of rapidly progressing breast cancer in Tunisia. *Cancer.* 46(12):2741-2746.

14. Ben Hamida A, Labidi IS, Mrad K, Charafe-Jauffret E, Ben Arab S, *et al.* (2008) Markers of subtypes in inflammatory breast cancer studied by immunohistochemistry: prominent expression of P-cadherin. *BMC Cancer.* 8:28.(doi):10.1186/1471-2407-1188-1128.

15. Li J, Gonzalez-Angulo AM, Allen PK, Yu TK, Woodward WA, *et al.* (2011) Triple-negative subtype predicts poor overall survival and high locoregional relapse in inflammatory breast cancer. *Oncologist.* 16(12):1675-1683. doi: 1610.1634/theoncologist.2011-0196. Epub 2011 Dec 1676.

16. Boyle P (2012) Triple-negative breast cancer: epidemiological considerations and recommendations. *Annals of oncology : official journal of the European Society for Medical Oncology / ESMO* 23 Suppl 6:vi7-12.

17. Prost S, Le MG, Douc-Rasy S, Ahomadegbe JC, Spielmann M, *et al.* (1994) Association of c-erbB2-gene amplification with poor prognosis in non-inflammatory breast carcinomas but not in carcinomas of the inflammatory type. *Int J Cancer.* 58(6):763-768.

18. Van Laere SJ, Van der Auwera I, Van den Eynden GG, van Dam P, Van Marck EA, *et al.* (2007) NF-kappaB activation in inflammatory breast cancer is associated with oestrogen receptor downregulation, secondary to EGFR and/or ErbB2 overexpression and MAPK hyperactivation. *British journal of cancer* 97(5):659-669.

19. Cabioglu N, Gong Y, Islam R, Broglio K, Sneige N, *et al.* (2007) Expression of growth factor and chemokine receptors: new insights in the biology of inflammatory breast cancer. *Annals of oncology : official journal of the European Society for Medical Oncology / ESMO*.

20. Rimawi MF, Shetty PB, Weiss HL, Schiff R, Osborne CK, *et al.* (2010) Epidermal growth factor receptor expression in breast cancer association with biologic phenotype and clinical outcomes. *Cancer* 116(5):1234-1242.

21. Zell JA, Tsang WY, Taylor TH, Mehta RS, & Anton-Culver H (2009) Prognostic impact of human epidermal growth factor-like receptor 2 and hormone receptor status in inflammatory breast cancer (IBC): analysis of 2,014 IBC patient cases from the California Cancer Registry. *Breast Cancer Res* 11(1):R9.

22. Turpin E, Bieche I, Bertheau P, Plassa LF, Lerebours F, *et al.* (2002) Increased incidence of ERBB2 overexpression and TP53 mutation in inflammatory breast cancer. *Oncogene* 21(49):7593-7597.

23. McCarthy NJ, Yang X, Linnoila IR, Merino MJ, Hewitt SM, *et al.* (2002) Microvessel density, expression of estrogen receptor alpha, MIB-1, p53, and c-erbB-2 in inflammatory breast cancer. *Clin Cancer Res.* 8(12):3857-3862.

24. Cheang MC, Voduc D, Bajdik C, Leung S, McKinney S, *et al.* (2008) Basal-like breast cancer defined by five biomarkers has superior prognostic value than triple-negative phenotype. *Clin Cancer Res.* 14(5):1368-1376. doi: 1310.1158/1078-0432.CCR-1307-1658.

25. Rakha EA, Elsheikh SE, Aleskandarany MA, Habashi HO, Green AR, *et al.* (2009) Triple-negative breast cancer: distinguishing between basal and nonbasal subtypes. *Clin Cancer Res.* 15(7):2302-2310. doi: 2310.1158/1078-0432.CCR-2308-2132. Epub 2009 Mar 2324.

26. Sawaki M, Ito Y, Akiyama F, Tokudome N, Horii R, *et al.* (2006) High prevalence of HER-2/neu and p53 overexpression in inflammatory breast cancer. *Breast Cancer* 13(2):172-178.

27. Bertucci F, Finetti P, & Birnbaum D (2012) Basal breast cancer: a complex and deadly molecular subtype. *Curr Mol Med.* 12(1):96-110.

28. Roy V & Perez EA (2009) Beyond trastuzumab: small molecule tyrosine kinase inhibitors in HER-2-positive breast cancer. *Oncologist.* 14(11):1061-1069. doi: 1010.1634/theoncologist.2009-0142. Epub 2009 Nov 1063.

29. Masuda H, Zhang D, Bartholomeusz C, Doihara H, Hortobagyi GN, *et al.* (2012) Role of epidermal growth factor receptor in breast cancer. *Breast Cancer Res Treat.* 136(2):331-345. doi: 310.1007/s10549-10012-12289-10549. Epub 12012 Oct 10517.

30. Yarden Y & Sliwkowski MX (2001) Untangling the ErbB signalling network. *Nat Rev Mol Cell Biol.* 2(2):127-137.

31. Lo HW, Hsu SC, & Hung MC (2006) EGFR signaling pathway in breast cancers: from traditional signal transduction to direct nuclear translocalization. *Breast Cancer Res Treat.* 95(3):211-218.

32. Lerebours F, Vacher S, Andrieu C, Espie M, Marty M, *et al.* (2008) NF-kappa B genes have a major role in inflammatory breast cancer. *BMC Cancer* 8:41.

33. Van Laere SJ, Van der Auwera I, Van den Eynden GG, Elst HJ, Weyler J, *et al.* (2006) Nuclear factor-kappaB signature of inflammatory breast cancer by cDNA microarray validated by quantitative real-time reverse transcription-PCR, immunohistochemistry, and nuclear factor-kappaB DNA-binding. *Clin Cancer Res* 12(11 Pt 1):3249-3256.

34. Van Laere S, Van der Auwera I, Van den Eynden GG, Fox SB, Bianchi F, *et al.* (2005) Distinct molecular signature of inflammatory breast cancer by cDNA microarray analysis. *Breast Cancer Res Treat* 93(3):237-246.

35. Bharti AC & Aggarwal BB (2002) Nuclear factor-kappa B and cancer: its role in prevention and therapy. *Biochem Pharmacol.* 64(5-6):883-888.

36. Karin M & Lin A (2002) NF-kappaB at the crossroads of life and death. *Nat Immunol.* 3(3):221-227.

37. Morgan MJ & Liu ZG (2011) Crosstalk of reactive oxygen species and NF-kappaB signaling. *Cell Res* 21(1):103-115.

38. Brosh R & Rotter V (2009) When mutants gain new powers: news from the mutant p53 field. *Nat Rev Cancer.* 9(10):701-713. doi: 710.1038/nrc2693. Epub 2009 Aug 1020.

39. Houchens NW & Merajver SD (2008) Molecular determinants of the inflammatory breast cancer phenotype. *Oncology (Williston Park)* 22(14):1556-1561; discussion 1561, 1565-1558, 1576.

40. Riou G, Le MG, Travagli JP, Levine AJ, & Moll UM (1993) Poor prognosis of p53 gene mutation and nuclear overexpression of p53 protein in inflammatory breast carcinoma. *J Natl Cancer Inst* 85(21):1765-1767.

41. Li CL, B.; Woodward, W.; Ueno, N.; Robertson, F.; Reuben, J.; Cristofanilli, M. (2009) p53 Mutation in Inflammatory Breast Cancer Cell Lines. *Thirty-Second Annual CTRC-AACR San Antonio Breast Cancer Symposium*, (Cancer Research).

42. Iwatsuki M, Mimori K, Yokobori T, Ishi H, Beppu T, *et al.* (2010) Epithelial-mesenchymal transition in cancer development and its clinical significance. *Cancer Sci.* 101(2):293-299. doi: 210.1111/j.1349-7006.2009.01419.x. Epub 02009 Oct 01428.

43. Wheelock MJ, Soler AP, & Knudsen KA (2001) Cadherin junctions in mammary tumors. *J Mammary Gland Biol Neoplasia.* 6(3):275-285.

44. Kleer CG, van Golen KL, Braun T, & Merajver SD (2001) Persistent E-cadherin expression in inflammatory breast cancer. *Modern pathology : an official journal of the United States and Canadian Academy of Pathology, Inc* 14(5):458-464.

45. Colpaert CG, Vermeulen PB, Benoy I, Soubry A, van Roy F, *et al.* (2003) Inflammatory breast cancer shows angiogenesis with high endothelial proliferation rate and strong E-cadherin expression. *Br J Cancer.* 88(5):718-725.

46. Silvera D, Arju R, Darvishian F, Levine PH, Zolfaghari L, *et al.* (2009) Essential role for eIF4GI overexpression in the pathogenesis of inflammatory breast cancer. *Nature cell biology* 11(7):903-908.

47. Gingras AC, Raught B, & Sonenberg N (2004) mTOR signaling to translation. *Curr Top Microbiol Immunol.* 279:169-197.

48. Van der Auwera I, Van Laere SJ, Van den Eynden GG, Benoy I, van Dam P, *et al.* (2004) Increased angiogenesis and lymphangiogenesis in inflammatory versus noninflammatory breast cancer by real-time reverse transcriptase-PCR gene expression quantification. *Clin Cancer Res.* 10(23):7965-7971.

49. Ferrara N, Gerber HP, & LeCouter J (2003) The biology of VEGF and its receptors. *Nat Med.* 9(6):669-676.

50. Silvera D & Schneider RJ (2009) Inflammatory breast cancer cells are constitutively adapted to hypoxia. *Cell cycle* 8(19):3091-3096.

51. Bieche I, Lerebours F, Tozlu S, Espie M, Marty M, *et al.* (2004) Molecular profiling of inflammatory breast cancer: identification of a poor-prognosis gene expression signature. *Clin Cancer Res* 10(20):6789-6795.

52. Braunstein S, Karpisheva K, Pola C, Goldberg J, Hochman T, *et al.* (2007) A hypoxia-controlled cap-dependent to cap-independent translation switch in breast cancer. *Molecular cell* 28(3):501-512.

53. Achen MG, Mann GB, & Stacker SA (2006) Targeting lymphangiogenesis to prevent tumour metastasis. *Br J Cancer.* 94(10):1355-1360.

54. Yamauchi H, Cristofanilli M, Nakamura S, Hortobagyi GN, & Ueno NT (2009) Molecular targets for treatment of inflammatory breast cancer. *Nature reviews. Clinical oncology*.

55. Duong T, Koopman P, & Francois M (2012) Tumor lymphangiogenesis as a potential therapeutic target. *J Oncol.* 2012:204946.(doi):10.1155/2012/204946. Epub 202012 Feb 204916.

56. Shirakawa K, Kobayashi H, Heike Y, Kawamoto S, Brechbiel MW, *et al.* (2002) Hemodynamics in vasculogenic mimicry and angiogenesis of inflammatory breast cancer xenograft. *Cancer Res.* 62(2):560-566.

57. Shirakawa K, Kobayashi H, Sobajima J, Hashimoto D, Shimizu A, *et al.* (2003) Inflammatory breast cancer: vasculogenic mimicry and its hemodynamics of an inflammatory breast cancer xenograft model. *Breast Cancer Res* 5(3):136-139.

58. Hanahan D & Weinberg RA (2000) The hallmarks of cancer. *Cell* 100(1):57-70.

59. Sinclair S & Swain SM (2010) Primary systemic chemotherapy for inflammatory breast cancer. *Cancer.* 116(11 Suppl):2821-2828. doi: 2810.1002/cncr.25166.

60. Dawood S, Ueno NT, & Cristofanilli M (2008) The medical treatment of inflammatory breast cancer. *Semin Oncol* 35(1):64-71.

61. Hortobagyi GN (1997) Anthracyclines in the treatment of cancer. An overview. *Drugs.* 54(Suppl 4):1-7.

62. Abal M, Andreu JM, & Barasoain I (2003) Taxanes: microtubule and centrosome targets, and cell cycle dependent mechanisms of action. *Curr Cancer Drug Targets.* 3(3):193-203.

63. Kell MR & Morrow M (2005) Surgical aspects of inflammatory breast cancer. *Breast Dis* 22:67-73.

64. Curcio LD, Rupp E, Williams WL, Chu DZ, Clarke K, *et al.* (1999) Beyond palliative mastectomy in inflammatory breast cancer--a reassessment of margin status. *Ann Surg Oncol* 6(3):249-254.

65. Fleming RY, Asmar L, Buzdar AU, McNeese MD, Ames FC, *et al.* (1997) Effectiveness of mastectomy by response to induction chemotherapy for control in inflammatory breast carcinoma. *Ann Surg Oncol* 4(6):452-461.

66. Liauw SL, Benda RK, Morris CG, & Mendenhall NP (2004) Inflammatory breast carcinoma: outcomes with trimodality therapy for nonmetastatic disease. *Cancer* 100(5):920-928.

67. Liao Z, Strom EA, Buzdar AU, Singletary SE, Hunt K, *et al.* (2000) Locoregional irradiation for inflammatory breast cancer: effectiveness of dose escalation in decreasing recurrence. *Int J Radiat Oncol Biol Phys* 47(5):1191-1200.

68. Jones KL & Buzdar AU (2004) A review of adjuvant hormonal therapy in breast cancer. *Endocr Relat Cancer.* 11(3):391-406.

69. Labidi SI, Mrad K, Mezlini A, Ouarda MA, Combes JD, *et al.* (2008) Inflammatory breast cancer in Tunisia in the era of multimodality therapy. *Ann Oncol.* 19(3):473-480. Epub 2007 Nov 2015.

70. Nahta R & Esteva FJ (2006) Herceptin: mechanisms of action and resistance. *Cancer Lett* 232(2):123-138.

71. Gianni L, Eiermann W, Semiglazov V, Manikhas A, Lluch A, *et al.* (2010) Neoadjuvant chemotherapy with trastuzumab followed by adjuvant trastuzumab versus neoadjuvant chemotherapy alone, in patients with HER2-positive locally advanced breast cancer (the NOAH trial): a randomised controlled superiority trial with a parallel HER2-negative cohort. *Lancet.* 375(9712):377-384. doi: 310.1016/S0140-6736(1009)61964-61964.

72. Esteva FJ, Valero V, Booser D, Guerra LT, Murray JL, *et al.* (2002) Phase II study of weekly docetaxel and trastuzumab for patients with HER-2-overexpressing metastatic breast cancer. *J Clin Oncol* 20(7):1800-1808.

73. Slamon DJ, Leyland-Jones B, Shak S, Fuchs H, Paton V, *et al.* (2001) Use of chemotherapy plus a monoclonal antibody against HER2 for metastatic breast cancer that overexpresses HER2. *N Engl J Med* 344(11):783-792.

74. Xia W, Mullin RJ, Keith BR, Liu LH, Ma H, *et al.* (2002) Anti-tumor activity of GW572016: a dual tyrosine kinase inhibitor blocks EGF activation of EGFR/erbB2 and downstream Erk1/2 and AKT pathways. *Oncogene* 21(41):6255-6263.

75. Xia W, Bisi J, Strum J, Liu L, Carrick K, *et al.* (2006) Regulation of survivin by ErbB2 signaling: therapeutic implications for ErbB2-overexpressing breast cancers. *Cancer Res* 66(3):1640-1647.

76. Dai CL, Tiwari AK, Wu CP, Su XD, Wang SR, *et al.* (2008) Lapatinib (Tykerb, GW572016) reverses multidrug resistance in cancer cells by inhibiting the activity of ATP-binding cassette subfamily B member 1 and G member 2. *Cancer Res* 68(19):7905-7914.

77. Polli JW, Humphreys JE, Harmon KA, Castellino S, O'Mara MJ, *et al.* (2008) The role of efflux and uptake transporters in [N-{3-chloro-4-[(3-fluorobenzyl)oxy]phenyl}-6-[5-({[2-(methylsulfonyl)ethyl]amino }methyl)-2-

furyl]-4-quinazolinamine (GW572016, lapatinib) disposition and drug interactions. *Drug Metab Dispos* 36(4):695-701.

78. Aird KM, Allensworth JL, Batinic-Haberle I, Lyerly HK, Dewhirst MW, *et al.* (2012) ErbB1/2 tyrosine kinase inhibitor mediates oxidative stress-induced apoptosis in inflammatory breast cancer cells. *Breast Cancer Res Treat* 132(1):109-119.

79. Johnston S, Trudeau M, Kaufman B, Boussen H, Blackwell K, *et al.* (2008) Phase II study of predictive biomarker profiles for response targeting human epidermal growth factor receptor 2 (HER-2) in advanced inflammatory breast cancer with lapatinib monotherapy. *J Clin Oncol* 26(7):1066-1072.

80. Boussen H, Cristofanilli M, Zaks T, DeSilvio M, Salazar V, *et al.* (2010) Phase II study to evaluate the efficacy and safety of neoadjuvant lapatinib plus paclitaxel in patients with inflammatory breast cancer. *J Clin Oncol.* 28(20):3248-3255. doi: 3210.1200/JCO.2009.3221.8594. Epub 2010 Jun 3247.

81. Chen FL, Xia W, & Spector NL (2008) Acquired resistance to small molecule ErbB2 tyrosine kinase inhibitors. *Clin Cancer Res* 14(21):6730-6734.

82. Wedam SB, Low JA, Yang SX, Chow CK, Choyke P, *et al.* (2006) Antiangiogenic and antitumor effects of bevacizumab in patients with inflammatory and locally advanced breast cancer. *J Clin Oncol* 24(5):769-777.

83. Overmoyer B, Fu P, Hoppel C, Radivoyevitch T, Shenk R, *et al.* (2007) Inflammatory breast cancer as a model disease to study tumor angiogenesis: results of a phase IB trial of combination SU5416 and doxorubicin. *Clin Cancer Res.* 13(19):5862-5868.

84. Cristofanilli M, Johnston SR, Manikhas A, Gomez HL, Gladkov O, *et al.* (2013) A randomized phase II study of lapatinib + pazopanib versus lapatinib in patients with HER2+ inflammatory breast cancer. *Breast Cancer Res Treat.* 137(2):471-482. doi: 410.1007/s10549-10012-12369-x. Epub 12012 Dec 10513.

85. van Golen KL, Davies S, Wu ZF, Wang Y, Bucana CD, *et al.* (1999) A novel putative low-affinity insulin-like growth factor-binding protein, LIBC (lost in

inflammatory breast cancer), and RhoC GTPase correlate with the inflammatory breast cancer phenotype. *Clin Cancer Res* 5(9):2511-2519.

86. van Golen KL, Bao L, DiVito MM, Wu Z, Prendergast GC, *et al.* (2002) Reversion of RhoC GTPase-induced inflammatory breast cancer phenotype by treatment with a farnesyl transferase inhibitor. *Mol Cancer Ther* 1(8):575-583.

87. Sparano JA, Moulder S, Kazi A, Coppola D, Negassa A, *et al.* (2009) Phase II trial of tipifarnib plus neoadjuvant doxorubicin-cyclophosphamide in patients with clinical stage IIB-IIIC breast cancer. *Clin Cancer Res* 15(8):2942-2948.

88. Cristofanilli M, Krishnamurthy S, Guerra L, Broglio K, Arun B, *et al.* (2006) A nonreplicating adenoviral vector that contains the wild-type p53 transgene combined with chemotherapy for primary breast cancer: safety, efficacy, and biologic activity of a novel gene-therapy approach. *Cancer.* 107(5):935-944.

89. Tomlinson JS, Alpaugh ML, & Barsky SH (2001) An intact overexpressed E-cadherin/alpha,beta-catenin axis characterizes the lymphovascular emboli of inflammatory breast carcinoma. *Cancer Res* 61(13):5231-5241.

90. Schmid P, Kuhnhardt D, Kiewe P, Lehenbauer-Dehm S, Schippinger W, *et al.* (2008) A phase I/II study of bortezomib and capecitabine in patients with metastatic breast cancer previously treated with taxanes and/or anthracyclines. *Ann Oncol.* 19(5):871-876. doi: 810.1093/annonc/mdm1569. Epub 2008 Jan 1021.

91. Molina MA, Sáez R, Ramsey EE, Garcia-Barchino M-J, Rojo F, *et al.* (2002) NH2-terminal Truncated HER-2 Protein but not Full-Length Receptor Is Associated with Nodal Metastasis in Human Breast Cancer. *Clinical Cancer Research* 8(2):347-353.

92. Scaltriti M, Rojo F, Ocana A, Anido J, Guzman M, *et al.* (2007) Expression of p95HER2, a truncated form of the HER2 receptor, and response to anti-HER2 therapies in breast cancer. *J Natl Cancer Inst* 99(8):628-638.

93. Nagy P, Friedlander E, Tanner M, Kapanen AI, Carraway KL, *et al.* (2005) Decreased accessibility and lack of activation of ErbB2 in JIMT-1, a herceptin-resistant, MUC4-expressing breast cancer cell line. *Cancer Res* 65(2):473-482.

94. Palyi-Krekk Z, Barok M, Isola J, Tammi M, Szollosi J, *et al.* (2007) Hyaluronan-induced masking of ErbB2 and CD44-enhanced trastuzumab internalisation in trastuzumab resistant breast cancer. *Eur J Cancer.* 43(16):2423-2433.

95. Nagata Y, Lan KH, Zhou X, Tan M, Esteva FJ, *et al.* (2004) PTEN activation contributes to tumor inhibition by trastuzumab, and loss of PTEN predicts trastuzumab resistance in patients. *Cancer Cell* 6(2):117-127.

96. Berns K, Horlings HM, Hennessy BT, Madiredjo M, Hijmans EM, *et al.* (2007) A functional genetic approach identifies the PI3K pathway as a major determinant of trastuzumab resistance in breast cancer. *Cancer Cell.* 12(4):395-402.

97. Huang CH, Mandelker D, Schmidt-Kittler O, Samuels Y, Velculescu VE, *et al.* (2007) The structure of a human p110alpha/p85alpha complex elucidates the effects of oncogenic PI3Kalpha mutations. *Science.* 318(5857):1744-1748.

98. Chan CT, Metz MZ, & Kane SE (2005) Differential sensitivities of trastuzumab (Herceptin)-resistant human breast cancer cells to phosphoinositide-3 kinase (PI-3K) and epidermal growth factor receptor (EGFR) kinase inhibitors. *Breast Cancer Res Treat* 91(2):187-201.

99. Lu Y, Zi X, & Pollak M (2004) Molecular mechanisms underlying IGF-I-induced attenuation of the growth-inhibitory activity of trastuzumab (Herceptin) on SKBR3 breast cancer cells. *Int J Cancer.* 108(3):334-341.

100. Lu Y, Zi X, Zhao Y, Mascarenhas D, & Pollak M (2001) Insulin-like growth factor-I receptor signaling and resistance to trastuzumab (Herceptin). *J Natl Cancer Inst* 93(24):1852-1857.

101. Nahta R, Takahashi T, Ueno NT, Hung MC, & Esteva FJ (2004) P27(kip1) down-regulation is associated with trastuzumab resistance in breast cancer cells. *Cancer Res* 64(11):3981-3986.

102. Yakes FM, Chinratanalab W, Ritter CA, King W, Seelig S, *et al.* (2002) Herceptin-induced inhibition of phosphatidylinositol-3 kinase and Akt Is required for antibody-mediated effects on p27, cyclin D1, and antitumor action. *Cancer Res* 62(14):4132-4141.

103. Aird KM, Ding X, Baras A, Wei J, Morse MA, *et al.* (2008) Trastuzumab signaling in ErbB2-overexpressing inflammatory breast cancer correlates with X-linked inhibitor of apoptosis protein expression. *Mol Cancer Ther* 7(1):38-47.

104. Mohd Sharial MS, Crown J, & Hennessy BT (2012) Overcoming resistance and restoring sensitivity to HER2-targeted therapies in breast cancer. *Ann Oncol.* 23(12):3007-3016. doi: 3010.1093/annonc/mds3200. Epub 2012 Aug 3002.

105. Dave B, Migliaccio I, Gutierrez MC, Wu M-F, Chamness GC, *et al.* (2011) Loss of Phosphatase and Tensin Homolog or Phosphoinositol-3 Kinase Activation and Response to Trastuzumab or Lapatinib in Human Epidermal Growth Factor Receptor 2–Overexpressing Locally Advanced Breast Cancers. *Journal of Clinical Oncology* 29(2):166-173.

106. O'Brien NA, Browne BC, Chow L, Wang Y, Ginther C, *et al.* (2010) Activated phosphoinositide 3-kinase/AKT signaling confers resistance to trastuzumab but not lapatinib. *Mol Cancer Ther.* 9(6):1489-1502. doi: 1410.1158/1535-7163.MCT-1409-1171. Epub 2010 May 1425.

107. Scaltriti M, Chandarlapaty S, Prudkin L, Aura C, Jimenez J, *et al.* (2010) Clinical benefit of lapatinib-based therapy in patients with human epidermal growth factor receptor 2-positive breast tumors coexpressing the truncated p95HER2 receptor. *Clin Cancer Res.* 16(9):2688-2695. doi: 2610.1158/1078-0432.CCR-2609-3407. Epub 2010 Apr 2620.

108. Xia W, Liu LH, Ho P, & Spector NL (2004) Truncated ErbB2 receptor (p95ErbB2) is regulated by heregulin through heterodimer formation with ErbB3 yet remains sensitive to the dual EGFR/ErbB2 kinase inhibitor GW572016. *Oncogene* 23(3):646-653.

109. Nahta R, Yuan LX, Du Y, & Esteva FJ (2007) Lapatinib induces apoptosis in trastuzumab-resistant breast cancer cells: effects on insulin-like growth factor I signaling. *Mol Cancer Ther* 6(2):667-674.

110. Xia W, Bacus S, Hegde P, Husain I, Strum J, *et al.* (2006) A model of acquired autoresistance to a potent ErbB2 tyrosine kinase inhibitor and a therapeutic strategy to prevent its onset in breast cancer. *Proc Natl Acad Sci U S A* 103(20):7795-7800.

111. Xia W, Bacus S, Husain I, Liu L, Zhao S, *et al.* (2010) Resistance to ErbB2 tyrosine kinase inhibitors in breast cancer is mediated by calcium-dependent activation of RelA. *Mol Cancer Ther* 9(2):292-299.

112. Wetterskog D, Shiu KK, Chong I, Meijer T, Mackay A, *et al.* (2013) Identification of novel determinants of resistance to lapatinib in ERBB2-amplified cancers. *Oncogene* 11(10):41.

113. Martin AP, Miller A, Emad L, Rahmani M, Walker T, *et al.* (2008) Lapatinib resistance in HCT116 cells is mediated by elevated MCL-1 expression and decreased BAK activation and not by ERBB receptor kinase mutation. *Mol Pharmacol* 74(3):807-822.

114. Aird KM, Ghanayem RB, Peplinski S, Lyerly HK, & Devi GR (2010) X-linked inhibitor of apoptosis protein inhibits apoptosis in inflammatory breast cancer cells with acquired resistance to an ErbB1/2 tyrosine kinase inhibitor. *Mol Cancer Ther* 9(5):1432-1442.

115. Jin Z & El-Deiry WS (2005) Overview of cell death signaling pathways. *Cancer Biol Ther* 4(2):139-163.

116. Riedl SJ & Shi Y (2004) Molecular mechanisms of caspase regulation during apoptosis. *Nat Rev Mol Cell Biol.* 5(11):897-907.

117. Elmore S (2007) Apoptosis: a review of programmed cell death. *Toxicol Pathol* 35(4):495-516.

118. Asakura T & Ohkawa K (2004) Chemotherapeutic agents that induce mitochondrial apoptosis. *Curr Cancer Drug Targets.* 4(7):577-590.

119. Cory S, Huang DC, & Adams JM (2003) The Bcl-2 family: roles in cell survival and oncogenesis. *Oncogene.* 22(53):8590-8607.

120. Wang X (2001) The expanding role of mitochondria in apoptosis. *Genes Dev* 15(22):2922-2933.

121. Sartorius U, Schmitz I, & Krammer PH (2001) Molecular mechanisms of death-receptor-mediated apoptosis. *Chembiochem* 2(1):20-29.

122. Carlo-Stella C, Lavazza C, Locatelli A, Vigano L, Gianni AM, *et al.* (2007) Targeting TRAIL agonistic receptors for cancer therapy. *Clin Cancer Res.* 13(8):2313-2317.

123. Cory S & Adams JM (2002) The Bcl2 family: regulators of the cellular life-or-death switch. *Nature reviews. Cancer* 2(9):647-656.

124. Fadeel B & Orrenius S (2005) Apoptosis: a basic biological phenomenon with wide-ranging implications in human disease. *Journal of internal medicine* 258(6):479-517.

125. Salvesen GS & Duckett CS (2002) IAP proteins: blocking the road to death's door. *Nature reviews. Molecular cell biology* 3(6):401-410.

126. Eckelman BP & Salvesen GS (2006) The human anti-apoptotic proteins cIAP1 and cIAP2 bind but do not inhibit caspases. *J Biol Chem.* 281(6):3254-3260. Epub 2005 Dec 3258.

127. Eckelman BP, Salvesen GS, & Scott FL (2006) Human inhibitor of apoptosis proteins: why XIAP is the black sheep of the family. *EMBO reports* 7(10):988-994.

128. Shi Y (2004) Caspase activation, inhibition, and reactivation: a mechanistic view. *Protein Sci* 13(8):1979-1987.

129. Huang H, Joazeiro CA, Bonfoco E, Kamada S, Leverson JD, *et al.* (2000) The inhibitor of apoptosis, cIAP2, functions as a ubiquitin-protein ligase and promotes in vitro monoubiquitination of caspases 3 and 7. *J Biol Chem* 275(35):26661-26664.

130. Suzuki Y, Nakabayashi Y, & Takahashi R (2001) Ubiquitin-protein ligase activity of X-linked inhibitor of apoptosis protein promotes proteasomal degradation of caspase-3 and enhances its anti-apoptotic effect in Fas-induced cell death. *Proc Natl Acad Sci U S A* 98(15):8662-8667.

131. Morizane Y, Honda R, Fukami K, & Yasuda H (2005) X-linked inhibitor of apoptosis functions as ubiquitin ligase toward mature caspase-9 and cytosolic Smac/DIABLO. *J Biochem* 137(2):125-132.

132. Galban S & Duckett CS (2010) XIAP as a ubiquitin ligase in cellular signaling. *Cell Death Differ* 17(1):54-60.

133. Schile AJ, Garcia-Fernandez M, & Steller H (2008) Regulation of apoptosis by XIAP ubiquitin-ligase activity. *Genes Dev* 22(16):2256-2266.

134. Ni T, Li W, & Zou F (2005) The ubiquitin ligase ability of IAPs regulates apoptosis. *IUBMB Life* 57(12):779-785.

135. Feltham R, Khan N, & Silke J (2012) IAPS and ubiquitylation. *IUBMB Life.* 64(5):411-418. doi: 410.1002/iub.1565. Epub 2012 Feb 1023.

136. MacFarlane M, Merrison W, Bratton SB, & Cohen GM (2002) Proteasome-mediated degradation of Smac during apoptosis: XIAP promotes Smac ubiquitination in vitro. *J Biol Chem* 277(39):36611-36616.

137. Hu S & Yang X (2003) Cellular inhibitor of apoptosis 1 and 2 are ubiquitin ligases for the apoptosis inducer Smac/DIABLO. *J Biol Chem* 278(12):10055-10060.

138. Vucic D, Franklin MC, Wallweber HJ, Das K, Eckelman BP, *et al.* (2005) Engineering ML-IAP to produce an extraordinarily potent caspase 9 inhibitor: implications for Smac-dependent anti-apoptotic activity of ML-IAP. *Biochem J.* 385(Pt 1):11-20.

139. Sax JK, Fei P, Murphy ME, Bernhard E, Korsmeyer SJ, *et al.* (2002) BID regulation by p53 contributes to chemosensitivity. *Nat Cell Biol.* 4(11):842-849.

140. Perego P, Giarola M, Righetti SC, Supino R, Caserini C, *et al.* (1996) Association between cisplatin resistance and mutation of p53 gene and reduced bax expression in ovarian carcinoma cell systems. *Cancer Res.* 56(3):556-562.

141. Igney FH & Krammer PH (2002) Death and anti-death: tumour resistance to apoptosis. *Nat Rev Cancer.* 2(4):277-288.

142. Soengas MS, Capodieci P, Polsky D, Mora J, Esteller M, *et al.* (2001) Inactivation of the apoptosis effector Apaf-1 in malignant melanoma. *Nature.* 409(6817):207-211.

143. Sun Y, Orrenius S, Pervaiz S, & Fadeel B (2005) Plasma membrane sequestration of apoptotic protease-activating factor-1 in human B-lymphoma cells: a novel mechanism of chemoresistance. *Blood* 105(10):4070-4077.

144. Isobe N, Onodera H, Mori A, Shimada Y, Yang W, *et al.* (2004) Caspase-3 expression in human gastric carcinoma and its clinical significance. *Oncology.* 66(3):201-209.

145. Fulda S, Kufer MU, Meyer E, van Valen F, Dockhorn-Dworniczak B, *et al.* (2001) Sensitization for death receptor- or drug-induced apoptosis by re-expression of caspase-8 through demethylation or gene transfer. *Oncogene* 20(41):5865-5877.

146. Teitz T, Wei T, Valentine MB, Vanin EF, Grenet J, *et al.* (2000) Caspase 8 is deleted or silenced preferentially in childhood neuroblastomas with amplification of MYCN. *Nat Med.* 6(5):529-535.

147. Pingoud-Meier C, Lang D, Janss AJ, Rorke LB, Phillips PC, *et al.* (2003) Loss of caspase-8 protein expression correlates with unfavorable survival outcome in childhood medulloblastoma. *Clin Cancer Res.* 9(17):6401-6409.

148. Zuzak TJ, Steinhoff DF, Sutton LN, Phillips PC, Eggert A, *et al.* (2002) Loss of caspase-8 mRNA expression is common in childhood primitive neuroectodermal brain tumour/medulloblastoma. *Eur J Cancer.* 38(1):83-91.

149. Takita J, Yang HW, Chen YY, Hanada R, Yamamoto K, *et al.* (2001) Allelic imbalance on chromosome 2q and alterations of the caspase 8 gene in neuroblastoma. *Oncogene.* 20(32):4424-4432.

150. Mandruzzato S, Brasseur F, Andry G, Boon T, & van der Bruggen P (1997) A CASP-8 mutation recognized by cytolytic T lymphocytes on a human head and neck carcinoma. *J Exp Med.* 186(5):785-793.

151. Liu B, Peng D, Lu Y, Jin W, & Fan Z (2002) A novel single amino acid deletion caspase-8 mutant in cancer cells that lost proapoptotic activity. *J Biol Chem.* 277(33):30159-30164. Epub 32002 Jun 30157.

152. Shivapurkar N, Reddy J, Matta H, Sathyanarayana UG, Huang CX, *et al.* (2002) Loss of expression of death-inducing signaling complex (DISC) components in lung cancer cell lines and the influence of MYC amplification. *Oncogene.* 21(55):8510-8514.

153. Shivapurkar N, Toyooka S, Eby MT, Huang CX, Sathyanarayana UG, *et al.* (2002) Differential inactivation of caspase-8 in lung cancers. *Cancer Biol Ther.* 1(1):65-69.

154. Cheng J, Zhou T, Liu C, Shapiro JP, Brauer MJ, *et al.* (1994) Protection from Fas-mediated apoptosis by a soluble form of the Fas molecule. *Science.* 263(5154):1759-1762.

155. Midis GP, Shen Y, & Owen-Schaub LB (1996) Elevated soluble Fas (sFas) levels in nonhematopoietic human malignancy. *Cancer Res.* 56(17):3870-3874.

156. Ugurel S, Rappl G, Tilgen W, & Reinhold U (2001) Increased soluble CD95 (sFas/CD95) serum level correlates with poor prognosis in melanoma patients. *Clin Cancer Res.* 7(5):1282-1286.

157. Takeda K, Hayakawa Y, Smyth MJ, Kayagaki N, Yamaguchi N, *et al.* (2001) Involvement of tumor necrosis factor-related apoptosis-inducing ligand in surveillance of tumor metastasis by liver natural killer cells. *Nat Med.* 7(1):94-100.

158. Tourneur L, Delluc S, Levy V, Valensi F, Radford-Weiss I, *et al.* (2004) Absence or low expression of fas-associated protein with death domain in acute myeloid leukemia cells predicts resistance to chemotherapy and poor outcome. *Cancer Res.* 64(21):8101-8108.

159. Irmler M, Thome M, Hahne M, Schneider P, Hofmann K, *et al.* (1997) Inhibition of death receptor signals by cellular FLIP. *Nature.* 388(6638):190-195.

160. Kataoka T (2005) The caspase-8 modulator c-FLIP. *Crit Rev Immunol.* 25(1):31-58.

161. Plati J, Bucur O, & Khosravi-Far R (2008) Dysregulation of apoptotic signaling in cancer: molecular mechanisms and therapeutic opportunities. *J Cell Biochem.* 104(4):1124-1149. doi: 1110.1002/jcb.21707.

162. Zhang X, Jin TG, Yang H, DeWolf WC, Khosravi-Far R, *et al.* (2004) Persistent c-FLIP(L) expression is necessary and sufficient to maintain resistance to tumor necrosis factor-related apoptosis-inducing ligand-mediated apoptosis in prostate cancer. *Cancer Res.* 64(19):7086-7091.

163. Korkolopoulou P, Saetta AA, Levidou G, Gigelou F, Lazaris A, *et al.* (2007) c-FLIP expression in colorectal carcinomas: association with Fas/FasL expression and prognostic implications. *Histopathology.* 51(2):150-156. Epub 2007 Jun 2008.

164. Weiss LM, Warnke RA, Sklar J, & Cleary ML (1987) Molecular analysis of the t(14;18) chromosomal translocation in malignant lymphomas. *N Engl J Med.* 317(19):1185-1189.

165. Campos L, Rouault JP, Sabido O, Oriol P, Roubi N, *et al.* (1993) High expression of bcl-2 protein in acute myeloid leukemia cells is associated with poor response to chemotherapy. *Blood.* 81(11):3091-3096.

166. Pepper C, Bentley P, & Hoy T (1996) Regulation of clinical chemoresistance by bcl-2 and bax oncoproteins in B-cell chronic lymphocytic leukaemia. *Br J Haematol.* 95(3):513-517.

167. Brinkmann U, Mansfield E, & Pastan I (1997) Effects of BCL-2 overexpression on the sensitivity of MCF-7 breast cancer cells to ricin, diphtheria and Pseudomonas toxin and immunotoxins. *Apoptosis.* 2(2):192-198.

168. Real PJ, Sierra A, De Juan A, Segovia JC, Lopez-Vega JM, *et al.* (2002) Resistance to chemotherapy via Stat3-dependent overexpression of Bcl-2 in metastatic breast cancer cells. *Oncogene.* 21(50):7611-7618.

169. Krajewska M, Moss SF, Krajewski S, Song K, Holt PR, *et al.* (1996) Elevated expression of Bcl-X and reduced Bak in primary colorectal adenocarcinomas. *Cancer Res.* 56(10):2422-2427.

170. Castilla C, Congregado B, Chinchon D, Torrubia FJ, Japon MA, *et al.* (2006) Bcl-xL is overexpressed in hormone-resistant prostate cancer and promotes survival of LNCaP cells via interaction with proapoptotic Bak. *Endocrinology.* 147(10):4960-4967. Epub 2006 Jun 4922.

171. Amundson SA, Myers TG, Scudiero D, Kitada S, Reed JC, *et al.* (2000) An informatics approach identifying markers of chemosensitivity in human cancer cell lines. *Cancer Res.* 60(21):6101-6110.

172. Kaufmann SH, Karp JE, Svingen PA, Krajewski S, Burke PJ, *et al.* (1998) Elevated expression of the apoptotic regulator Mcl-1 at the time of leukemic relapse. *Blood.* 91(3):991-1000.

173. Kitada S, Andersen J, Akar S, Zapata JM, Takayama S, *et al.* (1998) Expression of apoptosis-regulating proteins in chronic lymphocytic leukemia: correlations with In vitro and In vivo chemoresponses. *Blood.* 91(9):3379-3389.

174. Brimmell M, Mendiola R, Mangion J, & Packham G (1998) BAX frameshift mutations in cell lines derived from human haemopoietic malignancies are associated with resistance to apoptosis and microsatellite instability. *Oncogene.* 16(14):1803-1812.

175. Rampino N, Yamamoto H, Ionov Y, Li Y, Sawai H, *et al.* (1997) Somatic frameshift mutations in the BAX gene in colon cancers of the microsatellite mutator phenotype. *Science.* 275(5302):967-969.

176. Kim MS, Kim SS, Yoo NJ, & Lee SH (2012) Rare somatic mutation of pro-apoptotic BAX and BAK genes in common human cancers. *Tumori.* 98(6):149e-151e. doi: 110.1700/1217.13509.

177. Meijerink JP, Mensink EJ, Wang K, Sedlak TW, Sloetjes AW, *et al.* (1998) Hematopoietic malignancies demonstrate loss-of-function mutations of BAX. *Blood.* 91(8):2991-2997.

178. McConkey DJ, Chandra J, Wright S, Plunkett W, McDonnell TJ, *et al.* (1996) Apoptosis sensitivity in chronic lymphocytic leukemia is determined by endogenous endonuclease content and relative expression of BCL-2 and BAX. *J Immunol.* 156(7):2624-2630.

179. Ionov Y, Yamamoto H, Krajewski S, Reed JC, & Perucho M (2000) Mutational inactivation of the proapoptotic gene BAX confers selective advantage during tumor clonal evolution. *Proc Natl Acad Sci U S A.* 97(20):10872-10877.

180. Krajewski S, Blomqvist C, Franssila K, Krajewska M, Wasenius VM, *et al.* (1995) Reduced expression of proapoptotic gene BAX is associated with poor response rates to combination chemotherapy and shorter survival in women with metastatic breast adenocarcinoma. *Cancer Res.* 55(19):4471-4478.

181. Yang L, Cao Z, Yan H, & Wood WC (2003) Coexistence of high levels of apoptotic signaling and inhibitor of apoptosis proteins in human tumor cells: implication for cancer specific therapy. *Cancer Res.* 63(20):6815-6824.

182. Ambrosini G, Adida C, & Altieri DC (1997) A novel anti-apoptosis gene, survivin, expressed in cancer and lymphoma. *Nature medicine* 3(8):917-921.

183. Deveraux QL & Reed JC (1999) IAP family proteins--suppressors of apoptosis. *Genes Dev* 13(3):239-252.

184. Reed JC (2002) Apoptosis-based therapies. *Nat Rev Drug Discov.* 1(2):111-121.

185. Sarela AI, Macadam RC, Farmery SM, Markham AF, & Guillou PJ (2000) Expression of the antiapoptosis gene, survivin, predicts death from recurrent colorectal carcinoma. *Gut.* 46(5):645-650.

186. Lu CD, Altieri DC, & Tanigawa N (1998) Expression of a novel antiapoptosis gene, survivin, correlated with tumor cell apoptosis and p53 accumulation in gastric carcinomas. *Cancer Res.* 58(9):1808-1812.

187. Adida C, Berrebi D, Peuchmaur M, Reyes-Mugica M, & Altieri DC (1998) Anti-apoptosis gene, survivin, and prognosis of neuroblastoma. *Lancet.* 351(9106):882-883.

188. Reed JC (1999) Dysregulation of apoptosis in cancer. *J Clin Oncol.* 17(9):2941-2953.

189. Dai Z, Zhu WG, Morrison CD, Brena RM, Smiraglia DJ, *et al.* (2003) A comprehensive search for DNA amplification in lung cancer identifies inhibitors

of apoptosis cIAP1 and cIAP2 as candidate oncogenes. *Hum Mol Genet.* 12(7):791-801.

190. Imoto I, Yang ZQ, Pimkhaokham A, Tsuda H, Shimada Y, *et al.* (2001) Identification of cIAP1 as a candidate target gene within an amplicon at 11q22 in esophageal squamous cell carcinomas. *Cancer Res.* 61(18):6629-6634.

191. Dierlamm J, Baens M, Wlodarska I, Stefanova-Ouzounova M, Hernandez JM, *et al.* (1999) The apoptosis inhibitor gene API2 and a novel 18q gene, MLT, are recurrently rearranged in the t(11;18)(q21;q21) associated with mucosa-associated lymphoid tissue lymphomas. *Blood.* 93(11):3601-3609.

192. Uren AG, O'Rourke K, Aravind LA, Pisabarro MT, Seshagiri S, *et al.* (2000) Identification of paracaspases and metacaspases: two ancient families of caspase-like proteins, one of which plays a key role in MALT lymphoma. *Mol Cell.* 6(4):961-967.

193. Krajewska M, Krajewski S, Banares S, Huang X, Turner B, *et al.* (2003) Elevated expression of inhibitor of apoptosis proteins in prostate cancer. *Clin Cancer Res* 9(13):4914-4925.

194. Nachmias B, Ashhab Y, Bucholtz V, Drize O, Kadouri L, *et al.* (2003) Caspase-mediated cleavage converts Livin from an antiapoptotic to a proapoptotic factor: implications for drug-resistant melanoma. *Cancer Res* 63(19):6340-6349.

195. Vucic D, Stennicke HR, Pisabarro MT, Salvesen GS, & Dixit VM (2000) ML-IAP, a novel inhibitor of apoptosis that is preferentially expressed in human melanomas. *Curr Biol* 10(21):1359-1366.

196. Deveraux QL, Takahashi R, Salvesen GS, & Reed JC (1997) X-linked IAP is a direct inhibitor of cell-death proteases. *Nature* 388(6639):300-304.

197. Hofer-Warbinek R, Schmid JA, Stehlik C, Binder BR, Lipp J, *et al.* (2000) Activation of NF-kappa B by XIAP, the X chromosome-linked inhibitor of apoptosis, in endothelial cells involves TAK1. *J Biol Chem* 275(29):22064-22068.

198. Lu M, Lin SC, Huang Y, Kang YJ, Rich R, *et al.* (2007) XIAP induces NF-kappaB activation via the BIR1/TAB1 interaction and BIR1 dimerization. *Mol Cell.* 26(5):689-702.

199. Burstein E, Ganesh L, Dick RD, van De Sluis B, Wilkinson JC, *et al.* (2004) A novel role for XIAP in copper homeostasis through regulation of MURR1. *The EMBO journal* 23(1):244-254.

200. Ibrahim AM, Mansour IM, Wilson MM, Mokhtar DA, Helal AM, *et al.* (2012) Study of Survivin and X-Linked Inhibitor of Apoptosis Protein (XIAP) Genes in Acute Myeloid Leukemia (AML). *Lab Hematol.* 18(1):1-10.

201. Yang XH, Feng ZE, Yan M, Hanada S, Zuo H, *et al.* (2012) XIAP is a predictor of cisplatin-based chemotherapy response and prognosis for patients with advanced head and neck cancer. *PLoS One.* 7(3):e31601. Epub 32012 Mar 31605.

202. Markovic O, Marisavljevic D, Cemerikic V, Perunicic M, Savic S, *et al.* (2011) Clinical and prognostic significance of apoptotic profile in patients with newly diagnosed nodal diffuse large B-cell lymphoma (DLBCL). *Eur J Haematol.* 86(3):246-255. doi: 210.1111/j.1600-0609.2010.01567.x.

203. Sung KW, Choi J, Hwang YK, Lee SJ, Kim HJ, *et al.* (2009) Overexpression of X-linked inhibitor of apoptosis protein (XIAP) is an independent unfavorable prognostic factor in childhood de novo acute myeloid leukemia. *J Korean Med Sci.* 24(4):605-613. doi: 610.3346/jkms.2009.3324.3344.3605. Epub 2009 Jul 3329.

204. Kluger HM, McCarthy MM, Alvero AB, Sznol M, Ariyan S, *et al.* (2007) The X-linked inhibitor of apoptosis protein (XIAP) is up-regulated in metastatic melanoma, and XIAP cleavage by Phenoxodiol is associated with Carboplatin sensitization. *J Transl Med.* 5:6.

205. Frenzel LP, Patz M, Pallasch CP, Brinker R, Claasen J, *et al.* (2011) Novel X-linked inhibitor of apoptosis inhibiting compound as sensitizer for TRAIL-mediated apoptosis in chronic lymphocytic leukaemia with poor prognosis. *Br J Haematol.* 152(2):191-200. doi: 110.1111/j.1365-2141.2010.08426.x. Epub 02010 Nov 08423.

206. Gu LQ, Li FY, Zhao L, Liu Y, Chu Q, *et al.* (2010) Association of XIAP and P2X7 receptor expression with lymph node metastasis in papillary thyroid carcinoma. *Endocrine.* 38(2):276-282. Epub 2010 Oct 2023.

207. Burstein DE, Idrees MT, Li G, Wu M, & Kalir T (2008) Immunohistochemical detection of the X-linked inhibitor of apoptosis protein (XIAP) in cervical squamous intraepithelial neoplasia and squamous carcinoma. *Ann Diagn Pathol.* 12(2):85-89. doi: 10.1016/j.anndiagpath.2007.1004.1008. Epub 2007 Oct 1018.

208. Nagi C, Xiao GQ, Li G, Genden E, & Burstein DE (2007) Immunohistochemical detection of X-linked inhibitor of apoptosis in head and neck squamous cell carcinoma. *Ann Diagn Pathol.* 11(6):402-406. Epub 2007 Sep 2014.

209. Shi YH, Ding WX, Zhou J, He JY, Xu Y, *et al.* (2008) Expression of X-linked inhibitor-of-apoptosis protein in hepatocellular carcinoma promotes metastasis and tumor recurrence. *Hepatology.* 48(2):497-507. doi: 410.1002/hep.22393.

210. Seligson DB, Hongo F, Huerta-Yepez S, Mizutani Y, Miki T, *et al.* (2007) Expression of X-linked inhibitor of apoptosis protein is a strong predictor of human prostate cancer recurrence. *Clin Cancer Res* 13(20):6056-6063.

211. Kim MA, Lee HE, Lee HS, Yang HK, & Kim WH (2011) Expression of apoptosis-related proteins and its clinical implication in surgically resected gastric carcinoma. *Virchows Arch.* 459(5):503-510. Epub 2011 Sep 2027.

212. Zhang Y, Zhu J, Tang Y, Li F, Zhou H, *et al.* (2011) X-linked inhibitor of apoptosis positive nuclear labeling: a new independent prognostic biomarker of breast invasive ductal carcinoma. *Diagn Pathol.* 6:49.

213. Hussain AR, Uddin S, Ahmed M, Bu R, Ahmed SO, *et al.* (2010) Prognostic significance of XIAP expression in DLBCL and effect of its inhibition on AKT signalling. *J Pathol.* 222(2):180-190.

214. Augello C, Caruso L, Maggioni M, Donadon M, Montorsi M, *et al.* (2009) Inhibitors of apoptosis proteins (IAPs) expression and their prognostic significance in hepatocellular carcinoma. *BMC Cancer.* 9:125.

215. Jaffer S, Orta L, Sunkara S, Sabo E, & Burstein DE (2007) Immunohistochemical detection of antiapoptotic protein X-linked inhibitor of apoptosis in mammary carcinoma. *Hum Pathol* 38(6):864-870.

216. Li B, Zhang YD, & Tian BN (2007) [Expression of X-linked inhibitor of apoptosis protein in colorectal cancer tissues]. *Nan Fang Yi Ke Da Xue Xue Bao.* 27(11):1746-1748.

217. Li X, Ma X, Lu X, Cui L, & Dong W (2007) [Expression of inhibitor of apoptosis protein XIAP in laryngeal carcinoma and its clinicopathological significance]. *Lin Chung Er Bi Yan Hou Tou Jing Wai Ke Za Zhi.* 21(21):973-975.

218. Jin HS, Lee DH, Kim DH, Chung JH, Lee SJ, *et al.* (2009) cIAP1, cIAP2, and XIAP act cooperatively via nonredundant pathways to regulate genotoxic stress-induced nuclear factor-kappaB activation. *Cancer Res* 69(5):1782-1791.

219. Levkau B, Garton KJ, Ferri N, Kloke K, Nofer JR, *et al.* (2001) xIAP induces cell-cycle arrest and activates nuclear factor-kappaB : new survival pathways disabled by caspase-mediated cleavage during apoptosis of human endothelial cells. *Circ Res* 88(3):282-290.

220. Makishima T, Yoshimi M, Komiyama S, Hara N, & Nishimoto T (2000) A subunit of the mammalian oligosaccharyltransferase, DAD1, interacts with Mcl-1, one of the bcl-2 protein family. *J Biochem.* 128(3):399-405.

221. Sanna MG, da Silva Correia J, Luo Y, Chuang B, Paulson LM, *et al.* (2002) ILPIP, a novel anti-apoptotic protein that enhances XIAP-mediated activation of JNK1 and protection against apoptosis. *J Biol Chem* 277(34):30454-30462.

222. Bertucci F, Finetti P, Rougemont J, Charafe-Jauffret E, Nasser V, *et al.* (2004) Gene expression profiling for molecular characterization of inflammatory breast cancer and prediction of response to chemotherapy. *Cancer Res* 64(23):8558-8565.

223. Nguyen DM, Sam K, Tsimelzon A, Li X, Wong H, *et al.* (2006) Molecular heterogeneity of inflammatory breast cancer: a hyperproliferative phenotype. *Clin Cancer Res* 12(17):5047-5054.

224. Iwamoto T, Bianchini G, Qi Y, Cristofanilli M, Lucci A, *et al.* (2011) Different gene expressions are associated with the different molecular subtypes of inflammatory breast cancer. *Breast Cancer Res Treat* 125(3):785-795.

225. Kurokawa M, Kim J, Geradts J, Matsuura K, Liu L, *et al.* (2013) A network of substrates of the E3 ubiquitin ligases MDM2 and HUWE1 control apoptosis independently of p53. *Science signaling* 6(274):ra32.

226. Bartosz G (2009) Reactive oxygen species: destroyers or messengers? *Biochem Pharmacol.* 77(8):1303-1315. doi: 1310.1016/j.bcp.2008.1311.1009. Epub 2008 Nov 1324.

227. Forman HJ, Maiorino M, & Ursini F (2010) Signaling functions of reactive oxygen species. *Biochemistry.* 49(5):835-842. doi: 810.1021/bi9020378.

228. Rhee SG, Chang TS, Bae YS, Lee SR, & Kang SW (2003) Cellular regulation by hydrogen peroxide. *J Am Soc Nephrol.* 14(8 Suppl 3):S211-215.

229. de Keizer PL, Burgering BM, & Dansen TB (2011) Forkhead box o as a sensor, mediator, and regulator of redox signaling. *Antioxid Redox Signal.* 14(6):1093-1106. doi: 1010.1089/ars.2010.3403. Epub 2010 Sep 1020.

230. Finkel T (2011) Signal transduction by reactive oxygen species. *J Cell Biol.* 194(1):7-15. doi: 10.1083/jcb.201102095.

231. Rhee SG, Bae YS, Lee SR, & Kwon J (2000) Hydrogen peroxide: a key messenger that modulates protein phosphorylation through cysteine oxidation. *Sci STKE.* 2000(53):pe1.

232. McCubrey JA, Steelman LS, Chappell WH, Abrams SL, Wong EW, *et al.* (2007) Roles of the Raf/MEK/ERK pathway in cell growth, malignant transformation and drug resistance. *Biochim Biophys Acta.* 1773(8):1263-1284. Epub 2006 Oct 1267.

233. Knebel A, Rahmsdorf HJ, Ullrich A, & Herrlich P (1996) Dephosphorylation of receptor tyrosine kinases as target of regulation by radiation, oxidants or alkylating agents. *The EMBO journal* 15(19):5314-5325.

234. Lander HM, Milbank AJ, Tauras JM, Hajjar DP, Hempstead BL, *et al.* (1996) Redox regulation of cell signalling. *Nature* 381(6581):380-381.

235. Manda G, Nechifor MT, & Neagu T (2009) Reactive oxygen species, cancer and anti-cancer therapies. *Curr Chem Biol* 3(1):22-46.

236. Mallis RJ, Buss JE, & Thomas JA (2001) Oxidative modification of H-ras: S-thiolation and S-nitrosylation of reactive cysteines. *The Biochemical journal* 355(Pt 1):145-153.

237. Funato Y, Michiue T, Asashima M, & Miki H (2006) The thioredoxin-related redox-regulating protein nucleoredoxin inhibits Wnt-beta-catenin signalling through dishevelled. *Nat Cell Biol.* 8(5):501-508. Epub 2006 Apr 2002.

238. Gough DR & Cotter TG (2011) Hydrogen peroxide: a Jekyll and Hyde signalling molecule. *Cell Death Dis.* 2:e213.(doi):10.1038/cddis.2011.1096.

239. Kim LC, Song L, & Haura EB (2009) Src kinases as therapeutic targets for cancer. *Nature reviews. Clinical oncology* 6(10):587-595.

240. D'Autreaux B & Toledano MB (2007) ROS as signalling molecules: mechanisms that generate specificity in ROS homeostasis. *Nat Rev Mol Cell Biol.* 8(10):813-824.

241. Orrenius S, Gogvadze V, & Zhivotovsky B (2007) Mitochondrial oxidative stress: implications for cell death. *Annu Rev Pharmacol Toxicol.* 47:143-183.

242. Mates JM, Segura JA, Alonso FJ, & Marquez J (2012) Oxidative stress in apoptosis and cancer: an update. *Arch Toxicol.* 86(11):1649-1665. doi: 1610.1007/s00204-00012-00906-00203. Epub 02012 Jul 00219.

243. Wang JY (2001) DNA damage and apoptosis. *Cell Death Differ.* 8(11):1047-1048.

244. Yakes FM & Van Houten B (1997) Mitochondrial DNA damage is more extensive and persists longer than nuclear DNA damage in human cells following oxidative stress. *Proc Natl Acad Sci U S A.* 94(2):514-519.

245. Starke-Reed PE & Oliver CN (1989) Protein oxidation and proteolysis during aging and oxidative stress. *Arch Biochem Biophys.* 275(2):559-567.

246. Cecarini V, Gee J, Fioretti E, Amici M, Angeletti M, *et al.* (2007) Protein oxidation and cellular homeostasis: Emphasis on metabolism. *Biochim Biophys Acta.* 1773(2):93-104. Epub 2006 Aug 2030.

247. Esterbauer H, Schaur RJ, & Zollner H (1991) Chemistry and biochemistry of 4-hydroxynonenal, malonaldehyde and related aldehydes. *Free Radic Biol Med.* 11(1):81-128.

248. Avery SV (2011) Molecular targets of oxidative stress. *The Biochemical journal* 434(2):201-210.

249. Feig DI, Reid TM, & Loeb LA (1994) Reactive oxygen species in tumorigenesis. *Cancer Res.* 54(7 Suppl):1890s-1894s.

250. Mates JM, Segura JA, Alonso FJ, & Marquez J (2008) Intracellular redox status and oxidative stress: implications for cell proliferation, apoptosis, and carcinogenesis. *Arch Toxicol.* 82(5):273-299. doi: 210.1007/s00204-00008-00304-z. Epub 02008 Apr 00229.

251. Martin KR & Barrett JC (2002) Reactive oxygen species as double-edged swords in cellular processes: low-dose cell signaling versus high-dose toxicity. *Hum Exp Toxicol.* 21(2):71-75.

252. Singh KK (2004) Mitochondria damage checkpoint in apoptosis and genome stability. *FEMS Yeast Res.* 5(2):127-132.

253. Trachootham D, Alexandre J, & Huang P (2009) Targeting cancer cells by ROS-mediated mechanisms: a radical therapeutic approach? *Nature reviews. Drug discovery* 8(7):579-591.

254. Foley J, Nickerson NK, Nam S, Allen KT, Gilmore JL, *et al.* (2010) EGFR signaling in breast cancer: bad to the bone. *Seminars in cell & developmental biology* 21(9):951-960.

255. Klijn JG, Berns PM, Schmitz PI, & Foekens JA (1992) The clinical significance of epidermal growth factor receptor (EGF-R) in human breast cancer: a review on 5232 patients. *Endocrine reviews* 13(1):3-17.

256. Castaneda CA, Cortes-Funes H, Gomez HL, & Ciruelos EM (2010) The phosphatidyl inositol 3-kinase/AKT signaling pathway in breast cancer. *Cancer metastasis reviews* 29(4):751-759.

257. Zhang X, Tang N, Hadden TJ, & Rishi AK (2011) Akt, FoxO and regulation of apoptosis. *Biochim Biophys Acta.* 1813(11):1978-1986. doi: 1910.1016/j.bbamcr.2011.1903.1010. Epub 2011 Mar 1931.

258. Balmanno K & Cook SJ (2009) Tumour cell survival signalling by the ERK1/2 pathway. *Cell Death Differ* 16(3):368-377.

259. Gilles C, Polette M, Mestdagt M, Nawrocki-Raby B, Ruggeri P, *et al.* (2003) Transactivation of vimentin by beta-catenin in human breast cancer cells. *Cancer Res* 63(10):2658-2664.

260. Kang DH (2002) Oxidative stress, DNA damage, and breast cancer. *AACN Clin Issues.* 13(4):540-549.

261. Yook JI, Li XY, Ota I, Hu C, Kim HS, *et al.* (2006) A Wnt-Axin2-GSK3beta cascade regulates Snail1 activity in breast cancer cells. *Nature cell biology* 8(12):1398-1406.

262. Woodward WA, Chen MS, Behbod F, Alfaro MP, Buchholz TA, *et al.* (2007) WNT/beta-catenin mediates radiation resistance of mouse mammary progenitor cells. *Proc Natl Acad Sci U S A* 104(2):618-623.

263. Chen MS, Woodward WA, Behbod F, Peddibhotla S, Alfaro MP, *et al.* (2007) Wnt/beta-catenin mediates radiation resistance of Sca1+ progenitors in an immortalized mammary gland cell line. *Journal of cell science* 120(Pt 3):468-477.

264. Trachootham D, Zhang W, & Huang P (2009) Oxidative Stress and Drug Resistance in Cancer. *Drug Resistance in Cancer Cells*, eds Siddik ZH & Mehta K (Springer US), pp 137-175.

265. Brown NS & Bicknell R (2001) Hypoxia and oxidative stress in breast cancer. Oxidative stress: its effects on the growth, metastatic potential and response to therapy of breast cancer. *Breast Cancer Res.* 3(5):323-327. Epub 2001 Jul 2023.

266. Janero DR (1990) Malondialdehyde and thiobarbituric acid-reactivity as diagnostic indices of lipid peroxidation and peroxidative tissue injury. *Free Radic Biol Med.* 9(6):515-540.

267. Guetens G, De Boeck G, Highley M, van Oosterom AT, & de Bruijn EA (2002) Oxidative DNA damage: biological significance and methods of analysis. *Crit Rev Clin Lab Sci.* 39(4-5):331-457.

268. Tas F, Hansel H, Belce A, Ilvan S, Argon A, *et al.* (2005) Oxidative stress in breast cancer. *Med Oncol.* 22(1):11-15.

269. Portakal O, Ozkaya O, Erden Inal M, Bozan B, Kosan M, *et al.* (2000) Coenzyme Q10 concentrations and antioxidant status in tissues of breast cancer patients. *Clin Biochem.* 33(4):279-284.

270. Kumaraguruparan R, Subapriya R, Viswanathan P, & Nagini S (2002) Tissue lipid peroxidation and antioxidant status in patients with adenocarcinoma of the breast. *Clin Chim Acta.* 325(1-2):165-170.

271. Kumaraguruparan R, Kabalimoorthy J, & Nagini S (2005) Correlation of tissue lipid peroxidation and antioxidants with clinical stage and menopausal status in patients with adenocarcinoma of the breast. *Clin Biochem.* 38(2):154-158.

272. Huang J, Tan PH, Tan BK, & Bay BH (2004) GST-pi expression correlates with oxidative stress and apoptosis in breast cancer. *Oncol Rep.* 12(4):921-925.

273. Balendiran GK, Dabur R, & Fraser D (2004) The role of glutathione in cancer. *Cell Biochem Funct* 22(6):343-352.

274. Jardim BV, Moschetta MG, Leonel C, Gelaleti GB, Regiani VR, *et al.* (2013) Glutathione and glutathione peroxidase expression in breast cancer: An immunohistochemical and molecular study. *Oncol Rep* 13(10).

275. Chen EI, Hewel J, Krueger JS, Tiraby C, Weber MR, *et al.* (2007) Adaptation of energy metabolism in breast cancer brain metastases. *Cancer Res.* 67(4):1472-1486.

276. Singh B, Tai K, Madan S, Raythatha MR, Cady AM, *et al.* (2012) Selection of metastatic breast cancer cells based on adaptability of their metabolic state. *PLoS*

One. 7(5):e36510. doi: 36510.31371/journal.pone.0036510. Epub 0032012 May 0036513.

277. Ballatori N, Krance SM, Notenboom S, Shi S, Tieu K, *et al.* (2009) Glutathione dysregulation and the etiology and progression of human diseases. *Biol Chem.* 390(3):191-214. doi: 110.1515/BC.2009.1033.

278. Doroshow JH, Akman S, Esworthy S, Chu FF, & Burke T (1991) Doxorubicin resistance conferred by selective enhancement of intracellular glutathione peroxidase or superoxide dismutase content in human MCF-7 breast cancer cells. *Free Radic Res Commun.* 12-13(Pt 2):779-781.

279. Kalinina EV, Chernov NN, Saprin AN, Kotova YN, Andreev YA, *et al.* (2006) Changes in expression of genes encoding antioxidant enzymes, heme oxygenase-1, Bcl-2, and Bcl-xl and in level of reactive oxygen species in tumor cells resistant to doxorubicin. *Biochemistry (Mosc)* 71(11):1200-1206.

280. Schiff R, Reddy P, Ahotupa M, Coronado-Heinsohn E, Grim M, *et al.* (2000) Oxidative stress and AP-1 activity in tamoxifen-resistant breast tumors in vivo. *J Natl Cancer Inst* 92(23):1926-1934.

281. Karin M (2006) Nuclear factor-kappaB in cancer development and progression. *Nature* 441(7092):431-436.

282. Kaspar JW, Niture SK, & Jaiswal AK (2009) Nrf2:INrf2 (Keap1) signaling in oxidative stress. *Free Radic Biol Med.* 47(9):1304-1309. doi: 1310.1016/j.freeradbiomed.2009.1307.1035. Epub 2009 Aug 1307.

283. Mitsuishi Y, Motohashi H, & Yamamoto M (2012) The Keap1-Nrf2 system in cancers: stress response and anabolic metabolism. *Front Oncol.* 2:200.(doi):10.3389/fonc.2012.00200. Epub 02012 Dec 00226.

284. Dimberg LY, Anderson CK, Camidge R, Behbakht K, Thorburn A, *et al.* (2013) On the TRAIL to successful cancer therapy? Predicting and counteracting resistance against TRAIL-based therapeutics. *Oncogene* 32(11):1341-1350.

285. Bellezza I, Mierla AL, & Minelli A (2010) Nrf2 and NF-κB and Their Concerted Modulation in Cancer Pathogenesis and Progression. *Cancers* 2(2):483-497.

286. Song NY, Kim DH, Kim EH, Na HK, Kim NJ, *et al.* (2011) Multidrug resistance-associated protein 1 mediates 15-deoxy-Delta(12,14)-prostaglandin J2-induced expression of glutamate cysteine ligase expression via Nrf2 signaling in human breast cancer cells. *Chem Res Toxicol.* 24(8):1231-1241. doi: 1210.1021/tx200090n. Epub 202011 Jul 200025.

287. Woodward WA, Debeb BG, Xu W, & Buchholz TA (2010) Overcoming radiation resistance in inflammatory breast cancer. *Cancer* 116(11 Suppl):2840-2845.

288. Loignon M, Miao W, Hu L, Bier A, Bismar TA, *et al.* (2009) Cul3 overexpression depletes Nrf2 in breast cancer and is associated with sensitivity to carcinogens, to oxidative stress, and to chemotherapy. *Mol Cancer Ther.* 8(8):2432-2440. doi: 2410.1158/1535-7163.MCT-2408-1186. Epub 2009 Jul 2428.

289. Zhong Y, Zhang F, Sun Z, Zhou W, Li ZY, *et al.* (2012) Drug resistance associates with activation of Nrf2 in MCF-7/DOX cells, and wogonin reverses it by down-regulating Nrf2-mediated cellular defense response. *Mol Carcinog* 16(10):21921.

290. Kim SK, Yang JW, Kim MR, Roh SH, Kim HG, *et al.* (2008) Increased expression of Nrf2/ARE-dependent anti-oxidant proteins in tamoxifen-resistant breast cancer cells. *Free Radic Biol Med.* 45(4):537-546. doi: 510.1016/j.freeradbiomed.2008.1005.1011. Epub 2008 May 1024.

291. Smirnov AS, Ruzov AS, Budanov AV, Prokhortchouk AV, Ivanov AV, *et al.* (2001) High constitutive level of NF-kappaB is crucial for viability of adenocarcinoma cells. *Cell Death Differ.* 8(6):621-630.

292. Wu JT & Kral JG (2005) The NF-kappaB/IkappaB signaling system: a molecular target in breast cancer therapy. *J Surg Res.* 123(1):158-169.

293. Sprowl JA, Reed K, Armstrong SR, Lanner C, Guo B, *et al.* (2012) Alterations in tumor necrosis factor signaling pathways are associated with cytotoxicity and resistance to taxanes: a study in isogenic resistant tumor cells. *Breast Cancer Res.* 14(1):R2.

294. Zhou Y, Eppenberger-Castori S, Eppenberger U, & Benz CC (2005) The NFkappaB pathway and endocrine-resistant breast cancer. *Endocr Relat Cancer.* 12(Suppl 1):S37-46.

295. Musgrove EA & Sutherland RL (2009) Biological determinants of endocrine resistance in breast cancer. *Nature reviews. Cancer* 9(9):631-643.

296. Guo G, Yan-Sanders Y, Lyn-Cook BD, Wang T, Tamae D, *et al.* (2003) Manganese superoxide dismutase-mediated gene expression in radiation-induced adaptive responses. *Mol Cell Biol.* 23(7):2362-2378.

297. DeGraffenried LA, Friedrichs WE, Fulcher L, Fernandes G, Silva JM, *et al.* (2003) Eicosapentaenoic acid restores tamoxifen sensitivity in breast cancer cells with high Akt activity. *Ann Oncol.* 14(7):1051-1056.

298. deGraffenried LA, Chandrasekar B, Friedrichs WE, Donzis E, Silva J, *et al.* (2004) NF-kappa B inhibition markedly enhances sensitivity of resistant breast cancer tumor cells to tamoxifen. *Ann Oncol.* 15(6):885-890.

299. Tokunaga E, Kimura Y, Oki E, Ueda N, Futatsugi M, *et al.* (2006) Akt is frequently activated in HER2/neu-positive breast cancers and associated with poor prognosis among hormone-treated patients. *Int J Cancer.* 118(2):284-289.

300. Liang K, Jin W, Knuefermann C, Schmidt M, Mills GB, *et al.* (2003) Targeting the phosphatidylinositol 3-kinase/Akt pathway for enhancing breast cancer cells to radiotherapy. *Mol Cancer Ther.* 2(4):353-360.

301. Soderlund K, Perez-Tenorio G, & Stal O (2005) Activation of the phosphatidylinositol 3-kinase/Akt pathway prevents radiation-induced apoptosis in breast cancer cells. *Int J Oncol.* 26(1):25-32.

302. Weinstein-Oppenheimer CR, Henriquez-Roldan CF, Davis JM, Navolanic PM, Saleh OA, *et al.* (2001) Role of the Raf signal transduction cascade in the in vitro resistance to the anticancer drug doxorubicin. *Clin Cancer Res* 7(9):2898-2907.

303. Li Z, Wang N, Fang J, Huang J, Tian F, *et al.* (2012) Role of PKC-ERK signaling in tamoxifen-induced apoptosis and tamoxifen resistance in human breast cancer cells. *Oncol Rep* 27(6):1879-1886.

304. Svensson S, Jirstrom K, Ryden L, Roos G, Emdin S, *et al.* (2005) ERK phosphorylation is linked to VEGFR2 expression and Ets-2 phosphorylation in breast cancer and is associated with tamoxifen treatment resistance and small tumours with good prognosis. *Oncogene* 24(27):4370-4379.

305. Schor NF, Kagan VE, Liang Y, Yan C, Tyurina Y, *et al.* (2004) Exploiting oxidative stress and signaling in chemotherapy of resistant neoplasms. *Biochemistry (Mosc)* 69(1):38-44.

306. Foster FM, Owens TW, Tanianis-Hughes J, Clarke RB, Brennan K, *et al.* (2009) Targeting inhibitor of apoptosis proteins in combination with ErbB antagonists in breast cancer. *Breast cancer research : BCR* 11(3):R41.

307. Fandy TE, Shankar S, & Srivastava RK (2008) Smac/DIABLO enhances the therapeutic potential of chemotherapeutic drugs and irradiation, and sensitizes TRAIL-resistant breast cancer cells. *Molecular cancer* 7:60.

308. Tian H, Zhang B, Di J, Jiang G, Chen F, *et al.* (2012) Keap1: one stone kills three birds Nrf2, IKKbeta and Bcl-2/Bcl-xL. *Cancer Lett.* 325(1):26-34. doi: 10.1016/j.canlet.2012.1006.1007. Epub 2012 Jun 1026.

309. Meng F, Liu L, Chin PC, & D'Mello SR (2002) Akt is a downstream target of NF-kappa B. *J Biol Chem* 277(33):29674-29680.

310. Li F & Sethi G (2010) Targeting transcription factor NF-kappaB to overcome chemoresistance and radioresistance in cancer therapy. *Biochim Biophys Acta.* 1805(2):167-180. doi: 110.1016/j.bbcan.2010.1001.1002. Epub 2010 Jan 1014.

311. Sizemore N, Leung S, & Stark GR (1999) Activation of phosphatidylinositol 3-kinase in response to interleukin-1 leads to phosphorylation and activation of the NF-kappaB p65/RelA subunit. *Molecular and cellular biology* 19(7):4798-4805.

312. Forozan F, Veldman R, Ammerman CA, Parsa NZ, Kallioniemi A, *et al.* (1999) Molecular cytogenetic analysis of 11 new breast cancer cell lines. *British journal of cancer* 81(8):1328-1334.

313. Robertson FM, Chu K, Fernandes SV, Mu Z, Zhang X, *et al.* (2012) Genomic profiling of pre-clinical models of inflammatory breast cancer identifies a signature of epithelial plasticity and suppression of TGFβ signaling. *J Clin Exp Pathol* 2(5).

314. Klopp AH, Lacerda L, Gupta A, Debeb BG, Solley T, *et al.* (2010) Mesenchymal stem cells promote mammosphere formation and decrease E-cadherin in normal and malignant breast cells. *PloS one* 5(8):e12180.

315. Choi SL, Kim SJ, Lee KT, Kim J, Mu J, *et al.* (2001) The regulation of AMP-activated protein kinase by H(2)O(2). *Biochem Biophys Res Commun* 287(1):92-97.

316. Allensworth JL, Sauer SJ, Lyerly HK, Morse MA, & Devi GR (2013) Smac mimetic Birinapant induces apoptosis and enhances TRAIL potency in inflammatory breast cancer cells in an IAP-dependent and TNF-alpha-independent mechanism. *Breast Cancer Res Treat.* 137(2):359-371. doi: 310.1007/s10549-10012-12352-10546. Epub 12012 Dec 10547.

317. Batinic-Haberle I, Rajic Z, Tovmasyan A, Reboucas JS, Ye X, *et al.* (2011) Diverse functions of cationic Mn(III) N-substituted pyridylporphyrins, recognized as SOD mimics. *Free radical biology & medicine* 51(5):1035-1053.

318. Mosmann T (1983) Rapid colorimetric assay for cellular growth and survival: application to proliferation and cytotoxicity assays. *J. Immunol. Methods* 65(1-2):55-63.

319. Amantana A, London CA, Iversen PL, & Devi GR (2004) X-linked inhibitor of apoptosis protein inhibition induces apoptosis and enhances chemotherapy sensitivity in human prostate cancer cells. *Mol Cancer Ther* 3(6):699-707.

320. Williams KP, Allensworth JL, Ingram SM, Smith GR, Aldrich AJ, *et al.* (2013) Quantitative high-throughput efficacy profiling of approved oncology drugs in inflammatory breast cancer models of acquired drug resistance and re-sensitization. *Cancer Lett* 17(13):00386-00388.

321. Nikolovska-Coleska Z, Xu L, Hu Z, Tomita Y, Li P, *et al.* (2004) Discovery of embelin as a cell-permeable, small-molecular weight inhibitor of XIAP through

structure-based computational screening of a traditional herbal medicine three-dimensional structure database. *J Med Chem* 47(10):2430-2440.

322. Robinson JS, Klionsky DJ, Banta LM, & Emr SD (1988) Protein sorting in Saccharomyces cerevisiae: isolation of mutants defective in the delivery and processing of multiple vacuolar hydrolases. *Molecular and cellular biology* 8(11):4936-4948.

323. Puig S, Lee J, Lau M, & Thiele DJ (2002) Biochemical and genetic analyses of yeast and human high affinity copper transporters suggest a conserved mechanism for copper uptake. *J Biol Chem.* 277(29):26021-26030. Epub 22002 Apr 26030.

324. Pena MM, Koch KA, & Thiele DJ (1998) Dynamic regulation of copper uptake and detoxification genes in Saccharomyces cerevisiae. *Mol Cell Biol.* 18(5):2514-2523.

325. Reeder NL, Kaplan J, Xu J, Youngquist RS, Wallace J, *et al.* (2011) Zinc pyrithione inhibits yeast growth through copper influx and inactivation of iron-sulfur proteins. *Antimicrob Agents Chemother.* 55(12):5753-5760. doi: 5710.1128/AAC.00724-00711. Epub 02011 Sep 00726.

326. Chou TC & Talalay P (1984) Quantitative analysis of dose-effect relationships: the combined effects of multiple drugs or enzyme inhibitors. *Advances in enzyme regulation* 22:27-55.

327. Goldfarb JM & Pippen JE (2011) Inflammatory breast cancer: the experience of Baylor University Medical Center at Dallas. *Proc (Bayl Univ Med Cent).* 24(2):86-88.

328. Dawood S, Broglio K, Buzdar AU, Hortobagyi GN, & Giordano SH (2010) Prognosis of women with metastatic breast cancer by HER2 status and trastuzumab treatment: an institutional-based review. *J Clin Oncol* 28(1):92-98.

329. Petrelli F, Cabiddu M, Ghilardi M, & Barni S (2009) Current data of targeted therapies for the treatment of triple-negative advanced breast cancer: empiricism or evidence-based? *Expert Opin Investig Drugs.* 18(10):1467-1477. doi: 1410.1517/13543780903222268.

330. Burris HA, 3rd, Hurwitz HI, Dees EC, Dowlati A, Blackwell KL, *et al.* (2005) Phase I safety, pharmacokinetics, and clinical activity study of lapatinib (GW572016), a reversible dual inhibitor of epidermal growth factor receptor tyrosine kinases, in heavily pretreated patients with metastatic carcinomas. *J Clin Oncol* 23(23):5305-5313.

331. Aird KM, Ghanayem RB, Peplinski S, Lyerly HK, & Devi GR (2010) X-Linked inhibitor of apoptosis protein inhibits apoptosis in inflammatory breast cancer cells with acquired resistance to an ErbB1/2 tyrosine kinase inhibitor. *Mol. Cancer Ther.* 9:1431-1442.

332. Aird KM, Allensworth JL, Batinic-Haberle I, Lyerly HK, Dewhirst MW, *et al.* (2012) ErbB1/2 tyrosine kinase inhibitor mediates oxidative stress-induced apoptosis in inflammatory breast cancer cells. *Breast Cancer Res. Treat.* 132:109-119.

333. Wolpaw AJ, Shimada K, Skouta R, Welsch ME, Akavia UD, *et al.* (2011) Modulatory profiling identifies mechanisms of small molecule-induced cell death. *Proc Natl Acad Sci USA* 108:E771-780.

334. Valiathan C, McFaline JL, & Samson LD (2011) A rapid survival assay to measure drug-induced cytotoxicity and cell cycle effects. *DNA Repair* 11:92-98.

335. Kuo WL, Das D, Ziyad S, Bhattacharya S, Gibb WJ, *et al.* (2009) A systems analysis of the chemosensitivity of breast cancer cells to the polyamine analogue PG-11047. *BMC Med.* 7(1):77.

336. Heiser LM, Sadanandam A, Kuo WL, Benz SC, Goldstein TC, *et al.* (2012) Subtype and pathway specific responses to anticancer compounds in breast cancer. *Proc Natl Acad Sci USA* 109(8):2724-2729.

337. Dong HM, Liu G, Hou YF, Wu J, Lu JS, *et al.* (2007) Dominant-negative E-cadherin inhibits the invasiveness of inflammatory breast cancer cells in vitro. *J. Cancer Res. Clin. Oncol.* 133(2):83-92.

338. Hoffmeyer MR, Wall KM, & Dharmawardhane SF (2005) In vitro analysis of the invasive phenotype of SUM 149, an inflammatory breast cancer cell line. *Cancer Cell Int* 5(1):11.

339. Ignatoski K & Ethier S (1999) Constitutive activation of pp125fak in newly isolated human breast cancer cell lines. *Breast Cancer Res. Treat.* 54(2):173-182.

340. Singh B, Irving L, Tai K, & Lucci A (2010) Overexpression of COX-2 in Celecoxib-resistant breast cancer cell lines. *J. Surg. Res.* 163:235-243.

341. Wu M, Wu Z, Rosenthal D, Rhee E, & Merajver S (2010) Characterization of the roles of RHOC and RHOA GTPases in invasion, motility, and matrix adhesion in inflammatory and aggressive breast cancers. *Cancer* 116(S11):2768-2782.

342. Cardaci S, Filomeni G, & Ciriolo MR (2012) Redox implications of AMPK-mediated signal transduction beyond energetic clues. *J. Cell Sci.* 125(9):2115-2125.

343. Sharma SV, Lee DY, Li B, Quinlan MP, Takahashi F, *et al.* (2010) A chromatin-mediated reversible drug-tolerant state in cancer cell subpopulations. *Cell* 141(1):69-80.

344. Charafe-Jauffret E, Ginestier C, Iovino F, Tarpin C, Diebel M, *et al.* (2010) Aldehyde dehydrogenase 1–Positive cancer stem cells mediate metastasis and poor clinical outcome in inflammatory breast cancer. *Clin. Cancer Res.* 16(1):45-55.

345. Debeb BG, Cohen EN, Boley K, Freiter EM, Li L, *et al.* (2012) Pre-clinical studies of Notch signaling inhibitor RO4929097 in inflammatory breast cancer cells. *Breast Cancer Res. Treat.* 134:495-510.

346. Rosenthal DT, Zhang J, Bao L, Zhu L, Wu Z, *et al.* (2012) RhoC Impacts the Metastatic Potential and Abundance of Breast Cancer Stem Cells. *PLoS One* 7(7):e40979.

347. Anderson WF, Chu KC, & Chang S (2003) Inflammatory breast carcinoma and noninflammatory locally advanced breast carcinoma: distinct clinicopathologic entities? *J Clin Oncol* 21(12):2254-2259.

348. Van Laere S, Van der Auwera I, Van den Eynden G, Van Hummelen P, van Dam P, *et al.* (2007) Distinct molecular phenotype of inflammatory breast cancer compared to non-inflammatory breast cancer using Affymetrix-based genome-wide gene-expression analysis. *British journal of cancer* 97(8):1165-1174.

349. Wang J, Liu Y, Ji R, Gu Q, Zhao X, *et al.* (2010) Prognostic value of the X-linked inhibitor of apoptosis protein for invasive ductal breast cancer with triple-negative phenotype. *Hum Pathol* 41(8):1186-1195.

350. Liston P, Fong WG, & Korneluk RG (2003) The inhibitors of apoptosis: there is more to life than Bcl2. *Oncogene* 22(53):8568-8580.

351. LaCasse EC, Baird S, Korneluk RG, & MacKenzie AE (1998) The inhibitors of apoptosis (IAPs) and their emerging role in cancer. *Oncogene* 17(25):3247-3259.

352. Nachmias B, Ashhab Y, & Ben-Yehuda D (2004) The inhibitor of apoptosis protein family (IAPs): an emerging therapeutic target in cancer. *Semin Cancer Biol* 14(4):231-243.

353. Schimmer AD, Dalili S, Batey RA, & Riedl SJ (2006) Targeting XIAP for the treatment of malignancy. *Cell Death Differ* 13(2):179-188.

354. Kashkar H (2010) X-linked inhibitor of apoptosis: a chemoresistance factor or a hollow promise. *Clin Cancer Res* 16(18):4496-4502.

355. Fulda S & Vucic D (2012) Targeting IAP proteins for therapeutic intervention in cancer. *Nature reviews. Drug discovery* 11(2):109-124.

356. Flanagan L, Sebastia J, Tuffy LP, Spring A, Lichawska A, *et al.* (2010) XIAP impairs Smac release from the mitochondria during apoptosis. *Cell death & disease* 1:e49.

357. Pluta P, Cebula-Obrzut B, Ehemann V, Pluta A, Wierzbowska A, *et al.* (2011) Correlation of Smac/DIABLO protein expression with the clinico-pathological features of breast cancer patients. *Neoplasma* 58(5):430-435.

358. Vince JE, Wong WW, Khan N, Feltham R, Chau D, *et al.* (2007) IAP antagonists target cIAP1 to induce TNFalpha-dependent apoptosis. *Cell* 131(4):682-693.

359. Wu H, Tschopp J, & Lin SC (2007) Smac mimetics and TNFalpha: a dangerous liaison? *Cell* 131(4):655-658.

360. Bertrand MJ, Milutinovic S, Dickson KM, Ho WC, Boudreault A, *et al.* (2008) cIAP1 and cIAP2 facilitate cancer cell survival by functioning as E3 ligases that promote RIP1 ubiquitination. *Molecular cell* 30(6):689-700.

361. Lu J, Bai L, Sun H, Nikolovska-Coleska Z, McEachern D, *et al.* (2008) SM-164: a novel, bivalent Smac mimetic that induces apoptosis and tumor regression by concurrent removal of the blockade of cIAP-1/2 and XIAP. *Cancer Res* 68(22):9384-9393.

362. Petersen SL, Wang L, Yalcin-Chin A, Li L, Peyton M, *et al.* (2007) Autocrine TNFalpha signaling renders human cancer cells susceptible to Smac-mimetic-induced apoptosis. *Cancer Cell* 12(5):445-456.

363. Varfolomeev E, Blankenship JW, Wayson SM, Fedorova AV, Kayagaki N, *et al.* (2007) IAP antagonists induce autoubiquitination of c-IAPs, NF-kappaB activation, and TNFalpha-dependent apoptosis. *Cell* 131(4):669-681.

364. Condon SM (2011) Chapter 13 - The Discovery and Development of Smac Mimetics—Small-Molecule Antagonists of the Inhibitor of Apoptosis Proteins. *Annual Reports in Medicinal Chemistry*, ed John EM (Academic Press), Vol Volume 46, pp 211-226.

365. Arnt CR, Chiorean MV, Heldebrant MP, Gores GJ, & Kaufmann SH (2002) Synthetic Smac/DIABLO peptides enhance the effects of chemotherapeutic agents by binding XIAP and cIAP1 in situ. *J Biol Chem* 277(46):44236-44243.

366. Emeagi PU, Van Lint S, Goyvaerts C, Maenhout S, Cauwels A, *et al.* (2012) Proinflammatory characteristics of SMAC/DIABLO-induced cell death in antitumor therapy. *Cancer Res* 72(6):1342-1352.

367. Fulda S, Wick W, Weller M, & Debatin KM (2002) Smac agonists sensitize for Apo2L/TRAIL- or anticancer drug-induced apoptosis and induce regression of malignant glioma in vivo. *Nature medicine* 8(8):808-815.

368. Guo F, Nimmanapalli R, Paranawithana S, Wittman S, Griffin D, *et al.* (2002) Ectopic overexpression of second mitochondria-derived activator of caspases (Smac/DIABLO) or cotreatment with N-terminus of Smac/DIABLO peptide potentiates epothilone B derivative-(BMS 247550) and Apo-2L/TRAIL-induced apoptosis. *Blood* 99(9):3419-3426.

369. Wagner L, Marschall V, Karl S, Cristofanon S, Zobel K, *et al.* (2012 April 4 [Epub ahead of print]) Smac mimetic sensitizes glioblastoma cells to Temozolomide-induced apoptosis in a RIP1- and NF-kappaB-dependent manner. *Oncogene*.

370. Kim K, Fisher MJ, Xu SQ, & el-Deiry WS (2000) Molecular determinants of response to TRAIL in killing of normal and cancer cells. *Clin Cancer Res* 6(2):335-346.

371. Papenfuss K, Cordier SM, & Walczak H (2008) Death receptors as targets for anti-cancer therapy. *Journal of cellular and molecular medicine* 12(6B):2566-2585.

372. Ashkenazi A, Pai RC, Fong S, Leung S, Lawrence DA, *et al.* (1999) Safety and antitumor activity of recombinant soluble Apo2 ligand. *J Clin Invest.* 104(2):155-162.

373. Zhang L & Fang B (2005) Mechanisms of resistance to TRAIL-induced apoptosis in cancer. *Cancer Gene Ther* 12(3):228-237.

374. Aggarwal BB, Bhardwaj U, & Takada Y (2004) Regulation of TRAIL-induced apoptosis by ectopic expression of antiapoptotic factors. *Vitam Horm* 67:453-483.

375. Chawla-Sarkar M, Bae SI, Reu FJ, Jacobs BS, Lindner DJ, *et al.* (2004) Downregulation of Bcl-2, FLIP or IAPs (XIAP and survivin) by siRNAs sensitizes resistant melanoma cells to Apo2L/TRAIL-induced apoptosis. *Cell Death Differ* 11(8):915-923.

376. Cummins JM, Kohli M, Rago C, Kinzler KW, Vogelstein B, *et al.* (2004) X-linked inhibitor of apoptosis protein (XIAP) is a nonredundant modulator of tumor necrosis factor-related apoptosis-inducing ligand (TRAIL)-mediated apoptosis in human cancer cells. *Cancer Res* 64(9):3006-3008.

377. Shankar S & Srivastava RK (2004) Enhancement of therapeutic potential of TRAIL by cancer chemotherapy and irradiation: mechanisms and clinical implications. *Drug Resist Updat* 7(2):139-156.

378. Chinnaiyan AM, Prasad U, Shankar S, Hamstra DA, Shanaiah M, *et al.* (2000) Combined effect of tumor necrosis factor-related apoptosis-inducing ligand and ionizing radiation in breast cancer therapy. *Proc Natl Acad Sci U S A* 97(4):1754-1759.

379. Rahman M, Davis SR, Pumphrey JG, Bao J, Nau MM, *et al.* (2009) TRAIL induces apoptosis in triple-negative breast cancer cells with a mesenchymal phenotype. *Breast Cancer Res Treat* 113(2):217-230.

380. Braeuer SJ, Buneker C, Mohr A, & Zwacka RM (2006) Constitutively activated nuclear factor-kappaB, but not induced NF-kappaB, leads to TRAIL resistance by up-regulation of X-linked inhibitor of apoptosis protein in human cancer cells. *Mol Cancer Res* 4(10):715-728.

381. Shin SI, Freedman VH, Risser R, & Pollack R (1975) Tumorigenicity of virus-transformed cells in nude mice is correlated specifically with anchorage independent growth in vitro. *Proc Natl Acad Sci U S A* 72(11):4435-4439.

382. Debeb BG, Cohen EN, Boley K, Freiter EM, Li L, *et al.* (2012) Pre-clinical studies of Notch signaling inhibitor RO4929097 in inflammatory breast cancer cells. *Breast Cancer Res Treat* 134(2):495-510.

383. Jinesh GG, Chunduru S, & Kamat AM (2012) Smac mimetic enables the anticancer action of BCG-stimulated neutrophils through TNF-alpha but not through TRAIL and FasL. *Journal of leukocyte biology* 92(1):233-244.

384. Bai L, Chen W, Wang X, Ju W, Xu S, *et al.* (2009) Attenuating Smac mimetic compound 3-induced NF-kappaB activation by luteolin leads to synergistic cytotoxicity in cancer cells. *Journal of cellular biochemistry* 108(5):1125-1131.

385. Moujalled DM, Cook WD, Lluis JM, Khan NR, Ahmed AU, *et al.* (2012) In mouse embryonic fibroblasts, neither caspase-8 nor cellular FLICE-inhibitory protein (FLIP) is necessary for TNF to activate NF-kappaB, but caspase-8 is required for

TNF to cause cell death, and induction of FLIP by NF-kappaB is required to prevent it. *Cell Death Differ* 19(5):808-815.

386. Stadel D, Cristofanon S, Abhari BA, Deshayes K, Zobel K, *et al.* (2011) Requirement of nuclear factor kappaB for Smac mimetic-mediated sensitization of pancreatic carcinoma cells for gemcitabine-induced apoptosis. *Neoplasia* 13(12):1162-1170.

387. Cifone MA & Fidler IJ (1980) Correlation of patterns of anchorage-independent growth with in vivo behavior of cells from a murine fibrosarcoma. *Proc Natl Acad Sci U S A* 77(2):1039-1043.

388. Eschenburg G, Eggert A, Schramm A, Lode HN, & Hundsdoerfer P (2012) Smac Mimetic LBW242 Sensitizes XIAP-Overexpressing Neuroblastoma Cells for TNF-alpha-Independent Apoptosis. *Cancer Res* 72(10):2645-2656.

389. Agostinelli E & Seiler N (2006) Non-irradiation-derived reactive oxygen species (ROS) and cancer: therapeutic implications. *Amino Acids* 31(3):341-355.

390. Maiti AK (2012) Reactive oxygen species reduction is a key underlying mechanism of drug resistance in cancer chemotherapy. *Chemotherapy* 1(2).

391. Ahn KS, Sethi G, & Aggarwal BB (2007) Embelin, an inhibitor of X chromosome-linked inhibitor-of-apoptosis protein, blocks nuclear factor-kappaB (NF-kappaB) signaling pathway leading to suppression of NF-kappaB-regulated antiapoptotic and metastatic gene products. *Mol Pharmacol* 71(1):209-219.

392. Chitra M, Sukumar E, Suja V, & Devi CS (1994) Antitumor, anti-inflammatory and analgesic property of embelin, a plant product. *Chemotherapy* 40(2):109-113.

393. Sung B, Ravindran J, Prasad S, Pandey MK, & Aggarwal BB (2010) Gossypol induces death receptor-5 through activation of the ROS-ERK-CHOP pathway and sensitizes colon cancer cells to TRAIL. *J Biol Chem* 285(46):35418-35427.

394. Tazzari PL, Tabellini G, Ricci F, Papa V, Bortul R, *et al.* (2008) Synergistic proapoptotic activity of recombinant TRAIL plus the Akt inhibitor Perifosine in acute myelogenous leukemia cells. *Cancer Res* 68(22):9394-9403.

395. Yodkeeree S, Sung B, Limtrakul P, & Aggarwal BB (2009) Zerumbone enhances TRAIL-induced apoptosis through the induction of death receptors in human colon cancer cells: Evidence for an essential role of reactive oxygen species. *Cancer Res* 69(16):6581-6589.

396. Micheau O (2003) Cellular FLICE-inhibitory protein: an attractive therapeutic target? *Expert Opin Ther Targets* 7(4):559-573.

397. Kavuri SM, Geserick P, Berg D, Dimitrova DP, Feoktistova M, *et al.* (2011) Cellular FLICE-inhibitory protein (cFLIP) isoforms block CD95- and TRAIL death receptor-induced gene induction irrespective of processing of caspase-8 or cFLIP in the death-inducing signaling complex. *J Biol Chem* 286(19):16631-16646.

398. Garcia-Garcia C, Fumarola C, Navaratnam N, Carling D, & Lopez-Rivas A (2010) AMPK-independent down-regulation of cFLIP and sensitization to TRAIL-induced apoptosis by AMPK activators. *Biochemical pharmacology* 79(6):853-863.

399. Opel D, Naumann I, Schneider M, Bertele D, Debatin KM, *et al.* (2011) Targeting aberrant PI3K/Akt activation by PI103 restores sensitivity to TRAIL-induced apoptosis in neuroblastoma. *Clin Cancer Res* 17(10):3233-3247.

400. Stagni V, Mingardi M, Santini S, Giaccari D, & Barila D (2010) ATM kinase activity modulates cFLIP protein levels: potential interplay between DNA damage signalling and TRAIL-induced apoptosis. *Carcinogenesis* 31(11):1956-1963.

401. Geserick P, Drewniok C, Hupe M, Haas TL, Diessenbacher P, *et al.* (2008) Suppression of cFLIP is sufficient to sensitize human melanoma cells to TRAIL- and CD95L-mediated apoptosis. *Oncogene* 27(22):3211-3220.

402. Ivanov VN, Zhou H, Partridge MA, & Hei TK (2009) Inhibition of ataxia telangiectasia mutated kinase activity enhances TRAIL-mediated apoptosis in human melanoma cells. *Cancer Res* 69(8):3510-3519.

403. Zhao X, Qiu W, Kung J, Zhao X, Peng X, *et al.* (2008) Bortezomib induces caspase-dependent apoptosis in Hodgkin lymphoma cell lines and is associated with reduced c-FLIP expression: a gene expression profiling study with implications for potential combination therapies. *Leuk Res* 32(2):275-285.

404. Olayioye MA, Kaufmann H, Pakusch M, Vaux DL, Lindeman GJ, *et al.* (2005) XIAP-deficiency leads to delayed lobuloalveolar development in the mammary gland. *Cell Death Differ* 12(1):87-90.

405. Lu Z & Xu S (2006) ERK1/2 MAP kinases in cell survival and apoptosis. *IUBMB Life* 58(11):621-631.

406. Xia Z, Dickens M, Raingeaud J, Davis RJ, & Greenberg ME (1995) Opposing effects of ERK and JNK-p38 MAP kinases on apoptosis. *Science* 270(5240):1326-1331.

407. Nagata Y & Todokoro K (1999) Requirement of activation of JNK and p38 for environmental stress-induced erythroid differentiation and apoptosis and of inhibition of ERK for apoptosis. *Blood* 94(3):853-863.

408. Chang H, Lin H, Yi L, Zhu J, Zhou Y, *et al.* (2010) 3,6-Dihydroxyflavone induces apoptosis in leukemia HL-60 cell via reactive oxygen species-mediated p38 MAPK/JNK pathway. *Eur J Pharmacol* 648(1-3):31-38.

409. Zhuang S & Schnellmann RG (2006) A death-promoting role for extracellular signal-regulated kinase. *J Pharmacol Exp Ther* 319(3):991-997.

410. Cagnol S & Chambard JC (2010) ERK and cell death: mechanisms of ERK-induced cell death--apoptosis, autophagy and senescence. *Febs J* 277(1):2-21.

411. Pelicano H, Carney D, & Huang P (2004) ROS stress in cancer cells and therapeutic implications. *Drug Resist Updat.* 7(2):97-110.

412. Ozben T (2007) Oxidative stress and apoptosis: impact on cancer therapy. *J Pharm Sci.* 96(9):2181-2196.

413. Fang J, Seki T, & Maeda H (2009) Therapeutic strategies by modulating oxygen stress in cancer and inflammation. *Adv Drug Deliv Rev.* 61(4):290-302. doi: 210.1016/j.addr.2009.1002.1005. Epub 2009 Feb 1026.

414. Nguyen T, Nioi P, & Pickett CB (2009) The Nrf2-antioxidant response element signaling pathway and its activation by oxidative stress. *J Biol Chem.*

284(20):13291-13295. doi: 13210.11074/jbc.R900010200. Epub 900012009 Jan 900010230.

415. Allensworth JL, Aird KM, Aldrich AJ, Batinic-Haberle I, & Devi GR (2012) XIAP Inhibition and Generation of Reactive Oxygen Species Enhances TRAIL Sensitivity in Inflammatory Breast Cancer Cells. *Mol Cancer Ther*.

416. Eneanya DI, Bianchine JR, Duran DO, & Andresen BD (1981) The actions of metabolic fate of disulfiram. *Annu Rev Pharmacol Toxicol.* 21:575-596.

417. Fuller RK & Gordis E (2004) Does disulfiram have a role in alcoholism treatment today? *Addiction.* 99(1):21-24.

418. Schmitt SM, Frezza M, & Dou QP (2012) New applications of old metal-binding drugs in the treatment of human cancer. *Frontiers in bioscience (Scholar edition)* 4:375-391.

419. Conticello C, Martinetti D, Adamo L, Buccheri S, Giuffrida R, *et al.* (2012) Disulfiram, an old drug with new potential therapeutic uses for human hematological malignancies. *Int J Cancer.* 131(9):2197-2203. doi: 2110.1002/ijc.27482. Epub 22012 Mar 27427.

420. Liu P, Brown S, Goktug T, Channathodiyil P, Kannappan V, *et al.* (2012) Cytotoxic effect of disulfiram/copper on human glioblastoma cell lines and ALDH-positive cancer-stem-like cells. *Br J Cancer.* 107(9):1488-1497. doi: 1410.1038/bjc.2012.1442. Epub 2012 Oct 1482.

421. Yip NC, Fombon IS, Liu P, Brown S, Kannappan V, *et al.* (2011) Disulfiram modulated ROS-MAPK and NFkappaB pathways and targeted breast cancer cells with cancer stem cell-like properties. *British journal of cancer* 104(10):1564-1574.

422. Zhang H, Chen D, Ringler J, Chen W, Cui QC, *et al.* (2010) Disulfiram treatment facilitates phosphoinositide 3-kinase inhibition in human breast cancer cells in vitro and in vivo. *Cancer Res.* 70(10):3996-4004. doi: 3910.1158/0008-5472.CAN-3909-3752. Epub 2010 Apr 3927.

423. Li L, Yang H, Chen D, Cui C, & Dou QP (2008) Disulfiram promotes the conversion of carcinogenic cadmium to a proteasome inhibitor with pro-apoptotic activity in human cancer cells. *Toxicol Appl Pharmacol.* 229(2):206-214. doi: 210.1016/j.taap.2008.1001.1022. Epub 2008 Feb 1015.

424. Chen D, Cui QC, Yang H, & Dou QP (2006) Disulfiram, a clinically used anti-alcoholism drug and copper-binding agent, induces apoptotic cell death in breast cancer cultures and xenografts via inhibition of the proteasome activity. *Cancer Res* 66(21):10425-10433.

425. Lin J, Haffner MC, Zhang Y, Lee BH, Brennen WN, *et al.* (2011) Disulfiram is a DNA demethylating agent and inhibits prostate cancer cell growth. *Prostate* 71(4):333-343.

426. Guo X, Xu B, Pandey S, Goessl E, Brown J, *et al.* (2010) Disulfiram/copper complex inhibiting NFkappaB activity and potentiating cytotoxic effect of gemcitabine on colon and breast cancer cell lines. *Cancer Lett* 290(1):104-113.

427. Iljin K, Ketola K, Vainio P, Halonen P, Kohonen P, *et al.* (2009) High-throughput cell-based screening of 4910 known drugs and drug-like small molecules identifies disulfiram as an inhibitor of prostate cancer cell growth. *Clin Cancer Res.* 15(19):6070-6078. doi: 6010.1158/1078-0432.CCR-6009-1035. Epub 2009 Sep 6029.

428. Cen D, Brayton D, Shahandeh B, Meyskens FL, Jr., & Farmer PJ (2004) Disulfiram facilitates intracellular Cu uptake and induces apoptosis in human melanoma cells. *J Med Chem.* 47(27):6914-6920.

429. White C, Lee J, Kambe T, Fritsche K, & Petris MJ (2009) A role for the ATP7A copper-transporting ATPase in macrophage bactericidal activity. *J Biol Chem* 284(49):33949-33956.

430. Trombetta LD, Toulon M, & Jamall IS (1988) Protective effects of glutathione on diethyldithiocarbamate (DDC) cytotoxicity: a possible mechanism. *Toxicol Appl Pharmacol.* 93(1):154-164.

431. Nobel CI, Kimland M, Lind B, Orrenius S, & Slater AF (1995) Dithiocarbamates induce apoptosis in thymocytes by raising the intracellular level of redox-active copper. *J Biol Chem.* 270(44):26202-26208.

432. Clemens MJ, Bushell M, & Morley SJ (1998) Degradation of eukaryotic polypeptide chain initiation factor (eIF) 4G in response to induction of apoptosis in human lymphoma cell lines. *Oncogene* 17(22):2921-2931.

433. Morley SJ, McKendrick L, & Bushell M (1998) Cleavage of translation initiation factor 4G (eIF4G) during anti-Fas IgM-induced apoptosis does not require signalling through the p38 mitogen-activated protein (MAP) kinase. *FEBS letters* 438(1-2):41-48.

434. Johansson B (1992) A review of the pharmacokinetics and pharmacodynamics of disulfiram and its metabolites. *Acta psychiatrica Scandinavica. Supplementum* 369:15-26.

435. Ma I & Allan AL (2011) The role of human aldehyde dehydrogenase in normal and cancer stem cells. *Stem cell reviews* 7(2):292-306.

436. Kim MP, Fleming JB, Wang H, Abbruzzese JL, Choi W, *et al.* (2011) ALDH activity selectively defines an enhanced tumor-initiating cell population relative to CD133 expression in human pancreatic adenocarcinoma. *PloS one* 6(6):e20636.

437. Yu C, Yao Z, Dai J, Zhang H, Escara-Wilke J, *et al.* (2011) ALDH activity indicates increased tumorigenic cells, but not cancer stem cells, in prostate cancer cell lines. *In vivo (Athens, Greece)* 25(1):69-76.

438. Boonyaratanakornkit JB, Yue L, Strachan LR, Scalapino KJ, LeBoit PE, *et al.* (2010) Selection of tumorigenic melanoma cells using ALDH. *The Journal of investigative dermatology* 130(12):2799-2808.

439. Croker AK, Goodale D, Chu J, Postenka C, Hedley BD, *et al.* (2009) High aldehyde dehydrogenase and expression of cancer stem cell markers selects for breast cancer cells with enhanced malignant and metastatic ability. *Journal of cellular and molecular medicine* 13(8B):2236-2252.

440. Acharya A, Das I, Chandhok D, & Saha T (2010) Redox regulation in cancer: a double-edged sword with therapeutic potential. *Oxidative medicine and cellular longevity* 3(1):23-34.

441. Karwicka E (2010) Role of glutathione in the multidrug resistance in cancer. *Adv Cell Biol* 1(1):1-20.

442. Estrela JM, Ortega A, & Obrador E (2006) Glutathione in cancer biology and therapy. *Critical reviews in clinical laboratory sciences* 43(2):143-181.

443. Lehmann K, Rickenbacher A, Jang JH, Oberkofler CE, Vonlanthen R, *et al.* (2012) New insight into hyperthermic intraperitoneal chemotherapy: induction of oxidative stress dramatically enhanced tumor killing in in vitro and in vivo models. *Ann Surg.* 256(5):730-737; discussion 737-738. doi: 710.1097/SLA.1090b1013e3182737517.

444. Dalla Pozza E, Donadelli M, Costanzo C, Zaniboni T, Dando I, *et al.* (2011) Gemcitabine response in pancreatic adenocarcinoma cells is synergistically enhanced by dithiocarbamate derivatives. *Free radical biology & medicine* 50(8):926-933.

445. Morrison BW, Doudican NA, Patel KR, & Orlow SJ (2010) Disulfiram induces copper-dependent stimulation of reactive oxygen species and activation of the extrinsic apoptotic pathway in melanoma. *Melanoma Res* 20(1):11-20.

446. Shian SG, Kao YR, Wu FY, & Wu CW (2003) Inhibition of invasion and angiogenesis by zinc-chelating agent disulfiram. *Mol Pharmacol.* 64(5):1076-1084.

447. Hadi SM, Ullah MF, Azmi AS, Ahmad A, Shamim U, *et al.* (2010) Resveratrol mobilizes endogenous copper in human peripheral lymphocytes leading to oxidative DNA breakage: a putative mechanism for chemoprevention of cancer. *Pharm Res.* 27(6):979-988. doi: 910.1007/s11095-11010-10055-11094. Epub 12010 Jan 11030.

448. Kuo HW, Chen SF, Wu CC, Chen DR, & Lee JH (2002) Serum and tissue trace elements in patients with breast cancer in Taiwan. *Biol Trace Elem Res.* 89(1):1-11.

449. Faiman MD, Jensen JC, & Lacoursiere RB (1984) Elimination kinetics of disulfiram in alcoholics after single and repeated doses. *Clinical pharmacology and therapeutics* 36(4):520-526.

450. Zhou J & Du Y (2012) Acquisition of resistance of pancreatic cancer cells to 2-methoxyestradiol is associated with the upregulation of manganese superoxide dismutase. *Mol Cancer Res* 10(6):768-777.

451. Cen D, Gonzalez RI, Buckmeier JA, Kahlon RS, Tohidian NB, *et al.* (2002) Disulfiram induces apoptosis in human melanoma cells: a redox-related process. *Mol Cancer Ther.* 1(3):197-204.

452. Brar SS, Grigg C, Wilson KS, Holder WD, Jr., Dreau D, *et al.* (2004) Disulfiram inhibits activating transcription factor/cyclic AMP-responsive element binding protein and human melanoma growth in a metal-dependent manner in vitro, in mice and in a patient with metastatic disease. *Mol Cancer Ther* 3(9):1049-1060.

453. Hothi P, Martins TJ, Chen L, Deleyrolle L, Yoon JG, *et al.* (2012) High-throughput chemical screens identify disulfiram as an inhibitor of human glioblastoma stem cells. *Oncotarget.* 3(10):1124-1136.

454. Navratilova J, Jungova P, Vanhara P, Preisler J, Kanicky V, *et al.* (2009) Copper ions regulate cytotoxicity of disulfiram to myeloid leukemia cells. *Int J Mol Med.* 24(5):661-670.

455. Brady GF, Galban S, Liu X, Basrur V, Gitlin JD, *et al.* (2010) Regulation of the copper chaperone CCS by XIAP-mediated ubiquitination. *Molecular and cellular biology*.

456. Lenassi M & Plemenitas A (2006) The role of p38 MAP kinase in cancer cell apoptosis. *Radiol Oncol* 40(1):51-56.

457. Kim JY, Yu SJ, Oh HJ, Lee JY, Kim Y, *et al.* (2011) Panaxydol induces apoptosis through an increased intracellular calcium level, activation of JNK and p38 MAPK and NADPH oxidase-dependent generation of reactive oxygen species. *Apoptosis.* 16(4):347-358. doi: 310.1007/s10495-10010-10567-10498.

458. Kim DS, Jeon BK, Lee YE, Woo WH, & Mun YJ (2012) Diosgenin Induces Apoptosis in HepG2 Cells through Generation of Reactive Oxygen Species and Mitochondrial Pathway. *Evid Based Complement Alternat Med.* 2012:981675.(doi):10.1155/2012/981675. Epub 982012 Jun 981676.

459. Sanchez Y, Amran D, Fernandez C, de Blas E, & Aller P (2008) Genistein selectively potentiates arsenic trioxide-induced apoptosis in human leukemia cells via reactive oxygen species generation and activation of reactive oxygen species-inducible protein kinases (p38-MAPK, AMPK). *Int J Cancer.* 123(5):1205-1214. doi: 1210.1002/ijc.23639.

460. Piccirillo S, Filomeni G, Brune B, Rotilio G, & Ciriolo MR (2009) Redox mechanisms involved in the selective activation of Nrf2-mediated resistance versus p53-dependent apoptosis in adenocarcinoma cells. *J Biol Chem.* 284(40):27721-27733. doi: 27710.21074/jbc.M27109.014837. Epub 012009 Jul 014830.

461. Filomeni G, Piccirillo S, Rotilio G, & Ciriolo MR (2012) p38(MAPK) and ERK1/2 dictate cell death/survival response to different pro-oxidant stimuli via p53 and Nrf2 in neuroblastoma cells SH-SY5Y. *Biochem Pharmacol.* 83(10):1349-1357. doi: 1310.1016/j.bcp.2012.1302.1003. Epub 2012 Feb 1349.

462. Kairisalo M, Korhonen L, Blomgren K, & Lindholm D (2007) X-linked inhibitor of apoptosis protein increases mitochondrial antioxidants through NF-kappaB activation. *Biochem Biophys Res Commun* 364(1):138-144.

463. Winsauer G, Resch U, Hofer-Warbinek R, Schichl YM, & de Martin R (2008) XIAP regulates bi-phasic NF-kappaB induction involving physical interaction and ubiquitination of MEKK2. *Cell Signal* 20(11):2107-2112.

464. Alison MR, Guppy NJ, Lim SM, & Nicholson LJ (2010) Finding cancer stem cells: are aldehyde dehydrogenases fit for purpose? *The Journal of pathology* 222(4):335-344.

465. Allahverdiyev AM, Bagirova M, Oztel ON, Yaman S, Abamor ES, *et al.* (2012) *Aldehyde Dehydrogenase: Cancer and Stem Cells*.

466. Ginestier C, Hur MH, Charafe-Jauffret E, Monville F, Dutcher J, *et al.* (2007) ALDH1 is a marker of normal and malignant human mammary stem cells and a predictor of poor clinical outcome. *Cell stem cell* 1(5):555-567.

467. Shenoy A, Butterworth E, & Huang EH (2012) ALDH as a marker for enriching tumorigenic human colonic stem cells. *Methods in molecular biology (Clifton, N.J.)* 916:373-385.

468. Abdullah LN & Chow EK (2013) Mechanisms of chemoresistance in cancer stem cells. *Clinical and translational medicine* 2(1):3.

469. Huang CP, Tsai MF, Chang TH, Tang WC, Chen SY, *et al.* (2013) ALDH-positive lung cancer stem cells confer resistance to epidermal growth factor receptor tyrosine kinase inhibitors. *Cancer Lett* 328(1):144-151.

470. Kobayashi CI & Suda T (2012) Regulation of reactive oxygen species in stem cells and cancer stem cells. *J Cell Physiol* 227(2):421-430.

471. Diehn M, Cho RW, Lobo NA, Kalisky T, Dorie MJ, *et al.* (2009) Association of reactive oxygen species levels and radioresistance in cancer stem cells. *Nature* 458(7239):780-783.

472. Singh S, Brocker C, Koppaka V, Chen Y, Jackson BC, *et al.* (2013) Aldehyde dehydrogenases in cellular responses to oxidative/electrophilic stress. *Free radical biology & medicine* 56:89-101.

473. Xu M, Cui J, Fu H, Proksch P, Lin W, *et al.* (2005) Embelin derivatives and their anticancer activity through microtubule disassembly. *Planta Med* 71(10):944-948.

474. Moreb JS (2008) Aldehyde dehydrogenase as a marker for stem cells. *Current stem cell research & therapy* 3(4):237-246.

475. Kitson TM (1975) The effect of disulfiram on the aldehyde dehydrogenases of sheep liver. *The Biochemical journal* 151(2):407-412.

476. Kitson TM (1981) The inactivation of aldehyde dehydrogenase by disulfiram in the presence of glutathione. *The Biochemical journal* 199(1):255-258.

477. Sharma SV, Lee DY, Li B, Quinlan MP, Takahashi F, *et al.* (2010) A chromatin-mediated reversible drug-tolerant state in cancer cell subpopulations. *Cell.* 141(1):69-80. doi: 10.1016/j.cell.2010.1002.1027.

478. Velasco-Velazquez MA, Homsi N, De La Fuente M, & Pestell RG (2012) Breast cancer stem cells. *The international journal of biochemistry & cell biology* 44(4):573-577.

479. Rainer PP, Doleschal B, Kirk JA, Sivakumaran V, Saad Z, *et al.* (2012) Sunitinib causes dose-dependent negative functional effects on myocardium and cardiomyocytes. *BJU international* 110(10):1455-1462.

480. Rahmani M, Davis EM, Crabtree TR, Habibi JR, Nguyen TK, *et al.* (2007) The kinase inhibitor sorafenib induces cell death through a process involving induction of endoplasmic reticulum stress. *Molecular and cellular biology* 27(15):5499-5513.

481. Wu J, Min R, Wu M, & Chen W (2011) Gefitinib induces mitochondrial-dependent apoptosis in Saccharomyces cerevisiae. *Molecular medicine reports* 4(2):357-362.

482. Courtin A, Richards FM, Bapiro TE, Bramhall JL, Neesse A, *et al.* (2013) Anti-Tumour Efficacy of Capecitabine in a Genetically Engineered Mouse Model of Pancreatic Cancer. *PloS one* 8(6):e67330.

483. Corna G, Santambrogio P, Minotti G, & Cairo G (2004) Doxorubicin paradoxically protects cardiomyocytes against iron-mediated toxicity: role of reactive oxygen species and ferritin. *J Biol Chem* 279(14):13738-13745.

484. Kubota M, Shimmura S, Miyashita H, Kawashima M, Kawakita T, *et al.* (2010) The anti-oxidative role of ABCG2 in corneal epithelial cells. *Investigative ophthalmology & visual science* 51(11):5617-5622.

485. Wallach-Dayan SB, Izbicki G, Cohen PY, Gerstl-Golan R, Fine A, *et al.* (2006) Bleomycin initiates apoptosis of lung epithelial cells by ROS but not by Fas/FasL pathway. *American journal of physiology. Lung cellular and molecular physiology* 290(4):L790-L796.

486. Lu Y, Azad N, Wang L, Iyer AK, Castranova V, *et al.* (2010) Phosphatidylinositol-3-kinase/akt regulates bleomycin-induced fibroblast proliferation and collagen production. *American journal of respiratory cell and molecular biology* 42(4):432-441.

487. Matsunaga T, Yamane Y, Iida K, Endo S, Banno Y, *et al.* (2011) Involvement of the aldo-keto reductase, AKR1B10, in mitomycin-c resistance through reactive oxygen species-dependent mechanisms. *Anti-cancer drugs* 22(5):402-408.

488. Shi K, Wang D, Cao X, & Ge Y (2013) Endoplasmic reticulum stress signaling is involved in mitomycin C (MMC)-induced apoptosis in human fibroblasts via PERK pathway. *PloS one* 8(3):e59330.

489. Resch U, Schichl YM, Sattler S, & de Martin R (2008) XIAP regulates intracellular ROS by enhancing antioxidant gene expression. *Biochem Biophys Res Commun* 375(1):156-161.

490. Zhu C, Xu F, Fukuda A, Wang X, Fukuda H, *et al.* (2007) X chromosome-linked inhibitor of apoptosis protein reduces oxidative stress after cerebral irradiation or hypoxia-ischemia through up-regulation of mitochondrial antioxidants. *Eur J Neurosci* 26(12):3402-3410.

491. Saito A, Hayashi T, Okuno S, Nishi T, & Chan PH (2004) Oxidative stress is associated with XIAP and Smac/DIABLO signaling pathways in mouse brains after transient focal cerebral ischemia. *Stroke* 35(6):1443-1448.

492. Githui EK, Makawiti DW, & Midiwo JO (1991) Changes in the concentrations of testosterone, luteinising hormone and progesterone associated with administration of embelin. *Contraception* 44(3):311-317.

493. Joshi R, Kamat JP, & Mukherjee T (2007) Free radical scavenging reactions and antioxidant activity of embelin: biochemical and pulse radiolytic studies. *Chem Biol Interact* 167(2):125-134.

494. Mufti AR, Burstein E, & Duckett CS (2007) XIAP: Cell death regulation meets copper homeostasis. *Arch Biochem Biophys*.

495. Il'yasova D, Scarbrough P, & Spasojevic I (2012) Urinary biomarkers of oxidative status. *Clinica chimica acta; international journal of clinical chemistry* 413(19-20):1446-1453.

496. Il'yasova D, Spasojevic I, Wang F, Tolun AA, Base K, *et al.* (2010) Urinary biomarkers of oxidative status in a clinical model of oxidative assault. *Cancer epidemiology, biomarkers & prevention : a publication of the American Association for Cancer Research, cosponsored by the American Society of Preventive Oncology* 19(6):1506-1510.

Biography

Jennifer L. Allensworth was born to David A. Nollsch and Rebecca J. Paine in Houston, Texas on May 8th, 1987. She lived with them there until graduating from Langham Creek High School in May of 2005. After high school, she attended The University of Texas at Austin where she majored in microbiology and began researching HPV-associated cervical cancer in the laboratory of Dr. Jon Huibregtse. It was during her time at UT Austin that Jennifer met and fell in love with her husband James Allensworth. She graduated with high honors in May of 2009 and married James in Austin, Texas on July 18th, 2009. Jennifer then moved to North Carolina to enroll in the Ph.D. program at Duke University, where she joined the Department of Pathology. She joined the laboratory of Dr. Gayathri R. Devi in November of 2009 and remained there to perform her thesis work studying mechanisms of therapeutic resistance in inflammatory breast cancer and the development of rational strategies to overcome that resistance.

EDUCATION

Duke University, Durham, NC (August 2009 – present)

Doctor of Philosophy

Department of Pathology

The University of Texas at Austin, Austin, TX (August 2005 – May 2009)

Bachelor of Science in Microbiology, High Honors

Department of Natural Sciences

HONORS, AWARDS, AND FELLOWSHIPS

1. Duke University Graduate School Travel Award, December 2012
2. Duke Viral Oncology Research Training Grant, 2010-2011
3. Duke University Chancellor's Scholarship, 2009-2010

PUBLICATIONS AND PRESENTATIONS

Peer-reviewed Publications

1. Williams KP, **Allensworth JL**, Ingram SM, Smith GR, Aldrich AJ, Sexton JZ, Lyerly HK, Devi GR. Quantitative high-throughput efficacy profiling of approved oncology drugs in inflammatory breast cancer models of acquired resistance and drug-resistance reversal. Cancer Letters, 2013: in press.
2. **Allensworth JL**, Sauer SJ, Lyerly HK, Morse MA, and Devi GR. Smac mimetic Birinapant induces apoptosis and enhances TRAIL potency in inflammatory breast cancer cells in an IAP-dependent and TNF-α-

independent mechanism. Breast Cancer Research and Treatment, 2013 Jan;137(2):359-71.

3. Rangwala F, Williams KP, Smith GR, Thomas Z, **Allensworth JL**, Lyerly HK, Diehl AM, Morse MA, and Devi GR. Differential effects of arsenic trioxide on chemosensitization in human hepatic tumor and stellate lines. BMC Cancer, 2012 Sep 10;12(1):402.
4. **Allensworth JL**, Aird KM, Aldrich AJ, Batinic-Haberle I, and Devi GR. XIAP inhibition and generation of reactive oxygen species enhances TRAIL sensitivity in inflammatory breast cancer cells. Molecular Cancer Therapeutics, 2012 Jul; 11(7):1518-27.
5. Aird KM, **Allensworth JL**, Batinic-Haberle I, Lyerly HK, Dewhirst MW, and Devi GR. ErbB1/2 tyrosine kinase inhibitor mediates oxidative stress-induced apoptosis in inflammatory breast cancer cells. Breast Cancer Research and Treatment, 2012 Feb; 132(1):109-19.
6. Ye X, Fels D, Tovamasyan A, Aird KM, Dedeugd C, **Allensworth JL**, Kos I, Park W, Spasojevic I, Devi GR, Dewhirst MW, Leong KW, and Batinic-Haberle I. Cytotoxic effects of Mn(III) N-alkylpyridylporphyrins in the presence of cellular reductant, ascorbate. Free Radical Research, 2011 Nov;45(11-12):1289-306.

Conference Presentations and Proceedings

1. **Allensworth JL**, Aird KM, Murray MB, and Devi GR. "Targeting X-linked inhibitor of apoptosis protein (XIAP) and redox adaptation to overcome acquired therapeutic resistance in IBC," 3rd International Inflammatory Breast Cancer Conference, Poster Presentation, (2012)
2. **Allensworth JL** and Devi GR. "XIAP regulates TRAIL-induced apoptosis in inflammatory breast cancer cells," San Antonio Breast Cancer Symposium, Poster Presentation, (2010).